

SEP 27 1989

AGARD-LS-150 (Revised)

C#2

AGARD-LS-150 (Revised)

AGARD

ADVISORY GROUP FOR AEROSPACE RESEARCH & DEVELOPMENT

7 RUE ANCELLE 92200 NEUILLY SUR SEINE FRANCE

AGARD LECTURE SERIES No.150

Design Methods in Solid Rocket Motors

Revised Version 1988

TECHNICAL REPORT
FREE COPY

PROPERTY OF U.S. AIR FORCE
AFDC TECHNICAL LIBRARY

NORTH ATLANTIC TREATY ORGANIZATION



DISTRIBUTION AND AVAILABILITY
ON BACK COVER

NORTH ATLANTIC TREATY ORGANIZATION
ADVISORY GROUP FOR AEROSPACE RESEARCH AND DEVELOPMENT
(ORGANISATION DU TRAITE DE L'ATLANTIQUE NORD)

AGARD Lecture Series No.150
REVISED VERSION 1988
DESIGN METHOD IN SOLID ROCKET MOTORS

The material in this revised publication was assembled to support a Lecture Series under the sponsorship of the Propulsion and Energetics Panel and the Consultant and Exchange Programme of AGARD presented on 18—19 April 1988 in London, United Kingdom, 21—22 April 1988 in Saint-Aubin de Medoc, France, 25—26 April 1988 in Neubiberg, Germany and on 28—29 April 1988 in Rome, Italy.

THE MISSION OF AGARD

According to its Charter, the mission of AGARD is to bring together the leading personalities of the NATO nations in the fields of science and technology relating to aerospace for the following purposes:

- Recommending effective ways for the member nations to use their research and development capabilities for the common benefit of the NATO community;
- Providing scientific and technical advice and assistance to the Military Committee in the field of aerospace research and development (with particular regard to its military application);
- Continuously stimulating advances in the aerospace sciences relevant to strengthening the common defence posture;
- Improving the co-operation among member nations in aerospace research and development;
- Exchange of scientific and technical information;
- Providing assistance to member nations for the purpose of increasing their scientific and technical potential;
- Rendering scientific and technical assistance, as requested, to other NATO bodies and to member nations in connection with research and development problems in the aerospace field.

The highest authority within AGARD is the National Delegates Board consisting of officially appointed senior representatives from each member nation. The mission of AGARD is carried out through the Panels which are composed of experts appointed by the National Delegates, the Consultant and Exchange Programme and the Aerospace Applications Studies Programme. The results of AGARD work are reported to the member nations and the NATO Authorities through the AGARD series of publications of which this is one.

Participation in AGARD activities is by invitation only and is normally limited to citizens of the NATO nations.

The content of this publication has been reproduced
directly from material supplied by AGARD or the authors.

Published April 1988

Copyright © AGARD 1988
All Rights Reserved

ISBN 92-835-0454-2



*Printed by Specialised Printing Services Limited
40 Chigwell Lane, Loughton, Essex IG10 3TZ*

PREFACE

This Lecture Series will try to summarize the current state-of-the-art in designing solid rocket motors and their components. The aim is to collect the experience of several countries in using new technologies and new methods which have been developed over the past ten years.

Specific sessions will deal with propellant grain, cases, nozzle, internal thermal insulations; the question of the general optimization of a solid rocket motor will be emphasized.

This Lecture Series, sponsored by the Propulsion and Energetics Panel of AGARD, has been implemented by the Consultant and Exchange Programme.

* * *

Ce cycle de conférences présente une synthèse de l'état de l'art dans le domaine de la conception des moteurs-fusées à propergol solide et de leurs éléments constitutifs. Les conférences présentées rassemblent les connaissances et le savoir-faire de plusieurs pays dans la mise en oeuvre des nouvelles technologies et de nouvelles méthodes qui ont été développées au cours de la dernière décennie.

Les exposés spécifiques portent sur le bloc de poudre, son enveloppe, les tuyères et la protection thermique interne, en mettant l'accent sur l'optimisation globale des moteurs fusées à propergol solide.

Ce cycle de conférences est présenté dans le cadre du Programme des Consultants et des Echanges, sous l'égide du Panel de Propulsion et d'Energétique de l'AGARD.

LIST OF AUTHORS/SPEAKERS

Lecture Series Director: Mr l'Ing. eng Chef D.Reydellet
Service Technique des Engins Balistiques
Direction des Engins
26, Boulevard Victor
75996 Paris Armées
France

AUTHORS/SPEAKERS

Mr H.Badham
Royal Ordnance Summerfield
Kidderminster Worcs DY11 7RZ
United Kingdom

Mr J.P.Denost
Aérospatiale/Aquitaine
Boîte Postale 11 Issac
33165 Saint-Medard en Jalles Cedex
France

Dr P.R.Evans
Hercules Corp.
Aerospace Products Division
Alleghany Ballistics Laboratory
P.O. Box 210, Rocket Center,
WV 26726
USA

Mr J.H.Hildreth
Air Force Rocket Propulsion Laboratory
Edwards Air Force Base
California 93523
USA

Mr A.Lampert
Bayern Chemie GmbH
Postfach 220
8012 Ottobrunn
Germany

Mr Le Merer
SEP/DPPC
Les Cinq Chemins — Le Haillan
33165 Saint-Medard-en-Jalles
France

Dr B.Lucas
BP No.2 Le Bouchet
91710 Vert Le Petit
France

Mr S.Scippa
SNIA/BPD
Corso Garibaldi 22
00034 Colleferro (Roma)
Italy

Mr G.P.Thorp
Royal Ordnance Summerfield
Kidderminster, Worcs DY11 7RZ
United Kingdom

Mr D.Thrasher
Air Force Rocket Propulsion Laboratory
Edwards Air Force Base
California 93523
USA

Mr A.Truchot
Agence Spatiale Européenne
Division STS-AR
8—10, rue Mario Nikis
75738 Paris Cedex 15
France

Dr B.Zeller
SNPE/CRB
BP No.2 Le Bouchet
91710 Vert le Petit
France

CONTENTS

	Page
PREFACE	iii
LIST OF AUTHORS/SPEAKERS	iv
	Reference
INTRODUCTION by D.Reydellet	1
ADVANCES IN SOLID ROCKET NOZZLE DESIGN AND ANALYSIS TECHNOLOGY IN THE UNITED STATES SINCE 1970 by J.H.Hildreth	2
DESIGN AND ANALYSIS OF SOLID ROCKET MOTOR NOZZLE by A.Truchot	3
COMPOSITE MOTOR CASE DESIGN by P.R.Evans	4A
OVERALL DESIGN OF SOLID ROCKET MOTORS by A.Lampert	4B*
DESIGN OF FILAMENT-WOUND ROCKET CASES by J.P.Denost	5
CONSIDERATIONS FOR DESIGNERS OF CASES FOR SMALL SOLID PROPELLANT ROCKET MOTORS by H.Badham and G.P.Thorp	6
PROPELLANT GRAIN DESIGN by S.Scippa	7
SOLID PROPELLANT GRAIN DESIGN by B.Zeller	8
STATE OF THE ART OF SOLID PROPELLANT ROCKET MOTOR GRAIN DESIGN IN THE UNITED STATES by D.I.Thrasher	9
DESIGN AND ANALYSIS OF SOLID ROCKET MOTOR INTERNAL INSULATION by A.Truchot	10
OVERALL OPTIMIZATION OF SOLID ROCKET MOTOR by A.Truchot	11
ROUND TABLE DISCUSSIONS	RTD
BIBLIOGRAPHY	B

*Not available at time of printing.

Introduction to the lecture series 150
by D. REYDELLET
"Ingénieur en Chef de l'Armement" (Colonel, Armement Corps)
Direction des Engins (Technical Directorate for Missiles)
26, boulevard Victor
75996 PARIS-ARMEES
FRANCE

1. FOREWORD

When looking back to the evolution of the solid rocket motor (SRM) propulsion for the past twenty years, the following fact is obvious : this evolution has been very similar to the one of the others techniques, despite of its specific features.

Eventually, the same revolutions has appeared in the materials field (tendency to the general use of composite materials), and in the modelization methods (general use of finite elements codes and, more recently, design methods with computer aids). The only area that is still relatively traditionnal, is the formulation of propellants, though the trend to specific performances (increasing of specific impulse or reducing of signature) has driven the technicians to formulate compositions that are closer to the explosives than to the conventional propellants.

On the other hand, it is obvious that the new materials for SRM propulsion are very specific. In addition their behaviour is often very difficult to modelize from a thermomechanical point of view. As a result, it has been necessary to adapt the general methods for the characterization of materials, the finite elements modelization, the validation of these modelizations, the qualification tests, and, generally speaking, all the techniques that are used in a development program. It is obviously necessary to make a periodical synthesis of these questions. In addition, there are very few synthetic publications in this field.

So we have to acknowledge AGARD once more for the opportunity we have to achieve this goal.

2. GOAL OF THE SESSION

The purpose is to collect the most important points concerning the design and computation methods used for SRMS. Of course, it is not possible in such a short time to deal completely with all the problems. However, I hope that the fundamental ideas and the most critical or difficult problems will be emphasized. I invite you to make a synthesis on this point at the end of the session.

Beside the question of the general optimization of SRM (that is a specific subject), every presentation will try to summarize all the problems that are to be solved by an office in charge of designing a new SRM or a component of SRM : choice of technologies, modelization, material characterization, choice of margin of safety, identification of critical points, computation validation, qualification tests.

For the design of every main component, you will mainly attend two or three presentations by speakers from different countries.

This is not a mistake, but a choice : it will allow you to look at the same question from several points of view, since the different lecturers have lived various experiences on a same subject.

Once more time, I invite you to try to make a synthesis tomorrow during the round table.

On the other hand, you will not find in these presentations a detailed paper dealing with the prediction by theoretical methods of the specific impulse of the propellants used for SRMS. Once more, it is not an error, but a choice : this question has already been dealt with by the WORKING GROUP nr. 17 of AGARD PEP (AGARD Report n° 230). For any question on this specific problem, please consult this document : you will find an evaluation of the different methods for predicting specific impulse of propellants with high Aluminium loads, from the most sophisticated analytical methods to the most simple semi-empirical methods; the question of the measurement accuracy of this parameter (especially under altitude simulation) is approached, and, at the end, the group recommends the use of a semi-empirical method as a common reference between the AGARD countries.

At last, beyond the presentations, it is obvious that this session has a secondary goal : that is to put together different specialists in SRM propulsion. Persons in the audience of this session must be also, if possible, active players. I do hope, from my point of view, that profitable conversations will be initiated, that you will not hesitate to ask questions in case you want to make clear by the speaker a difficult point, or if you want to share your experience on a special point.

3. ORGANIZATION OF THE SESSION

During this session, eight speakers will present the result of their experience in the field of their speciality. They are all professional people, whose skill is well known in the world of SRM and solid propellants.

In their country, they have all high responsibility in important civil or military programs. Despite that, they have devoted a lot of time to the preparation of their papers. I want now to address my deepest thanks to them. I think their best reward will probably be the interest in their work you are going to show through the questions that you will ask them, every time you will have the opportunity to do so, that is,

I hope, as often as possible. I will ask the speakers to be very watchful of the timing during the presentations, in order to save a sufficient time for questions at the end of each presentation. In addition, the session will end tomorrow with a round table, with all speakers; during this round table, you will be able to ask all the questions and make clear the points that you think the most important. In don't want now to detail all the papers that are going to be presented to you. I only want to set a list of the subjects and try to point out some important features.

3.1. Design and Computation of Nozzles

This topic will be presented by two speakers: Mr. J. HILDERTH (USA) and Mr. TRUCHOT (FRANCE). Obviously this component is very specific in comparison with other nozzles used in other propulsion techniques, specifically because of the very high exhaust gas temperature, their chemical and physical characteristics (especially with two phases).

At first, one can say that the problem is to choose the materials, along with their place in the nozzle (in a subsonic, sonic or supersonic flow). Then, the purpose is to solve a problem of design from a thermo-mechanical point of view (computation of the stresses as a result of the thermal expansion of the parts under the huge temperature differences everywhere). In addition, one must predict the erosion rate.

This technique has followed the general evolution during this last fifteen years : at first, only high temperature alloys (such as tungsten) or bulk graphite were used. Currently, the carbon-carbon composite are more and more used. On the other hand, the computation methods have experienced important changes : the general use of finite elements code allows now to perform the computation of mechanical margins of safety for every part of the nozzle.

With the recent progresses concerning the materials that are called "thermostructural", an important simplification in nozzle design can be hoped, since cold structural parts could be removed. However, a lot of technical and economical problems are still to be solved : quality insurance, non destructive tests, complete characterization of materials, verification of margin of safety...

3.2. Design and Computation of Cases

This topic will be presented by three speakers : Dr. P. EVANS (USA), Mr. DENOST (FRANCE) et Mr BADHAM (or Mr. THORP) (U.K.). The two first lecturers will present you the technologies and the design of composite cases for large SRM. In this field, progresses have been spectacular during these last twenty years : the first filament wound cases were using glass fiber (whose performances were increasing continuously), then an aramide fiber (trade mark : KEVLAR), and at last carbon (or graphite) fiber. At the same time, the development of computation methods was considerable; many difficulties were encountered for modeling filament wound cases by finite elements codes because of the very specific arrangements (successive monodirectional layers) of this composite material. The question was especially critical at the bonding between the vessel and the rest of the missile (design of skirts), and at the aft and forward polar fittings.

Nowadays , the state of the art allows to perform precise mechanical computations; however, the higher performances are, the more severe "small mistakes in designing details" are, in the same way, small defects can become very critical. As a result, many progresses are still to be made for quality insurance (in a general meaning, that is the problem of discovering and assessing critical defects).

The third speaker will deal with technologies and design methods used for cases of small SRM for tactical missiles. The concerns for this applications are very different, since other critical loads than the internal pressure (for instance, the problems of rigidity for very slender SRM) can be encountered. In addition, economical constraints can be preponderant. As a result, the materials that are choosen are often metallic alloys, although some composite reinforcement can be used in some cases.

3.3. Design and Computation of Propellant Grains

Three speakers will deal with this point : Dr. SCIPPA (ITALY), Dr. ZELLER (FRANCE), Mr. THRASHER (USA). The most important point for that subject is obviously the continuous evolutions of propellants : double-base, conventional composites, double-base composites... Every kind of propellant has a very particular ballistic and mechanical behaviour. A very general evolution is the use of cast bonded grains, that is the technique of casting the propellant directly in the case (which is already equipped with its internal thermal protections). The question of the bonding between propellant and thermal insulation is very critical. On the other hand, the techniques used for obtaining various shapes, by machining or integral molding have provided the designer with many degrees of freedom. Besides the conventionnal star cylindrical and axisymmetric grains, one can now use three dimensional shapes (for exemple : finocyl grains).

These solutions lead to optimal pressure history and high volumetric loading. This last point become possible from a mechanical point of view with the enhancement of the mechanical properties of the propellant. Modern propellant compositions are optimized for sophisticated requirements : high specific impulse and density, reduced signature (actually this requirement covers many different concerns). The methods used for mechanical computations of propellant grains were at first very simple. Nowadays, the most sophisticated finite elements codes are used (in certain case with three-dimensionnal capabilities). Dynamic loads can be modeled by taking in account the most various rheological behaviours (typically : linear or non-linear viscoelasticity). These methods allow the identification of the critical mechanical points, at low temperature and during firing as well. By using failure criteria, the margin of safety can be assessed. Since the critical points in the grain it self are rather well predicted, one must point out that the prediction of margin of safety at the bonding between propellant and thermal protection is still difficult. Some progresses are still to be made in that field.

A last, I want to remind you the questions of investigating the influence of aging, the quality insurance and the verification of margin of safety.

3.4. Design and Computation of Internal Thermal Insulations

This question will be analysed by only one paper presented by Mr. TRUCHOT (FRANCE). This is not a negligible problem, in reference to the relative magnitude of the thermal insulation's mass in the total inert mass of a modern SRM. Internal thermal insulations use elastomeric materials, with various loads (powders or fibers), that are designed to enhance the material's properties. The most important requirements are : erosion performances, low diffusivity, and (if possible) low density. In this fields, progresses have been spectacular these last years.

The design of internal thermal insulation is very difficult, especially concerning the prediction of the erosion rate : the role of the experimental knowledge is still very important.

3.5. General optimization of SRMS

Mr. TRUCHOT will present also a paper dealing with general optimization methods for SRMS, that have been developed extensively these last years. As a matter of fact, the emergence of computer aids for design has produced some applications for SRMS. These methods allow to generate SRM predesigns automatically; as a result, one can make better choices between different technologies and main geometrical parameters. These codes have some computation subroutines for components; these subroutines are more and more sophisticated; the designers are now able to provide a lot of predesign studies very quickly.

4. CONCLUSION

At the end of these two days, we will try to draw some conclusions together. I am sure that you will be convinced that solid rocket motor propulsion shows an extraordinary maturity.

I will not try to remind you the classical comparisons between various propulsion techniques. However, I would like to point out a few points about the future of solid propellants.

I'm strongly convinced that this kind of propulsion has still an important role to play in the future. It will be, of course, still present in its usual uses, such as military applications, for tactical or strategical missiles as well. The continuous progresses in performances, along with the very simple operational use, make the adequacy of SRM propulsion to that kind of application almost perfect.

In addition, it is obvious that solid propellants have not yet developed all their qualities for the space applications, and especially for large boosters; by the way, it seems to me that spectacular progresses are to be forecasted in the field of cost reduction. However, a recent and tragic accident make someone to doubt about the intrinsic reliability of SRMS. Some people may have the temptation to conclude that they are incompatible with manned space flights. This conclusion is obviously excessive, but this dramatic exemple must invite us to be careful.

It is very dangerous to believe that SRMS are so simple that nothing severe can happen, especially after a long successful series. In any case, the burning gases of solid propellants are always extremely dangerous; the huge mass of propellant grain is always a source of hazard, because of their very high specific energy. As a result, the safety studies (design, justifications, insurance and maintenance of safety) must always be looked at with the greatest care, under the direct authority of the program manager.

At last, I think the most important thing is to be aware of this fact (that could seem completely obvious) : a SRM can work only one time and, consequently, it is impossible to verify the operation of every specimen by an acceptance test.

The whole quality insurance rests on the margins of safety, but also on the process controls and on the performances of non destructive inspection tests.

If all the people involved in a program keep these simple ideas in their mind, I'm convinced that it is possible to reach a considerable level of reliability and safety; this level will lead to a very low failure probability.

As a result of all these elements, it is for me obvious that SRMS will be present for many applications, for after the year 2000.

Introduction à la lecture série 150
par D. REYDELLET
Ingénieur en Chef de l'Armement
Direction des Engins
26, boulevard Victor
75996 PARIS-ARMÉES
FRANCE

1. - GENERALITES

Si l'on observe l'évolution de la propulsion à propergol solide dans les vingt dernières années, on est frappé par le fait que, malgré la spécificité de ce domaine, l'évolution a été assez conforme à celle des autres techniques. En effet, les mêmes révolutions sont apparues dans le domaine des matériaux (tendance à l'utilisation généralisée des matériaux composites), et dans les méthodes de dimensionnement (utilisation à grande échelle des codes aux éléments finis, et, plus récemment des outils de conception assistés par ordinateurs). Le seul secteur relativement resté traditionnel est celui de la formulation des propergols, encore que, pour satisfaire à certaines performances (impulsion spécifique élevée ou recherche de discrétion) les techniciens soient de plus en plus tentés de faire appel à des compositions ayant plus de parenté avec les explosifs qu'avec les propergols traditionnels. Il est vrai par ailleurs que les nouveaux matériaux de la propulsion à poudre sont des matériaux très spécifiques. De plus, leur comportement est souvent difficile à modéliser au plan thermomécanique. Ils sont souvent utilisés dans des gammes de sollicitation très inusitées. C'est pourquoi, les méthodes générales de caractérisation des matériaux, de modélisation par éléments finis, de validation des modèles de calcul, d'essai de qualification en un mot toutes les techniques utilisées lors de la mise au point des matériels ont dû être adaptées. La nécessité de faire le point de manière périodique sur ces problèmes est absolument évidente. On doit ajouter qu'il existe très peu d'ouvrages de synthèse dans ce domaine.

C'est pourquoi, il convient de remercier une fois de plus l'AGARD pour l'occasion qui nous est donnée de réaliser cet objectif.

2. - OBJECTIF DE LA SESSION

Il s'agit de rassembler les éléments les plus importants relatifs aux règles de conception et de dimensionnement des propulseurs à poudre. Bien entendu, il n'est pas possible dans un temps aussi limité d'aller complètement jusqu'au fond des choses. Cependant, j'espère que seront dégagées au moins les idées fondamentales et soulignées les points les plus sensibles ou difficiles. Je vous engage à bien vouloir en faire le bilan en fin de session.

Si on excepte la question de l'optimisation générale des propulseurs, qui constitue un sujet à part, chaque exposé tentera de vous résumer de manière succincte l'ensemble des problèmes qui doivent être résolus par un bureau d'étude lors de la conception d'un nouveau propulseur ou de sous-ensemble de propulseur : choix des différentes technologies possibles, modélisation, caractérisation des matériaux, choix des coefficients de sécurité, inventaire des points critiques, vérification des calculs, essai de qualification, etc...

Pour le dimensionnement de chaque sous-ensemble majeur, vous assisterez généralement à deux ou trois présentations d'orateurs de pays différents. Ce fait ne constitue pas une erreur de programmation, mais un choix délibéré pour vous permettre d'aborder le même problème de manière différente, dans la mesure où les différents intervenants auront une expérience différente sur un même sujet. Je vous invite, une fois de plus, à tenter d'en faire la synthèse lors de table ronde de demain. Par ailleurs, vous ne trouverez pas dans ces présentations de papiers détaillés portant sur la détermination par des méthodes théoriques de l'impulsion spécifique des propergols utilisés dans les moteurs. Ce fait ne constitue pas un oubli, mais un choix délibéré : le sujet a déjà été traité par le groupe de travail n° 17 de l'AGARD (AGARD report n° 230). Pour toute question portant sur ce problème particulier, vous voudrez bien vous reporter à ce document où sont évaluées les différentes méthodes de prévision de l'impulsion spécifique des propergols fortement aluminisés depuis les méthodes analytiques les plus sophistiquées jusqu'aux méthodes semi-empiriques les plus simples; le problème de la précision de mesure de ce paramètre (notamment en altitude simulée) est abordé, et finalement, le groupe préconise l'utilisation d'une méthode semi-empirique, en tant que référence parmi les pays de l'AGARD.

Enfin, au-delà de la matière-même des conférences, il va sans dire que cette manifestation a aussi pour but de mettre en contact divers spécialistes de la propulsion à propergol solide. Les auditeurs de cette session doivent également, si possible, en être les acteurs actifs. Je souhaite personnellement que des échanges fructueux soient initiés, et que vous n'hésitez pas à prendre la parole soit pour faire éclaircir par l'orateur quelque point délicat, soit pour faire part de votre expérience propre sur un point particulier.

3. - DEROULEMENT DE LA SESSION

Au cours de cette session, huit conférenciers vont vous présenter le fruit de leur réflexion dans le domaine de leur spécialité. Ce sont tous de grands professionnels, dont la compétence est reconnue dans le monde de la propulsion à poudre et des propergols. Ils ont tous dans leur pays des responsabilités élevées dans de grands programmes civils ou militaires. Malgré cela, ils ont bien voulu consacrer beaucoup de temps à la préparation de leurs exposés. Qu'ils en soient dès maintenant collectivement et chaleureusement remerciés. Leur meilleure récompense sera sans doute les marques d'intérêt que vous voudrez bien manifester pour leur travail, grâce aux questions que vous ne manquerez pas de leur poser, chaque fois que vous en aurez l'occasion, c'est-à-dire, j'espère, le plus souvent possible. A cet effet, je demanderai aux conférenciers de bien vouloir être vigilants sur le respect de l'horaire lors des présentations, afin de ménager un temps suffisant à la fin de chaque séance pour les questions. Par ailleurs, la session sera clôturée demain par une table ronde réunissant tous les conférenciers, au cours de laquelle vous pourrez poser les questions et voir traiter les sujets qui vous tiennent à coeur.

Il n'entre pas dans mon propos de vous détailler la teneur des papiers qui vous seront exposés. Je me bornerai donc à lister les sujets abordés, en tentant d'en souligner les caractéristiques les plus importantes à mon sens.

3.1. Conception et dimensionnement des tuyères

Ce sujet vous sera exposé par deux orateurs : Mr J. HILDERTH (USA) et Mr TRUCHOT (FRANCE). Il va sans dire que la conception de ce sous-ensemble présente une originalité considérable par rapport aux tuyères utilisées dans les autres techniques de propulsion, par la température considérable des gaz, leur nature chimique, leur caractère biphasique.

On peut dire que, dans un premier temps, il s'agit d'un problème de choix de matériaux, diversifié suivant leur position dans la veine (zone sub, trans ou supersonique). Dans un deuxième temps, il s'agit de résoudre un problème d'architecture au plan thermomécanique (calculs de contrainte) liées aux dilatations produites par les énormes gradients de température dans toutes les pièces). Il faut également évaluer les performances en érosion.

Cette technique a subi l'évolution générale au cours des quinze dernières années : au départ, seuls les métaux réfractaires (tungstène) ou le graphite polycristallin étaient utilisés au col, le reste de la veine ayant recours au carbone ou à la silice phénolique. Actuellement, les matériaux carbone-carbone se généralisent. Par ailleurs, les méthodes de calcul ont évolué de manière considérable : la généralisation des calculs aux éléments finis permet désormais d'effectuer des calculs de marge de sécurité mécanique pour chacune des pièces des tuyères.

Les récents progrès de matériaux dits "thermostructuraux" permettent d'espérer une simplification considérable dans les architectures, par élimination des pièces structurales froides. Cependant, de nombreux problèmes techniques et économiques restent à résoudre : assurance de la qualité, contrôle non destructif, caractérisation complète des matériaux, vérification des marges de sécurité etc...

3.2. Conception et dimensionnement des structures

Ce sujet vous sera exposé par trois orateurs : Mr M. EVANS (USA), Mr DENOST (FRANCE) et Mr BADHAM ou Mr THORP (G.B.).

Les deux premiers vous présenteront les technologies et la conception des structures composites pour propulseurs de grande dimension. Dans ce domaine, les progrès ont été spectaculaires durant les vingt dernières années : les premiers enroulés filamentaires utilisaient de la fibre de verre, dont les performances n'ont fait qu'augmenter, puis une fibre polyamide (nom commercial : KEVLAR), et enfin des fibres de carbone. Parallèlement, les méthodes de calcul ont connu un développement considérable; de nombreuses difficultés ont été rencontrées dans la modélisation des structures roving par élément finis, compte tenu de la nature spécifique, en couches successives, de ce composite. Les problèmes sont particulièrement délicats aux liaisons entre le bidon et la virole du missile (conception des jupes) et aux embases avant et arrière.

L'état de l'art permet à l'heure actuelle d'effectuer des dimensionnements précis; cependant, plus les performances sont élevées, plus les "petites erreurs locales de dimensionnement" sont graves. De même, les défauts locaux peuvent devenir extrêmement critiques. C'est pourquoi, de nombreux progrès sont encore à attendre dans l'assurance de la qualité au sens large, c'est-à-dire dans la détermination et la détection des défauts critiques.

Le troisième orateur vous parlera des technologies et des conceptions de structure de propulseur de petite dimension adaptées aux missiles tactiques. Les préoccupations sont nettement différentes, puisque d'autres facteurs dimensionnants en dehors de la pression interne peuvent intervenir (par exemple la rigidité pour les propulseurs très élancés). Par ailleurs, les considérations d'ordre économique peuvent être prépondérantes. Dans ces conditions, les matériaux utilisés peuvent être plutôt métalliques, bien que pouvant avoir recours à des renforcements composites.

3.3. Conception et dimensionnement des chargements propulsifs

Trois orateurs vous développeront ce point : Dr SCIPPA (ITALY) Dr ZELLER (FRANCE) et Mr D. THRASHER (USA).

Ce sujet est bien entendu dominé par les évolutions des formulations des propergols : double-base, composites, double-base composite. Chaque famille a un comportement balistique et mécanique très particulier. Une évolution tout à fait générale est également la généralisation des blocs moulés-collés, dont le propergol est directement coulé à l'intérieur de la structure équipée de ses protections thermiques. Le problème du collage protection-thermique propergol est des plus crucial. Par ailleurs, les techniques d'obtention de formes variées, soit par usinage, soit par moulage intégral ont donné au concepteur de nombreux degrés de liberté. A côté des blocs à forme classique cylindrique étoilés, et des profils de révolution, on peut désormais utiliser des formes tridimensionnelles

(par exemple : bloc finocyl) conduisant à des évolutions balistiques optimales associées à des coefficients de remplissage élevés, rendus également possibles au plan mécanique par l'amélioration des propriétés mécaniques du propergol. Les formulations actuelles ont été adaptées à des exigences fonctionnelles de plus en plus importantes : forte impulsion spécifique, forte densité, éventuellement discrétion (en distinguant d'ailleurs de nombreuses sous-catégories dans cette spécification. Les méthodes de calcul mécanique des blocs initialement très rudimentaires, font actuellement appel aux codes aux éléments finis les plus élaborés (dans certains cas tri-dimensionnels), pouvant travailler en dynamique en prenant en compte des rhéologies de propergol les plus variées (typiquement : viscoélasticité plus ou moins linéaire). Ces méthodes permettent d'accéder aux points les plus contraints mécaniquement soit à basse température, soit en tir et, par l'intermédiaire d'un critère de rupture, évaluer les marges de dimensionnement. Si les points critiques du côté du propergol sont assez bien évalués de manière classique, on peut cependant souligner que le dimensionnement des marges de sécurité aux collage sont connues avec beaucoup moins de précision, et la vérification de ces marges encore plus problématiques. Il y a sans doute encore des progrès à faire dans ce domaine. Enfin, soulevons les problèmes soulevés par l'évaluation des caractéristiques en vieillissement, l'assurance de la qualité et la vérification des marges de sécurité.

3.4. Conception et dimensionnement des protections thermiques internes

Ce problème fera l'objet d'un seul papier, présenté par M. TRUCHOT (FRANCE). Cette question est loin d'être négligeable, si l'on se réfère à l'importance actuelle du poste "protection thermique" dans le devis-masse d'un propulseur moderne. Les protections thermiques internes des propulseurs utilisant des élastomères, comportent des charges soit pulvérulentes, soit fibreuses, destinées à améliorer leurs propriétés. Les propriétés requises sont : la résistance à l'ablation, le caractère isolant (faible diffusivité) et si possible, la faible densité. Là aussi, les progrès ont été spectaculaires ces dernières années. Le dimensionnement des protections thermiques est très délicat, notamment les prévisions de comportement en érosion et la part expérimentale est encore très importante.

3.5. Optimisation générale des propulseurs à poudre

Mr. TRUCHOT vous présentera également une communication sur les méthodes d'optimisation générales des propulseurs, qui ont fait l'objet de développements importants ces dernières années. En effet, l'avènement des méthodes de conception assistée par ordinateur a également eu des applications pour les propulseurs à poudre. Ces méthodes permettent de générer de manière automatique des avant-projets de propulseur, et donc de faire des choix éclairés en ce qui concerne les différentes technologies et les paramètres géométriques fondamentaux. Ces programmes comportent des modules de dimensionnement de sous-ensembles de plus en plus sophistiqués, et permettent donc d'augmenter considérablement l'aptitude des bureaux d'études à fournir rapidement des avant-projets et de multiples variantes.

4. - CONCLUSION

À l'issue de ces deux jours, nous essayerons de tirer quelques conclusions. Je suis certain que vous serez tous convaincus du degré de maturité extraordinaire atteint à ce jour par la propulsion à poudre.

Je ne tenterai pas les comparaisons classiques que l'on fait habituellement entre les divers modes de propulsion. Cependant, je voudrais souligner quelques points ayant trait à l'avenir du propergol solide.

Je suis intimement convaincu que ce mode de propulsion est encore promis à un grand avenir. Elle sera bien entendu toujours présente dans ses domaines privilégiés, à savoir les utilisations militaires, que ce soit pour les missiles tactiques ou stratégiques. Les progrès dans les performances, associés aux caractéristiques de simplicité opérationnelle, en font une technique parfaitement adaptée à ce type de besoin.

En outre, il est certain que les propergols solides n'ont pas dit leur dernier mot dans le domaine du lancement spatial, et principalement pour les étages d'appoint des gros lanceurs; en effet, il me semble que des progrès spectaculaires sont à attendre dans le domaine de la réduction des coûts.

Cependant, une actualité récente et dramatique a peut-être pu amener à douter de la fiabilité intrinsèque des propulseurs à poudre. Certains sont même tentés de conclure qu'ils sont incompatibles avec les vols spatiaux habités. Cette conclusion est bien évidemment excessive, mais ce malheureux exemple est là pour nous rappeler à la prudence. Il ne faut jamais considérer que les propulseurs à propergol solide sont des objets tellement simples que rien de vraiment dramatique ne peut arriver, surtout après une longue série de succès. Quoi qu'il en soit, les gaz de combustion des propergols sont toujours extrêmement dangereux; les masses considérables des chargements de propergols sont un facteur de risques très importants compte tenu de leur énergie spécifique très élevée. C'est pourquoi, les études liées à la sécurité (construction, justification, assurance et maintien de la sécurité) doivent toujours être menées avec la plus grande rigueur, sous l'autorité directe du responsable du programme.

Enfin, il me semble que le plus important est de bien avoir conscience du fait suivant totalement évident "a priori" : un propulseur ne peut servir qu'une seule fois, et, en conséquence, il est impossible de vérifier son bon fonctionnement en essai de recette. Toute l'assurance de la qualité réside dans les marges de dimensionnement, mais aussi dans la maîtrise des procédés de fabrication et les performances des moyens de contrôle non destructifs.

Si ces idées simples sont présentes à l'esprit de toutes les personnes impliquées dans le programme, il n'y a aucune raison pour qu'un niveau de fiabilité et de sécurité considérable ne puisse être atteint, et ceci quelle que soit la sévérité de l'objectif en terme de probabilité. Compte tenu de ces éléments, il me semble évident que l'on trouvera des propulseurs à propergol solide dans de multiples applications bien après l'an 2000.

Advances in Solid Rocket Nozzle Design and Analysis Technology in the United States Since 1970

Joseph H. Hildreth
Structural Analyst
United States Air Force Rocket Propulsion Laboratory
Edwards Air Force Base, California, USA

ABSTRACT

Since 1970 design and analysis technologies for solid rocket nozzles in the United States have experienced significant changes. These changes have been dictated primarily by increasingly severe operating environments. To a smaller but still significant degree, these changes have also been caused by outside influences. The environmental hazards of using materials incorporating asbestos is one example of these outside influences. This paper examines the evolution of the nozzle design and analysis in the US over the past decade. The discussion begins with a brief summary of generalized design requirements and follows with a description of the design evolution from tungsten and graphite based designs to the current carbon-carbon designs. The main causes for the incorporation of new technologies in the designs are identified.

A modestly technical description of the analysis processes that are employed in the design cycle is given. The portions of the analysis activities where increased technology has been incorporated are identified as well as the current trends for improved capabilities. The verification of the analysis procedures is a vital aspect of improving the analysis capabilities. The paper concludes with a description of some of the activities which have occurred to demonstrate the validity of the new analysis technology. These activities include code versus code comparisons as well as code versus laboratory measurement efforts. The code versus measurement efforts include investigations into threaded interfaces between the throat and exit cone parts and the behavior of carbon-carbon involute exit cones subjected to multiaxial loads.

INTRODUCTION

The technologies used in the design and development of solid rocket nozzles have been substantially improved over the last decade. The areas of improvement include materials, analysis techniques, testing techniques for measurement of material properties, and supporting computer technology. The advances in these technologies have made it possible to develop nozzles capable of surviving the more severe operating environments generated by current high performance motors. Conversely, these improvements also permit us to utilize the more established approaches more efficiently and with more confidence. The evolving technologies are based primarily on the advances in fiber reinforced carbon composite materials, generally referred to as carbon-carbon materials, but these technologies have also had a significant impact on our capacity to make use of the various phenolic nozzle materials as well.

The advances in technology are driven by the ever increasing demands of those who set the mission requirements for a particular system. The demands on solid rocket nozzle designs fall under two major headings; Payload and Range (or Delta V in the case of space motors). Air launch designs are also driven by a requirement for low observability, for example, minimum radar cross section and infrared signature. Another global requirement for the design of any nozzle is the need for high reliability. From these requirements, a number of additional design requirements begin to appear depending upon how the vehicle is sized and its specific mission, for example, motor operation time, overall vehicle length constraints, directional control of the vehicle (spin stabilized or thrust vector control), and overall system cost. Generalized design requirements for booster, space, and air launch systems are summarized in the following table:

TABLE 1
GENERALIZED NOZZLE DESIGN REQUIREMENTS

	<u>Booster</u>	<u>Space</u>	<u>Air Launch</u>
Burn Time (seconds)	120	120	< 20
Erosion (mils/sec)	15-20	15	< 15
Expansion Ratio	10	100+	10-20
TVC	Sometimes	Sometimes	Sometimes
Vehicle Length (relative importance)	Moderate	Moderate	Moderate
Nozzle Weight (relative importance)	Moderate	Moderate-High	Moderate-Low
Cost (relative importance)	Moderate	Low	High
Production Time	Low	Low	Moderate
Reliability	High	High	High

Although they are not mission related requirements, environmental considerations have played a role in nozzle design. Materials containing asbestos, such as adhesives and phenolic insulators, are being eliminated due to health hazards to the manufacturers. Similarly, other materials have changed somewhat because of environmental restrictions on waste products produced during their manufacture.

The items listed in Table 1 have a significant impact upon the technologies to be considered for a particular design and thus upon the design techniques that must be used in the design process. For booster and space motor applications, the requirements on burn time, erosion, and, to some extent, TVC have greatly impacted the forward region of the nozzle. This is particularly true for the throat and the approach region to the throat. The nozzle weight and expansion ratio requirements have produced substantial changes in the exit cone. These requirements have resulted in the need to use very thin walled constructions that do not require a surrounding structure to support the mechanical loads. In the air launch arena, the geometry of the nozzle has not been changed as drastically as have space nozzle designs, but the materials selection has been significantly affected. The design considerations of burn time, pulsed and nonpulsed operation, and production time and cost result in constant trade-offs between materials. For example, low cost and rapidly producible materials generally do not perform very well in terms of erosion performance. The increased thermal loads occurring in pulsed operation have dictated the use of carbon-carbon materials in the throat.

DESIGN HISTORY

Over the past decade, the space nozzles have evolved from all graphite and phenolic structures to the use of tungsten or molybdenum throats surrounded by graphite and phenolic to throats of pyrolytic graphite washers surrounded by graphite and phenolics, finally, to a design consisting of a single piece of carbon-carbon for the throat/entrance, and either an all phenolic or a carbon-carbon exit cone. Booster designs, on the other hand, have changed very little. The design evolution for air launch nozzles has been very similar to that of the space nozzles. The air launched nozzles have progressed from tungsten throats to pyrolytic graphite washers and, most recently, to 3 directional and 4 directional carbon-carbon inserts for the throat. Materials surrounding the throat insert consist of tape wrapped ablatives and monolithic graphites. Exit cones for air launched nozzles are typically tape wrapped phenolics.

The design trends for nozzles are illustrated in Figures 1 through 6. Figure 1 is a conceptual drawing of an early 70's booster nozzle. The significant feature of this design is that all of the flame side parts are tape wrapped phenolics. Carbon and graphite cloth phenolic were the most common of these. The exit cone required a metal shell for structural support because the charring phenolic materials had insufficient strength to withstand the applied loads. Consequently, additional insulative material had to be added to keep the metal shell from melting. In the mid 70's, space nozzles incorporated a pyrolytic graphite washer pack in the throat and a low density carbon phenolic exit cone liner to reduce weight. This design represented a significant increase in the severity of the operating environment over a phenolic based design. The use of the pyrolytic graphite material in the throat permitted operating in a more severe environment while maintaining a reasonable throat erosion rate. On the negative side, these throat packs experienced the formation of rather large steps and gaps along the nozzle surface. These irregularities were caused by enhanced erosion at the interfaces between individual washers and differential erosion rates between the washer pack and the surrounding materials.

The design shown in Figure 2 approached a new generation in nozzle design beyond the technology of the space nozzle designs in the mid 70's. This design retains the pyrolytic graphite washer pack in the throat to minimize the throat erosion, but a single forward and aft piece of carbon-carbon material was used for throat retention. Additionally, the exit cone was made of a carbon-carbon involute material instead of an ablative. This meant that the exit cone no longer required a structural shell. A significant weight savings was realized because the metal shell was eliminated and the exit cone liner was much thinner. Some back surface insulation was still required to protect equipment surrounding the nozzle, but this was satisfied with the use of a light weight graphite felt. The nozzle shown in Figure 3 represents another major step forward. This nozzle uses a one piece 3 directional carbon-carbon throat and entrance piece, referred to as the ITE, to minimize the number of components in the design.

A similar evolutionary process for air launch nozzles is shown in Figures 4 through 6. The nozzle in Figure 4 represents a typical air launch configuration from the mid 1970's. The inlet and exit materials are carbon phenolics. The throat region is assembled from a tungsten throat piece surrounded by monolithic graphite. The entire structure is surrounded by a metal shell which supplies all of the structural support for the nozzle. Figure 5 shows a design from the late 70's. This design incorporates a pyrolytic graphite throat pack surrounded by phenolics and bulk graphite. The pyrolytic graphite washers reduced the erosion in the throat of the air launched design, but incurred some of the same penalty as the space nozzles due to the formation of relatively large steps and gaps. Figure 6 is a more modern design incorporating a carbon-carbon throat piece which provides better erosion performance and results in fewer parts. The thermal loads on the throat during pulse motor operation require the use of a carbon-carbon material for survival.

STRUCTURAL ANALYSIS TECHNOLOGY

The evolution in the nozzle designs has required a similar change in the design and analysis technologies. As the requirements have become more severe, the analytical methods have become more complex, and the area of analytical emphasis has changed. The all-ablative designs, such as in Figure 1, are critical in terms of the amount of erosion and the char depth. Char refers to the phase change in the material when the temperature has reached the point where the phenolic resin pyrolyzes. A great deal of effort was expended to understand the materials' thermochemistry so that the amount of erosion and the char depth could be determined prior to testing. The results of these efforts were subsequently

incorporated into the analysis techniques. With the appearance of pyrolytic graphite washers, a new emphasis came into being. Pyrolytic graphite has a greatly increased resistance to erosion compared to the ablative materials. This produced a substantial differential in the eroded surface across material boundaries and produced a highly irregular surface comprised of steps and gaps between components. As a result, a significant effort was undertaken to determine the effects of these steps and gaps on the efficiency of the nozzle and structural integrity. Pyrolytic graphite is also highly anisotropic in strength and modulus. This severely challenged the structural analysis techniques.

The search for a solution to the performance losses caused by the steps and gaps led to the use of more erosion-resistant materials to surround the washer throat packs. Figure 3 shows a design using both a 3 directional carbon-carbon material and a 2 directional carbon-carbon involute material to control the amount of erosion. At this same time, the carbon-carbon involute exit cone made its debut. These materials produced a new emphasis on the analytical technology. The 3 directional carbon-carbon materials experienced most of their difficulties during processing, so many of the efforts with 3 directional materials were focused on processing issues, but not necessarily from an analytical view point. Most of these efforts were approached empirically. The 2 directional involute materials represented an analytical challenge which had not been addressed previously. This was due to the unique torsional displacement response to even axisymmetric loads on the exit cone such as internal pressure. The standard axisymmetric formulations of commonly used computer programs could not account for this and were in substantial error predicting stresses and strains. After the space nozzle designs progressed to a configuration such as in Figure 3, the concern over erosion effectively disappeared. The 3 directional and 2 directional carbon-carbon erosion rates, at the expansion ratio where the materials interface, are similar enough that significant steps do not form. Also, since the entrance and throat are now a single piece of material, no steps form here either. This greatly reduced the analytical difficulties relating to erosion prediction. However, the design and analysis tasks were complicated due to the presence of a threaded interface between the ITE and exit cone. In the next several paragraphs, the capabilities being used in the various computer tools will be described.

The structural assessment of a new nozzle design must consider a number of issues which will determine the approach that has to be used. In addition to the environmental loads, temperature and pressure, these issues include interfaces between materials, the specific materials to be used, and operational considerations such as the requirement for thrust vector control (TVC). Nearly all of the nozzle designs produced over the past several years have been designed assuming the problem to be strictly axisymmetric. These methods have been shown to be incorrect for involute exit cones and are obviously incorrect for loads and boundary conditions that are not axisymmetric, as in the case of a vectored nozzle. The need for higher performance requires that the designs be more efficient with the use of materials which, in turn, requires that the design and analysis methods be much more accurate. Three dimensional analysis approaches are being used more often in order to achieve the accuracy. The most obvious example of this is the analysis approach to the involute exit cone that has evolved over the last five or six years. The involute exit cone will twist under an internal pressure load causing the problem to be 3 dimensional. Until fairly recently it was believed that an axisymmetric analysis was sufficient. It has now been demonstrated that, not only are the results of an axisymmetric analysis incorrect in magnitude, they are frequently incorrect in type, predicting compression instead of tension or vice versa. Figure 7 is a plot of the axial stress distribution through the thickness of the part from a representative structural analysis of an involute exit cone. This analysis was conducted using an axisymmetric approach and a 3 dimensional approach. It is clear from this figure that the use of an improper model can generate very wrong answers. This realization led to a series of programs that resulted in a 3 dimensional finite element model which properly accounts for the material orientation angles and the torsional behavior of an involute part.

The analysis of a nozzle in a vectored condition is also a 3 dimensional problem which is normally treated using an axisymmetric model. Typically, this problem is addressed by performing two or three different axisymmetric analyses. One model is used to investigate the unvectored or normal nozzle position, a second model to incorporate the loads seen by one "side" of the vectored nozzle in the plane of vectoring, and a third model to investigate the other "side" of the vectored nozzle. These models of the vectored nozzle are axisymmetric approximations of real 3 dimensional problem, and the intent is to bracket the actual conditions. If the analyses can show that the nozzle will survive at these limits, then the nozzle is considered structurally sound. As will be discussed later, determining the gas flow conditions in the nozzle is an important part of the analysis procedures. At this time, a 3 dimensional flow analysis methodology does not exist that can model the flow conditions in appropriate detail and still fit on existing computer facilities. Therefore, this part of the analysis also involves a substantial amount of approximation with one dimensional and axisymmetric tools.

Another issue that has received a significant amount of attention is the interfaces between dissimilar materials, particularly the threaded interfaces. The design depicted in Figure 3 is relatively simple in terms of the configuration of the flame surface components. This simplicity is achieved by using a threaded attachment between the ITE and exit cone. The integrity of the threaded interface in the pictured design is critical, particularly so since it is a vectorable design and the vectoring loads must be transferred through the threaded joint. Only recently have there been serious efforts to correctly model the joint. Most often the thread area is modeled as a continuous material with estimated properties to account for all of the phenomena that occur. Thread shear tests would then be run at room temperature to verify the structural strength of the interface. Figure 8 shows a finite element model that uses this approach to modeling the thread response. Figure 9 is an enlargement of the thread area in Figure 8 with the "thread" elements shaded. An accurate approach to model the behavior of the threaded joint requires a nonlinear solution that can account for the opening and closing of gaps between the dissimilar materials as well as the frictional loads that are developed, see Figure 10. Additionally, since the joint is frequently filled with adhesive, the effects of the adhesive as it degrades with temperature must also be included. Due to the complexity of the model required to capture these highly nonlinear responses, this type of analysis is generally performed using only a portion of the overall nozzle structure, while the analysis of the total nozzle assembly

incorporates a crude approximation on the thread area.

Excluding the metal components of the nozzle, the materials used in current nozzle designs are orthotropic in behavior. This means that there are three mutually perpendicular material directions. Depending upon the specific material, the material properties can be significantly different in all three directions. In addition, the effective properties in a single direction are different depending upon whether the loading is tensile or compressive (see Figure 11) and upon the temperature of the material at a particular location in the nozzle. Generally speaking, all of the materials exhibit some degree of nonlinearity in their stress-strain responses. The typical structural analysis code stores the material property information in a series of tables based on the temperature at which the properties were measured. Figure 12 illustrates these data in terms of the stress-strain curves. The code accounts for the temperature dependence by linearly interpolating between the values stored in the tables, the circled temperatures in Figure 12. Nearly all of the codes model the difference in the properties due to the type of loading with a bilinear curve fit to the data, Figure 11. Some codes will also approximate the nonlinearity of the tension only and compression only portions of the curve with an additional bilinear fit, Figure 13. More recently, with the trend toward using 3 dimensional analyses, the nonlinear response is modelled as an actual curve. There are two approaches to modeling the actual curve. The first is to input the stress-strain coordinates explicitly using a sufficient number of coordinates to describe the actual curve. This is the simplest approach to implement and is being used. However, this approach requires a significant amount of data to properly model the response since the program will linearly interpolate between the input values. A scattered set of data will cause large flat spots along the curve and produce a bad model. The second approach is to fit some form of nonlinear curve through the measured data and then use this equation for the required information. This approach is much more difficult to implement and the results are dependent upon the quality of the curve fit to the actual response. The Jones-Nelson-Morgan model (Ref. 1) is an example of the latter method. This model fits a curve of the form:

$$\text{Property} = A(1 - BU^C)$$

through the measured data, Figure 14. In this equation A, B, and C are curve fit coefficients and U is the strain energy of the material. "Property" is the value of the material property for a given value of U. This represents a state variable approach since the variable U is the strain energy of the material (energy stored in the body due to deformation). This method requires transitioning to a different type of curve, usually linear, at some point because the form of the curve fit does not prevent the model from going negative instead of reaching a limiting value. If the fit is to one of the material's moduli, then the implied stress-strain curve will appear as shown in Figure 15. In this case, the model transitions into a straight line with a positive slope.

The goal of the analyses is to determine if the design will survive before the hardware is actually built. To assess survivability, the analysis results are judged against a predetermined failure criteria. For the metal parts this does not present a problem, a Von Mises or Maximum Stress or Maximum Strain criteria seems to work quite well, particularly if the metal part is considered to fail when it reaches its yield point. However, a failure criterion for carbon-carbon materials has yet to be validated. The common practice is to use a maximum stress or strain based criterion or to use some form of a polynomial curve fit through measured strength data. One approach to a polynomial curve fit is the Tsai-Wu formulation or some variation of it (Ref. 2). This is a tensor equation involving second order terms of the form:

$$F_i \sigma_i + F_{ij} \sigma_i \sigma_j = 1 \quad i, j = 1, 2, \dots, 6$$

Figure 16 represents a hypothetical Tsai-Wu curve in the sigma 1, sigma 2 plane. Determining the coefficients, F, in this equation is difficult if not impossible in general, therefore, the form is typically limited to two directions (i, j = 1, 2). The coefficients can then be related to the various material strengths in the 1, 2 plane. Recently, a significant effort has been expended to develop a criterion that accounts for the interaction between simultaneous loads in several directions on the ultimate load carrying capability for 2D involute exit cones. This effort involved a series of flat panel, cylinder, and conical specimens loaded uniaxially and multiaxially to develop the data to define the failure surface. Some test results from this effort will be discussed later.

THEMAL ANALYSIS TECHNOLOGY

The other half of the design/analysis effort is the prediction of the thermal behavior of the nozzle. The objectives of the thermal analyses are to determine the in-depth temperature throughout the nozzle, to determine the material recession, and to define the surface pressures, all as functions of the burn time of the motor. This information is used separately by the designer to assess the insulative qualities of the nozzle for the protection of the low temperature parts and to confirm that there is sufficient material remaining at the end of motor operation to maintain nozzle integrity. In addition, this information serves as input data to the structural analyses to predict the thermo/mechanical response of the design and evaluate the survivability of the nozzle under the imposed thermal and mechanical loads. The thermal analysis techniques have undergone an evolution similar to the structural analysis methods. The more current approaches are gravitating toward 3 dimensional formulations to provide the sophistication necessary to address all of the appropriate analysis issues.

The thermal analysis methodology consists of a number of steps, each requiring its own approach and consequently its own computer code. The procedures perform a series of chemical and energy balances beginning with the free stream characteristics in the motor chamber, progressing into supersonic flow, then determining the momentum and energy transfer through the boundary layer and finally considering the

conduction of the thermal energy through the various materials of the nozzle. The various methodologies can consider conduction, convection, radiation, thermally degrading materials, mass removal, two-phase gas kinetics, and particle impact.

The analyses are generally performed as a series of sequential steps. Each step develops information that becomes part of the input to the next step. The process begins with the free stream calculations. These calculations use the propellant formulation, heats of formation, and the motor chamber conditions and produce the velocity, pressure, and temperature profiles at the outer edge of the boundary layer down the length of the nozzle. The first analytical approaches to this problem used a 1D isentropic expansion model. This approach is applicable only in the supersonic region of the nozzle and ignores any two dimensional effects in the flow field. The most recent development activities involve this part of the thermal analysis cycle. The use of aluminized propellants result in the presence of aluminum droplets in the exhaust gas, commonly referred to as two-phase flow. The early isentropic flow analyses ignored the presence of these droplets. Current methods have included the effects of two-phase flow into their methodologies and have extended the analysis model to include the subsonic region upstream of the throat as well as the effects of submergence into the motor chamber.

The next step in the thermal analysis procedures considers the effects of the boundary layer. Using the velocities, pressures, and temperatures previously calculated, this step determines the heat and mass transfer coefficients at specific points along the nozzle surface. The early methodologies for these calculations assumed that the boundary layer formed on a smooth wall. It has since been shown that the surface roughness of the nozzle wall has a significant effect in the form of an augmentation of the heat transfer to the wall. In the newer approaches, methods have been implemented to account for the surface roughness, transpiration, and acceleration as well as the boundary layer properties. At this point the chemical kinetics on the nozzle surface must be determined. The computerized methods that accomplish this are based on a predetermined number of chemical reactions such as the reaction between carbon and water at high temperature to yield carbon monoxide and hydrogen. The accuracy of the results of the kinetic calculations are thus dependent upon the selection of reactions built into the computer codes. The selected reactions have had to change over time because of the use of different materials for nozzle components and the increase in surface temperatures (greater than 5500°R) due to the use of hotter burning propellants. If the nozzle design incorporates ablative materials, either on the surface or as backup insulators, the release of the pyrolysis gases and the subsequent change in the material's composition and thermal properties must also be taken into account.

Once all of the free stream, boundary layer, and surface calculations are made, the prediction of the in-depth temperatures can be made. All of the previous calculations develop information that serve as input data to the in-depth temperature predictions and establish the boundary conditions for the problem. Early on, all of the thermal analysis methods were one dimensional. This required the analyst to perform the calculations at a number of different axial stations and manually smooth the data between the analysis points. More recently, some of these procedures have been expanded to a two dimensional formulation. Now, in the case of the in-depth temperature calculations, the procedures are gravitating toward 3 dimensional techniques. In addition, the in-depth temperature calculations, which were traditionally based on finite difference solution methods, are being reformulated using finite element methods. Using the finite element formulations makes the transfer of data between the thermal analysis and the structural analysis much easier and more accurate. The finite difference approaches used geometry models that were optimized for that type of solution and did not have as much generality in terms of the applied boundary conditions. The finite element formulations for the thermal analyses permit the use of a geometry model that is exactly the same as the model used in the structural analyses without significantly impacting the accuracy of the thermal calculations.

While it is not necessarily obvious, another rapidly developing technology that has had a major effect on all of the nozzle analysis capabilities is the improvement in computational capacity that has happened over the last decade. Indeed, it has been mainly due to the development of the 32 bit super mini computers that has allowed us to incorporate the increased complexity into the analysis approaches. Also, due to the development of these computers, the industry has been able to develop the computer aided design and modeling (CAD/CAM) software that permits the human mind to deal effectively with the magnitude of the input and output data for the analyses. While the computer technology has made huge advances that allow more accurate and complex analyses to be attempted, further advances are needed to permit solving the current problems. For example, significant increases in machine capacity and speed are required to model the 3 dimensional flow problem and to sufficiently model the throat region of the nozzle as an integral part of the entire nozzle assembly.

VERIFICATION

Development of more capable analytical techniques is important. However, these new or improved techniques must be verified before much faith can be placed in the results they produce. The most positive way of verifying the analytical methods is to compare the predictions directly to measured data. This can only be accomplished for cases where accurate measurements can be made. For instance, one cannot expect to verify high temperature strain calculations because it is nearly impossible to measure the data. Another way that some limited verification for an analysis technique can be obtained is to compare its predictions against predictions made using other analysis tools. While this does not provide assurances that the predicted numbers are realistic, it does determine how well predictions based on one computer code compare with the same predictions made with another code. The assumption that is made in using this approach is that the second code has already achieved some credibility for correctly performing the analyses. Both of these verification techniques have been used to gain confidence with a specific analysis tool.

The first example of comparing one analysis against another is shown in Figure 17. The problem is a hypothetical ITE insert subjected to a highly specialized set of boundary conditions. The purpose of

the exercise was to assess the sensitivity of the mathematical models to numerical approximations, and not to analyze an ITE subjected to realistic firing conditions. The boundary conditions for this exercise permitted formulating an exact elasticity solution to the problem, against which typical finite element solutions could be compared. Likewise, the material properties, shown in Table 2, were tailored so the exact solution was available. Figures 18 and 19 show examples of the results obtained through this exercise. Figure 18 is a plot of the circumferential stress through roughly the midplane of the model. The various data sets, A,B,C,etc., represent results submitted by several different organizations. In this figure, all analyses appear to be quite good. Figure 19 is a plot of the axial stress for this same problem, and, as can be readily seen, the various solutions do not compare nearly as well. Evaluation of the various answers showed that the main reason for the discrepancies in the results was the care given to the modeling of the traction boundary conditions. The traction conditions that were supplied with the problem description were not smooth. If the analyst was not careful, the variation in the tractions, coupled with the numerical approximations inherent in the finite element models, could produce serious problems with the solution. This exercise was a clear reminder that too much confidence is often placed in the computer to give the correct answer without applying the engineering judgement to check the results.

TABLE 2
ITE ROUND ROBIN MATERIAL PROPERTIES

Engineering Moduli	
$E_z = 105,000,000./r$ psi	$G_{rz} = 2,100,000./r$ psi
$E_\theta = 70,000,000./r$ psi	$\nu_{z\theta} = \nu_{zr} = \nu_{\theta r} = .05$
$E_r = 35,000,000./r$ psi	
Where $\nu_{ij} = -\epsilon_j/\epsilon_i$ under uniaxial stress σ_i	
and r = radial coordinate	
Free Thermal Strains	
$e_z = .0000114666 * r$	
$e_\theta = .000007 * r$	
$e_r = .000015 * r$	

Figure 20 shows the geometry for another code versus code modeling exercise that occurred recently. In this case, the problem was developed around an involute exit cone and was intended to assess the capability of the various finite element and other approaches for modeling the involute response. Figures 21 and 22 show comparisons of the results for three different modeling approaches. The dashed line in Figure 21 and the solid line in Figure 22 represent the results from a variational approach incorporating a finite difference equation solver. The open symbols in both figures are the results from a fully three dimensional finite element approach, and the remaining data came from a 2D axisymmetric approach that had been modified to account for the circumferential degree of freedom. The results from all three types of analyses agree very well. Since the 3 dimensional finite element model used in these analyses had previously achieved some credibility based on comparison with measured data, the other two models have now achieved some level of credibility as well.

Earlier, it was mentioned that the analysis methods had to be improved to properly predict the behavior of an involute exit cone. Part of that series of efforts addressed nonlinear response and multiaxial load behavior. Figures 23 and 24 show two cylinder specimens that were tested to failure under combined compression and internal pressure loads. The measured hoop stress-strain behavior for these two specimens is shown in Figure 25. These two tests were part of a test matrix to verify an improved analysis model. The predicted response using the new model is shown by the open circles connected by the solid line in the figure. As can be seen, the model's predicted behavior agrees quite well with the measured data. It is also apparent from this figure that predictions using a linear analysis methodology would be in substantial error. The argument could be raised that this is data on an involute cylinder, and that conclusions drawn from this data might not apply to actual exit cones. Figure 26 shows the test configuration for a subscale involute cone. This test setup was used to measure the room temperature response of an actual exit cone geometry under combined loads. Figure 27 shows a cone specimen that was tested to failure under combined internal pressure and axial compression. Figures 28 and 29 are plots of the measured test data for the hoop and axial directions and the pretest predicted behavior using the new model. Here, again, the correlation is quite good. It would seem safe to conclude that the new model represents a significant improvement over the previous methods. However, this level of verification is still not definitive. The model's ability to predict high temperature response remains unproven, as well as the existence of any scaling effects for full size parts.

Another important finding came from the nonlinear model development and test effort. The material properties used in these analyses were measured using specimens cut from flat panels made from the same raw materials and coprocessed with the cylinders and cones. The performance of the model to accurately predict the response of the cylinders and cones has provided some hard evidence that properties measured from flat panel specimens are, in fact, representative of the actual response of the exit cone. This is very important because property measurements using specimens excised from actual exit cones and tag end rings are questionable, due to the curvature of the specimens. It is also extremely difficult to measure the cross ply response using excised specimens due to the small radial dimension of the part. Carefully made flat panels can be constructed to provide specimens of

sufficient thickness to determine cross ply properties, and do not have any curvature to corrupt the data.

The threaded joint between the ITE and exit cone is a very important interface and the ability to analyze it is less than satisfactory. Efforts have been undertaken to understand and properly model this interface. The capability to predict the response of threaded metal parts was developed a number of years ago to address drilling technology for the oil industry. These same methods, when applied to solid rocket nozzles, do not adequately solve the problem. Research and development efforts have been sponsored to address the threaded interface for nozzles. Figure 30 shows two photoelastic specimens using two of the most commonly used thread forms for nozzles. The objective of these tests was to assess the performance of existing analysis tools for solving the nozzle thread interface problem. Figures 31 and 32 show the results of these photoelastic tests compared against the analytical predictions for both thread types. The predictions were made using three different finite element codes. These predictions are labeled as Code 1, 2, and 3 in the figures. All three of the predictions were made using an axisymmetric model. Code 1 represented the industry standard for nozzle analysis at the time. Using this approach, the threads were either ignored or, as was done for these analyses, pseudo-thread properties were fabricated to estimate the response for the thread elements.

Code 2 is a descendant of Code 1 incorporating a specialized interface element. This element is a 4 node quadrilateral element of zero width that carries only compressive and shear loads along its length. Code 3 is a general purpose three dimensional code with an axisymmetric interface capability. The interface "element" consists of two nodes, each associated with one side of the interface and an angle that represents the slope of the interface at the location of the nodes. This element carries only compressive and shear loads. From Figures 31 and 32, the predictions agree reasonably well with the photoelastic measurements. One would have hoped for better agreement because this configuration represents the "ideal" case; an isotropic, well characterized material at constant temperature. A second type of thread shear test is shown in Figure 33. This test used real nozzle materials and attempted to measure data at each thread root on the 3 directional part. Figure 34 is a plot of the room temperature strain measurements against the pretest predictions. The strain measurements were made with small gauges located at the root of each thread as indicated by the filled dots marked A1 thru A5. The predictions were made using the same codes used for the photoelastic case. The scatter in the measured data might be due in part to experimental error, but variations in the thread clearances most probably represent the largest effect. The analyses assumed that the threads were perfect thus producing a smooth variation in load. This illuminates one of the biggest challenges to accurately analyzing the behavior of the threads, how to incorporate the as-built geometry.

In a follow-on program an effort was made to determine the important mechanisms of thread behavior in carbon-carbon parts. Knowing these mechanisms, it should be possible to develop appropriate computer models that properly predict the response of the threaded interface. Part of the testing in this effort used specimens that represented segments of the cylindrical interface region. These specimens could either be curved sections, excised from the cylindrical interface, or specially machined rectangular pieces removed from the cylindrical carbon-carbon parts, see Figure 35. Either specimen represented approximately 15 degrees of the 360 degree interface. A special test fixture had to be built to test these specimens (Ref. 3). Figure 36 is a schematic of the test fixture which installs on a standard load frame. Using this specimen design allowed gathering the maximum amount of data from a limited amount of material and permitted making photographic records of the exposed face of the joint while the test was in progress. Figure 37 shows a set of these photographs for a sawtooth thread form with a 30 degree thread surface angle. Figure 38 shows the load/deflection curves for this same thread form. In this specific case the specimen included an adhesive bond that had been precharred. In Figure 39, the load/deflection curves from Figure 38 are simplified and represented by the dashed lines. The other lines in the figure represent various degrees of modification to the finite element model in an attempt to match the measured behavior. The modifications to the model were cumulative in nature and ended with the following assumptions:

1. Shear yield stress set to 500 psi,
2. As built thread engagement (use correct number of active threads),
3. ITE's shear and Young's moduli set to 60 ksi,
4. Tension side of threads assumed to be unbonded.

The order of these assumptions matches the designations Mod 1 through Mod 4 on Figure 39. The last modification caused the computer results to lie within the bounds of the initial slopes of the measured responses. It should be noted here that this modeling exercise was not intended to match the complete load/deflection curve, but instead to uncover the major influences on the thread behavior. Further analysis cases were run to capture the joint behavior after the threads became totally unbonded and could move relative to each other. To accomplish this, an average load level was chosen for total unbonding based on the measured data, the open square in Figure 40. Then different coefficients of friction were tried for the interface element input. The extension lines from the open square in Figure 40 are for friction coefficients of 0.2 and 0.5. Estimates of effective coefficients of friction were made from the measured axial and lateral loads. The calculated effective coefficients of friction ranged from 0.18 to 0.79 for the 30 degree sawtooth threads with a charred bond.

The results of the segmented thread specimen tests which are most meaningful to modeling issues indicate that:

- a) Bonding improves the load carrying capacity of the joint even after charring. For the ACME threads the increase was about a factor of 2. This means that an effective model of the joint cannot ignore the adhesive bond.
- b) The effective coefficient of friction at the interface in the presence of charred C34 cement is greater than 0.2.

SUMMARY

In summary, the design approaches for solid rocket nozzles and the analytical methods used to develop these designs have changed substantially during the past decade. Although the nozzle designs have tended to become somewhat more simplified, the demands that the design requirements place on the new nozzle designs force the use of greater analytical complexity. The nozzle designs have progressed toward minimizing the number of parts and reducing the surface erosion as much as possible. The most significant changes have been the incorporation of 3 directional carbon-carbon throats for space and air launch nozzle types, and the use of the 2D carbon-carbon involute exit cone in space nozzle designs. The continuing trend for the design of nozzles is to incorporate higher performance materials by part replacement without substantially altering the configuration. The most significant improvement in the analytical techniques is the capacity to effectively model the behavior of the involute exit cone. The current trend in nozzle analysis is to make wider use of nonlinear and 3 dimensional analytical techniques.

The work which most needs to be done to improve the nozzle design capabilities is in the area of material technology. The science and understanding of the manufacturing processes of the nozzle materials is one of the most important areas to be researched. We must understand the influences of changes in the raw materials and manufacturing processes on the ultimate performance of the nozzle part. In terms of analytical capabilities, two problems come to the forefront as the greatest challenges. One is the proper modeling of the threaded interface between the throat and exit cone. This joint is a key feature of current nozzles and must be properly designed. The second is the capability to analyze ablative materials. These materials decompose with time in the nozzle environment evolving gas and drastically changing their character in terms of thermal and mechanical response. All of these phenomena must be considered to accurately predict nozzle performance.

REFERENCES

- 1) Jones, Robert M., Mechanics of Composite Materials With Different Moduli in Tension and Compression, AFOSR TR-78-1400, July 1978.
- 2) Jones, Robert M., Mechanics of Composite Materials, McGraw-Hill, 1975, pp 76-83.
- 3) Jortner, J. and Pfeifer, W.H., "Experimental Study of Strength, Deformation, and Failure Modes of Threaded Joints Between 2D and 3D Carbon-Carbons", ASME Booklet AD-11, 1986.

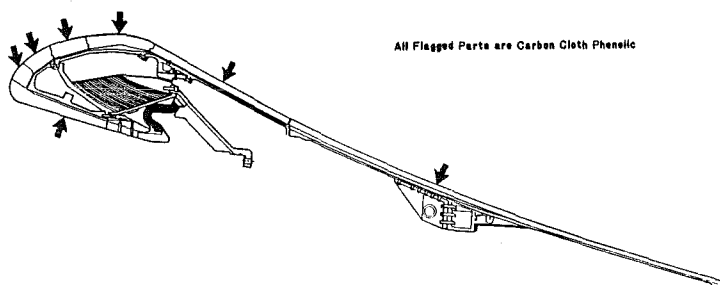


Fig. 1. Modern phenolic based nozzle.

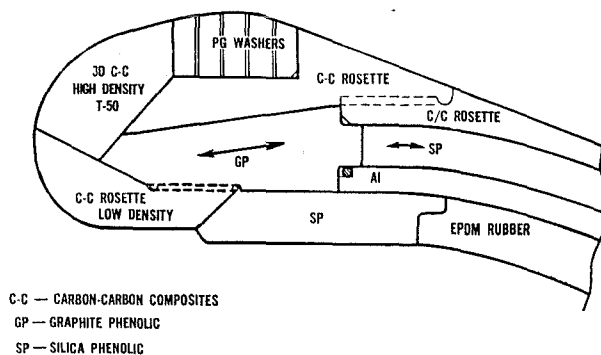


Fig. 2. Space nozzle - late 1970's.

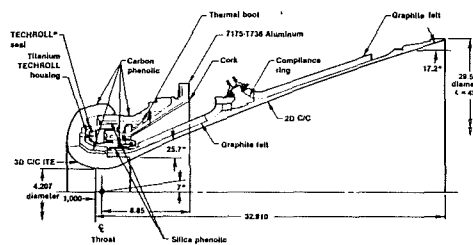


Fig. 3. Space nozzle - early 1980's.

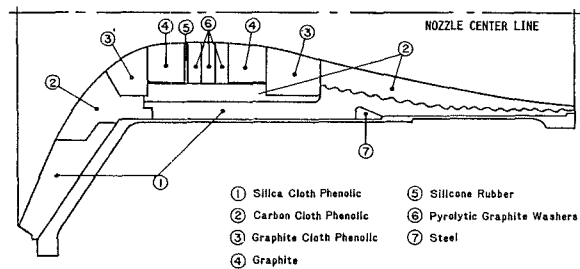


Fig. 4. Air launch nozzle - mid 1970's.

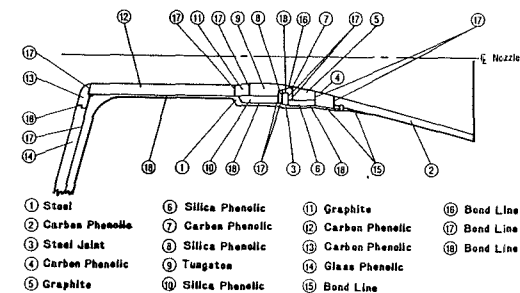


Fig. 5. Air launch nozzle - late 1970's.

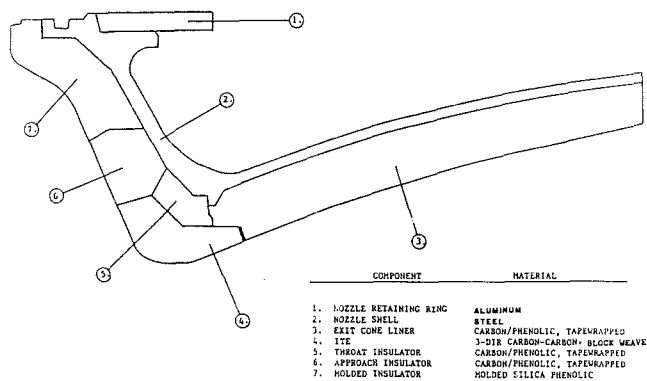


Fig. 6. Air launch nozzle - early 1980's.

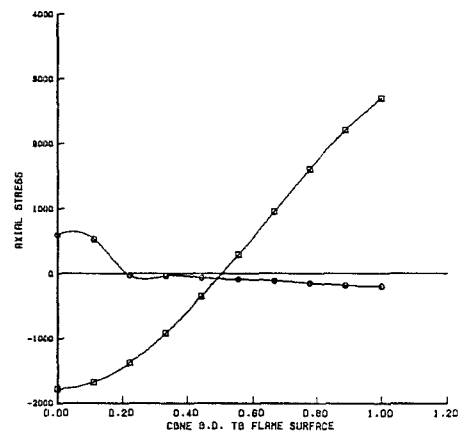


Fig. 7. Comparison of results between involute and axisymmetric models.

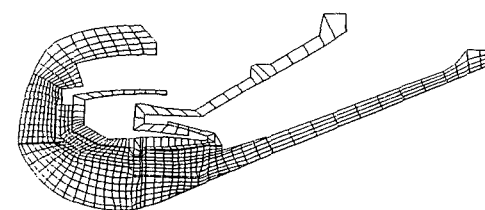


Fig. 8. Typical finite element model to analyze nozzle assembly.

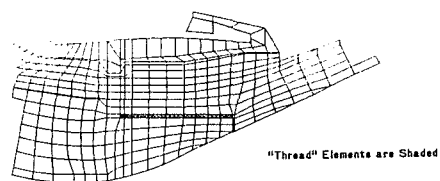


Fig. 9. Enlargement of pseudo thread-elements in nozzle assembly model.

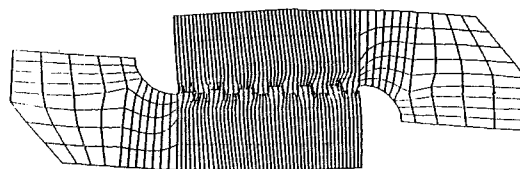


Fig. 10. Deformed geometry for detailed thread analysis model.

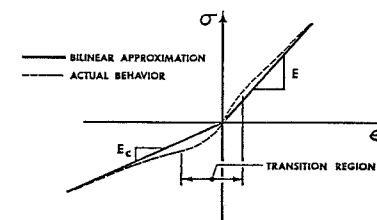


Fig. 11. Bilinear material model versus actual stress-strain behavior.

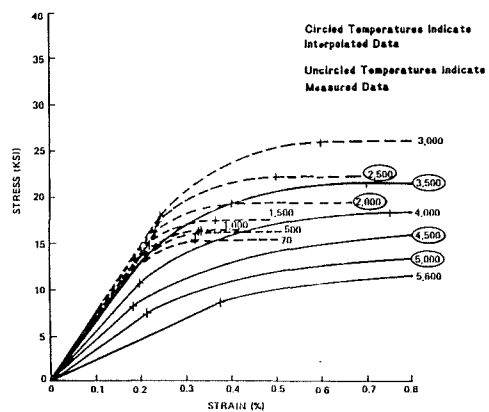


Fig. 12. Typical stress-strain versus temperature data.

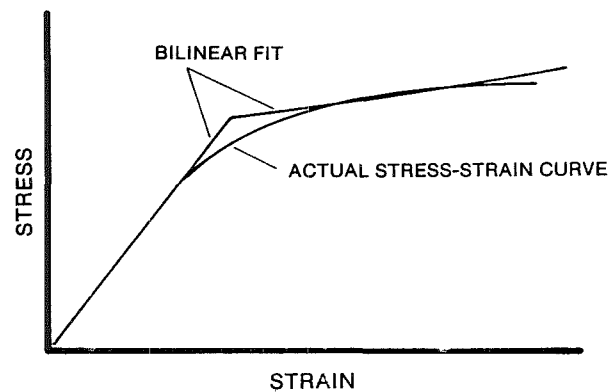


Fig. 13. Bilinear fit to tension only stress-strain curve.

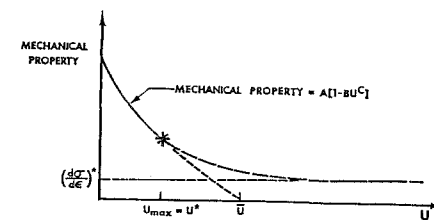
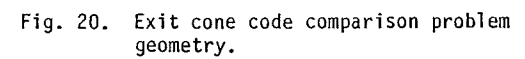
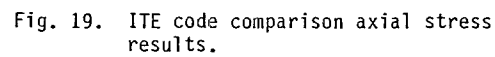
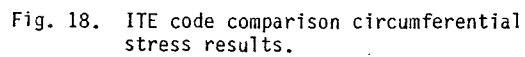
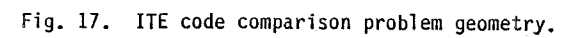
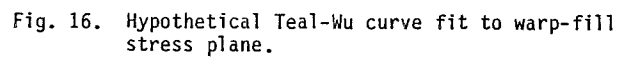
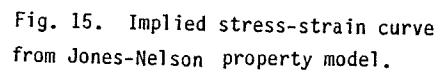


Fig. 14. Jones-Nelson curve fit to typical mechanical property.



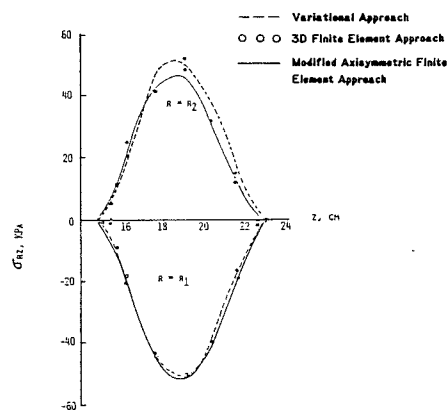


Fig. 21. Exit cone code comparison R-Z shear stress results.

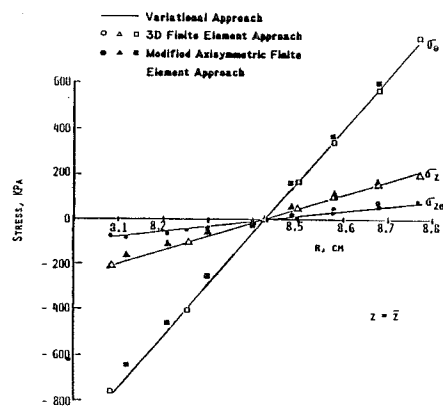


Fig. 22. Exit cone code comparison mid-section stresses.

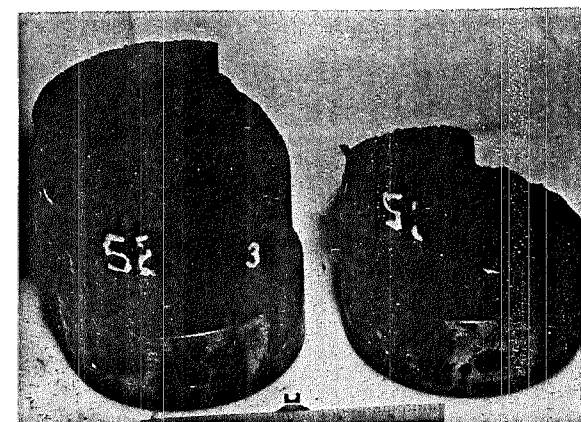


Fig. 23. Involute cylinder (#585) failed under biaxial loads (axial compression and internal pressure).

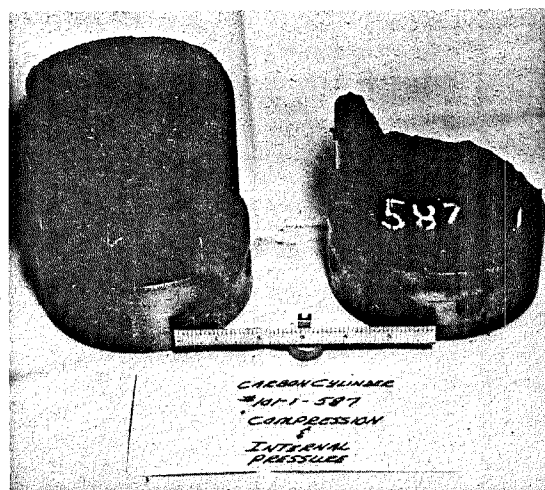


Fig. 24. Involute cylinder (#587) failed under biaxial loads (axial compression and internal pressure).

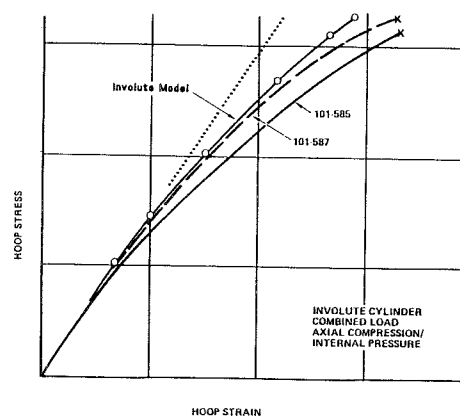


Fig. 25. Measured versus predicted response for cylinders under biaxial loads.

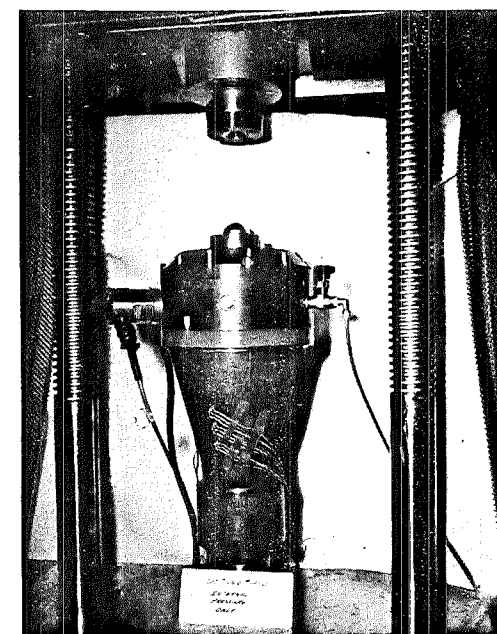


Fig. 26. Involute core specimen for biaxial load test.

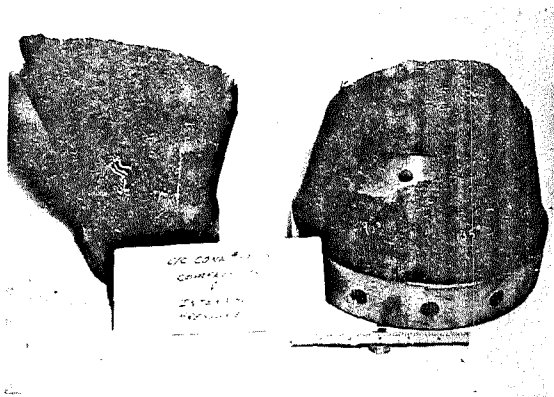


Fig. 27. Failed cone after biaxial test.

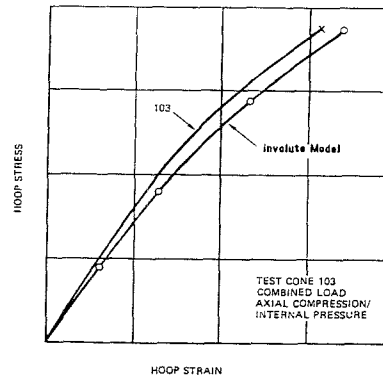


Fig. 28. Measured versus predicted hoop response for cone under biaxial loads

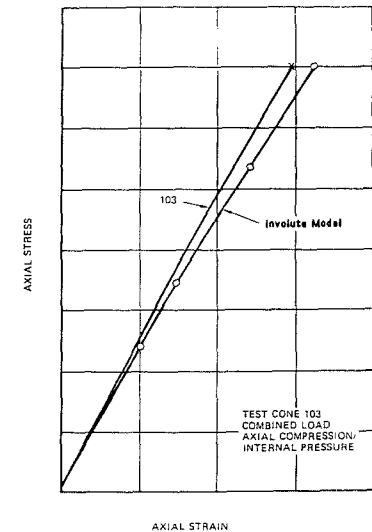


Fig. 29. Measured versus predicted axial response for cone under biaxial loads.

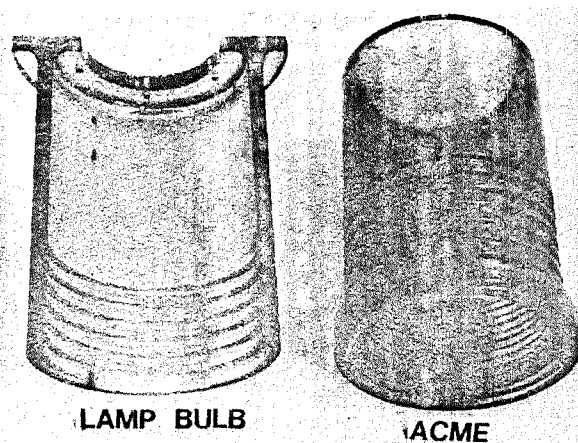


Fig. 30. Photoelastic specimens for two thread forms.

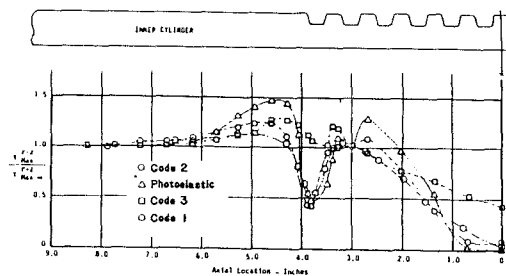


Fig. 31. Measured versus predicted results for ACME thread form.

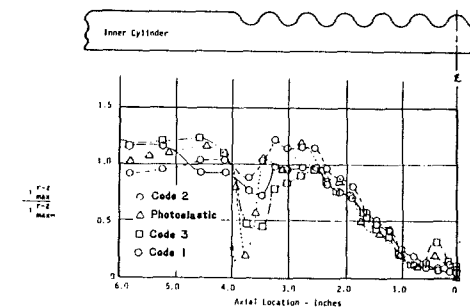


Fig. 32. Measured versus predicted results for lamp bulb thread form.

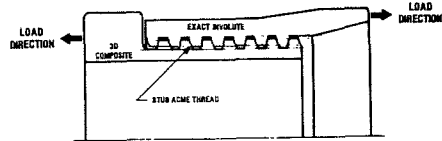


Fig. 33. All carbon-carbon thread test specimen.

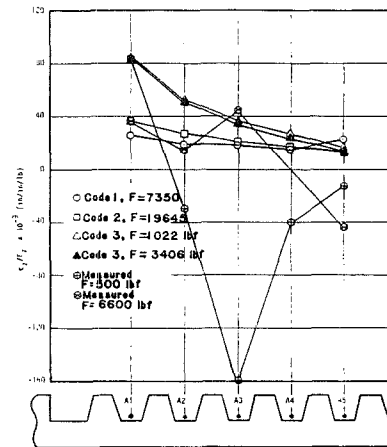


Fig. 34. Measured versus predicted response in thread roots.

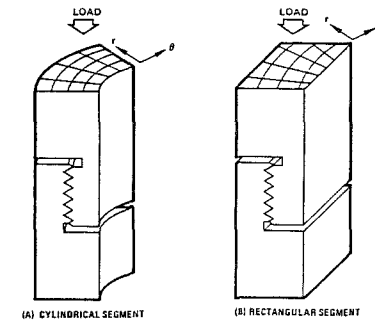


Fig. 35. Segment specimens for testing threaded joint configurations.

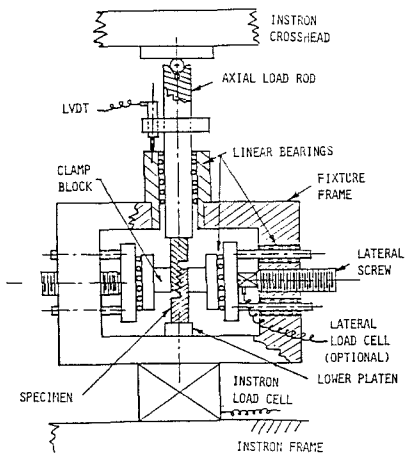


Fig. 36. Test fixture for thread segment specimens.

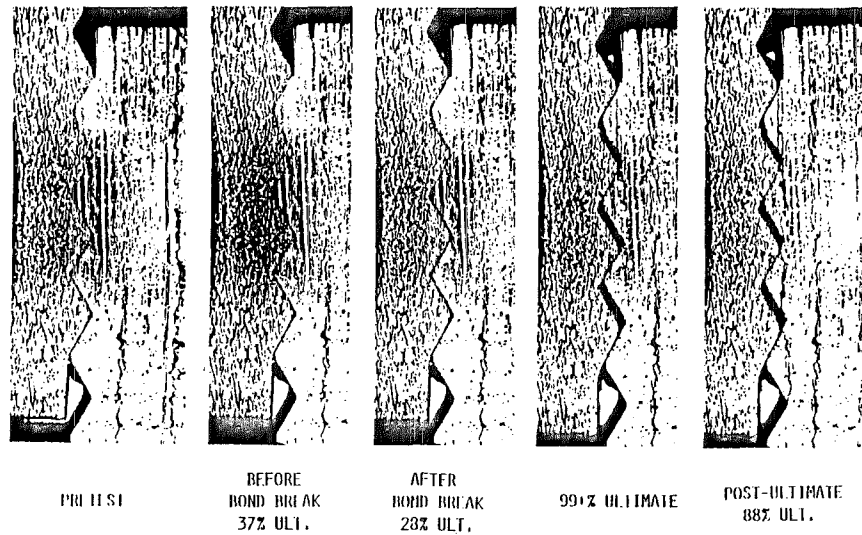


Fig. 37. Photographs of deformations for 30 degree V thread test.

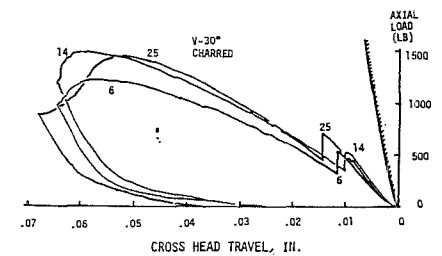


Fig. 38. Load-displacement results for 30 degree V thread tests.

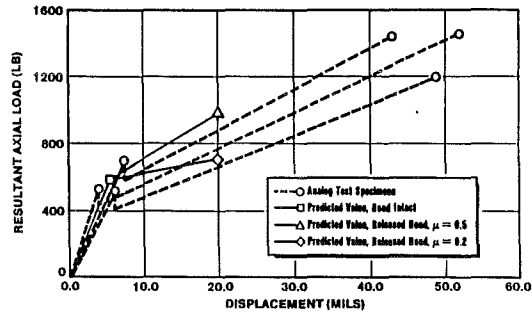


Fig. 40. Measured versus calculated response for model with friction.

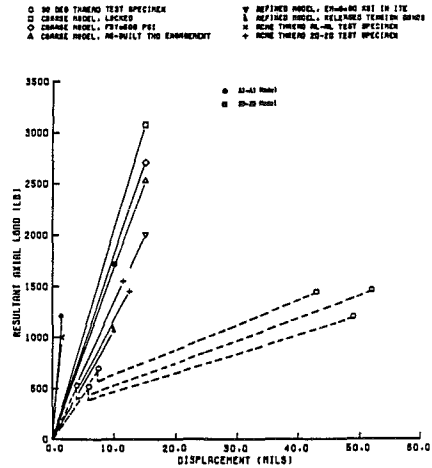


Fig. 39. Measured versus calculated response for various model assumptions.

DESIGN AND ANALYSIS OF SOLID ROCKET MOTOR NOZZLE

by

Mr A.Truchot
Agence Spatiale Européenne
Division STS-AR
8-10, rue Mario Nikis
75738 Paris Cedex 15
France

ABSTRACT

The objective of this paper is to present the different methods used to design and analyse solid rocket motor nozzles. In a preliminary phase, the typical requirements and parameters required to design a nozzle are discussed. Afterwards the general process of the design is detailed : nozzle configuration, aerodynamic contour design, selection and sizing of liners and insulators, etc... In a second step, the different systems used to control the motor thrust or to improve the performance, such as extendible exit cone, are presented. To conclude the presentation, the different steps of the nozzle analysis are presented. For each step (aerodynamic, thermal and structural) the different computer programs used are presented (principle, possibilities, limitations).

1. - INTRODUCTION

The main function of a solid rocket motor nozzle is to channel and control expansion of hot gases coming from the chamber, thus creating the motor thrust.

The scale and complexity of a nozzle are dependant on the application of the motor (ballistic, space or tactical) and the level of performance required. Thus for tactical applications, with low burning time and reduced scale, the nozzle is often a simple device made up of metal or classical reinforced plastic. However for ballistic or space applications, the scale and complexity are of more importance due to the greater dimensions (greater than one meter), the more important burning time (1 to 2 minutes) and the higher level of performance required.

This paper deals mainly with large solid rocket motor nozzles ; however some examples of tactical missile applications will be presented.

2. - GENERAL REQUIREMENTS

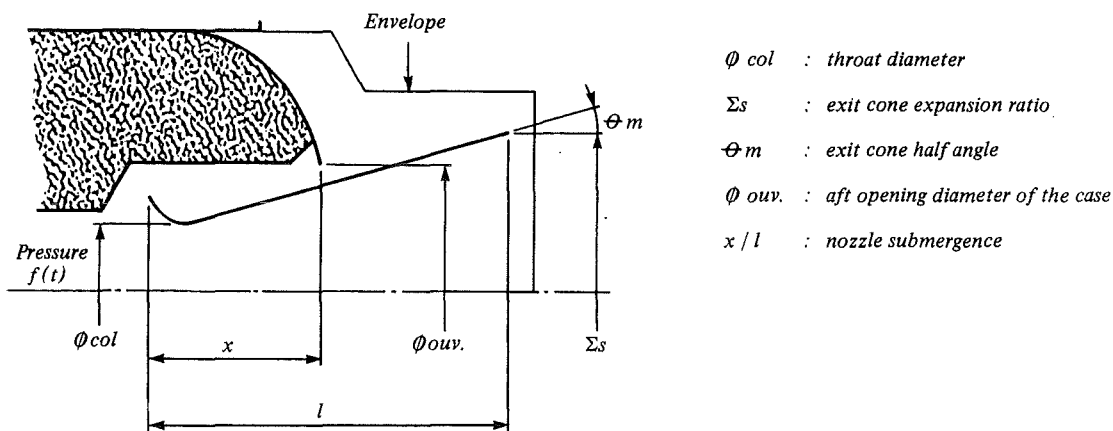


Fig. 1 - NOZZLE PARAMETERS

In order to design a nozzle, a certain number of specific parameters are required such as throat diameter, exit cone expansion ratio and half angle, aft opening diameter of the case and nozzle submergence. A great number of these parameters are a result of the overall optimization of the motor based upon the general requirements of the propulsion system. Some of these parameters are left to the discretion of the designer or imposed by the storage or operating environment. These different requirements and parameters are summarized below.

Operating conditions (pressure, burn time) :

The mechanical design is usually performed with the maximum expected operating pressure and the thermal design with the maximum burn time.

Throat area - Throat area variation :

The throat area variation can be compensated by the grain design. The throat erosion is a function of several parameters such as chamber pressure, burn time, nozzle configuration and grain design. On this point several iterations between grain design and nozzle design may be required.

Propellant type :

The characteristics of the propellant such as combustion temperature, erosion and oxidation properties are of great importance to select nozzle materials (liners and insulators).

Envelope limit :

The envelope limit is usually a vehicle designer requirement. In some systems, the envelope can be restricted by guidance or navigation equipment.

Exit cone expansion ratio :

The optimum exit cone expansion ratio is dependant on the external pressure. The optimum efficiency of the nozzle is obtained with a static pressure at the exit plane equal to the external pressure. Thus for first stage, expansion ratios from 7 to 15 are usual. Expansion ratios from 15 to 80 may be used for upper stage or high altitude vehicles.

Nozzle submergence :

For a same exit cone expansion ratio, an increase of the submergence allows a decrease of the external part of the nozzle, thus leading to an improvement of performance for limited length motors. The nozzle submergence is usually a result of the overall optimization of the motor.

Thrust vector control :

The thrust vector angle is a vehicle designer requirement. The most usual device currently used for ballistic or space applications is the flexible bearing allowing thrust vector angles from 3 to 15 degrees.

Case interface :

The motor inert weight is minimized when the aft opening diameter of the case is minimum. Sometimes a minimum diameter may be required in order to cast the propellant into the motor case.

Performance - Cost - Reliability - Development time :

Nozzle technologies, such as materials or thrust vector control systems are functions of the performance, cost, reliability and development time objectives. These considerations can restrict the use of certain efficient technologies, because they are not sufficiently demonstrated.

Environment - Storage - Life time :

These different considerations must be taken into account for the materials selection ; thus, certain elastomers are incompatible with a low storage temperature.

3. - NOZZLE DESIGN

3.1. Configuration

The nozzle can be external to the motor or submerged into the combustion chamber :

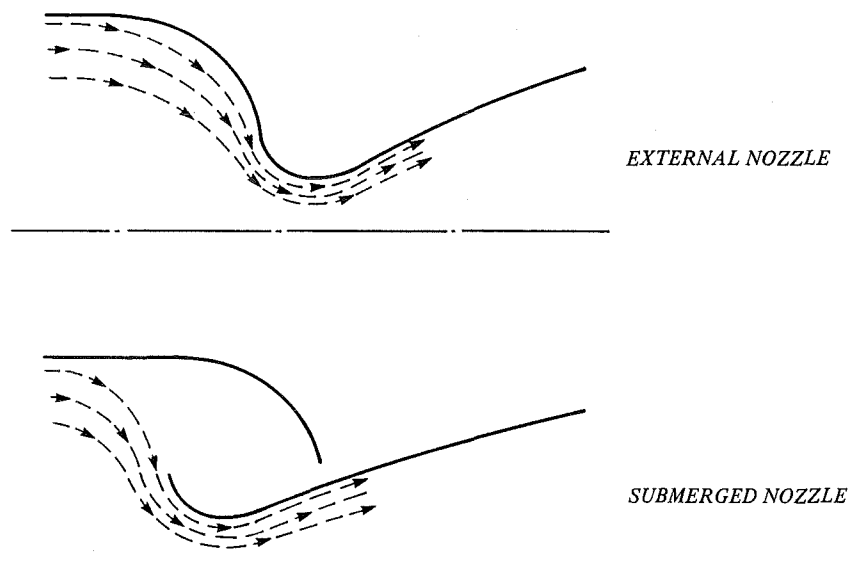


Fig. 2 - NOZZLE CONFIGURATIONS

These two configurations lead to different internal flow fields. The distance to the grain of an external nozzle is increased, thus giving a lower erosion of the throat. However the aft dome internal insulation erosion is greater due to the importance of the gas velocity near the wall.

An external configuration is usual with fixed nozzle and non limited length motors, thus giving a more simple design at a lower cost.

The submerged configuration allows an increase of the performance for limited length motors. However this configuration leads to a more complex design and a higher cost. A submerged configuration is usual with movable nozzles ; thus, in the case of a flexible bearing, the articulation is located in a low mach number area (see figure 3).

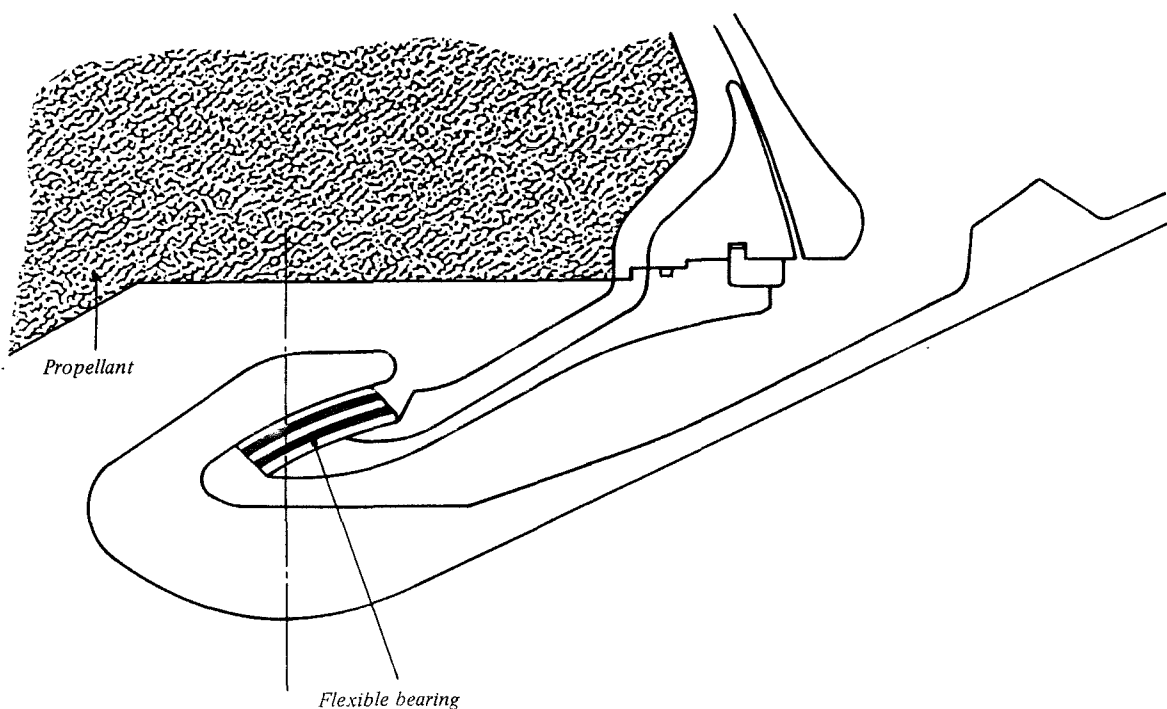


Fig. 3 - MOVABLE NOZZLE

An other possible configuration is the four nozzle design. This configuration has been used on the first generations of solid rocket motors to provide thrust vector control. With the development of omniaxial thrust vector control systems, the four nozzle configuration has considerably declined in usefulness. Single nozzle systems provide a higher efficiency at a lower cost.

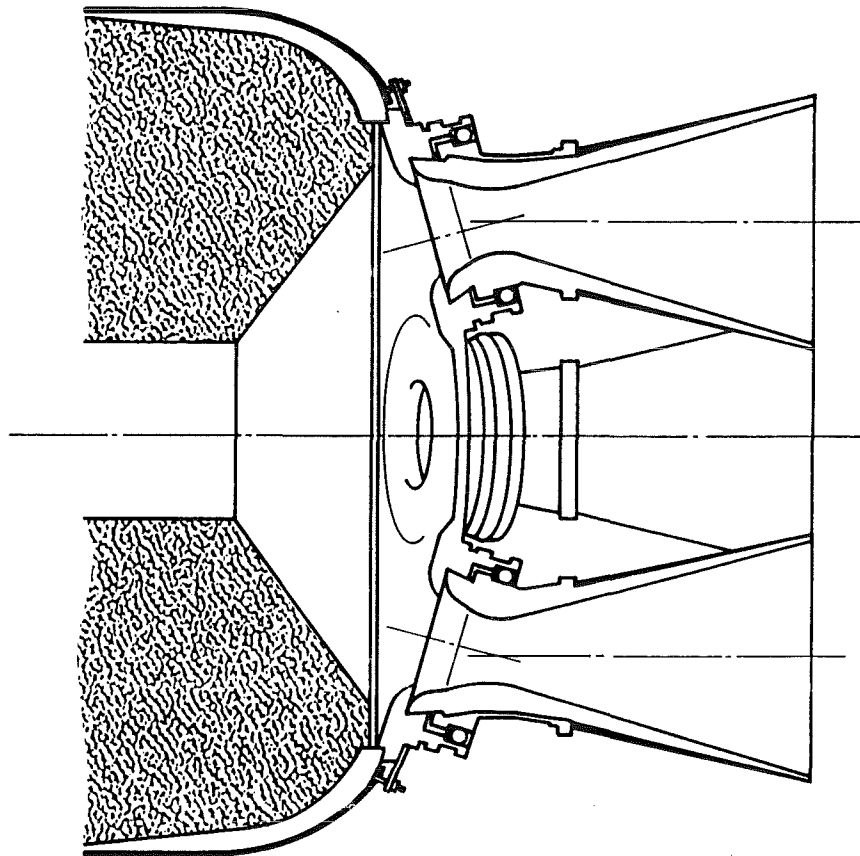


Fig. 4 - FOUR NOZZLE CONFIGURATION

An usual configuration for tactical applications is the blast tube nozzle. This design is used to accommodate guidance or navigation equipment.

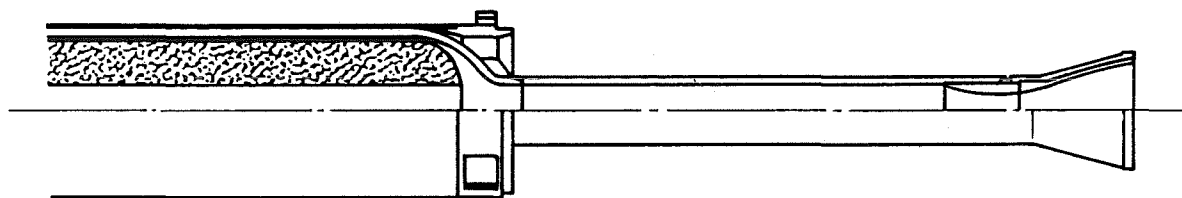


Fig. 5 - NOZZLE WITH BLAST TUBE

3.2. Aerodynamic contour design

The general configuration of the nozzle aerodynamic contour is presented in figure 6.

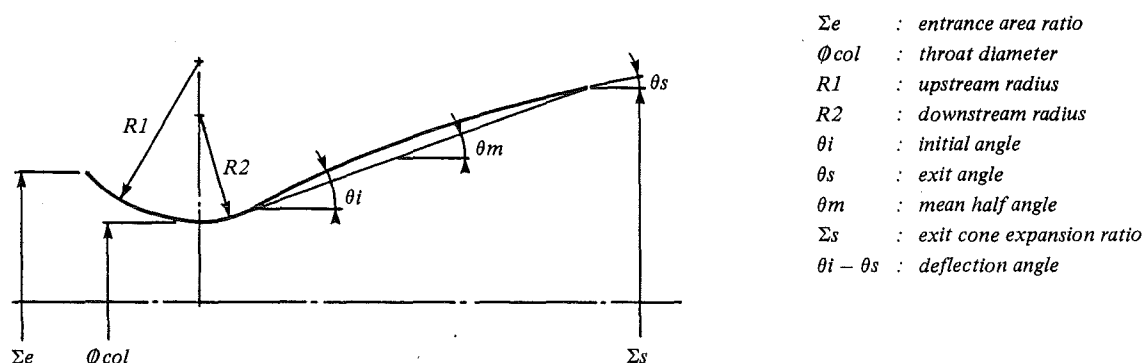


Fig. 6 - AERODYNAMIC CONTOUR

In the subsonic area, contraction ratios from 2.5 to 3.5 and nose tip lengths greater than the throat radius are usual. These rules are based on both aerodynamic and thermal considerations (see reference [17]). In the exit area a contoured shape is desirable in order to limit divergence losses. However in the case of aluminized propellants the deflection angle is limited by particules impacting on the tip of the exit cone. Typical values of deflection angles are in the range of 9 to 14 degrees.

For the same deflection angle and same length of the exit cone, an increase of the half mean angle leads to an increase of both the expansion ratio and divergence losses. The optimum value of the half mean angle is a compromise between these two aspects.

3.3. Thermal liner and insulator materials

After designing the aerodynamic contour, the next step of the design consists in selecting and sizing thermal liners and insulators. The thermal liner is exposed directly to the hot gases and forms the aerodynamic contour of the nozzle. The insulator serves to protect structural parts of the nozzle. Sometimes, a same material can achieve different functions at the same time ; it is the case of phenolic materials, which can serve as both liners and insulators.

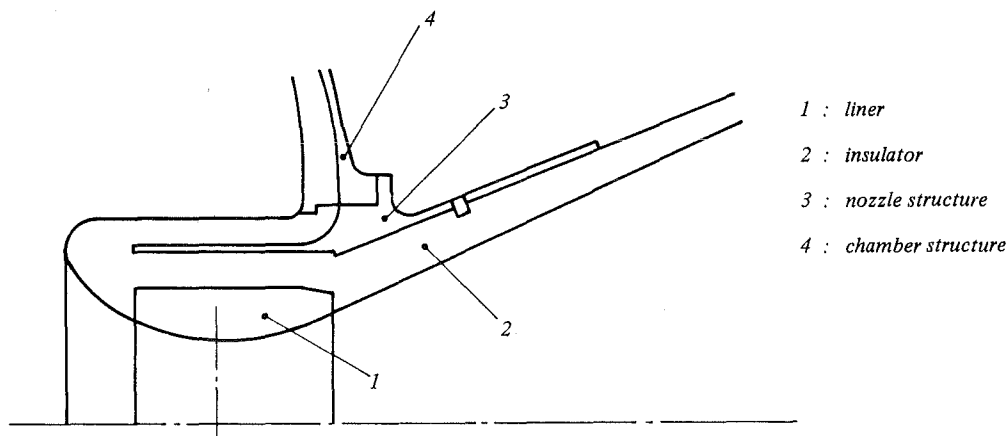


Fig. 7 - NOZZLE MATERIALS

In a first step, the nozzle thermal design is performed taking into account experience obtained in firing tests, certain empirical correlations and one dimensionnal simplified thermal analyses. This preliminary design is afterwards refined during the thermal analysis of the nozzle (see § 6.2. Thermal analysis).

3.3.1. Thermal liner materials

a) Refractory metals :

These metals have been used on the first generations of solid rocket motor nozzles. Tungsten with its very high melting point (3410°C) has been used as throat material. The main drawback of these metals is the density (19.3 in the case of tungsten). For this reason, these metals are rarely used at the present time.

b) Graphites :

Two classes of graphite have been used : the polycrystalline graphite and the pyrolytic graphite. These materials are able to withstand very high temperatures (greater than 2600°C) but present a low thermal shock resistance and an unpredictable thermomechanical behavior. For these reasons the use of graphite has considerably declined.

An example of a nozzle using graphite washers in the throat area is presented in figure 8.

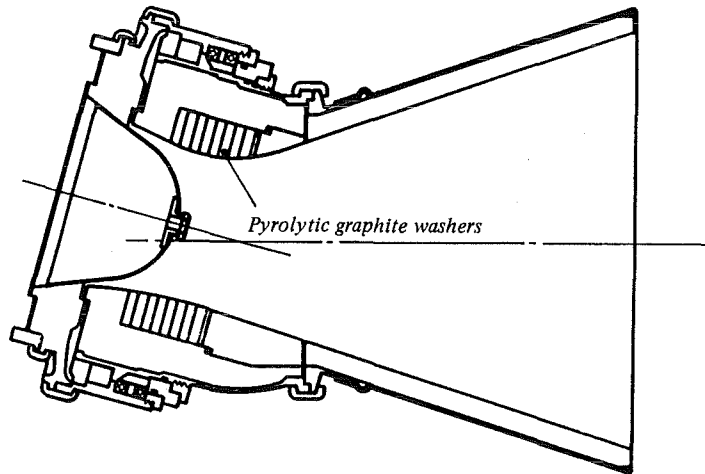


Fig. 8 - NOZZLE WITH PYROLYTIC GRAPHITE WASHERS IN THE THROAT

c) Ablative materials :

An ablative material is made up of a refractory reinforcement and a polymer resin. Different sorts of reinforcement are possible such as carbon, graphite, silica, glass or asbestos. Phenolic matrices are extensively used for this application because they give off high levels of char during the pyrolysis which occurs during the motor combustion. The pyrolysis starts approximately at 300°C and increases the thermal protection effect ; indeed most of the chemical reactions involved are endothermic thus absorbing energy. The pyrolysis is accompanied with an important outgassing, which must be taken into account for the design.

Carbon, graphite or silica phenolics are the most commonly used ablative materials. Typical thermal and mechanical properties of these materials are summarized in table 1.

	CARBON-PHENOLIC	GRAPHITE-PHENOLIC	SILICA-PHENOLIC
Density	1.40 - 1.50	1.35 - 1.54	1.70 - 1.80
Tensile strength (MPa)	110 - 140	40 - 150	80 - 190
Ablation temperature (°C)	2500	2500	1700
Heat diffusivity (m ² /s)	0.5 - 0.8 10 ⁻⁶	1 - 1.5 10 ⁻⁶	0.2 - 0.3 10 ⁻⁶

TABLE 1

These materials present low density, good insulating properties and high ablation temperatures. The use of a carbon or graphite reinforcement gives a higher ablation temperature than that of silica. Silica phenolics can be used in areas less exposed to thermal loads such as the downstream part of the exit cone in order to decrease the cost ; indeed the price per kilogram of silica fibers is approximately one third that of carbon fibers.

Carbon or graphite phenolics can be used in the throat area. This technology is used at the present time for the nozzle of the Space Shuttle Solid Rocket Booster ; at the development time, a carbon-carbon throat would have been too expensive because of the large size of the nozzle. However this technology leads to the following drawbacks, a higher ablation rate and a more complex design. Moreover, the throat must be segmented in several parts in order to achieve the proper thermomechanical behavior of the nozzle.

Ablative parts can be molded. This process is well suited for small parts produced in large quantities. For larger sizes and reduced quantities, tape wrap or lay-up (see figures 9 and 10) are less expensive. For parts such as exit cone, tape wrap is usually the most economical solution. The reinforcement can be parallel to the center line or inclined at a certain angle.

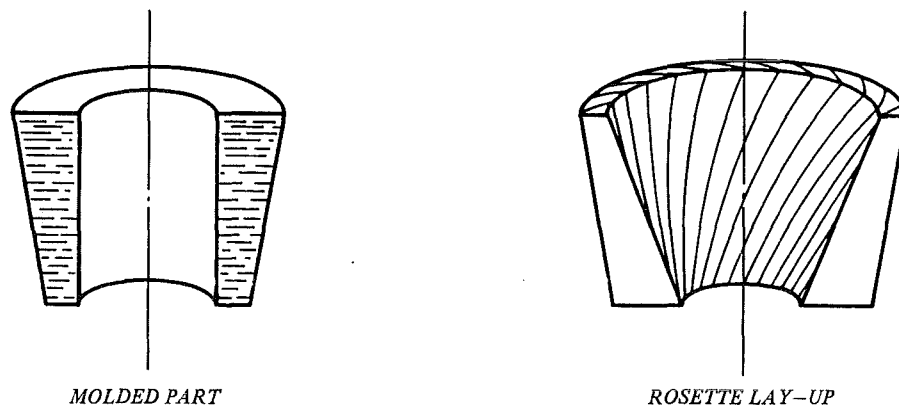


Fig. 9 - MOLDED OR LAID-UP PARTS

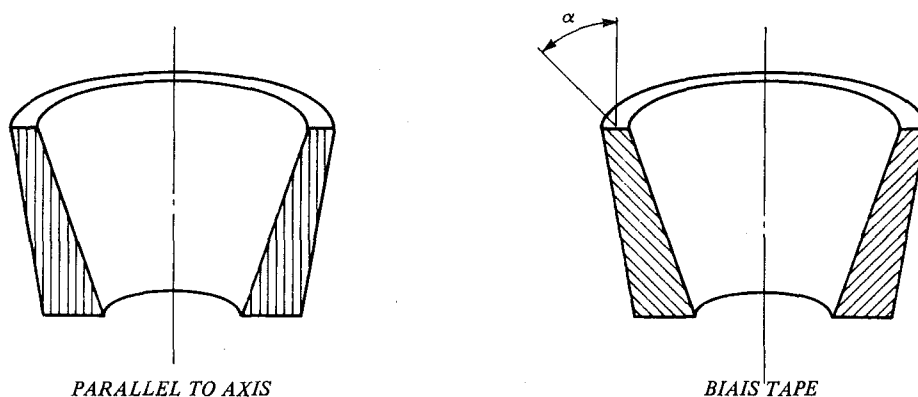


Fig. 10 - TAPE WRAP

d) Carbon-carbon :

Carbon-carbon materials present many advantages compared to other liner materials : low density, good thermal shock behavior, excellent erosion resistance and more reproducible thermomechanical behavior.

Most modern nozzles use one-piece carbon-carbon integral throat and entrance. These monobloc parts are heavily loaded by the thermal gradients during the motor combustion. This type of one-piece design presented in figure 11, has enabled great simplifications and an improvement of reliability by eliminating throat failure.

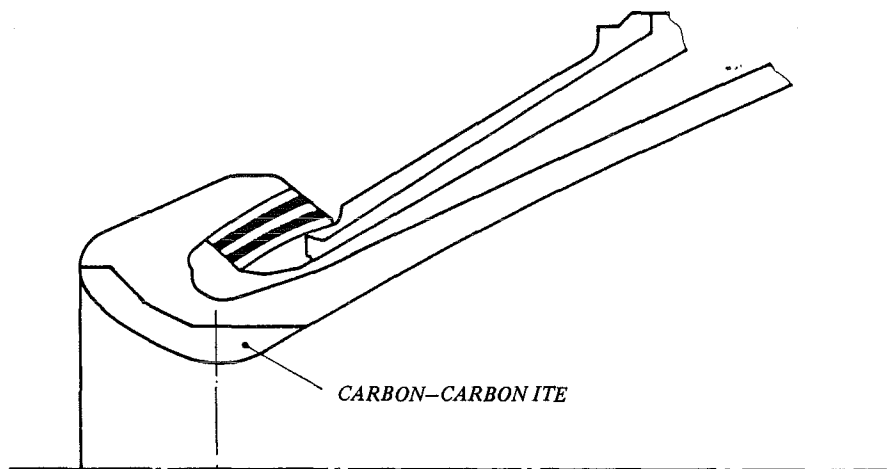


Fig. 11 - CARBON-CARBON INTEGRAL THROAT AND ENTRANCE

The fabrication of a carbon-carbon part involves two phases :

. Preform construction :

The preform construction can be performed by different processes such as carbon clothes lay-up, multidirectional weaving and pultruded carbon rods arrangement.

. Densification process :

The densification consists to fill up the preform porosity by a carbon matrix. There are basically two methods to deposit the matrix into the substate. In the liquid impregnation method, a resin or a pitch is injected into the preform and charred in order to create the carbon matrix. In the chemical vapor deposition process a deposit of pyrocarbon is obtained by cracking a gaseous hydrocarbure.

The different densification cycles are repeated until the required density of the part is obtained. Lastly a final graphitization of the matrix is performed at temperatures greater than 2000°C. Typical densities in the throat area may vary from 1.9 to 2.0 ; however, for weight saving, lower densities are desirable in less severe erosion environments such as exit cones (1.5 to 1.6 g/cc).

3.3.2. Insulators

Nozzle insulators can be divided into the three following classes :

a) Elastomers :

These materials are mainly used for internal insulation. They can be used also for nozzles in subsonic areas exposed to very low mach numbers.

b) Phenolic insulators :

Phenolic insulators have already been presented as liner materials (see § 3.3.1. c) Ablative materials). These materials present excellent thermal insulation properties. The thermal protection effect is increased by the ablation process, which occurs during the firing ; indeed most of the chemical reactions involved are endothermic thus absorbing energy.

Silica phenolic diffusivity is two to three times less than the diffusivity of carbon phenolic, but its use is limited in temperature because of the lower ablation temperature (1700°C).

Phenolic insulators present some limitations. The degradation of the matrix, which occurs during firing leads to poor mechanical properties at elevated temperatures. Outgassing of pyrolysis gasses may induce stresses in other parts of the nozzle ; moreover the modelisation of phenolic insulators for thermomechanical analysis is difficult due to the chemical change in the material.

c) Thermostable insulators :

An insulator is said to be thermostable when its reinforcement and matrix are both refractory. Different combinations of matrix and reinforcement are possible using carbon or ceramics. These new materials currently in development are very promising (see § 3.5. Multifunction materials).

3.4. Structural materials

The structural materials form the mechanical component of the nozzle. The most usual materials are metals (aluminium, steel, titanium) and reinforced plastics (carbon or glass epoxy).

3.5. Multifunction materials

Some composite materials have the capability to achieve different functions at the same time. It is the case of carbon-carbon for exit cones and thermostable insulators. They can serve at the same time as liner, insulator and structural materials.

3.5.1. Carbon-carbon exit cone

A freestanding carbon-carbon exit cone presents the following advantages : a lower inert mass thus increasing performance and a reduction of the number of parts thus decreasing nozzle complexity.

The nozzle of the Apogee Boost Motor MAGE II is presented in figure 12. This nozzle, which has been developed in 1980 by SEP, uses a carbon-carbon exit cone. 15 firing tests have already been successfully performed.

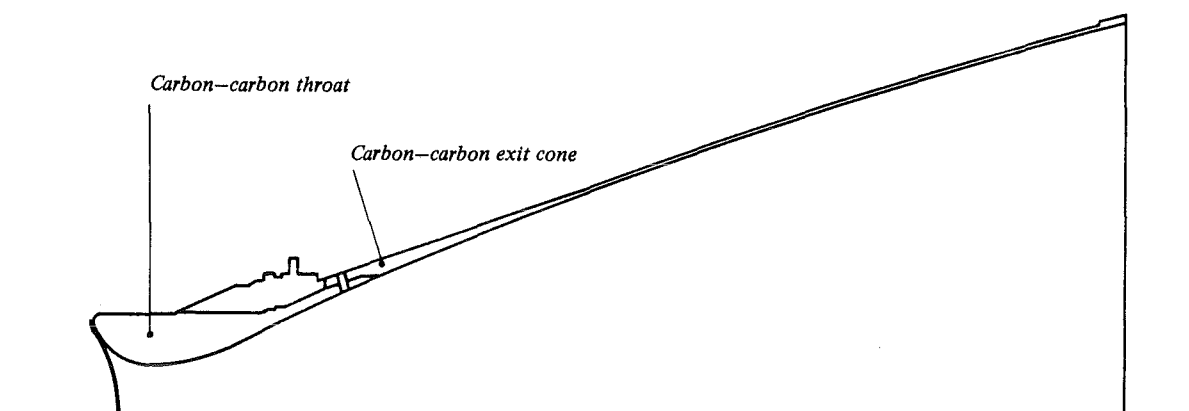


Fig. 12 - MAGE 2 NOZZLE

The main drawback of carbon-carbon exit cones is currently the cost ; indeed for the different operational applications, the preform construction is hand-performed by an involute process (STAR 30, IUS, MAGE II).

However the development of new methods enabling the construction of large multidirectional reinforced preforms will increase the applications of carbon-carbon exit cones by decreasing the cost. Thus for freestanding exit cones, SEP has developed a new carbon-carbon material called NOVOLTEX. This new material is characterized by a fully automated preform construction and a very fine spacing texture.

3.5.2. Thermostable insulators

A thermostable insulator is made up of a multidirectional carbon or ceramic reinforcement and a carbon or ceramic matrix. The final mechanical and thermal properties are a main function of the combination of reinforcement and matrix. These new materials currently in development are presented in reference [6]. Some typical thermal and structural properties for these materials are summarized in table 2.

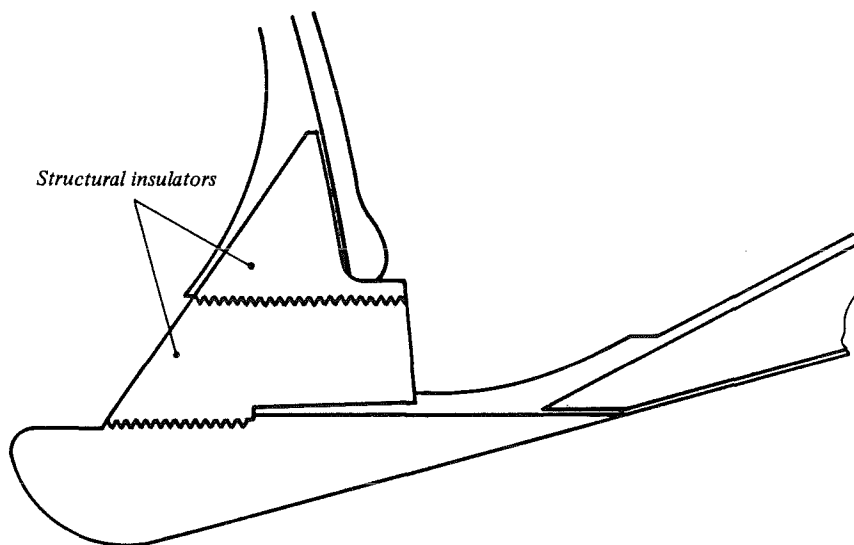
Reinforcement / Matrix	Density	Ultimate tensile strength	Heat diffusivity $10^{-6} \text{ m}^2 / \text{s}$	Temperature of use
Carbon-alumina	2.3	100	1.8	1800°C
Alumina-carbon	1.7	55	0.8	1500°C
Alumina + - carbon carbon	1.55	55	0.7	> 2000°C
Carbon-carbon	1.60	70	3.0	> 2000°C
Carbon-zirconia	2.3	100	1.1	2000°C

TABLE 2

Compared to phenolic insulators, thermostable insulators present the following advantages :

- . no outgassing
- . excellent mechanical properties at elevated temperature
- . more predictable thermomechanical behavior
- . design simplifications
- . decrease of the nozzle assembly time.

A nozzle using thermostable insulators is presented in figure 13. Design and development of this nozzle, fired in 1982, are presented with more details in reference [5].

**Fig. 13 - CSD - SEP MOTOR NOZZLE**

Vectoring loads can be transmitted by thermostable insulators. An example is presented in figure 14. The vectoring loads are applied directly to the exit cone and transmitted to the flexible bearing by a monobloc part, which achieves at the same time a mechanical function (transmission of vectoring loads) and a thermal function to protect the flexible bearing.

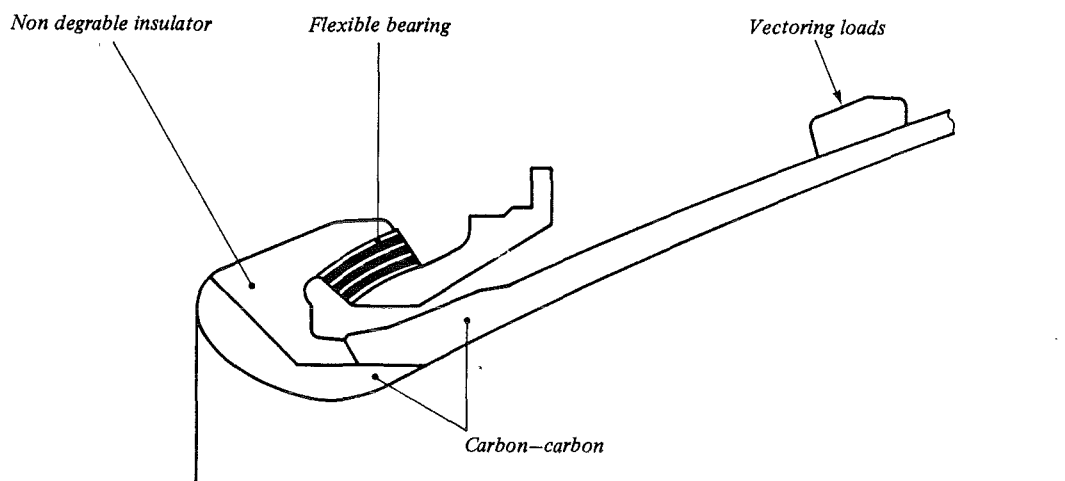


Fig. 14 - NON DEGRADABLE INSULATORS APPLICATION

4. - THRUST VECTOR CONTROL

In many solid rocket motors thrust vector control is required. The nozzle itself can provide TVC ; it is the case of movable nozzles hinged by a flexible bearing, a ball and socket, or a hydraulic bearing joint. The nozzle can also be combined to an attached device acting on the nozzle supersonic stream : fluid injection, jet vanes, etc...

4.1. Movable nozzles

a) Four nozzle configuration :

The four nozzle configuration has been used on the first generation of solid rocket motors. The thrust is controlled by a selective orientation of each canted nozzle.

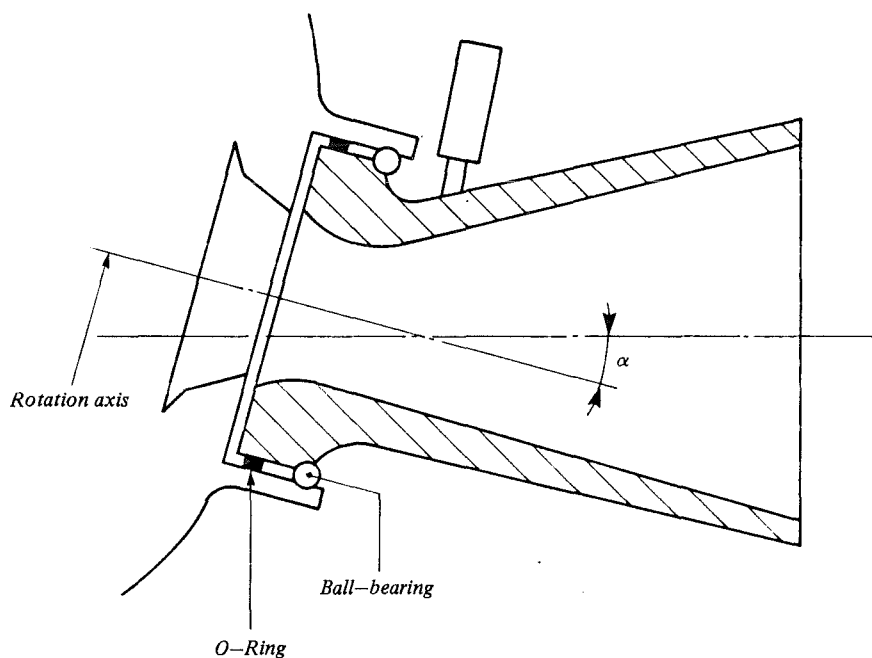


Fig. 15 - ROTATING CANTED NOZZLE - PRINCIPLE

The use of this very complex technology has considerably decreased over the past years. Single nozzle systems provide a higher efficiency at a lower cost.

b) Flexible bearing :

A flexible bearing is made up of alternate spherical segments of elastomeric and rigid shims (see figure 16).

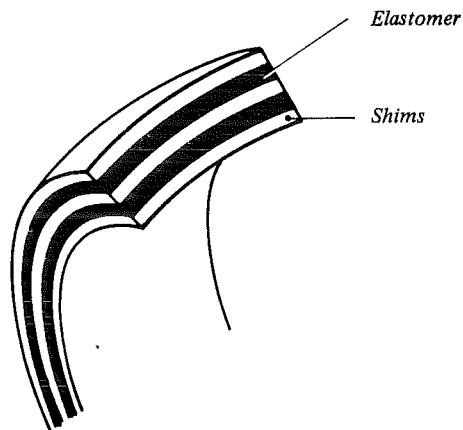


Fig. 16 - FLEXIBLE BEARING - PRINCIPLE

The flexible bearing enables control of both pitch and yaw attitudes of the missile. If a roll movement control is necessary, it is controlled by a other system.

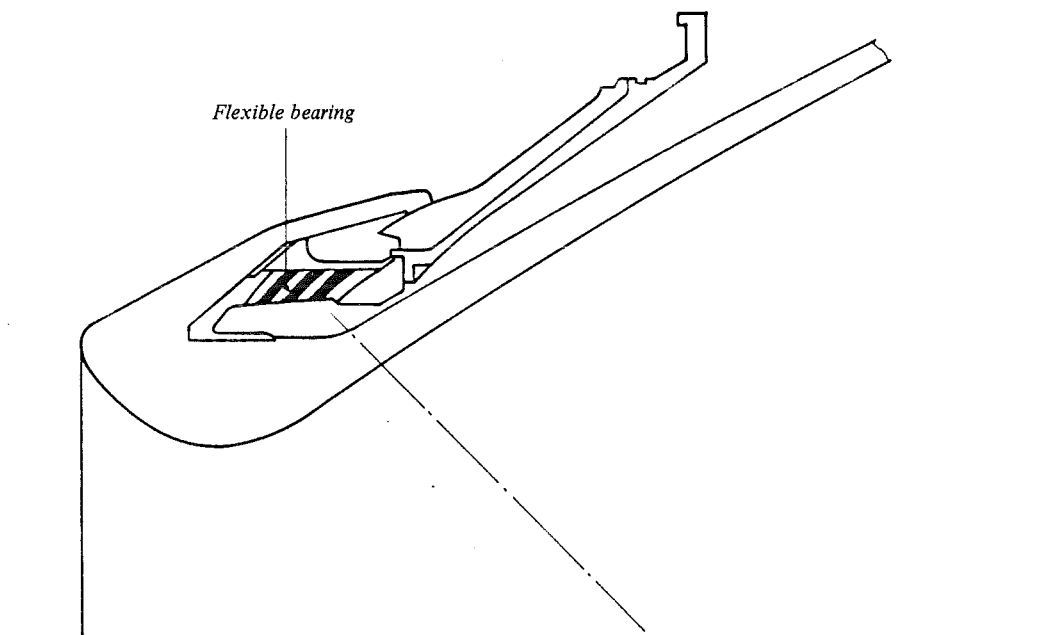


Fig. 17 - NOZZLE HINGED BY A FLEXIBLE BEARING

Two designs are possible depending on the position of the pivot point. These two configurations are called upstream and downstream pivot point configurations.

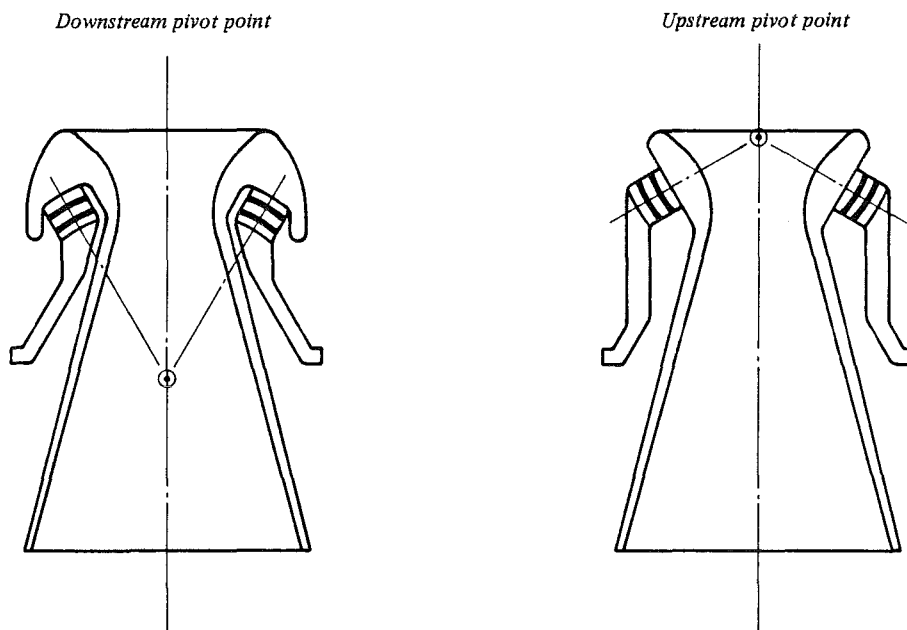


Fig. 18 - FLEXIBLE BEARING CONFIGURATIONS

The flexible bearing is the most widely used device in modern nozzles for ballistic or space applications. The use of a downstream pivot point allows a better protection of the joint which is located in a low mach number area.

c) Hydraulic bearing :

The principle of a hydraulic bearing is presented in figure 19. The joint consists of a fluid contained in a rubber membrane, thus reacting to the nozzle blow-off load. This technology is used at the present time for the motors of the orbital transfer vehicle IUS (see figure 19).

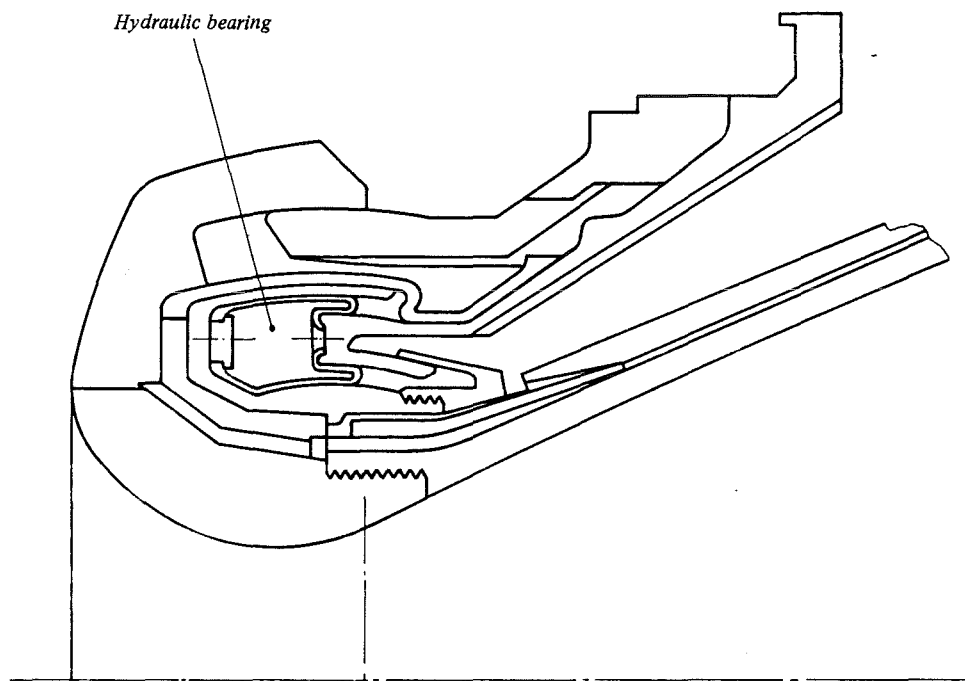


Fig. 19 - HYDRAULIC BEARING - PRINCIPLE

A low torque value is associated to the hydraulic bearing ; in the IUS, this characteristic allows the transmission of vectoring loads directly by the carbon-carbon exit cone and the phenolic insulators.

d) Ball and socket :

The ball and socket joint consists of two spherical sliding surfaces, thus giving an omnidirectional orientation to the nozzle. Low friction coefficient materials are desirable in order to minimize the torque value. If the joint is made of teflon, it is called "cold ball and socket", and must be protected by thermal insulators, because the use of teflon is limited by temperature. Carbon-carbon can also be used ; the joint is called "hot ball and socket" and can withstand higher temperatures in the range of 1000 to 2000°C (see figure 20).

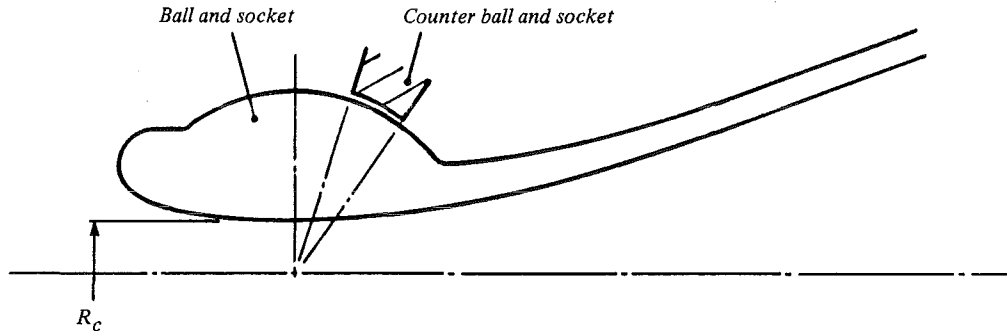


Fig. 20 - BALL AND SOCKET - PRINCIPLE

e) Supersonic splitline nozzles :

In most movable nozzle designs, the splitline between the fixed and movable portion of the nozzle is located in the subsonic area of the nozzle. This splitline can also be located in the supersonic area. An example is presented in figure 21.

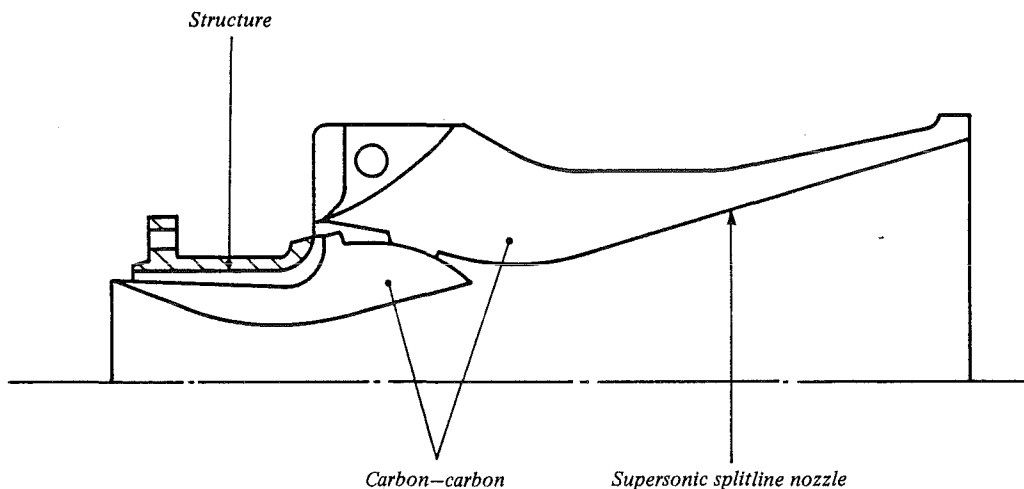


Fig. 21 - SUPERSONIC SPLITLINE NOZZLE

This nozzle is made up of a carbon-carbon throat and exit cone hinged by a hot ball and socket. This nozzle has been developed by SEP and fired for a cooperation program with the company ARC. The test motor was representative of a tactical missile motor with a low burning time and a non aluminized propellant. The firing test was successful and demonstrated an 18° thrust vector angle. The supersonic splitline nozzle presents two advantages :

- . a high vector angle capability : the exit cone steering angle is amplified by a factor ranging from 1.2 to 1.7 created by the supersonic deflection effect,
- . an important design simplification by reducing the number of parts.

However the concept presents limitations with aluminized propellants because of the erosion by particules impacting on the exit cone.

4.2. Attached systems acting on the nozzle flow

Two categories of attached systems acting on the nozzle flow have been used to provide TVC for solid rocket motors :

- a) fluid injection
- b) solid devices introduced into the nozzle supersonic stream.

4.2.1. Fluid injection

When a jet of fluid is injected into a supersonic stream, a side force is created as a result of both momentum of the jet and the dynamic and chemical interactions of the jet with the primary flow.

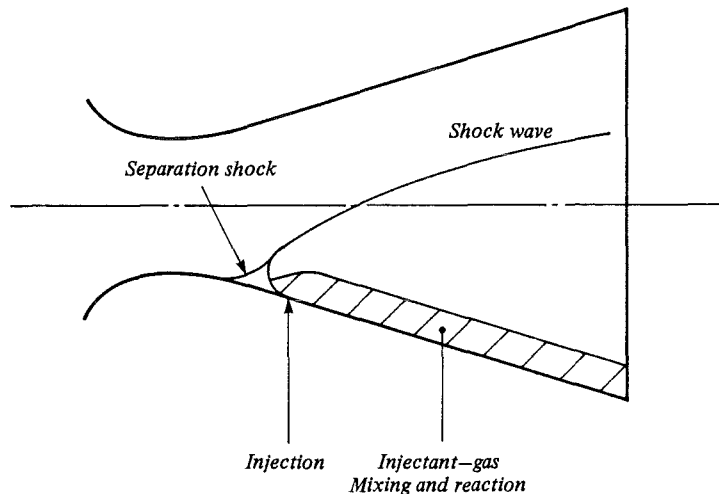


Fig. 22 - FLUID INJECTION - PRINCIPLE

The main advantage of fluid injection is the design simplification of the nozzle compared to that of movable nozzles. The main drawback is the increase of inert mass due to the transported fluid. For this reason the use of this technology has considerably declined over the past years. However the current development of hot gas valves using modern ceramic-ceramic materials enables the controlled injection of hot gases coming directly from the combustion chamber. This gives new interest to this technology.

4.2.2. Solid device introduced into the nozzle supersonic stream

Several systems have been used mainly for tactical applications ; two examples are presented in figures 23 and 24. The system presented in figure 24 consists of 4 jet vanes, which are able to control pitch, yaw and roll attitudes of the missile. This category of systems present some limitations by the thermal and mechanical loads induced on the device by the nozzle flow.

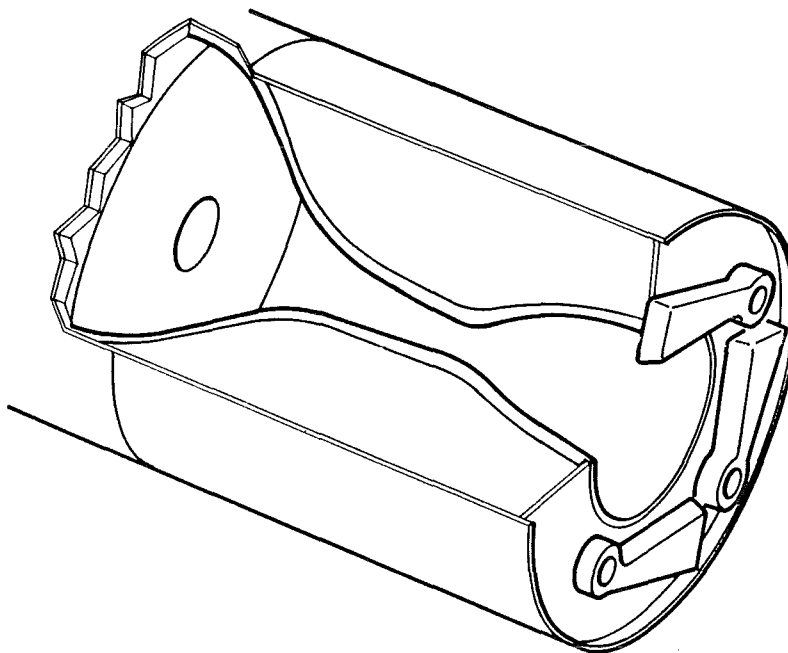


Fig. 23 - MECHANICAL DEVICE INTRODUCED INTO THE NOZZLE FLOW

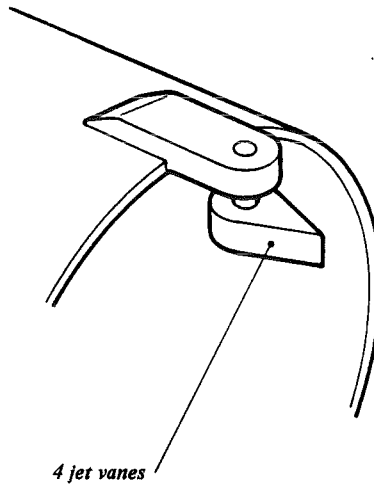


Fig. 24 - JET VANES

5. - EXTENDIBLE EXIT CONE

The principle of an extendible exit cone is to increase the exit cone expansion ratio in a limited external volume of the nozzle. This concept is well suited for limited length motors, such as submarine based missile motors and allows on increase of the performance by 6 to 8 percent.

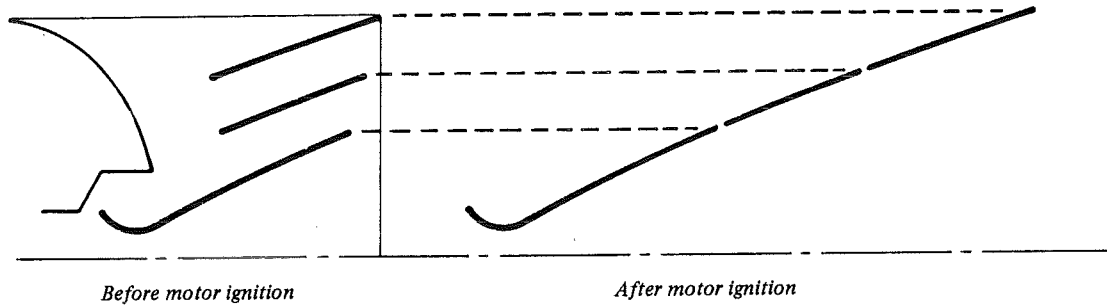


Fig. 25 - EXTENDIBLE EXIT CONE - PRINCIPLE

The experience of SEP in the field of extendible exit cone deployed after motor ignition is summarized in reference [8]. This demonstration program has enabled investigation of four concepts incorporating carbon-carbon cones and petals (see figure 26).

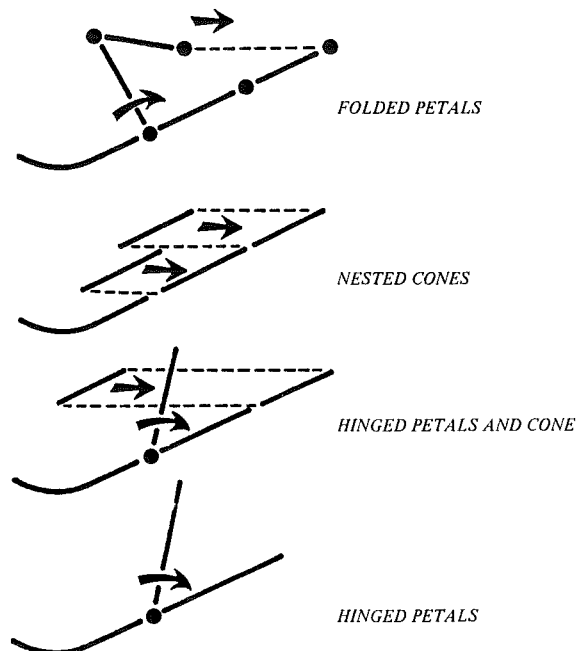


Fig. 26 - EEC CONCEPTS

6. - NOZZLE ANALYSIS

The nozzle analysis is usually conducted in 3 steps.

Aerodynamic analysis :

The goal of this analysis is to predict the performance and calculate the loads induced by the aerodynamic flow.

Thermal analysis :

This step consists to calculate the in-depth temperature distribution in the nozzle in order to verify the structural integrity of the mechanical parts.

Thermomechanical analysis :

This analysis is the last step of the nozzle analysis process. This step uses the results obtained during the two previous steps : the aerodynamic pressure and in depth temperature distribution.

The results obtained at each step and the recommendations of analysis people are taken into account by the nozzle designer. Several iterations are often required between the design and the analysis in order to obtain the optimum configuration of the nozzle.

6.1. Aerodynamic analysis

In a preliminary phase, the thermodynamic properties of exhaust products are evaluated by using a slightly modified version of the Nasa Lewis thermochemical analysis. This analysis is based on a free-energy calculation with the following assumptions :

- . one dimensional flow
- . non viscous and adiabatic flow
- . chemical equilibrium
- . velocity and thermal equilibrium of condensed and gas phases.

The inputs required are the following :

- . elemental composition of the propellant
- . heat of formation of the propellant at the operating grain temperature
- . motor operating pressure (average)
- . expansion ratio of the exit cone.

This analysis leads to a maximum theoretical specific impulse (I_{sv}^{th}). However the effective expansion achieved by the nozzle is different from this ideal case. The different performance losses are the following :

Flow divergence :

This effect depends on the exit cone geometry. The main influence parameters are the half mean angle and the deflection angle.

Two phase flow :

In the case of aluminized propellant, the two phase flow effect may represent a loss ranging from 3 to 5 %.

Viscosity effect :

The friction on the boundary layer may induce a loss ranging from 1 to 1.5 %.

Heat loss :

This loss is induced by the heat transfer at the nozzle wall.

Chemical non equilibrium :

This loss is due to the finite rate of chemical reactions, that do not allow the total energy of these reactions to be released during the expansion process through the nozzle.

Nozzle erosion :

This loss is mainly reflected by the expansion ratio decrease due to the change of the throat diameter during the firing.

The method used at SEP for performance prediction is described with more details in reference [3]. It consists of evaluating separately each effect, and cumulating these losses in order to obtain the effective nozzle efficiency. The results obtained by this method are in good accordance with experimental results. Some typical values of specific impulse losses are given in table 3.

Isv th losses	Typical value %
Flow divergence	2 - 3 %
Two phase flow	3 - 4 %
Viscosity loss	1 - 1.5 %
Heat transfer	0.5 %
Chemical non equilibrium	0.5 %
Throat erosion	0.5 %
TOTAL	9 - 10 %

TABLE 3

As shown in table 3, the flow divergence and two phase flow effects are preponderant and represent more than 60 % of the total loss. They are currently evaluated in two steps. Initially a bidimensional monophasic program enables the calculation of flow divergence loss. Afterwards, a bidimensionnal diphasic program gives by a comparison with the results obtained previously the two phase flow effects. These programs consider only the trans - and supersonic stream of the nozzle and use stationary methods ; for instance the supersonic stream is analyzed by a method of characteristics.

A new computer program presented in reference [9] is currently under development. This program will be able to analyse directly a two dimensional two phase flow. This program is based upon a non steady state approach solving the Euler equations with a Mac Cormack's explicite finite difference scheme. This new program will be able to take into account the subsonic area of the nozzle and to improve the performance prediction. An example of results of a flow field analysis performed with this new program is presented in figure 27. In the first case, the flow is supposed to be monophasic ; as shown the results are very different from those obtained by the second calculation assuming a two phase flow.

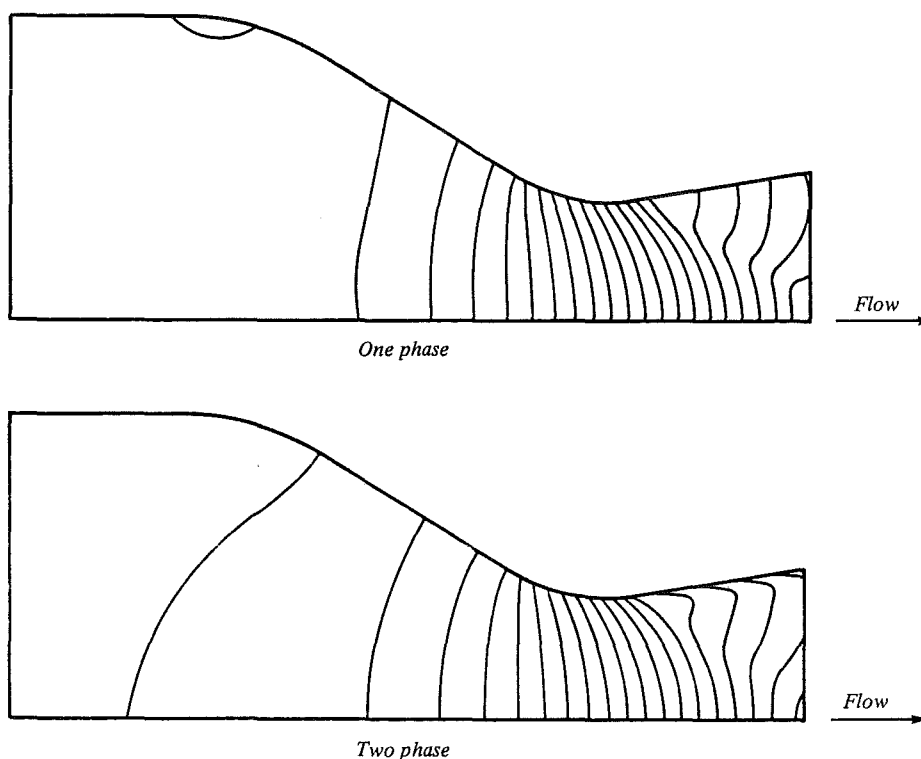


Fig. 27 - NOZZLE MACH NUMBER CONTOUR

6.2. Thermal analysis

The initial sizing of liner and insulator thicknesses is usually performed with material erosion data and one dimensional thermal calculation. This design is afterwards analysed with more refined techniques using two dimensional computer programs taking into account the ablation.

6.2.1. Thermal analysis characteristics

The thermal analysis presents the following characteristics :

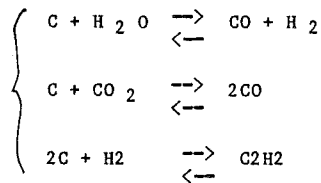
- . the anisotropic and temperature dependant materials properties
- . the very high convective and radiative heat flux ($> 10 \text{ MW/m}^2$)
- . the analysis must predict and take into account the ablation by hot gases.

6.2.2. Boundary conditions

Convection : the convective heat flux is usually preponderant in the total heat exchange.

Radiation : the radiative heat flux is important during the first seconds of the combustion, for which the difference of temperature between the wall and the hot gases is maximum.

Mass transfer : the heat flux resulting of this effect may represent 10 % of the total heat flux. The chemical reactions taken into account are the following :



The boundary conditions are determined in the three following steps :

(1) Calculation of transport properties (specific heat, viscosity, thermal conductivity and mass diffusion coefficients) for use in boundary layer thermodynamic analysis.

(2) Calculation of chemical surface recession rate considering the chemical reaction between the material and the combustion products.

6.2.3. Conduction calculation

The transient heat conduction problem is solved by a two dimensional finite difference scheme taking into account the surface recession and the thermochemical boundary conditions at the wall. Figure 28 shows the typical analytical results for a nozzle at a given combustion time.

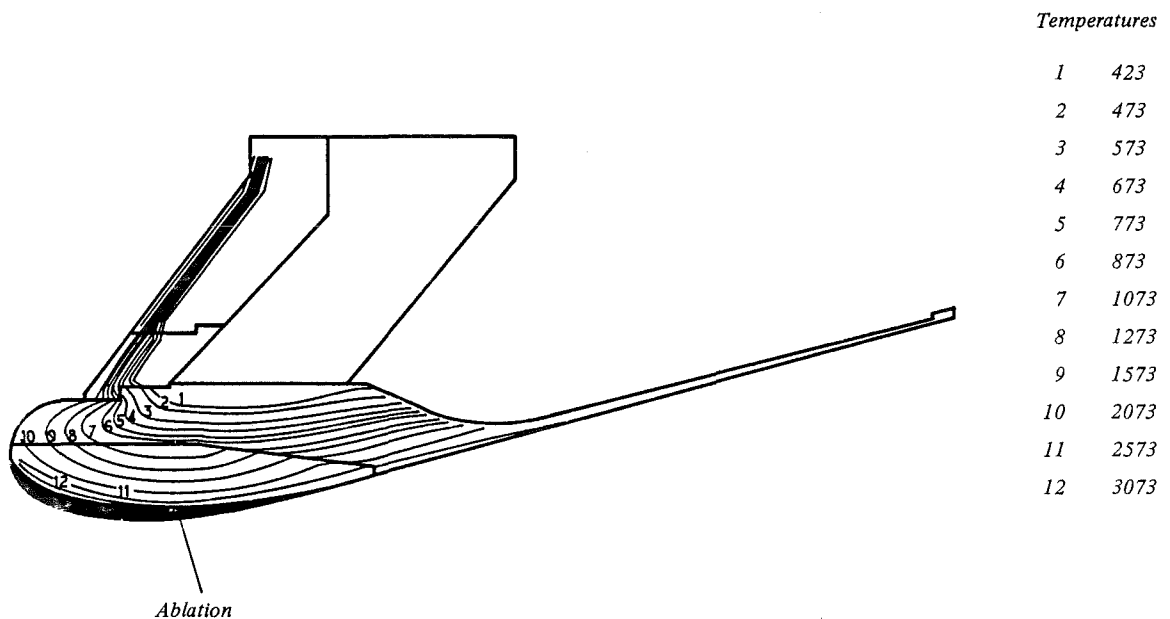


Fig. 28 - IN-DEPTH TEMPERATURE DISTRIBUTION EVALUATION

6.2.4. Developments underway

The following developments are underway :

- . improvement of boundary layer analysis
- . in depth temperature calculation with a finite element scheme in order to perform the thermal and thermo-mechanical analysis in one step. This development will enable transient thermomechanical analysis taking into account "the history of the load".

6.3. Thermomechanical analysis

The structural analysis is performed at given combustion times. The structural analysis presents the following characteristics :

- . very severe thermal gradients
- . anisotropic and temperature dependant materials properties
- . non linearity of stress-strain curves
- . geometry non linearities (gaps, etc...).

6.3.1. Characteristics of materials

Nozzle materials are usually considered orthotropic. The structural behavior evaluation requires for each direction, the stress-strain curves, the Poisson's effect, the shear moduli and expansion ratios. These values must be measured at different temperatures. The characterization must be performed with samples fabricated with industrial conditions representative of the nozzle part process. An example of stress-strain curves for a carbon-carbon is presented in figure 29.

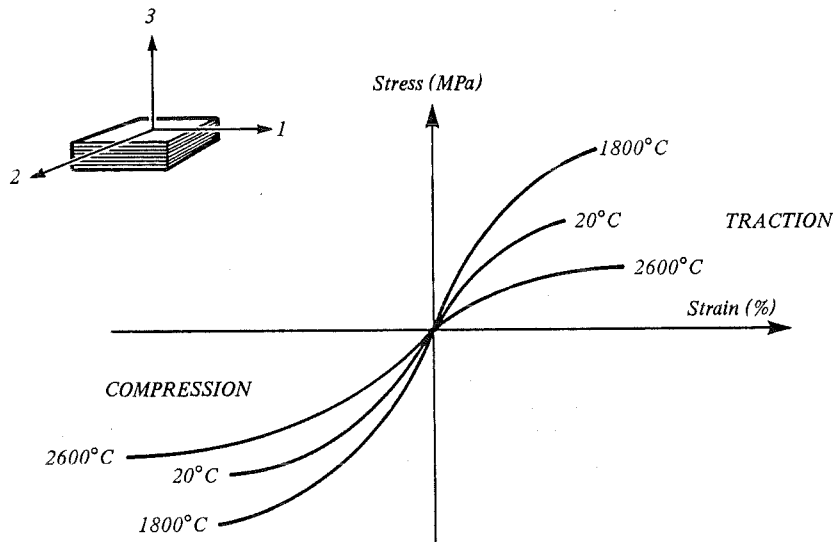


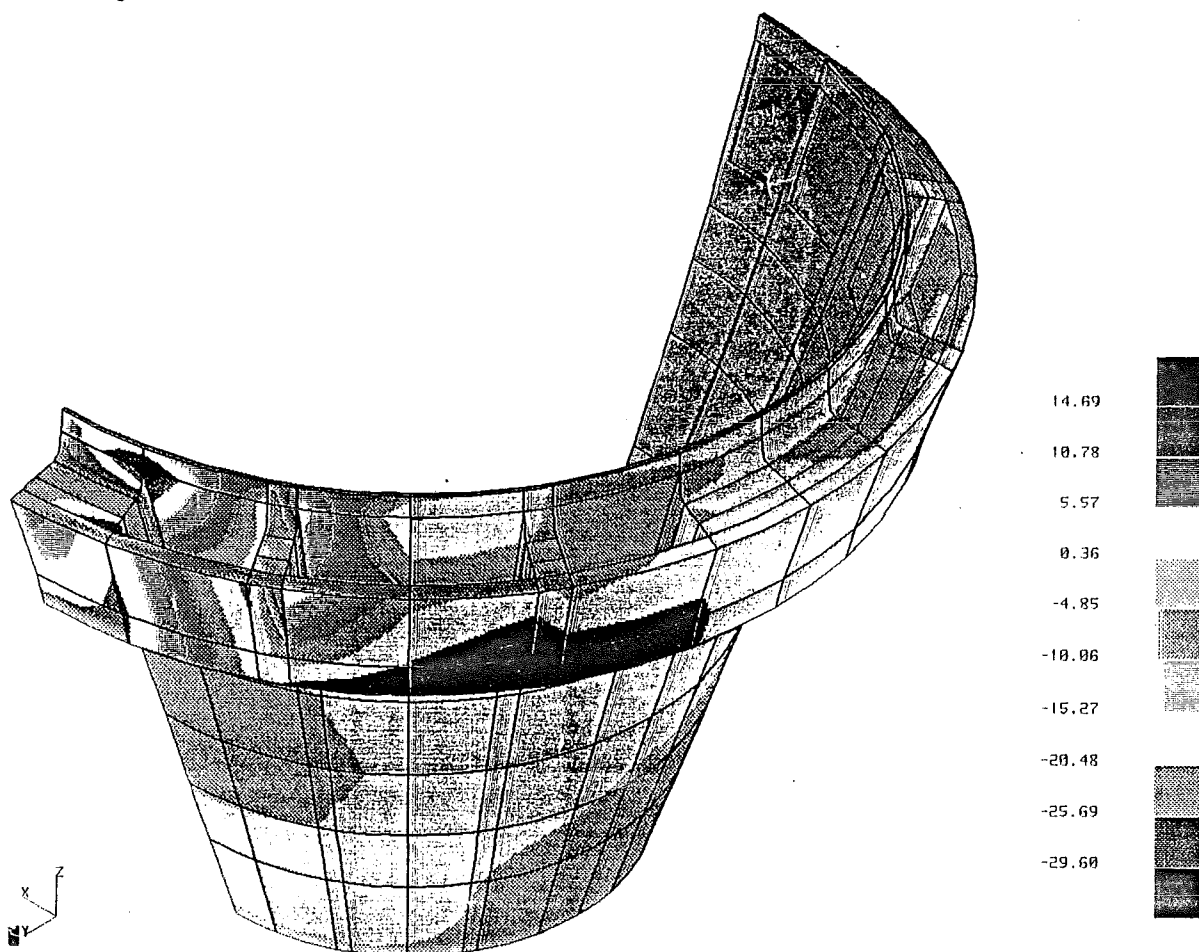
Fig. 29 - EXAMPLE OF STRESS-STRAIN CURVES FOR A CARBON-CARBON

6.3.2. Calculation of stress and strain

The analysis is performed with a finite element computer program (code MARC see reference [5]). The loads applied to the nozzle can be aerodynamic pressure, thermal gradients or external loads such as actuation loads, vibration.

Two to four combustion times are selected, for which the parameters are the most significative (thermal gradient, chamber pressure, temperature). The modeling must take into account the surface recession due to ablation. The stress and strain calculation is performed with an incremental iterative technique in order to consider the different non linearities (non linearity of stress-strain curves, gaps in the nozzle assembly). An example of stress distribution in a carbon-carbon exit cone subjected to actuation loads is presented in figure 30.

Fig. 30 - STRESS DISTRIBUTION IN A CARBON-CARBON EXIT CONE



The nozzle structure factor of safety is determined with maximum stress or maximum strain criteria. These criteria consist of comparing for each direction the calculated stress or strain with the maximum value obtained on samples.

6.3.3. Further development

The use of the same finite element modeling for thermal and structural analysis will enable the achievement of transient thermomechanical analyses with a better adaptation of the modeling to the thermal gradients. An example of automatic remodeling between different combustion times is presented in figure 31. These developments enable the taking into account of inelastic behavior of the materials, the history of load and the effects of damage.

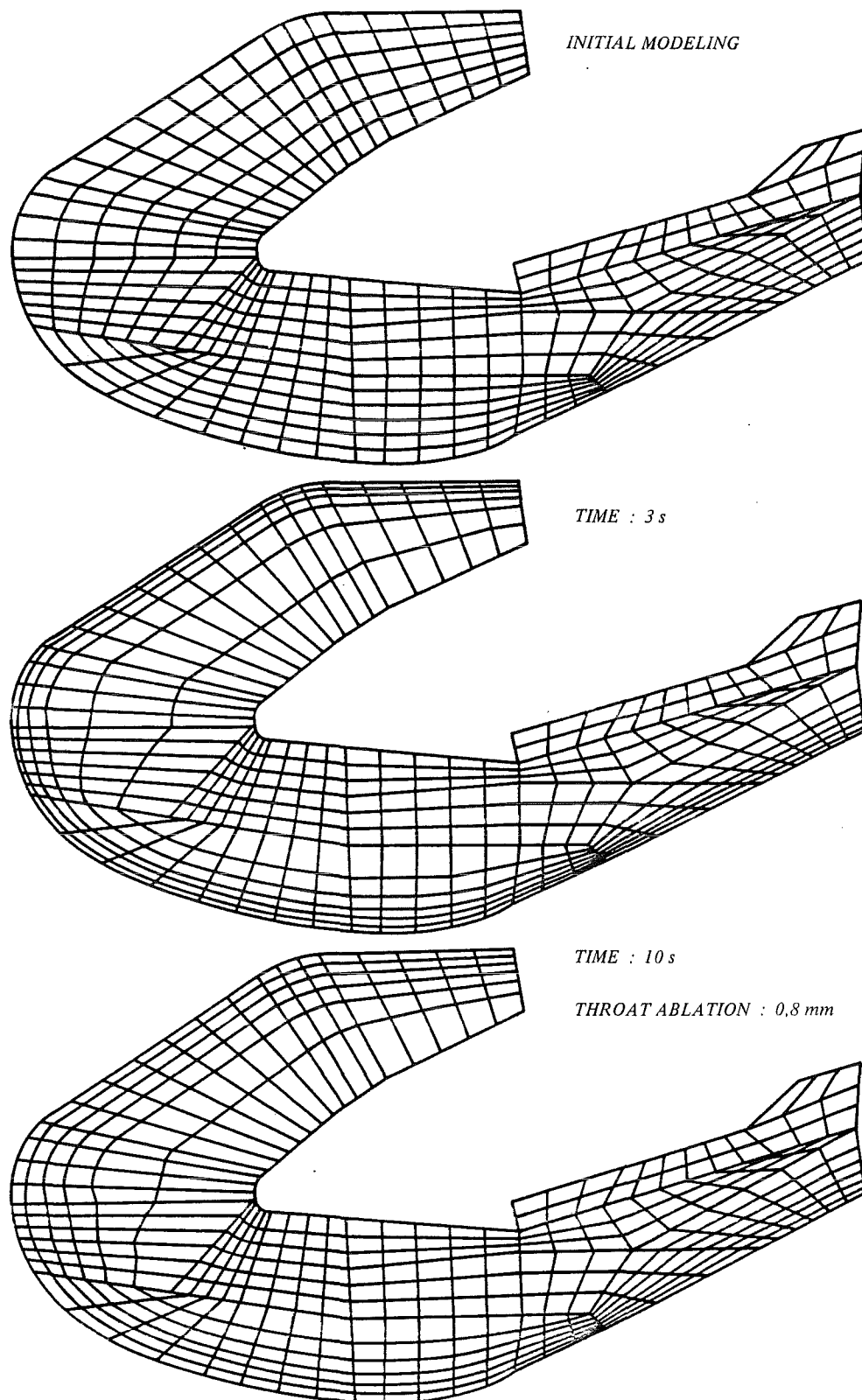


Fig. 31 - THERMOMECHANICAL ANALYSIS WITH AUTOMATIC REMODELING

7. - CONCLUSION

A lot of improvements have been performed in the field of nozzle materials over the past ten years. Most modern nozzles use one piece carbon-carbon integral throat and entrance. The current development of new methods allowing the construction of large multidirectional reinforced preforms, will increase the applications of carbon-carbon exit cones. Ceramic-ceramic insulators are emerging. They will greatly simplify the design of nozzles, thus leading to an improvement of both performance and reliability.

In parallel, the analysis methods have been enhanced. Thus the different computer programs, which have been developed have allowed great improvements of performance prediction and thermostructural behavior evaluation.

COMPOSITE MOTOR CASE DESIGN

by
 Dr. P. R. Evans
 Department Manager, Structures & Analysis
 Hercules Incorporated (Aerospace Products Group)
 Allegany Ballistics Laboratory
 P.O. Box 210
 Rocket Center, WV 26726
 USA

SUMMARY

Information is presented on the design of composite cases for rocket motors. Typical design requirements are discussed, including pressure, axial and bending loads and thermal loading. Material technology discussed includes filament winding resins and glass, Kevlar and graphite fibers. Design features discussed include the pressure vessel body, skirts, polar adapters and other attachments. Typical qualification testing and inspection techniques are presented.

OBJECTIVE

The objective of this lecture is to provide an overview of the design and verification of filament wound motor cases for use in solid rocket motors.

BACKGROUND

The motor case for a solid propulsion rocket motor serves: (a) to protect and "store" the propellant grain until the motor is used, (b) as a combustion chamber for high pressure, high temperature burning of the grain during motor operation, (c) to mechanically/structurally interface with other motor components like the nozzle, igniter, internal insulation, handling/carrying brackets, etc., and (d) usually as a primary airframe during missile flight. Motor cases may be very large like the Space Shuttle Solid Rocket motor or quite small man-operated tactical units. The design requirements dictated by the missile's size and mission profile encompass wide ranges of mechanical and thermal loadings which can occur during the manufacture, storage, operational deployment, and flight history of a given missile.

Since the motor case is an inert or non-energy-contributing missile component, the design objective is to make the case as lightweight as possible, within the bounds of technology and cost. This will result in a higher motor mass fraction (propellant weight/total motor weight) and high motor and missile "performance" (range, delta velocity, etc.). Case designs utilizing structural composites, laminates of high strength fibrous materials like fiberglass, Kevlar and graphite (carbon) with matrix materials like epoxies, typically result in significantly lower weights than metallic designs. The nature and behavior of composite materials dictate distinctly different design and quality verification methodologies than would be required for metal case designs.

The "typical" solid rocket motor case is basically a double-domed right circular cylinder with openings in both domes and cylindrical extensions called "skirts" (Figure 1). The aft opening interfaces with the nozzle. The forward opening accommodates the igniter and safe/arm. The forward opening may be absent altogether if an aft igniter is utilized. The "skirts" are integral extensions of the case body which serve as structurally-capable attachment interfaces for other missile stages or hardware packages. The motor case interior is covered with an insulator which provides thermal protection and flow erosion resistance in those regions where the propellant burns to the wall before the entire grain is consumed. A case bond system chemically attaches the grain to the case wall interior and insulator. Additionally, numerous conduits, ducts, and attach/carry features may be required on the case. A particular design challenge present on most large intercontinental-capable motors is thrust termination ports--specific regions of the case pressure vessel which must be penetrated or destructed in a controlled manner on command, to depressurize and extinguish the propellant grain.

The solid rocket motor case is essentially a minimum-weight pressure vessel, one whose design is complicated by the presence of significant levels of thrust and bending as well as locally concentrated loads from the skirts and any attachments. Solid rocket motors typically operate from 500 to 3500 psi. Appreciable thermal loads are also present, since the propellant grain combusts at 5-6000°F and aeroheating can result in exterior surface temperatures in excess of 1200°F.

CASE DESIGN APPROACH

Mechanical and thermal loads and geometry constraints are usually supplied to the designer. Factors of safety or load factors typically vary somewhat from customer-to-customer (Navy, Army, AF, NASA, etc.) and for a specific missile. Internal pressure is often the dominant load. A typical factor of safety requires the minimum vessel burst

strength to be 1.25 times greater than maximum expected operating pressure, MEOP, ("hot firing", maximum pressure-increasing tolerances, manufacturing variability). For some air-launched applications or man-portable motors, this factor may be increased to 1.4 or 1.5 for the flight period while the motor is within a specified distance of the launch point. Other mechanical load factors like bending and thrust may have values higher or lower than that selected for pressure, depending upon the precision with which their limit magnitudes can be predicted and their criticality. Thermal loads require particular attention since the mechanical properties of composite degrade appreciable at temperatures well below those affecting metals. Such loads may be accommodated by imposing maximum (or minimum) temperature limits on the case structural region and requiring insulation thicknesses adequate to insure that the temperature limits are never exceeded. Even so, the mechanical strengths and stiffnesses of the structural materials must be known across the allowable temperature range for all of the other environmental bounds imposed and for the design life of the motor. Since composite materials are sensitive to temperature, moisture and other "environmental" exposures and since composites "age"--particularly the resin matrix materials--the subject of material properties characterization is pivotal to efficient and effective composite case design.

Consider the "typical" motor case (Figure 2). Since pressure loads usually dominate the design we will, for preliminary design sizing, treat the case as a "thin shell, a membrane"; i.e., one in which the stresses do not vary through the thickness. At any point on the vessel, the in-plane membrane loads are a combination of: (a) those due to internal pressure (determinable if the local radii of curvatures of the membrane are known), and (b) those due to thrust and bending of the shell body (determinable if the shell thickness is known). For example, in the simplified case shown in Figure 2, in the cylindrical section the hoop and axial membrane loads are given by Eq.'s (1) and (2):

$$(1) \text{ Hoop Line Load} = N_H \text{ (lb/in.)} = N_{HP} = PR, \text{ lb/in.}$$

$$(2) \text{ Axial Line Load} = N_A \text{ (lb/in.)} = N_{AP} \pm N_{AM} - N_{AT}, \\ = \frac{PR}{2} \pm \frac{M}{\pi R^2} - \frac{T}{2\pi R}, \text{ lb/in.}$$

where: P = motor design pressure = $(FS)(MEOP)$, psi

R = motor case radius, in.

M = case body bending moment = $(FS)(\text{Limit Bending})$, in.-lb

T = motor design thrust $(FS)(\text{Limit Thrust})$, lb

If the motor case were of metal, the wall thickness could be quickly determined by Eq. (3):

$$(3) \quad t_{\min.} = \frac{N_{\max.}}{\sigma_{\text{allow.}}}$$

$t_{\min.}$ = case wall design thickness

$N_{\max.}$ = N_H or N_A

$\sigma_{\text{allow.}}$ = allowable metal design stress

since metals are homogeneous and isotropic; i.e., their properties are essentially the same at all points and uniform in all directions.

Composites are highly inhomogeneous and anisotropic. Their properties vary considerably with location and direction, variations which may often be used to the designer's advantage.

COMPOSITE MATERIALS AND CONSTRUCTION

Composites are "laminates" of unidirectional "lamina" (Figure 3). The lamina, the basic building block, is a ply of continuous fibers lying side-by-side, parallel, and essentially one fiber thick. The fiber is bound together by a resin matrix. The resin matrix performs the critical functions of holding the fibers in place and transferring stresses from fiber-to-fiber through shear. The structural behavior of this "composite" of fiber and resin is dominated by the fiber.

Properties are highly directional, as compared with metals (Tables I and II). Unlike metals, composites are non-yielding and quite unforgiving of stress risers or local overloads.

The composite lamina is very strong and stiff in the direction of the fiber but is comparatively quite weak in other directions where only the resin matrix is available to resist loads. Accordingly, the designer must be sure to place adequate amounts of fiber in all load directions but has the distinct advantage of having to place at a given point only the amounts and in the directions required by the load state at that point. That is, the composite structure may be optimally designed.

A "laminate" consists of stacking plies of lamina to achieve a desired strength or stiffness. The resulting directional strength and stiffness is very dependent on the stackup. (Figure 4).

The composite motor case designer/analyst requires an extensive material property data base, one which recognizes that the strengths and stiffnesses of a given composite can vary substantially with temperature, moisture content, and time.

The theoretical strength of a given fiber--as measured by a strand or "tow" test--is seldom realized in a pressure vessel (primarily due to less than perfect fiber collimation). The "delivered strength" often varies significantly with changes in winding resin. Since the "deliverable fiber strength" must be known before even a preliminary design can be developed, various laboratory specimens have been utilized to provide design data. Resin coated strands, unidirectional "dogbones" cut from layed-up plates, filament wound rings and actual pressure vessels have been employed. Only the latter have provided reasonably satisfactory results and even then significant size scale effects occur and verification typically requires the bursting of full scale cases.

For detailed analysis purposes, the constitute stiffnesses E_{11} , E_{22} , G_{12} , and μ_{12} are required to be known for each lamina material at each temperature which must be evaluated. Corresponding strengths are required to allow calculation of margins of safety. These properties may be generated by means of fairly large numbers of small scale laboratory specimens like dogbones and plates. Since most such specimens are not really "filament windable", press cured plates are often used, resulting in some parameters like compressive and shear stresses and strengths of the specimen differing somewhat from those in the wound vessel.

The complexity of determining allowable strengths, in tension, compression and shear, and encompassing all environmental exposure conditions, results in major emphasis being placed on: (a) in-process control during case manufacture to assure unit-to-unit variability is minimized, and (b) proof and ultimate structural testing of full scale cases to verify design margin.

FILAMENT WOUND MOTOR CASES

The basic approach used for fabricating composite motor cases is "filament winding" (Figure 5), placing alternating layers of "helix" or "polar" wraps with "90°" or "hoop" wraps onto a mandrel shaped to form the desired case interior profile. The helix or polar wraps carry all of the axial membrane load and, to an extent depending on the "winding" or "wrap" angle, α , a portion of the hoop membrane load. That portion of the hoop load beyond the hoop-capacity of the helix wraps is then carried by the hoop wraps. The helix layers encompass the entire vessel surface--cylinder and ends--like a cocoon, while the hoops cover only the cylindrical section. Once all helices and hoops are in place, the matrix resin is cured, either thermally or by microwave, and the mandrel removed, leaving a rigid lightweight vessel.

The fiber is placed or "wound" as a continuous "band" consisting of several "tows" or "rovings" of fiber placed side-by-side--one tow coming from each spool of fiber as packaged by the fiber manufacturer. The bandwidth and "band density" (thickness) is a design variable which may be selected to result in thick or thin layers and wide or narrow bands. The fiber may be "wet wound"; i.e., passed as a dry fiber through a resin bath while the winding operation is occurring. An alternate approach is to use "prepregged" tow--fiber which has already been saturated (impregnated) with matrix material (resin) and the resin partially cured (B-staged) to a handleable condition but being under cured to the extent that it will reflow during elevated temperature cure. This latter characteristic allows for uniform fiber tensioning (collimation) due to mandrel expansion before resin set.

Domes and the Helix Angle - The partially or totally closed ends of filament wound motor cases are called "domes" and are very efficient structural closures. Proper dome design is a major design feature of filament wound cases and is the determining factor in defining what the helix winding angle must be for the cylindrical section. The polar opening diameter in relation to the cylinder diameter sets the angle which the helix band must have as it crosses the "dome tangent" the junction of cylinder and dome (Figure 6). The larger the polar opening and the wider the bandwidth in relation to the cylinder diameter, the higher the helix angle at the tangent must be. Large polar openings (greater than 60-70% of the vessel diameter) are severely stressed and structurally untenable.

Crossing the tangent at any other angle than the theoretically correct one defined by Eq. (4):

$$(4) \quad \alpha = \arcsin \frac{R_P + BW/2}{R_E}$$

will result in the fiber band wanting to slip sideways since the theoretically correct angle is also the "geodesic" or friction-free path angle. Further, a unique dome shape (Figure 7) may be defined which is "geodesic" along its entire path and also results in an "isotensoid" condition--constant tension stress in all fibers at all points when the vessel is pressure loaded. This unique dome shape and specific winding angle cannot be

substantially deviated from if a high strength structurally well-behaved composite dome is to result. The isotenoid condition drives most or all of the membrane load into the strong and stiff fiber and away from the much weaker resin. The properly designed dome utilizes the variations in local hoop and meridional radii of curvature to offset fiber thickness build up and angle change (low to high--90° at the pole) to maintain constant fiber stress. This is attained by increasing the meridional radius of curvature to offset the propensity for decreased stress with decreasing diameter and increasing fiber thickness in moving from the tangent to the pole.

Since the typical case has a different size polar opening at the two ends and a constant body diameter, a helix angle perfect for one dome cannot be perfect for the other unless it changes along the body--a condition which can be utilized to only a quite limited extent unless wasteful building of helix thickness at one end can be tolerated. In practice, within limits, the helix angle crossing the tangent can be one which is "deviated"; i.e., different from the theoretical, by a few degrees. The result will be a variation in stress in each individual filament as it traces its path over the dome, the variation in fiber or filament stress being accommodated by shear stresses in the resin. Therefore, both domes are typically "deviated" by small amounts. If the cylinder is long relative to the diameter, a gradual change in helix angle from one end to the other may also be utilized. To the designer, this means that he is not free to choose one polar opening size independent of the other.

The detailed design and analysis of practical domes--particularly as complicated by the presence of skirts causing local large stiffness gradients and bending stresses--constitute much of the design challenge for composite cases.

Skirts - Skirts, cylindrical extensions of the case body, typically must carry appreciable mechanical loads. They are basically rigid tubes or rings which must be attached to the relatively flexible case body "membrane" without creating unacceptable stress risers due to locally increased stiffness and in-plane bending (Figure 8). Their behavior, even with the aid of sophisticated finite element design/analysis codes, remains quite difficult to predict. Empiricism in design and full scale testing are still much used for this feature.

DESIGNING THE CASE WALL

When the nominal cylindrical winding angle is established, the thicknesses of hoop and helix composite necessary to carry the body membrane loads may be determined by "netting design"; i.e., by assuming that all of the membrane load is carried by the fibers alone (E_{22} , G_{12} , $\nu_{12} = 0$). Any required reinforcements are similarly preliminarily designed for regions where concentrated loads or local discontinuities occur (skirts, attach lugs, T.T. ports, pole piece regions, etc.). Once the preliminary design is established, iterative design/analysis utilizing powerful finite element computational codes and extensive materials models and data bases are used to refine the design. The analysis codes, materials models and data bases are typically proprietary to the designing company.

For a vessel composed of helix layers at a winding angle of α and hoop layers at 90°, the required thicknesses of hoop fiber t'_{90} and helix fiber t'_{α} of strength σ'_{90} and σ'_{α} may be predicted by Eq.'s (5) and (6):

$$(5) \quad t'_{\alpha} = \frac{N_{\phi}}{\sigma'_{\alpha} \cos^2 \alpha}$$

$$(6) \quad t'_{90} = \frac{N_{\theta} - N_{\phi} \tan^2 \alpha}{\sigma'_{90}}$$

where: t'_{α} = total equivalent helix fiber thickness, in.

t'_{90} = total equivalent hoop fiber thickness, in.

σ'_{α} = helix fiber tensile strength, psi

σ'_{90} = hoop fiber tensile strength, psi

N_{ϕ} = meridional (axial) line load, lb/in.

N_{θ} = hoop line load, lb/in.

When the total required fiber thicknesses are ascertained, the designer determines the number of hoop and helix composite layers by selecting layer thicknesses. Note that the values t' are for "fiber only" and do not include resin. Total composite thickness will depend on the final in-situ resin content which is dependent on processing variables like winding tension, diameter, and winding angle. A typical value is 40% resin by volume.

A DESIGN EXAMPLE

Determine the required hoop and helix thicknesses for a 12-in. diameter cylindrical composite vessel, subjected to pressure only, to achieve a burst pressure of 4000 psi.

Assume the helix winding angle is 25° and a 60% fiber volume (V_f) is achieved. The fiber is graphite with a hoop fiber strength of 600 ksi and a helix fiber strength of 500 ksi.

For pressure only, the axial and hoop membrane loads are as shown by Eq.'s (7), (8), (9), and (10):

$$(7) \quad N_\phi = \frac{PR}{2} = \text{axial membrane load}$$

$$(8) \quad N_\theta = PR = \text{hoop membrane load}$$

$$(9) \quad t'_\alpha = \frac{N_\phi}{\sigma'_\alpha \cos^2 \alpha} = \frac{PR}{2\sigma'_\alpha \cos^2 \alpha}$$

$$= \frac{(4000 \text{ lb/in.}^2)(6 \text{ in.})}{2(500,000 \text{ lb/in.}^2) \cos^2 25^\circ} = 0.029 \text{ in.}$$

$$(10) \quad t'_{90} = \frac{N_\theta - N_\phi \tan^2 \alpha}{\sigma'_{90}} = \frac{PR - \frac{PR}{2} (\tan^2 \alpha)}{\sigma'_{90}}$$

$$= \frac{PR (1 - 0.5 \tan^2 \alpha)}{\sigma'_{90}} = \frac{(4000 \text{ lb/in.}^2)(6 \text{ in.})(1 - 0.5 \tan^2 25^\circ)}{(600,000 \text{ lb/in.}^2)}$$

$$= 0.036 \text{ in.}$$

For a 60% fiber volume, the corresponding composite hoop and helix thicknesses are shown by Eq.'s (11) and (12):

$$(11) \quad t_\alpha = 0.029/0.6 = 0.049$$

$$(12) \quad t_{90} = 0.036/0.6 = 0.060$$

$$0.109 \text{ in.}$$

The density of the composite, ρ_C , is given by Eq. (13):

$$(13) \quad \rho_C = V_f \rho_f + V_R \rho_R = (0.6)(0.065) + (0.4)(0.043) = 0.056 \text{ lb/in.}^3$$

and the weight per inch of cylinder is given by Eq. (14):

$$(14) \quad \omega = \pi D t \rho = (\pi)(12)(0.109)(0.056) = 0.23 \text{ lb/in.}$$

A comparable high strength steel case of, say, D6AC steel at an ultimate strength of 225 ksi would require a wall thickness as given by Eq. (15):

$$(15) \quad t = PR/\sigma = 4000 \times 6/225,000 = 0.107 \text{ in.}$$

which would result in a weight per inch of cylinder as given by Eq. (16):

$$(16) \quad \omega = (\pi)(12)(0.283)(0.107) = 1.14 \text{ lb/in.}$$

or five times as much.

COMPOSITE MATERIALS TECHNOLOGY

A wide range of fiber and matrix materials are available. Fibers include glass, Kevlar and graphite/carbon (Table III). An epoxy resin is typically used as the matrix material but emerging requirements for structural performance at higher temperatures is creating interest in more exotic resins like the polyimides for some uses.

Fiberglass was used for most earlier applications (Polaris, C3 Poseidon). It is relatively high density but inexpensive. Kevlar, much lower in density and higher in specific strength, is presently in wide use (Trident C4, Pershing II, Peacekeeper). The graphite/carbon fibers have improved dramatically in recent years and, while slightly higher in density than Kevlar, their substantially higher delivered fiber strength in pressure vessels and consequently higher specific strength makes them the frequent materials of choice today.

Conventional bisphenol-A based epoxies continue to dominate matrix technology. They are inexpensive and easily processed either as a prepreg or a wet wind. These resins do soften at temperatures beyond 300-350°F. Vessel pressure carrying capability is reasonably well retained even somewhat beyond these temperatures. However, composite compression and shear strengths essentially disappear at or somewhat beyond the "Heat Distortion Temperature", the temperature at which a cured resin experiences a sharp

drop-off of mechanical properties. External and internal insulators are used to maintain case wall temperatures low enough to assure structural performance.

Polymeric materials exist which possess superior high temperature capabilities (Table IV). These materials are substantially more difficult to process, typically requiring the use of an autoclave, and attempts to use them for wound pressure vessels have resulted in reduced burst strength with a given fiber as compared with that attained with a conventional epoxy, so they cannot be considered state-of-the-art today.

QUALITY CONTROL AND VERIFICATION

The hydroproof test is widely utilized as the final determinant of the acceptability of a given motor case. Of course, during manufacture, material and component quality and consistency of manufacturing processes are rigidly controlled. Non-destructive testing techniques like X-ray, and to a lesser extent ultrasonics and acoustic emission, are used to establish unit-to-unit "fingerprints" but the ultimate determinant of a "good" case is the passing of hydroproof.

Strain gages are widely utilized at key stress points for routine proof testing. The strains are compared with the body of data from prior units for any significant deviation.

Hydroproof testing can and often does include the application of limit levels of other load conditions like thrust and bending. Once a case design is established by initial structural tests, typically several more cases are destructively ultimate tested to establish variability and design margins.

THE CHALLENGE, THE PAY-OFF AND THE FUTURE

The rocket motor designer is always being challenged to minimize the weight of the inert components. The case designer is confronted with a wide array of approaches and choices. Metals are rugged and durable, have long case histories and extensive data bases, are relatively simple to design with, and possess the ability to accommodate local overloads and stress risers through yielding--but metal cases are heavy. Structural composites provide much lighter cases, but the designer is obligated to understand and design to accommodate the non-homogeneity, anisotropy and non-yielding stress-strain behavior of the materials. They are also more temperature and environmental sensitive than metals. The pay-off is large if the designer understands the material behavior and is willing to master the design skills.

Composite cases have been state-of-the-art in the U.S. for strategic solid rockets for 30 years--due to their superior performance. They are now beginning to be used for tactical rocket cases because material and fabrication costs are becoming competitive, the material and design advances allow accommodation of the substantially more severe use environment, and the performance requirements of emerging systems require the improved performance.

TABLE I
METAL MATERIAL PROPERTIES

Material	Constitutive Properties			Density, ρ (lb/in. ³)	Tensile Strength, σ (ksi)	Specific Strength, σ/ρ
	E (msi)	G (msi)	μ			
AISI 4130 Steel	29.0	11.0	0.32	0.283	180	0.64×10^{-6}
D6AC Steel	29.0	11.0	0.32	0.283	220	0.78×10^{-6}
7075-T6 Aluminum	10.3	3.9	0.33	0.101	80	0.79×10^{-6}
64 Titanium	16.0	6.2	0.31	0.160	160	1.00×10^{-6}

TABLE II
FIBER, MATRIX AND COMPOSITE MATERIAL PROPERTIES

Material		Constitutive Properties				Strength			ρ lb/in. ³	σ_{11}/ρ 10 ⁶ in.
		E ₁₁ msi	E ₂₂ msi	G ₁₂ msi	μ_{12}	$\sigma_{11,T}$ ksi	$\sigma_{22,T}$ ksi	τ_{12} ksi		
FIBER	E-Glass	10.5	10.5	4.2	0.25	280.0	--	--	0.090	3.1
	S2 Glass	12.6	12.6	5.2	0.22	450.0	--	--	0.092	4.9
	Kevlar-49	18.0	0.6	0.4	0.30	370.0	--	--	0.052	7.1
	Graphite, IM	42.0	2.2	3.5	0.20	560.0	--	--	0.065	8.6
RESIN	Epoxy	0.4	0.4	0.2	0.38	12.0	12.0	7.5	0.043	0.3
LAMINA	E-Glass	6.7	1.8	0.8	0.25	150.0	6.0	6.0	0.070	2.1
	S2 Glass	8.8	1.9	0.9	0.30	250.0	9.9	8.8	0.072	3.5
	Kevlar-49	11.8	0.8	0.3	0.34	190.0	2.9	5.4	0.050	3.8
	Graphite, IM	25.2	1.3	0.6	0.30	340.0	9.6	10.2	0.56	6.1

TABLE III
REPRESENTATIVE FIBER AND COMPOSITE PROPERTIES

Material	Tow Properties					Pressure Vessel			Unidirectional Laminate	
	σ	E	ρ	$\$/lb$	σ/ρ 10^6 in.	Hoop Fiber Strength	PR/t	E_{axial} msi	σ_{11c} ksi	τ_{12} ksi
E-Glass	300	10.5	0.090	0.75	3.33	280	105	3.2	85.0	12.0
S2 Glass	550	12.6	0.092	5.00	5.98	450	170	3.8	100.0	13.5
Kevlar-49	545	18.0	0.052	18.00	10.48	370	140	4.1	40.0	6.0
Graphite, AS	580	34.0	0.065	21.00	8.92	480	180	8.0	200.0	17.5
Graphite, IM	700	42.0	0.065	31.00	10.77	560	210	9.3	200.0	17.5

TABLE IV
MATRIX RESINS

Material	Designa- tion	Heat Deflec. Temp. °F	Density lb/in. ³	Composite Compressive Strength, ksi					Utilization
				-65°F	77°F	250°F	450°F	600°F	
Bisphenol-A Epoxy	Hercules HBRF-55A	260	0.044	200	175	125	--	--	Trident
Epoxy Novalac	Hercules HARF-7A	400	0.041	155	130	105	--	--	Development Motors
Polyimide	PMR-15	680	0.047	75	62	59	50	40	Experimental

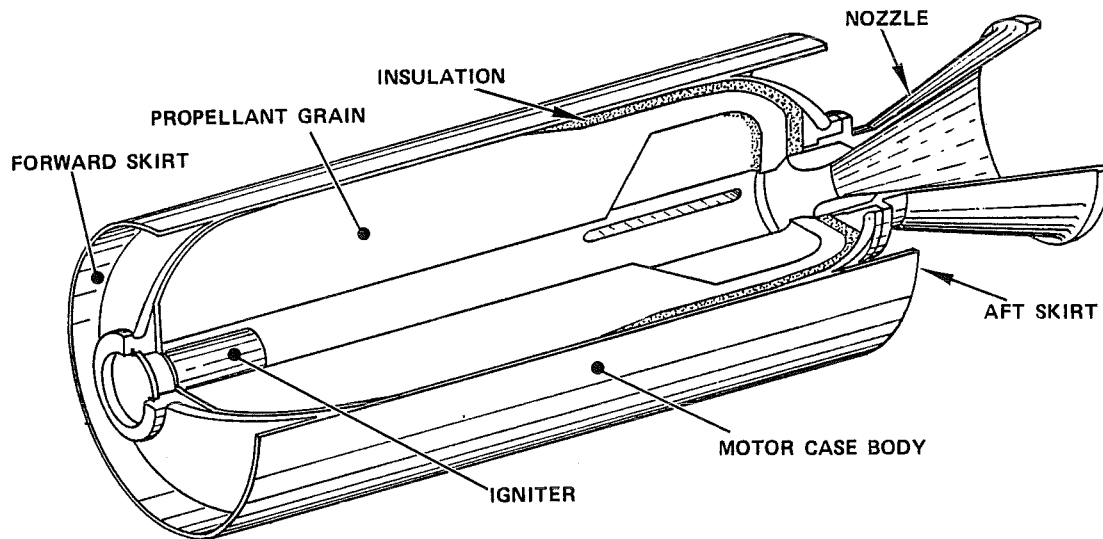


FIGURE 1. The Typical Rocket Motor Case Is A Double-Domed Cylindrical Pressure Vessel

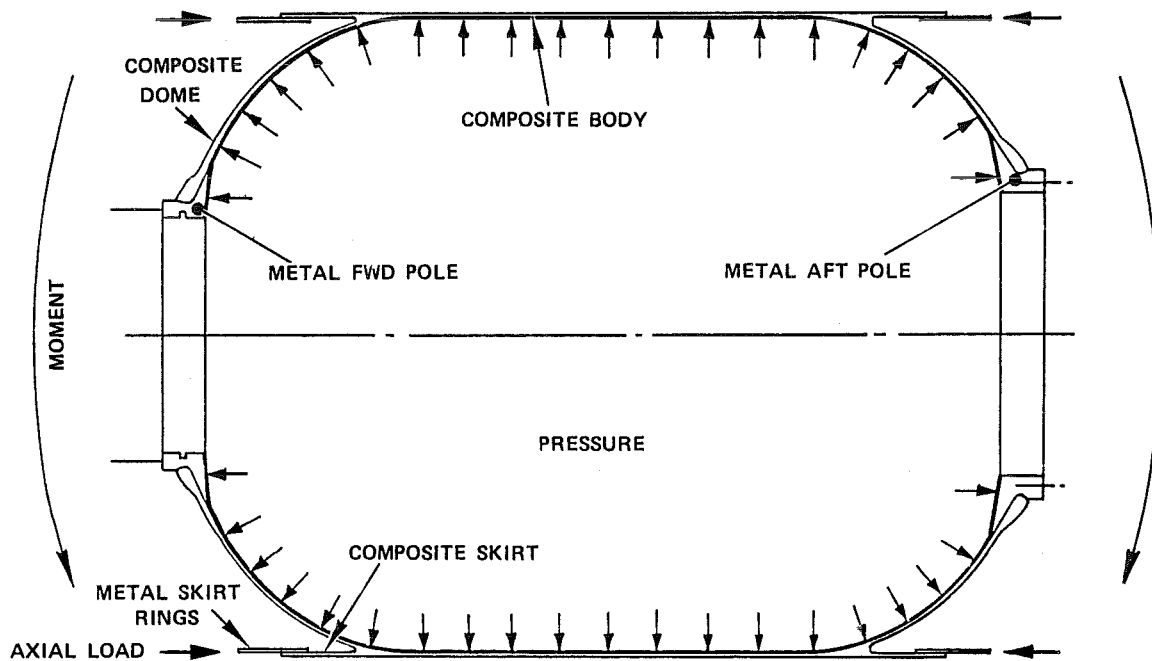


FIGURE 2. The Motor Case May Be Treated As A Membrane For Preliminary Design

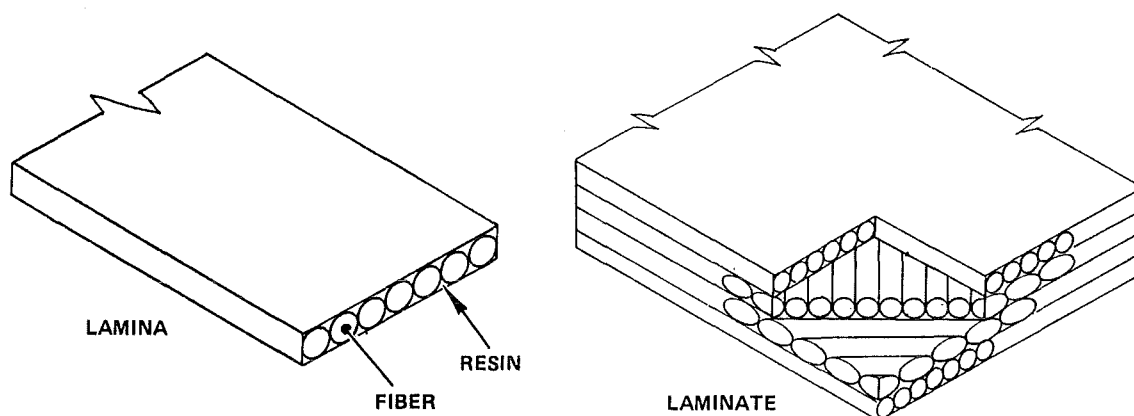


FIGURE 3. Laminate Composite Construction

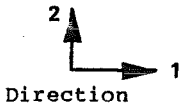
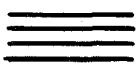



	Fiber Orientation	Laminate Properties			
		E_{11} msi	E_{22} msi	G_{12} msi	σ_{11} ksi
	0°	25.2	1.3	0.6	340.0
	90°	1.3	25.2	0.6	9.6
	$\pm 45^\circ$	2.2	2.2	6.5	170.0
	$0, 90^\circ$	13.3	13.3	0.6	170.0

FIGURE 4. Laminate Properties Depend On Stack-Up

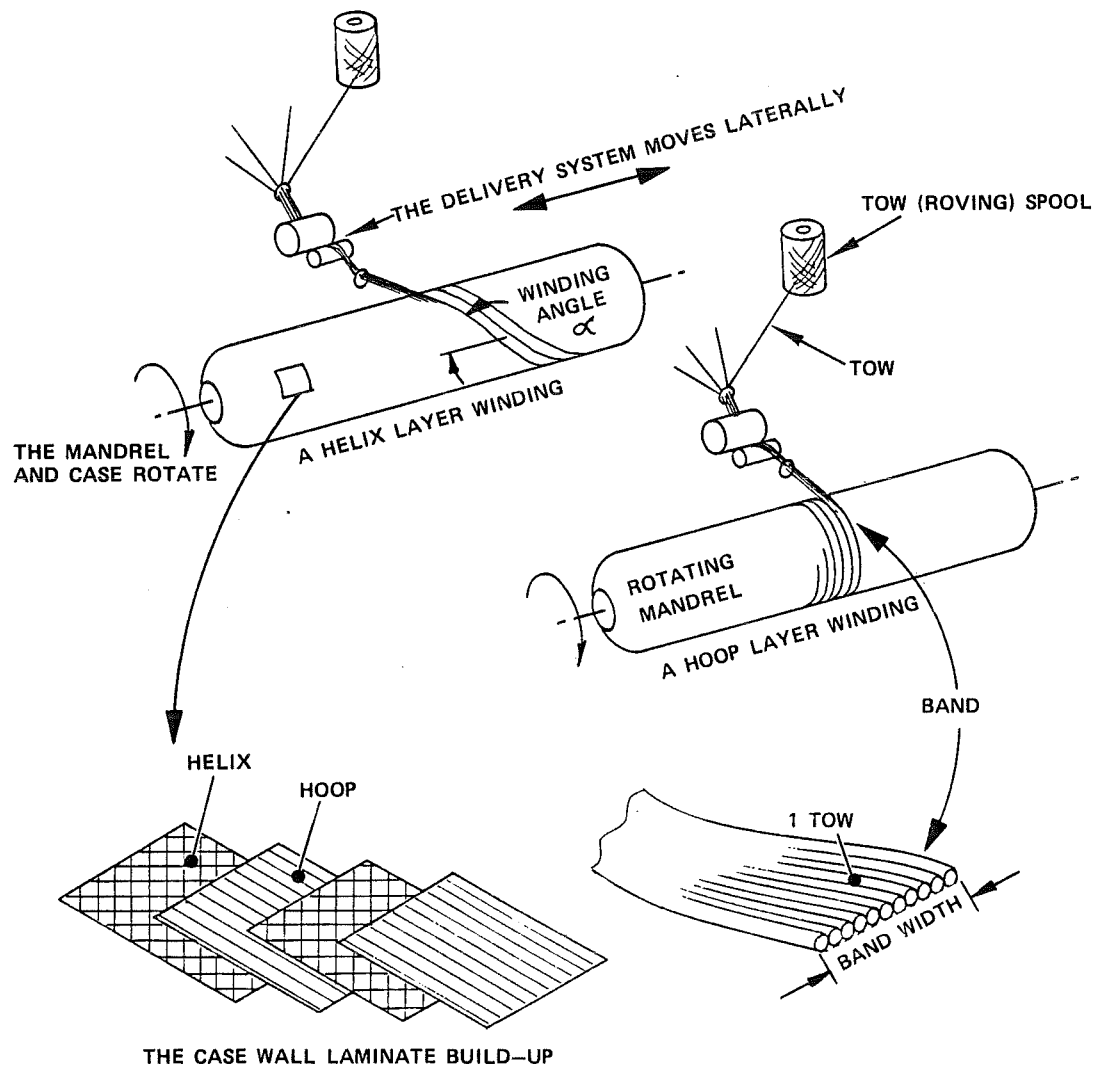


FIGURE 5. Composite Cases Are Wound Of Alternating Layers Of Hoop & Helix Material

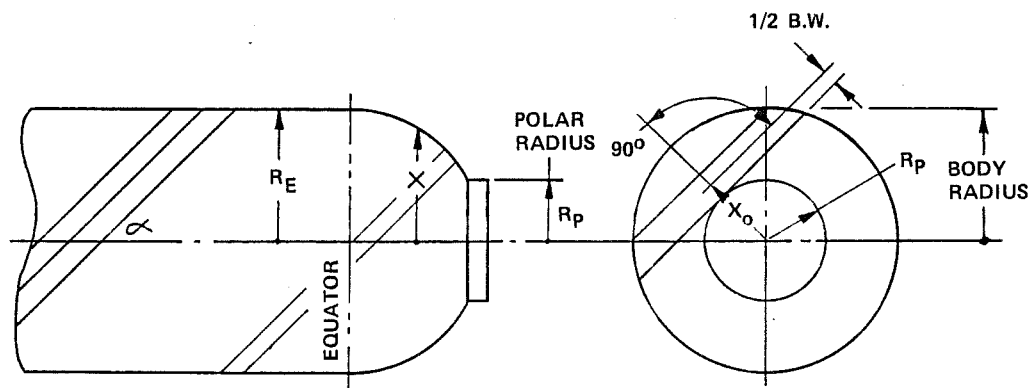


FIGURE 6. The Relative Diameters Of Polar Opening And Case Body Determine The Helix Winding Angle

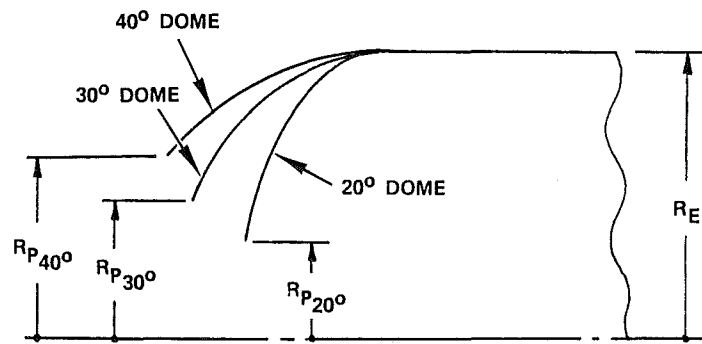


FIGURE 7. The Isotenoid Dome Shape Depends On The Body Helix Angle

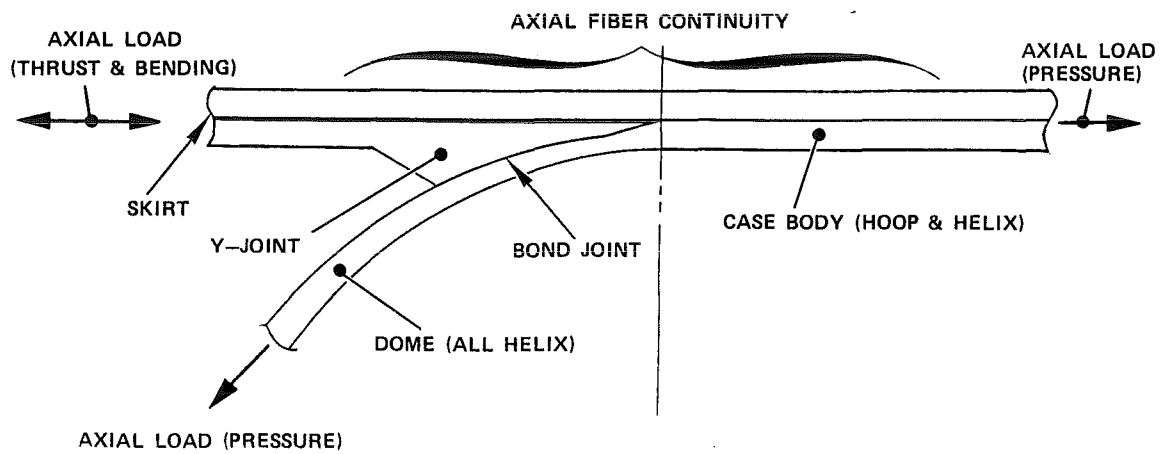


FIGURE 8. Skirts Are Attached By Bond Joints And Fiber Overwraps

DESIGN OF FILAMENT-WOUND ROCKET CASES

by

J.P. DENOST

Head of Programs for Filament-Wound Structures

AEROSPATIALE

St-Médard-en-Jalles

33165

FRANCE.

ABSTRACT

Our Company began developing methods for the design and sizing of filament-wound rocket cases in the early 1970's. Such methods have since evolved to the extent that rapid design and precise verification means are now available.

The purpose of this document is to outline these two approaches, to criticize them and to evidence their complementarity. Detailed presentations will be given to enable the reader to grasp the principal rules, and to gain such information as will enable him to develop them in specific fields.

This predominantly theoretical part will be completed by considerations relating to materials, their implementation and performances, and by a description of the major principles of fabrication of this type of structure.

NOTATIONS

A = area of a straight cross-section of the filament.

$\vec{b} = \vec{t} \wedge \vec{n}$.

$\vec{b}_S = \vec{t} \wedge \vec{n}_S$.

c = curvature of (Γ) in M ; $c > 0$.

C_1, C_2 = main centers of curvature of (S) in M .

$D = (1 + \rho'^2)^{\frac{1}{2}}$

d = symbol of derivation.

e = thickness of the vessel in M .

\vec{F} = action of the mandrel on the filament, by filament unit length.

g = terrestrial constant of gravitation.

H = orthogonal projection of M on the revolution axis of (S) .

$k = tg\gamma$.

L = axial distance between the two polar openings of the vessel.

M = running points of (Γ) and of (S) .

m = mass of the vessel.

\vec{n} = unit vector of the main positive semi-norm of (Γ) in M .

N = number of filaments cut per unit length of a parallel.

\vec{n}_S = unit vector of the internal semi-norm at (S) in M .

N_ϕ = value in M of the internal membrane stress in the direction of \vec{t}_ϕ , by unit length of the parallel; for tensile stress: $N_\phi > 0$.

N_θ = value in M of the internal membrane stress in the direction of \vec{t}_θ , by unit length of the meridian; for tensile stress: $N_\theta > 0$.

O = point of origin of the datum mark (x, y, z) ; situated in the plane of junction between the head and the cylindrical part.

p = value of internal pressure; $p > 0$.

$q = \frac{pV}{mg}$.

R_1, R_2 = principal radii of curvature of (S) in M ; $R_i = MC_i \cdot \vec{n}_S$ ($i = 1, 2$).

s = curvilinear abscissa of M on (Γ) oriented.

S = mean surface of the vessel; revolution surface where the concavity of the meridian is turned towards the axis of revolution.

- \vec{t} = unit vector of the positive semi-tangent of (Γ) in M ; $\vec{t} \cdot \vec{z} > 0$.
 T = value of tension in the filament ; $T > 0$.
 \vec{t}_ϕ = unit vector of the positive semi-tangent of the meridian in M ; $\vec{t}_\phi \cdot \vec{z} > 0$.
 \vec{t}_θ = unit vector of the positive semi-tangent of the parallel in M oriented by \vec{z} .
 u = ρ' .
 v = $\frac{\rho}{\rho_o}$.
 V = internal volume of the vessel.
 x, y, z = coordinates of M in relation to the general datum mark.
 $(\vec{x}, \vec{y}, \vec{z})$ = direct orthonormal base of the general datum mark ; \vec{z} : carried by the axis of revolution of (S) .
 α = measurement in radians of the angle of the pair of vectors (\vec{t}_ϕ, \vec{t}) ; if $(\vec{t}_\phi \wedge \vec{t}) \cdot \vec{n}_s > 0$:
 $0 < \alpha < \frac{\pi}{2}$.
 Γ = curve represented by the filament.
 θ = measurement in radians of the angle of the pair of vectors (\vec{x}, \vec{HM}) ; $\theta = \int_{M_0}^M \theta' dz$,
 θ' being expressed by the relation (36).
 λ = $\vec{F} \cdot \vec{t}$.
 μ = $\vec{F} \cdot \vec{n}_s$.
 v = $\vec{F} \cdot \vec{b}_s$.
 ρ = HM .
 ρ_{F_1}, ρ_{F_2} = radii of the polar openings of the two heads.
 σ_f = stress in the filament ; $\sigma_f = \frac{T}{A}$.
 ϕ = measurement in radians of the angle of the pair of vectors $(\vec{z}, -\vec{n}_s)$; if $(\vec{n}_s \wedge \vec{z}) \cdot \vec{t}_\theta > 0$:
 $0 < \phi < \pi$.
 χ = titer by volume of fiber in the composite.
 Ψ = measurement in radians of the angle of the pair of vectors (\vec{n}_s, \vec{n}) ; if $(\vec{n}_s \wedge \vec{n}) \cdot \vec{t} > 0$:
 $0 < \Psi < \frac{\pi}{2}$.

Particular notations :

- $()'$ = symbol of derivation in relation to the variable z .
 o = index affecting all parameters evaluated for $z = 0$.

1. INTRODUCTION

Filament-winding technology has been in use now for approximately 25 years in the fabrication of the rocket cases of the various French programs.

Such programs have been civilian (DIAMANT) and military (MSBS, SSBS).

This technology has essentially made it possible to replace metal by composites, thus reducing the inert weight to the benefit of the range of the carrier. Furthermore, filament winding is an automated fabrication method providing simultaneously rapidity, economy and quality.

Resin impregnated fibers have evolved over the years. The initial structures were made with glass fiber. Subsequently, Kevlar appeared, and more recently carbon. Each development has served to further reinforce the advantage of composites over metal.

While the production facilities installed evolved rapidly to meet the requirements mainly of military program, design facilities have been perfected more progressively.

In the early 1960's, the definition of a structure was obtained by predominantly empirical methods. Experimentation made it possible to obtain a product meeting requirements. Some years were necessary for designers to exert their skills in this field, starting by the establishment of relatively simple methods in the latter part of the 1960's.

The development of data-processing in France, and later the appearance of calculation programs gradually led to the sophisticated working methods of the mid-1970's. Finally, today, stress is laid on computerized design (CAD) and more recently on the connection possible between CAD and CAM. Nevertheless, so-called "light-weight" methods, geared to providing rapid answers to questions which do not immediately require a high degree of precision and above all to enabling operators not to lose the understanding of the physical phenomena, are still being developed and used.

Concomitantly, with calculations requiring an ever-increasing number of characteristics, characterization programs were established by designers for filament-wound composites, giving rise to major research efforts providing a constant level of activity for Materials and Trials Laboratories.

The main purpose of this document is to present the methods of design and justification of filament-wound rocket cases. A critical analysis of the so-called "light-weight" methods and of computer facilities will serve to demonstrate how our Company uses them complementarily.

This will take up the major part, but short chapters clearly had to be included to present on the one hand how problems are posed, generally, and on the other hand to present methods of fabrication and experimental certification.

Finally, reverting to calculations, a few basic mathematical notions must be developed, in as condensed a form as possible, to enable the reader to understand, without wearying him, the aim being to provide the few basic notions necessary to enable anyone who so wishes to develop models geared to his specific applications.

2. STATEMENT OF THE PROBLEM

2.1 DESCRIPTION OF THE CASE

An illustration of the main sub-assemblies of the case is necessary for a better understanding of what is to follow. This is given in Figure 1 below.

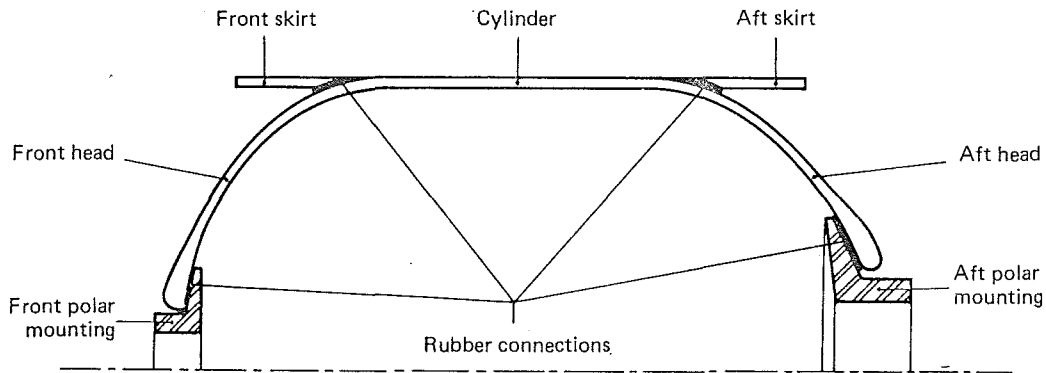


Figure 1

This illustration shows details of :

- the two skirts, which are two short cylinders, connecting the shell of the case with the rest of the carrier,
- the cylinder and the two heads, both filament-wound, the principles of design and of justification of which will be presented below,
- the two metal polar mountings, which reinforce the openings and provide connection with other components, such as the igniter plug forward and the nozzle aft,
- rubber connections between the vessel and the skirts on the one hand and between the vessel and the polar mountings on the other hand.

The vessel (the cylindrical part and the heads) are thus filament-wound. In this phase of fabrication, two types of winding are employed :

- firstly, so-called "satellite" winding, to make up the two heads and the cylinder, by a succession of loops tangential to the two openings,
- secondly, so-called "circumferential" winding, on the cylindrical part only in such a way that the filaments are laid practically perpendicular to the generatrices.

2.2 MAIN SPECIFICATIONS

The technical specifications of such a product are given in a detailed and voluminous document from which we have drawn the main elements.

2.2.1 RESISTANCE TO MECHANICAL STRESS

Mechanical stresses come from the internal pressure exerted by combustion of the powder upon operation of the stage involved, and from the tensile and flexural stresses born mainly by the skirts during the carrier's lifetime.

Moreover, thermal stresses have to be taken into account during the propulsion phases.

Certification regulations associated with these stresses are such that the structure, as new, must have a safety coefficient of : $K > 1.4$.

Furthermore, the various sub-assemblies must remain in the elastic field for loads equal to 1.15 times the nominal loads. This latter specification is verified experimentally for each specimen prior to delivery to the end-customer.

2.2.2 AGING

Each specimen manufactured must be capable of fulfilling all its functions with a probability over a minimum value throughout its operational lifetime.

2.2.3 GEOMETRY

Geometric specifications are laid down in order to :

- meet the maximum dimensions set both for when at rest and in operation,
- ensure interface conditions with the rest of the carrier.

2.2.4 FILLING WITH POWDER

Structural integrity must be maintained throughout the filling phase. Briefly, this involves both temperature and internal pressure stresses over a fixed period of time.

2.3 RESISTANCE TO INTERNAL OPERATING PRESSURE

In this document, we shall deal with the design and justification of such a structure when submitted to what is in all cases the greatest stress : that of internal pressure due to the combustion of the powder during the operation of the stage involved.

Moreover, whilst numerous components are subjected to stress from this internal pressure, the most critical sub-assembly for optimisation is the cylindrical part and the two heads, which is why particular attention will be given in the following paragraphs to detailing their design and justification.

Problems relating to the skirts will not be dealt with, given their low weight and given the conventional notions familiar to any designer. On the other hand, the design of the aft polar mounting will be briefly presented as its mass occasionally makes optimisation necessary.

2.4 STATEMENT OF THE PROBLEM SPECIFIC TO FILAMENT WINDING

The filament-wound cylindrical part is designed very simply, by determining the respective thicknesses of the two windings involved required to ensure the proper resistance to internal pressure. The calculation method will be presented in a specific paragraph.

The problem of the design of the two heads is quite different. The shape of each head, and the trajectory of the filaments on the head have to be determined simultaneously to provide for their optimized fabrication.

The figure below illustrates the notations given at the beginning of this document, and how the problem is posed.

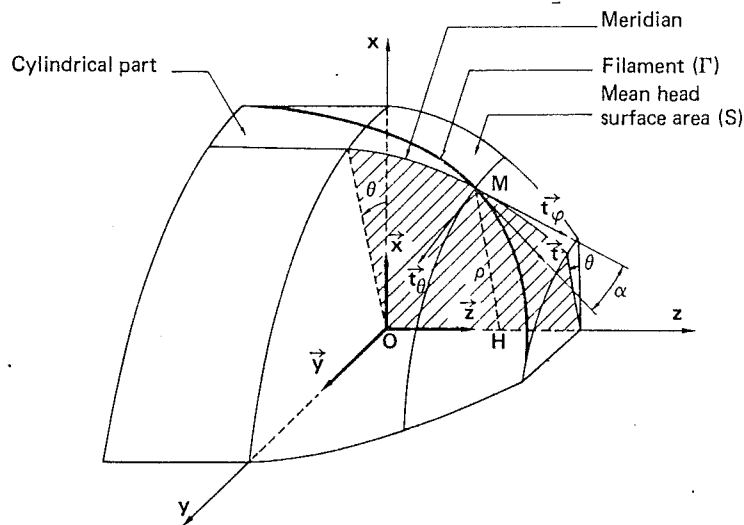


Figure 2

The shape of the vessel is defined by the function $\rho(z)$. The lay-up of the filament during winding, i.e. the line (Γ) , is defined by the function $\alpha(z)$.

The problem thus includes two unknown functions. Two conditions involving these two functions will therefore be necessary. The following chapters will reveal how this has led to the development of different design methods.

3. DESIGN

A separation will be made in design methods between :

- the cylindrical filament-wound part,
- the filament-wound part on the heads.

We shall take here the term "net method" to cover the theoretical notions to be developed. With this method, we shall consider that at any given point the filament-wound structure has stiffness and resistance only in the direction of the filaments, to the exclusion of any other direction.

3.1 ANALYSIS OF THE CYLINDRICAL PART

Given the notations, we can write :

$$N_{\phi} = N_{\phi s} + N_{\phi c} , \quad (1)$$

$$N_{\theta} = N_{\theta s} + N_{\theta c} . \quad (2)$$

With :

$$N_{\phi} = \frac{PR}{2} ,$$

$$N_{\theta} = PR .$$

Furthermore, the basic hypothesis of the net method leads to :

$$N_{\phi c} = 0 . \quad (3)$$

The resultant of the stress $N_{\theta c}$ is easily expressed by :

$$N_{\theta c} = \chi e_c \sigma_{fc} . \quad (4)$$

For satellite winding, the figure shown below must be taken into account :

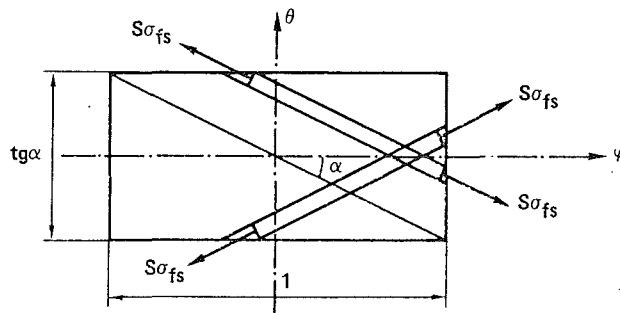


Figure 3

In view of the notations, the following can be expressed as shown in the figure :

$$N \operatorname{tg} \alpha \cdot S \sigma_{fs} \cos \alpha = N_{\phi s} \operatorname{tg} \alpha , \quad (5)$$

$$N \operatorname{tg} \alpha \cdot S \sigma_{fs} \sin \alpha = N_{\theta s} . \quad (6)$$

Moreover, it is possible to express the thickness of composite of the satellite winding by :

$$e_s = N \frac{S}{\chi \cos \alpha} . \quad (7)$$

Relations (5), (6) and (7) lead to :

$$N_{\phi s} = \chi e_s \sigma_{fs} \cos^2 \alpha , \quad (8)$$

$$N_{\theta s} = \chi e_s \sigma_{fs} \sin^2 \alpha . \quad (9)$$

Relations (1) and (2), by using the expressions of $N_{\phi s}$, $N_{\theta s}$, $N_{\phi c}$, $N_{\theta c}$, lead to :

$$\frac{PR}{2} = \chi e_s \sigma_{fs} \cos^2 \alpha \quad (R = \rho o) ,$$

$$PR = \chi e_s \sigma_{fs} \sin^2 \alpha + \chi e_c \sigma_{fc} .$$

These two relations make it possible to obtain the expression of stresses in the filaments of the two windings in the cylindrical part :

$$\sigma_{fs} = \frac{PR}{2 \chi e_s \cos^2 \alpha} , \quad (10)$$

$$\sigma_{fc} = \frac{PR}{\chi e_c} \left(1 - \frac{\operatorname{tg}^2 \alpha}{2} \right) . \quad (11)$$

The latter relations are widely used in designing the cylindrical part of the rocket tanks. They are simple and enable a rapid definition of the necessary thickness of composite material to obtain a level of stress imposed in the fibers.

N.B. :

a - If circumferential winding is eliminated, it can easily be deduced that the winding angle is to be such that :

$$\operatorname{tg}^2 \alpha = 2 \quad \text{i.e. } \alpha = 54.7^\circ .$$

It will be demonstrated later that the value of the winding angle α in the cylindrical part imposes the dimensions of the openings in the heads. To maintain geometric freedom on this point, it is therefore always necessary to perform a circumferential winding.

b - If the filaments belonging to both types of winding are subjected on the same level of stress, from (10) and (11) it can easily be deduced that :

$$\frac{e_c}{e_s} = 3 \cos^2 \alpha - 1 .$$

3.2 ANALYSIS OF THE HEADS

3.2.1 OUTLINE OF PRINCIPLES

The problem of defining thickness in the cylindrical part has been studied in the previous paragraph. The shape of the heads and the lay-up line of the filaments must now be defined. Paragraph 2.4 evidenced that two conditions are necessary to address the problem.

Three approaches will be detailed. Their presentation will follow in the same way as their chronological use ; this will make it possible to highlight the limits of each approach, the problems concretely encountered and what justified the move to the next method.

3.2.2 "ISOTENSOID" DESIGN

This is based on the following two conditions :

- the filaments alone counterbalance the stresses from internal pressure (net method),
- stress in the filaments is constant along their entire length.

3.2.2.1 EXPRESSION OF THE FIRST CONDITION

The heads being only in satellite winding, relations (8) and (9) lead to :

$$\frac{N_\theta}{N_\phi} = \operatorname{tg}^2 \alpha . \quad (12)$$

Moreover, it is supposed that the tank is subjected only to extension stresses. The expressions of N_θ and N_ϕ are then as follows :

$$N_\phi = \frac{PR_2}{2} , \quad (13)$$

$$N_\theta = \frac{PR_2}{2} \left(2 - \frac{R_2}{R_1} \right) . \quad (14)$$

Furthermore, it is easy to demonstrate that :

$$R_1 = - \frac{(1 + \rho'^2)^{3/2}}{\rho''} , \quad (15)$$

$$R_2 = \rho \sqrt{1 + \rho'^2} . \quad (16)$$

Thus, the final expression of the first condition (net method) is :

$$2 - \frac{R_2}{R_1} = \operatorname{tg}^2 \alpha \quad \text{i.e.,}$$

$$2 + \frac{\rho \rho''}{1 + \rho'^2} = \operatorname{tg}^2 \alpha . \quad (17)$$

3.2.2.2 EXPRESSION OF THE SECOND CONDITION

This second condition requires that the stress in the filament be constant. The expression of this stress is deduced from the relation (8).

$$\sigma_{fs} = \frac{N_\phi}{\chi e_s \cos^2 \alpha} . \quad (18)$$

To transform this expression into a suitable form, the local thickness of the tank wall must first be determined.

Relation (7) makes it possible to write :

$$e_s = N \frac{S}{\chi \cos \alpha} , \quad (\text{at any given point}),$$

$$e_{so} = N \frac{S}{\chi \cos \alpha_o} , \quad (\text{at the junction between one of the heads and the cylinder}).$$

Moreover, account is taken of the fact all the filaments which cut the parallel to the junction between head and cylinder also cut the parallel through the point considered. This is translated by :

$$2 \pi \rho N = 2 \pi \rho_0 N_0 .$$

This provides the relation which expresses the local thickness :

$$e_s = e_{s0} \frac{\rho_0 \cos \alpha_0}{\rho \cos \alpha} . \quad (19)$$

Whence, with the help of (13), (18) and (20) :

$$\sigma_{fs} = \frac{\rho \rho_0^2 \sqrt{1 + \rho_0'^2}}{2 \chi e_{s0} \rho_0 \cos \alpha_0 \cos \alpha} . \quad (20)$$

Requiring that the stress in the filament is constant therefore consists of writing the second condition in the following manner :

$$\rho^2 \frac{\sqrt{1 + \rho'^2}}{\cos \alpha} = K . \quad (21)$$

3.2.2.3 DETERMINATION OF THE MERIDIAN AND OF THE WINDING LAW

The meridian of the surface head (S) and the winding law are defined by the functions $\rho(z)$ and $\alpha(z)$ respectively.

The two functions are solutions of the differential system consisting of equations (17) and (21) recalled below :

$$\begin{aligned} 2 + \frac{\rho \rho''}{1 + \rho'^2} &= \operatorname{tg}^2 \alpha , \\ \frac{\rho^2 \sqrt{1 + \rho'^2}}{\cos \alpha} &= K . \end{aligned}$$

These two equations make it possible first of all to demonstrate a simple relation. The derivation with respect to z of equation (21) leads, after simplification, to :

$$2 \rho' + \rho' \frac{\rho \rho''}{1 + \rho'^2} + \rho \operatorname{tg} \alpha \cdot \alpha' = 0 .$$

Taking into account the expression of $\frac{\rho \rho''}{1 + \rho'^2}$ deduced from (17), this becomes :

$$2 \rho' + \rho' (\operatorname{tg}^2 \alpha - 2) + \rho \operatorname{tg} \alpha \cdot \alpha' = 0 \text{ i.e.,}$$

$$\rho' \sin \alpha + \rho \cos \alpha \cdot \alpha' = 0 ,$$

$$\text{or finally : } \rho \sin \alpha = C \operatorname{te} . \quad (22)$$

This relation between the winding angle and the local radius is very simple and, in this particular case (isotensoid design), makes it possible to obtain the winding law when the head is geometrically defined.

As will be demonstrated later, relation (22) is a characteristic property of the geodesic lines belonging to a revolving surface.

Thus, it has been shown that designing a tank head such that the filaments alone counterbalance the stresses due to internal pressure by being subjected to a constant stress means that these filaments will be laid following the geodesic lines of the mean surface of the tank.

As for the determination of the geometric shape of the mean line of the heads of a tank, the following mathematical developments make it possible to specify the function linking the coordinates ρ and z .

After elimination of the variable α , the relations (17) and (22) lead to :

$$3 + \frac{\rho \rho''}{1 + \rho'^2} = \frac{K^2}{\rho^4 (1 + \rho'^2)} . \quad (23)$$

Another form can be deduced :

$$\rho^6 (1 + \rho'^2) + \rho^6 (1 + \rho'^2)' = K^2 (\rho^2)' .$$

The integrated form of this latter relation is written as follows :

$$\rho^6 (1 + \rho'^2) = K^2 \rho^2 + C \quad (C = \text{integration constant}).$$

The constant C can be evaluated by writing the previous relation for $z = 0$.

$$\rho_0^6 = K^2 \rho_0^2 + C \quad (\rho_0' = 0) .$$

A few, simple mathematical manipulations lead to the final result :

$$z(u) = -\rho_0 \int_1^v \frac{\cos \alpha_0 \cdot t^3 dt}{\sqrt{(1 - t^2) [\cos^2 \alpha_0 \cdot t^2 (1 + t^2) - \sin^2 \alpha_0]}} . \quad (24)$$

From relation (24) the shape of each of the heads can be found. Relation (22) determines the winding law.

3.2.2.4 PRACTICAL APPLICATION

A tank has two heads, and therefore two planes of junction between the cylinder and the head.

The geodesic line on a cylinder is a helix. The winding angle α , which is constant, is the same at these two junctions.

$$\alpha_{01} = \alpha_{02} = \alpha_0.$$

At the openings of the two heads, $\alpha = 90^\circ$.

Relation (22) immediately leads to :

$$\rho_{F1} = \rho_{F2} = \rho_0 \sin \alpha_0.$$

The first finding is that the isotensoïd design only enables the fabrication of tanks with identical polar openings.

Moreover, relation (17) shows that the meridians of the heads present an inflexion point for α , such that :

$$\operatorname{tg}^2 \alpha = 2 \quad (\alpha \approx 54.7^\circ).$$

Practically speaking, the following rules are applied :

1. $\alpha_0 < \alpha < 54.7^\circ$. Relation (24) is used to define the shape of the heads.
2. $54.7^\circ < \alpha < 90^\circ$. The head is spherical, its radius being equal to the value taken by R_2 at the point of inflexion. The winding law is governed by relation (22). The structure includes a metal reinforcement called polar mounting (Fig. 1). Consequently, the first condition (equation 12) is no longer verified, and more complex calculation methods are necessary to study the behavior of this area. The point of inflexion is chosen to situate the beginning of the metal reinforcement.

In conclusion to the development of this first approach, it should be underscored that only tanks with equal openings can be made. In practical terms, for rocket cases, overall optimisation systematically leads to a small opening at the front to reduce the weight of the metal reinforcement with a large opening aft due to the dimensions of the nozzle.

Consequently, this approach cannot be systematically applied for such cases. On the other hand, it has the advantage of enabling simple and effective products as the stability of the filament is perfect during winding and the stress within the filament remains constant. We therefore produce small vessels for characterisation based on these principles.

3.2.3 "BALANCED PLANAR DESIGN"

3.2.3.1 STATEMENT OF THE PROBLEM

It has been demonstrated above that isotensoïd design cannot be used for the production of filament-wound structures meeting the specific requirements of rockets.

Moreover, the production facilities have winding machines specifically geared to laying filaments according to a trajectory within a plane. Design departments have therefore developed design methods based on the following two essential prerequisites :

1. The filaments alone counterbalance the stresses due to internal pressure.
2. The trajectory of the filaments is contained within a plane.

The figure below describes in a simplified form the configuration of the filament and of the mandrel.

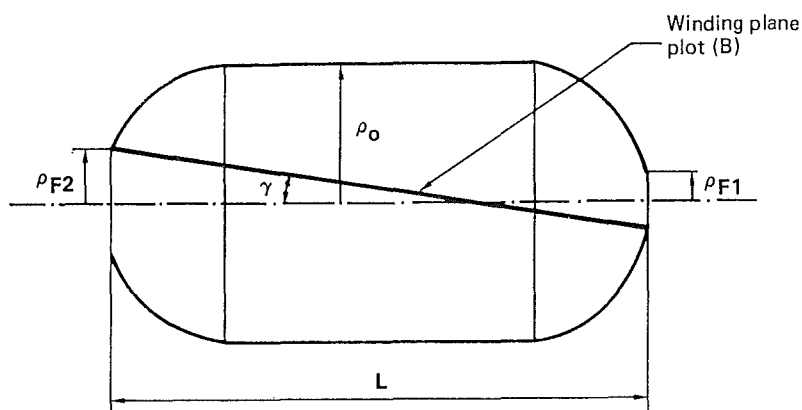


Figure 4

It should be noted that as the shapes of the heads and therefore their depths are only determined once the problem has been solved, the length of the cylindrical part is only known at the end of the calculation. On the other hand, the angle defining the "winding" plane is determined by :

$$\operatorname{tg} \gamma = \frac{\rho_{F1} + \rho_{F2}}{L}$$

(ρ_{F1} , ρ_{F2} , and L are fixed parameters for the designer).

The first condition that the parameters $\rho(z)$ and $\alpha(z)$ must meet is always expressed by relation (17). The second condition is obtained by saying that the trajectory of the filament is planar. This is covered in the following paragraph.

3.2.3.2 EXPRESSION OF THE SECOND CONDITION

The figure below summarizes the parameters and their geometric representations involved in the expression of the condition sought.

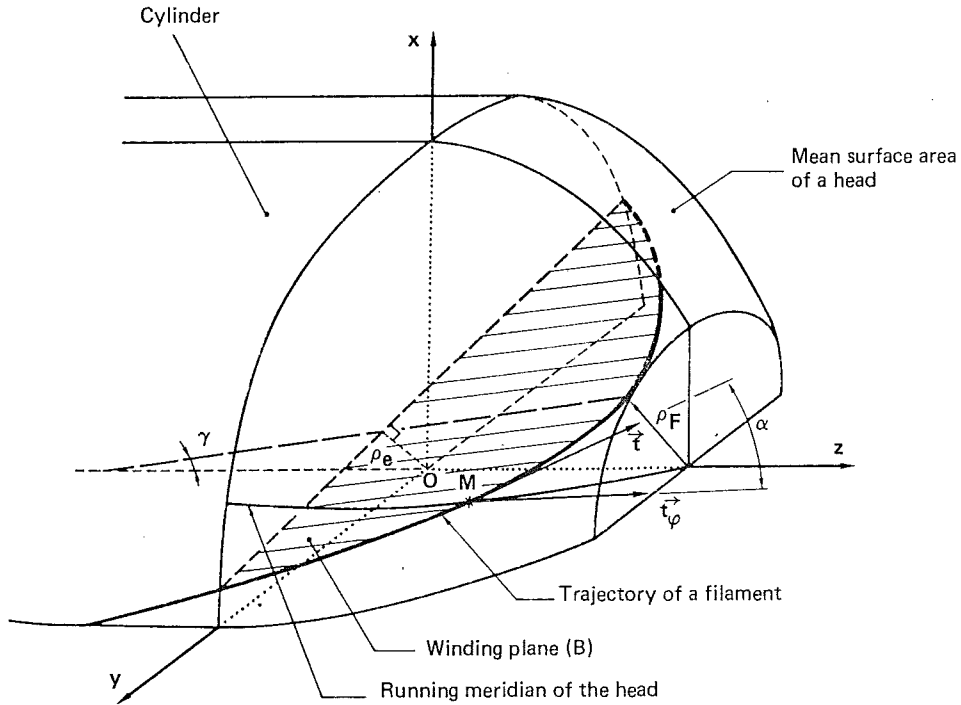


Figure 5

Lengthy calculations, that are not detailed here, provide the expression of the winding angle α by :

$$\operatorname{tg}^2 \alpha = \frac{[\rho \rho' - (z \operatorname{tg} \gamma + \rho_e) \operatorname{tg} \gamma]^2 + (\operatorname{tg}^2 \gamma - \rho'^2) [\rho^2 - (z \operatorname{tg} \gamma + \rho_e)^2]}{(1 + \rho'^2) [\rho^2 - (z \operatorname{tg} \gamma + \rho_e)^2]} \quad (25)$$

This equation, together with equation (17) forms the differential system involving $\rho(z)$ and $\alpha(z)$. The elimination of α leads to the second order differential equation of the function ρ :

$$[\rho \rho' - (z \operatorname{tg} \gamma + \rho_e) \operatorname{tg} \gamma]^2 = (2 - \operatorname{tg}^2 \gamma + 3 \rho'^2 + \rho \rho'') [\rho^2 - (z \operatorname{tg} \gamma + \rho_e)^2] \quad (26)$$

3.2.3.3 NUMERIC RESOLUTION

The Runge Kutta method is used to integrate numerically this type of equation.

To use this method, equation (26) of the second order is replaced by the following differential system of the first order :

$$\rho' = u, \quad (27)$$

$$u' = \frac{1}{\rho} \left\{ \frac{[u \rho - (z \operatorname{tg} \gamma + \rho_e) \operatorname{tg} \gamma]^2}{\rho^2 - (z \operatorname{tg} \gamma + \rho_e)^2} - 3 u^2 - 2 + \operatorname{tg}^2 \gamma \right\} \quad (28)$$

The two functions, ρ and u therefore verify two equations of the type :

$$\begin{cases} \rho' = f_1(u, \rho, z), \\ u' = f_2(u, \rho, z). \end{cases}$$

Under such conditions, if the functions ρ and u have values ρ_1 and u_1 for $z = z_1$, the values ρ_{i+1} and u_{i+1} for $z = z_1 + \Delta z$ are determined by performing the series of the following calculation (ref. 2).

$$-\rho'_{i0} = f_1(u_1, \rho_1, z_1),$$

$$u'_{i0} = f_2(u_1, \rho_1, z_1).$$

$$-\rho'_{i1} = f_1\left(u_1 + \frac{1}{2}u'_{i0}\Delta z, \rho_1 + \frac{1}{2}\rho'_{i0}\Delta z, z_1 + \frac{\Delta z}{2}\right),$$

$$u'_{i1} = f_2\left(u_1 + \frac{1}{2}u'_{i0}\Delta z, \rho_1 + \frac{1}{2}\rho'_{i0}\Delta z, z_1 + \frac{\Delta z}{2}\right).$$

$$-\rho'_{i2} = f_1\left(u_1 + \frac{1}{2}u'_{i1}\Delta z, \rho_1 + \frac{1}{2}\rho'_{i1}\Delta z, z_1 + \frac{\Delta z}{2}\right),$$

$$u'_{i2} = f_2\left(u_1 + \frac{1}{2}u'_{i1}\Delta z, \rho_1 + \frac{1}{2}\rho'_{i1}\Delta z, z_1 + \frac{\Delta z}{2}\right).$$

(29)

$$-\rho'_{i3} = f_1(u_1 + u'_{i2}\Delta z, \rho_1 + \rho'_{i2}\Delta z, z_1 + \Delta z),$$

$$u'_{i3} = f_2(u_1 + u'_{i2}\Delta z, \rho_1 + \rho'_{i2}\Delta z, z_1 + \Delta z).$$

$$-\rho_{i+1} = \rho_1 + \frac{\Delta z}{6}(\rho'_{i0} + 2\rho'_{i1} + 2\rho'_{i2} + \rho'_{i3}),$$

$$u_{i+1} = u_1 + \frac{\Delta z}{6}(u'_{i0} + 2u'_{i1} + 2u'_{i2} + u'_{i3}).$$

Knowing that for $z = 0$, $\rho = \rho_0$ and $u = \rho'_0 = 0$ the calculation can be started and subsequently makes it possible to determine a series of discrete values of the functions ρ and u , and of the function α using equation (25).

The design presented being based in particular on equation (17), the meridian of a head will present in the same way as for the isotenoid design a point of inflexion as soon as the winding angle reaches the value of 54.7° . The design rules given in the isotenoid formulation will again be applied for the shape of the meridian. On the other hand, winding will be planar beyond the point of inflexion, namely in the area of the polar metal reinforcement.

In practical terms, the shape of the meridian and the winding law will therefore be determined, by the previously described numeric integration, from the planes of the junctions between the heads and the cylinder, to the openings ($\alpha = 90^\circ$).

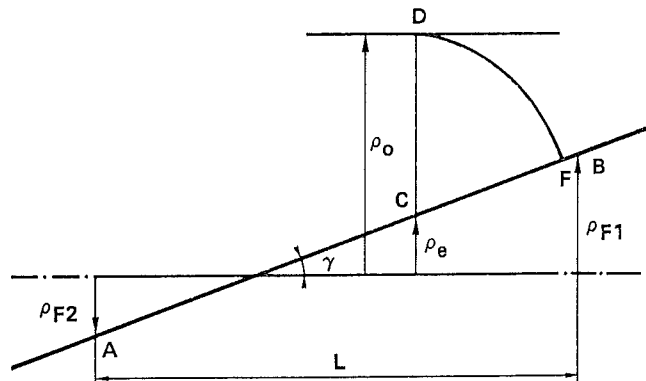


Figure 6

Nevertheless, it is to be noted that equation (28) involves the parameter ρ_e which positions the winding plane (figure 6). This parameter must be determined for each head so as to obtain the opening required. This aspect of the problem is evidenced in the figure above.

As the parameters ρ_{F1} , ρ_{F2} , and L are known, the points A and B and the angle γ are fixed.

By imposing a value for the parameter ρ_e the point D can be situated for a head, representing the beginning of the meridian for the head in question (ρ_0 is known).

The meridian can be constructed by numeric integration to the point F, where the winding angle assumes a value of 90° . This point F is only known at the end of the integration of the system (27), (28). The problem will only be solved when point F coincides with point B.

This shows that for each head the value ρ_e must be found, leading to a final point coinciding with A or B respectively. This will be done iteratively and automatically once the method is programmed.

3.2.3.4 CONCLUSIONS ON THE "BALANCED PLANAR" DESIGN

This method has the advantage, on the one hand, of leading to a design such that the composite material is only subjected to those stresses that are counterbalanced by the tension of the filaments, and, on the other hand, of presenting a winding method particularly well adapted to the power train of simple and fast-operating winding machines.

However, experience has shown that, during or after the winding phase, the filaments may slip, in certain cases. This leads to a position of equilibrium of the filament that is different from the position scheduled in the design of the product.

Any excessive occurrence of this phenomenon will bring about a drop in the fabrication quality and will adversely affect the performance of the structure.

Certain concrete examples have meant that this slippage phenomenon has been taken into account as from the initial design phase, leading to a third design method for vessels with unequal polar openings (ref.3), as will be explained in the following paragraphs.

3.2.4 BALANCED WINDING AND CONTROLLED STABILITY DESIGN

As indicated in the title, this design takes into account, on the one hand, the balancing of the forces due to internal pressure, and, on the other hand, the stability of the filament during or after the winding phase.

The following paragraph will evidence the parameters characterizing this stability.

3.2.4.1 ANALYSIS OF FILAMENT STABILITY DURING WINDING

During the winding phase, the filament is laid on the mandrel with a tension of T . Figure 7 illustrates the parameters involved in what follows.

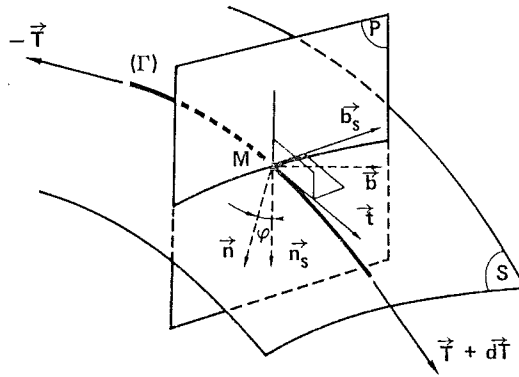


Figure 7

The mandrel exerts a force \vec{F} on the filament, per unit length of the filament, which can be written in the following form :

$$\vec{F} = \lambda \vec{t} + \mu \vec{n}_s + \nu \vec{b}_s .$$

By placing an infinitely small element of the filament in equilibrium, it can easily be demonstrated that the values λ , μ , ν have the following expressions :

$$\left\{ \begin{array}{l} \lambda = - \frac{dT}{ds} , \end{array} \right. \quad (30)$$

$$\left\{ \begin{array}{l} \mu = - Tc \cos \Psi , \end{array} \right. \quad (31)$$

$$\left\{ \begin{array}{l} \nu = - Tc \sin \Psi . \end{array} \right. \quad (32)$$

Under the effect of the tension T , the filament tends to slip in the direction of the vector \vec{b}_s . Furthermore, this tension "flattens" the filament against the mandrel.

The slippage tendency is thus characterized by :

$$k = \left| \frac{\nu}{\mu} \right| = \left| \tan \Psi \right| . \quad (33)$$

This relation shows that the angle Ψ is the value characterizing the stability of winding. Consequently, in the design presented here, this angle will be taken into account to express the second condition necessary to determine $\rho(z)$ and $\alpha(z)$.

3.2.4.2 EXPRESSION OF $\tan \Psi$

The method of obtaining the expression of this value is rather long. Only the main intermediary results will be presented in turn.

The components of the vectors \vec{n}_s and \vec{t} in the datum mark $(\vec{x}, \vec{y}, \vec{z})$ have the following expressions :

$$\vec{n}_s \left\{ \begin{array}{l} - \frac{\cos \theta}{D} , \\ - \frac{\sin \theta}{D} , \\ \frac{\rho'}{D} . \end{array} \right. \quad (34)$$

$$\vec{t} \left\{ \begin{array}{l} \frac{\rho' \cos \alpha \cos \theta}{D} - \sin \alpha \cdot \sin \theta, \\ \frac{\rho' \cos \alpha \sin \theta}{D} + \sin \alpha \cdot \cos \theta, \\ \frac{\cos \alpha}{D} \end{array} \right. \quad (35)$$

Expressions (35) are obtained taking into account the following relation :

$$\frac{d\theta}{dz} = \frac{D \operatorname{tg} \alpha}{\rho} \quad (36)$$

Subsequently, a vector parallel to \vec{n} can be obtained by calculating the components of the vector

$\frac{d\vec{t}}{dz}$:

$$\frac{d\vec{t}}{dz} \left\{ \begin{array}{l} \frac{\rho'' \cos \alpha \cos \theta}{D} - \frac{\rho' \alpha' \sin \alpha \cos \theta}{D} - \frac{\rho' \sin \alpha \sin \theta}{\rho} - \\ \alpha' \cos \alpha \sin \theta - \frac{\sin^2 \alpha \cos \theta}{\cos \alpha} \cdot \frac{D}{\rho} - \frac{\rho'^2 \rho''}{D^3} \cos \alpha \cdot \cos \theta, \\ \frac{\rho'' \cos \alpha \sin \theta}{D} - \frac{\rho' \alpha' \sin \alpha \sin \theta}{D} + \frac{\rho' \sin \alpha \cos \theta}{\rho} + \\ \alpha' \cos \alpha \cos \theta - \frac{\sin^2 \alpha \sin \theta}{\cos \alpha} \cdot \frac{D}{\rho} - \frac{\rho'^2 \rho''}{D^3} \cos \alpha \sin \theta, \\ - \frac{\alpha' \sin \alpha}{D} - \frac{\rho' \rho''}{D^3} \cos \alpha \end{array} \right. \quad (37)$$

The expression of $\operatorname{tg} \Psi$ is deduced from relations (34) and (37) :

$$\operatorname{tg} \Psi = \frac{(\alpha' \rho \cos \alpha + \rho' \sin \alpha) (1 + \rho'^2)}{\rho \rho'' \cos^2 \alpha - (1 + \rho'^2) \sin^2 \alpha} \quad (38)$$

Note :

A characteristic property of the geodesic curves of a revolving surface is that the normal vector at the surface and the main normal vector at the curve meet at all points.

They thus verify that $\Psi = 0$.

Relation (38) therefore indicates that : $\alpha' \rho \cos \alpha + \rho' \sin \alpha = 0$

Namely : $\rho \sin \alpha = C^{te}$

The assertion given in paragraph 3.2.2.3 is thus established, which demonstrates clearly that designing a so-called "isotensoid" vessel is equivalent to designing the same vessel laying up the filaments along the geodesic lines.

3.2.4.3 DETERMINATION OF THE GEOMETRY AND WINDING LAW

With the first condition unchanged, the problem is solved by integrating the following differential system :

$$\left\{ \begin{array}{l} 2 + \frac{\rho \rho''}{1 + \rho'^2} = \operatorname{tg}^2 \alpha, \\ \frac{(\alpha' \rho \cos \alpha + \rho' \sin \alpha) (1 + \rho'^2)}{\rho \rho'' \cos^2 \alpha - (1 + \rho'^2) \sin^2 \alpha} = k \end{array} \right. \quad (39)$$

Moreover, in what follows, designs will be sought such that the slippage tendency of the filaments remains constant along their entire length.

As before, the following first order system will be resolved by the Runge Kutta method :

Kutta :

$$\left\{ \begin{array}{l} \rho' = u, \\ u' = \frac{1 + u^2}{\rho} (\operatorname{tg}^2 \alpha - 2), \\ \alpha' = \frac{1}{\rho \cos \alpha} (2 k \cos^2 \alpha + u \sin \alpha) \end{array} \right. \quad (40)$$

The following system is resolved using equations of the same type as relations (29) extended to three functions $f_1(u, \rho, \alpha)$, $f_2(u, \rho, \alpha)$, $f_3(u, \rho, \alpha)$.

The first equation of the system (39) shows that this design again leads to the existence of a point of inflexion when the winding angle reaches the value of 54.7° . Beyond this point, the head has a spherical shape, with the radius being equal to the value of the second radius of curvature at that point, and the lay-up line of the filament is geodesic, thus ensuring the continuity of the winding angle.

Finally, the angle θ necessary to ensure the adjustment of the winding machine is obtained numerically using relation (36).

3.2.4.4 DESIGN OF THE CYLINDRICAL PART

The technique of winding with a constant slippage tendency can be used for the cylindrical part. In this case, the relation (38) is written as follows :

$$-\frac{\alpha' \rho \cos \alpha}{\sin^2 \alpha} = k$$

Thus, at two points M_1 and M_2 separated by a length l , the winding angles α_1 and α_2 verify :

$$\frac{1}{\sin \alpha_2} - \frac{1}{\sin \alpha_1} = \frac{kl}{\rho_o} \quad (41)$$

In the same way, the variation of the angle θ is obtained by using relations (36) and (41) :

$$\theta_2 - \theta_1 = \frac{1}{k} \left\{ \text{Log} \left[\frac{kl}{\rho_o} + \frac{1}{\sin \alpha_1} + \sqrt{\left(\frac{kl}{\rho_o} + \frac{1}{\sin \alpha_1} \right)^2 - 1} \right] - \text{Log} \left[\frac{1}{\sin \alpha_1} + \frac{1}{\text{tg} \alpha_1} \right] \right\} \quad (42)$$

3.2.4.5 APPLICATION OF WINDING WITH A CONSTANT SLIPPAGE TENDENCY

When the problem of designing a new vessel is posed, the parameters ρ_{F1} , ρ_{F2} and ρ_o are imposed. Moreover, an idea of the criticality of the problems to be solved has to be rapidly obtained. In certain cases, the technological risks have to be evaluated and the designer must be capable of taking decisions as to the nature of the composite material adapted to the problem posed. This has technical consequences and naturally a direct effect on the price of the product sold. This obviously involves an initial evaluation of the problem not requiring a very great accuracy.

That explains why the method presented above, that is used in our industrial fabrication, has been processed in such a way as to enable the very rapid evaluation of a few essential parameters, as illustrated in the following diagram that will be discussed below :

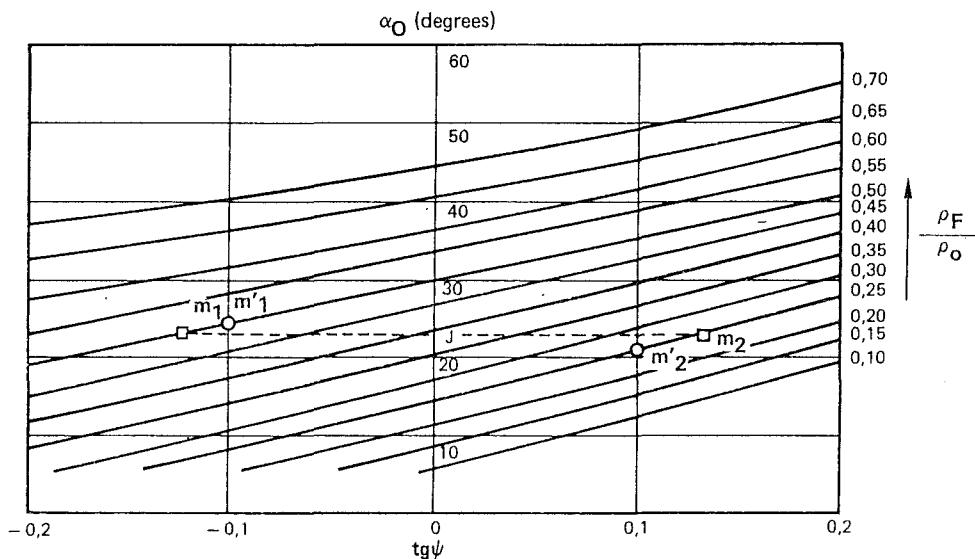


Figure 8

This diagram relates the parameters :

- α_o (winding angle at the junctions of the heads and the cylinder),
- ρ_F / ρ_o (what is called the opening ratio),
- $\text{tg} \Psi$ (slippage factor).

The tracing of this diagram is obtained by the systematic use of the program numerically resolving the system (40). Thus, the lines traced in Figure 8 have been drawn point by point.

The following example shows how this diagram can be used :

$$\rho_{F1} / \rho_o = 0.50 \quad (\text{aft head}) ,$$

$$\rho_{F2} / \rho_o = 0.25 \quad (\text{front head}) .$$

If a helicoidal trajectory is used for laying up the filaments on the cylinder, the winding angles at the two head/cylinder junctions are equal. In addition, in order to obtain the most stable winding possible, it will be accepted that the procedure must be such that the slippage factors are equal for both heads. Under such conditions, the points m_1 and m_2 therefore represent the two heads in the diagram, from which the following can be obtained :

$$\alpha_o \approx 23^\circ ,$$

$$|\text{tg} \Psi| = 0.13 \text{ i.e. } \Psi = 7.4^\circ .$$

Another possibility lies in choosing a winding law for the cylindrical part which presents a slippage tendency. In this case, the winding angles at the two ends of the cylinder may be different.

The points m'_1 and m'_2 always obtained by equalling the slippage tendency at the two heads, will then present a new solution to the problem.

In the present case, the slippage factor is reduced :

$$\operatorname{tg} \Psi = 0.10 \text{ i.e. } \Psi = 5.7^\circ .$$

Winding stability at the heads has thus been improved. By reading off the winding angle values at the head/cylinder junction from the diagram, the slippage factor can easily be calculated using relation (41).

3.2.4.6 DESIGN OF STRESS IN THE FILAMENTS

Relation (20), which gives the general expression of the local stress in the filaments, can be written :

$$\sigma_{fs} = H \frac{\rho^2 \sqrt{1 + \rho'^2}}{\cos \alpha} ,$$

with :

$$H = \frac{P}{2 \chi e_{so} \rho_o \cos \alpha_o} .$$

The expression of $\frac{d \sigma_{fs}}{dz}$ is written below :

$$\frac{d \sigma_{fs}}{dz} = H \left[\frac{2 \rho \rho' D}{\cos \alpha} + \frac{\rho^2 \rho' \rho''}{\cos \alpha \cdot D} + \rho^2 D \frac{\sin \alpha \cdot \alpha'}{\cos^2 \alpha} \right] .$$

Relation (17) makes it possible to eliminate ρ'' . After simplification, this becomes :

$$\frac{d \sigma_{fs}}{dz} = - 2 \rho H \operatorname{tg} \alpha \cdot D \cdot \operatorname{tg} \Psi . \quad (43)$$

By using the principle of equalizing the slippage tendencies on both heads, from Figure 8 it appears that :

- $\operatorname{tg} \Psi$ is negative for the head with the larger opening (aft head),
- $\operatorname{tg} \Psi$ is positive for the head with the smaller opening (front head).

Given this, it results from relation (43) that the stress in the filaments increases from the head/cylinder junction to the point of inflexion for the aft head, and decreases for the front head.

Therefore, without taking into account the phenomena of flexion that the theories developed hitherto cannot in fact take into account, it would appear that the aft head should always be thicker than the other head in order to allow for the maximum stress reached at the point of inflexion.

3.3 CONCLUSION ON DESIGN METHODS

These design methods presented above are today operational and are used almost daily. They are usable by employing simple equipment and software. The time required to obtain results is short (in the order of a day). The volume of inputs and outputs is low.

The results are complete, given that it is possible to obtain mainly :

- the overall geometry,
- the weights and volume of the filament-wound shell,
- the winding parameters for the winding machines,
- parameters making it possible to have an idea of the difficulties of fabrication.

Nevertheless, the hypotheses of these methods are such that verification of the extent to which the structure meets the specification must be undertaken, in particular to ensure that the local over-stresses are acceptable.

Furthermore, the metal reinforcements must be designed by calculations that the methods described cannot handle.

The following paragraph will describe the methods used to provide final justification of the structure before any irreversible fabrication phases are undertaken.

4. JUSTIFICATION

4.1 PRINCIPLES OF THE METHODS OF JUSTIFICATION

The working method consists of using a calculation method based on the technique of finite elements (S.A.M.C.E.F. developed by the LTAS of the University of Liège).

As the purpose is not to describe the method of finite elements, the major phenomena taken into account simultaneously to ensure as realistic a study as possible of the behavior of such structures will be listed, namely :

- the geometric non-linear behavior, related to the fact that the internal pressure, at equilibrium, is no longer exerted on the initial geometry but on the distorted geometry, is necessary to obtain displacements and a stress condition corresponding to reality,
- local anisotropy, which varies according to the winding angle and therefore the point taken of the structure, is an element that must be taken into account when creating the data card-indexes representing the terms of the Hooke matrix along the entire structure,
- elasto-plastic behavior laws are necessary to relate realistically the tensors of stress and distortions of the polar mountings,
- the existence of gap between polar mountings, blanking systems and their connections cannot be overlooked, and has led to the development of extensions to the SAMCEF software program.

4.2 PRESENTATION OF THE MAIN RESULTS

The results are printed on voluminous listings, from which a few representative plates have been taken.

1 - Stresses in the filaments :

These stresses are presented in plates of the type illustrated in the figure below :

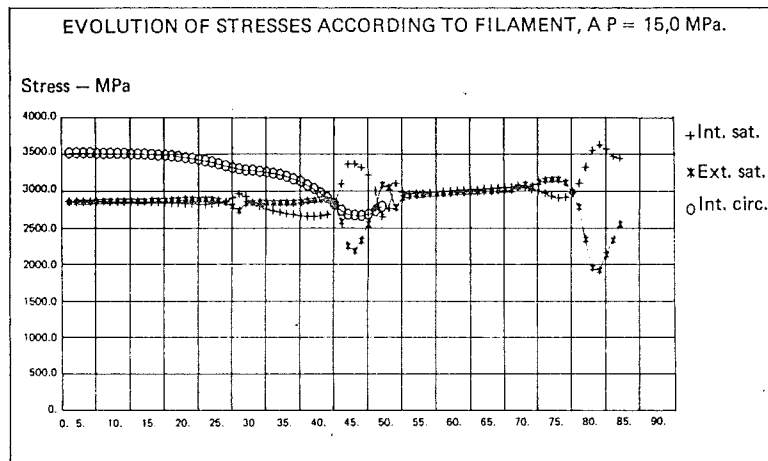


Figure 9

This figure indicates the evolution of the stresses from the middle of the cylinder to the opening of one of the two heads. Such stresses affect the internal and external layers in such a way that the local phenomena are evidenced. A more or less constant evolution can be noted, except :

- at the head/cylinder junction,
- in an area close to the opening.

Only the finite elements method can provide the maximum values reached and justify the reinforcement that had been defined on the basis of past experience.

2 - Stresses in the polar mountings

Several representations have been used over the past years to illustrate a two-dimensional stress condition as from numeric indexes providing on stress tensor per element of the modelization.

Currently, the designer is provided with coloured figures, defining zone by zone the levels reached. This type of figure is illustrated below :

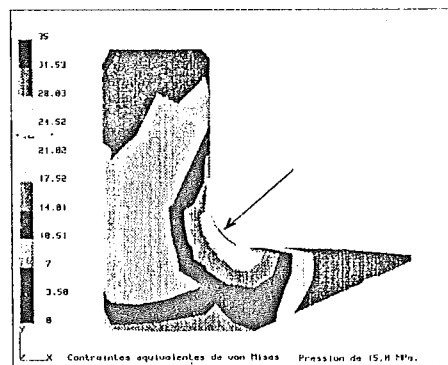


Figure 10

This figure shows a radial cross-section of a front polar mounting (small opening).

In this example, it can be seen that the area most subject to stress is in the ring marked by the arrow.

Multiple results are obtained and subjected to precise analysis, leading either to modifications, or to the decision to give the go-ahead for fabrication. Only the principal critical parameters for the behavior of the structure are mentioned, namely :

- shear between winding layers (possibility recently developed),
- shear of the rubber laminates connecting the winding and the polar mountings,
- general deflection of the structure to evaluate its size.

4.3 CRITICAL ANALYSIS OF DESIGN AND JUSTIFICATION METHODS

It is a rule in our company to consider that the existence of these two methods is necessary. The first has the qualities of being rapid, effective and able to allow users to retain an intuitive knowledge in regard to the influence of the main parameters on the results obtained. The second, longer and more expensive to use, is alone suitable for making it possible to draw the conclusion that the structure can be fabricated.

This is why it is necessary to maintain a balance between the use of these two methods, which we consider as complementary.

5. CHARACTERIZATION OF MATERIALS

This is a subject which deserves a document to itself and a special presentation. We shall confine ourselves here to presenting some of the more important principles, with a view to highlighting the importance of this characterization in the field of industrial production.

Characterization can be split into two main categories :

- work in connection with our knowledge of material properties, with a view to enabling the Designers to justify the product to be fabricated with access to information which is as complete as possible concerning the characteristics of the materials making up the winding and the composite.

The Calculation Department, for example, needs the laws of behavior linking the tensors of stress and distortion. Special tests are required to determine the terms of the Hooke's matrix if linear behavior is considered representative. This particular case, the simplest that can be chosen, nonetheless requires the determination of nine different coefficients.

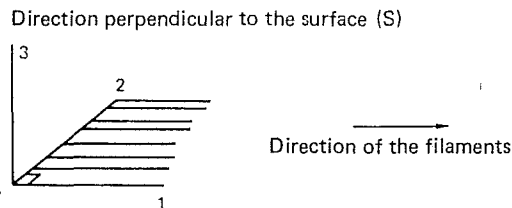


Figure 11

The relationships are written as follows :

$$\begin{bmatrix} \sigma_{11} \\ \sigma_{22} \\ \sigma_{33} \\ \sigma_{12} \\ \sigma_{13} \\ \sigma_{23} \end{bmatrix} = \begin{bmatrix} H_{11} & H_{12} & H_{13} & 0 & 0 & 0 \\ & H_{22} & H_{23} & 0 & 0 & 0 \\ & & H_{33} & 0 & 0 & 0 \\ \text{Sym} & & & G_{12} & 0 & 0 \\ & & & & G_{13} & 0 \\ & & & & & G_{23} \end{bmatrix} \begin{bmatrix} \varepsilon_{11} \\ \varepsilon_{22} \\ \varepsilon_{33} \\ \gamma_{12} \\ \gamma_{13} \\ \gamma_{23} \end{bmatrix} \quad (44)$$

Other methods in the 1970s based on the properties of the filaments and the resin made it possible to determine the elements of the relationship (44). Characterization of the constituents was then necessary.

Specific laws were sometimes necessary when the composite had non-linear relationships (σ, ε) (e.g. degradation of the composite by microfracturing of the resin when placed under internal pressure).

Moreover, in addition to the composite, the presence of rubber made it necessary to carry out experiments enabling the stress to be linked to the deformation. Curves of the following type were used :

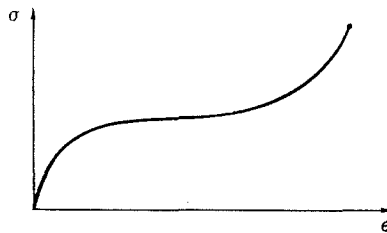


Figure 12

- The second category involves the characterization required to ensure that the product fabricated complies with the acceptance specifications for the materials.

There are any types of characterization, but we shall only deal here with those relating to winding.

The fibers are bought from manufacturers who deliver the material in such quantities as belong to a single fabrication batch. Before their use for the fabrication of a filament wound structure, samples of a similar design to the rockets are produced on a reduced scale (diameter 304 mm). The samples are subjected to rupture through internal pressure. The values obtained make it possible to decide whether or not the material can be used.

Less costly tests are carried out on unidirectional tows subjected to tensile strain. The former, more expensive, type of test, however, is more representative of the biaxial strains (meridian and parallel) existing in a real structure.

Characteristic material performance values will be given in paragraph 8.

6. FABRICATION

This paragraph will be devoted to the fabrication methods for this type of structure. It will be divided into three parts :

- a - description of the filament-winding machines,
- b - description of the main stages during fabrication,
- c - particular remarks on the method of obtaining the filament wound composite.

6.1 DESCRIPTION OF THE FILAMENT WINDING MACHINES

The filament winding machines we use are of two types, for which we shall use the following terms :

- vertical satellite machine,
- horizontal machine.

6.1.1 VERTICAL SATELLITE MACHINE

The operating principle of such a machine is represented in the figure below :

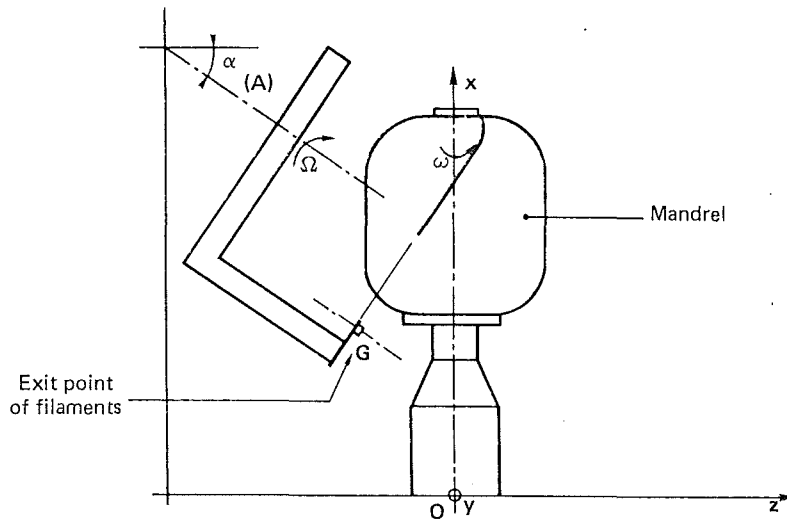


Figure 13

The mandrel is fixed to a supporting structure with a vertical axis. An arm, turning at a speed Ω , bears the filament routing and includes, at its end, a device whose purpose is to provide an outlet for the filaments prior to being laid on the mandrel.

If the mandrel is fixed, after several rotations of the arm the filaments will be laid by overlaying on a planar trajectory. For this reason, a slight rotation of the mandrel is necessary in order to cause a shift in the filament braid after one full rotation of the arm. This is how the mandrel is covered. When these shifts total 360° , one filament wound layer is completed.

The number of layers laid is defined by the thickness of composite required in order to comply with the resistance specifications (paragraph 3).

The configuration of some structures is such that there is no guarantee of the stability of planar winding. In order to solve this problem, the technique known as "modified planar filament winding" is used. This type of winding is achieved by turning the mandrel at a rotation speed ω . The filament laying trajectory is no longer planar. When the arm has completed a turn, the braid is no longer laid next to the previous braid. The ratio between the speeds ω and Ω is chosen in such a manner that there will be juxtaposition. This gives rise to star pattern winding.

This type of machine does not make it possible to rigorously respect the $\alpha(z)$ laws compatible with the form of mandrel defined by $\rho(z)$. Experience shows, however, that it is possible to approach the theoretic laws.

Moreover, these machines are simple, rapid and reliable. They also exist, and are there to be used. This is why this type of machine is still greatly used. We shall see below that they do nonetheless have certain limitations in regard to the type of implementation of the composite at the time of winding.

6.1.2 HORIZONTAL FILAMENT WINDING MACHINE

The operating principle of these machines is shown in the figure below :

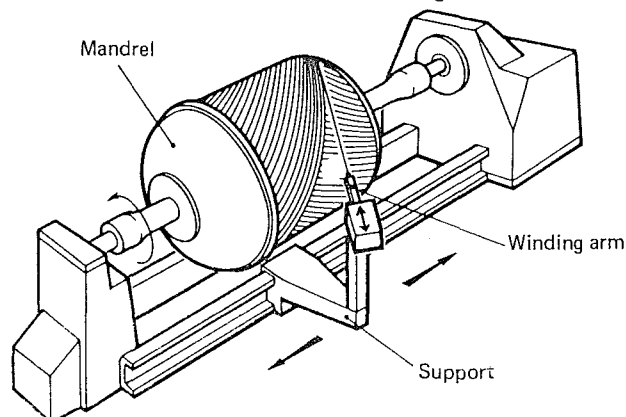


Figure 14

In the simplest case, the movements enabling a braid of filaments to be laid are :

- rotation of the mandrel,
- displacement of the mandrel holder parallel to the z direction,
- displacement of the winding arm in the y direction.

So, the point M which here symbolizes the winding head with its filament braid outlet, can be displaced in any manner on a plane parallel to z.

Improvements can be made in one particular field to enhance the quality of the filament winding.

The braid laid is, in practice, a group of tows themselves made up of several thousand filaments (the tow is the condition of the material as delivered by the manufacturer). Thus, the braid coming out of the winding head (M) has a certain width, generally around 20 mm. In order to reduce the length of this phase in production, we envisage increasing that width to around 50 mm. It is inevitable that the braid is not planar between point M and the point of tangency with the mandrel. This phenomenon, if over pronounced, may give rise to poor winding quality. In order to remedy this, a winding head with several degrees of freedom of rotation about point M is currently under development. These degrees of freedom will be programmed, as will the main movements described above.

This type of machine makes it possible to comply fully with the theoretical ($\alpha(z)$) winding laws defined in paragraph 3. Also, unlike the vertical machines, they make it possible to wind structures whatever the implementation of the composite (paragraph 6.3).

6.2 MAIN STAGES IN FABRICATION

The purpose of the fabrication of rocket cases is to provide the customer with a case ready to be loaded with powder and fitted with the nozzle prior to becoming a rocket stage ready for assembly with the rest of the vector.

Production is therefore broken down into the following stages :

- fabrication of the primary parts (frames and polar mountings),
- fabrication of the internal thermal protections fitted to the polar mountings by rubber lay-up in special molds. Vulcanization is performed by placing in a pressure oven (autoclave),
- fabrication of the mandrel by introducing sand and binder into molds fitted with protected thermal protections. The sand is rammed, then hardened by oven drying,
- assembly of the various parts thus produced to provide the mandrel ready for winding,
- securing the mandrel to the filament winding machine, and winding,
- polymerization of the composite in an oven (the skirts may be fabricated during the filament winding phase or after the first polymerization. In the latter case, a second polymerization cycle is required),
- extraction of the sand by adding warm water which disintegrates and washes out the sand,
- machining of the skirts, securing the skirt frames, and finishing operations,
- geometric examination and examination of critical areas such as bonds in particular. An important phase during inspection is pressure testing the case at an internal pressure equal to 1.15 times the maximum operating pressure.

Finally, the case is delivered.

6.3 IMPLEMENTATION OF THE COMPOSITE

Two methods are used. They involve the method of impregnating the filaments with resin.

The first method (the W method) consists in impregnating the tows during the winding phase immediately before the filaments are laid on the mandrel. We shall call this the WET technique.

The second (the P method) consists in impregnating the tows prior to the winding phase (sometimes several months earlier), subjecting the impregnated filaments to a thermal field to induce initial polymerization, then storing this product on reels at a temperature of -18°C. We shall call this Prepreg winding.

Both methods, of course, have their advantages and their drawbacks.

a - W method

This procedure is less costly than the P method. The stability of the filament during the winding phase, however, is sometimes poor.

b - P method

This procedure provides enhanced stability during the winding phase. It involves, however, increased cost in fabricating the case because of the extra time required to make Prepreg.

Another source of overcoat linked to quality improvement is the inspection of the product prior to use.

Finally, it should be noted (paragraph 3.2.4) that, in certain configurations, Prepreg is required in order to be able to wind the case.

7. EXPERIMENTAL QUALIFICATION

In addition to the experimental work whose purpose is to characterize the materials used in order to fabricate the case, a new case is subjected to destructive testing in order to determine its ultimate resistance.

The skirts are subjected to predetermined mechanical stresses providing the best possible representation of the severest stress conditions.

The rest of the case is subjected to destructive testing through the application of internal pressure, generally by introducing water into the wound capacity.

In addition, a mechanical effort applied to the rear link represents the thrust relief. The front skirt is therefore subjected to compressive stress.

This type of test should demonstrate that the failure pressure P_F is such that :

$$P_F > K \times P_{MO} ,$$

(P_{MO} = Maximum operating pressure) .

- The case is placed vertically in a pit. A great number of measurements are made in order to :
- make it possible to explain how the failure was initiated,
 - enable the calculation team to compare theoretical forecasts with reality,
 - provide the person in charge of powder loading with the deformation limits of the filament-wound case.

These measurements are carried out using displacement sensors and deformation gages.

The following areas in particular are measured :

- the middle of the cylindrical part in order to determine the strain on the circumferential winding,
- the skirt/cylinder bonds, which are areas of bending,
- the areas of composite near the polar mountings (areas of bending),
- the metal rear polar mounting which is always optimized as it is heavy due to the wide opening.

These tests are always long because of the dense instrumentation (250 measurement channels in major tests) and the use of extensive equipment :

- recording equipment which requires each measurement channel to be connected to a data acquisition system,
- heavy mechanical equipment in order to comply with safety requirements.

Lastly, systematic video and fast camera (≈ 3000 frames per sec.) recordings are made, covering the whole case insofar as possible, in order to be able to review the occurrence of the failure after the test.

The test pit is approximately 8 meters deep and approximately 7 meters in diameter.

The figure below gives more precise information on the details dealt with briefly in this paragraph.



Figure 15

8. RESULTS

In this paragraph, we shall present a number of results which can be used to evaluate :

- the performance of filament winding in comparison with certain metals,
- developments in the performance of filament wound products,
- the specific performance related to rocket cases.

8.1 COMPOSITE/METAL COMPARISON

We shall exclude here the performances indicated by suppliers for the purpose of this type of comparison. Performance obviously depends on the intrinsic qualities of the materials, but it also depends just as much on the object (geometry, stress) and the quality of the implementation which is determined by the development of good resins, in association with the proper thermal cycles, the winding quality, etc.

Therefore, the filament wound composite assessed here has been assessed by using failure stresses obtained on known samples, discussed in paragraph 5.

In addition, the stresses presented are obtained by taking account, not of the cross-sectional area of dry fibers, but of the total cross-section (dry fiber + impregnating resin).

Finally, the parameter adopted is σ / d (d = density of composite).

Results as of today are :

MATERIALS	σ / d
Glass composite	≈ 900
Kevlar composite	≈ 1400
Carbon composite (Hercules IM6)	≈ 1600 to 1800
Steel	≈ 200
Light alloy	≈ 170
Titanium	≈ 220

σ = expressed in MPa.

The advantages of composites are very considerable, as can be seen from comparison between the values shown in the above table.

It can also be seen that the fibers successively used - glass, Kevlar and carbon - have produced marked performance enhancement. The notion of the scale effect should be underlined here.

Experience has shown that it is not possible to judge performance solely on the basis of results obtained with small scale samples (diameter ≈ 300 mm).

It has been noted with glass and kevlar, that there is a significant decrease in performance as the dimensions of the case increase. This experimental fact, unexplained by our design department, is shown in the diagram below :

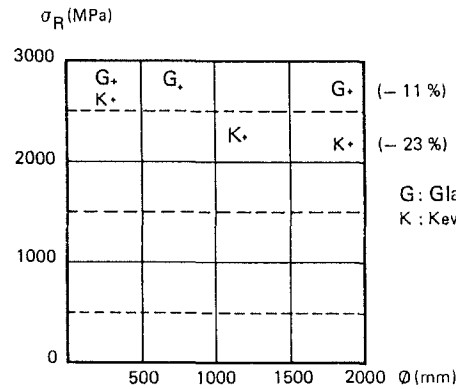


Figure 16

The following percentages are thus observed respectively :

- 23 % decrease ($\phi = 300$ mm to $\phi = 2000$ mm) for kevlar,
- 11 % decrease ($\phi = 300$ mm to $\phi = 2000$ mm) for glass.

This phenomenon has made it much more difficult to obtain a definition complying with the specifications when these materials were used.

Moreover, the performances observed during preliminary small scale tests being unobtainable on the real object, the inert mass of the case was increased.

As far as is known today, this phenomenon does not appear to exist in regard to carbon fibers, thus providing yet another advantage for this material.

8.2 PERFORMANCE FACTOR IN ROCKET CASES

The following magnitude is frequently used amongst industrialists fabricating such cases. It is defined as follows :

$$q = \frac{pV}{mg}$$

p = failure pressure.
V = internal volume.
m = mass of filament wound capacity.
g = terrestrial acceleration.

This factor has the dimension of a length. For countries using the metric system, it is generally expressed in kilometers.

This factor is, indeed, fairly representative of the criteria that fabricators wish to respect. q increases as :

- p increases (no comment),
- V increases, corresponding to the desire to be able to carry the greatest possible mass of powder,
- m decreases, corresponding to the smallest possible inert mass.

An increase in q , therefore, represents the desire that a given stage should provide the best possible contribution to the range of the vector.

It should, however, be noted that comparisons between cases should be made taking due account of the fact that the overall length is imposed by the case fabricator.

For the same quality of fabrication, a quick analysis will show that, all other things being equal, an increase in length gives rise to an increase in the performance factor.

This being so, we nonetheless present below, for information, the best performances achieved by our company in this field.

Diameter (mm)	1500	2000	1150
Materials	Glass	Kevlar	Carbon
q (km)	20	31	41

As the range of lengths is fairly close, it is clear to see the development resulting from the evolution of the fibers on the market.

8.3 INFORMATION ABOUT FUTURE DEVELOPMENTS

In regard to carbon fibers, two major producers are offering fibers with ever higher performance : the American HERCULES and the Japanese TORAYCA.

The HERCULES Corporation, after its AS4 and AS6 fibers, is now marketing the IM6 fiber, with a forecast :

$$\sigma_R = 5000 \text{ MPa (tow test)}$$

Another fiber, IM7, exists but is not widely marketed, with a forecast :

$$\sigma_R = 5500 \text{ MPa (tow test)}$$

Other fibers, currently at the laboratory stage, promise even higher levels.

The TORAYCA Corporation, after the T300 fiber (class AS4), is now marketing its T800 and T800H fibers which are respectively comparable to the IM6 and IM7 fibers.

More recently, this manufacturer has announced its T1000 fiber, with :

$$\sigma_R = 7000 \text{ MPa (tow test)}$$

It may therefore be seen that there is rapid development in the materials made available to fabricators of filament wound structures. This fact makes it all the more difficult to take certain decisions in that, when a program is launched, it is always necessary to have available the elements making it possible to use the best fibers, and these must be constantly evaluated and qualified for industrial application.

9. CONCLUSION

Experience in recent years in regard to both design and justification, has been detailed in this document (paragraphs 4 and 5). It is important to note that these methods have been developed in order to meet extremely precise requirements in regard to rocket cases, outlined in paragraph 2.

We wish to stress, for this is the result of constant effort on the part of our design team, the fact that we have always attempted to preserve rapidity in the field of pure design and accuracy in justification.

It should also be pointed out that there has been a constant effort to produce designs enabling our production team to fabricate quality structures at the least possible cost. Remarks relating to the choice between the WET and Prepreg methods, or to filament winding stability are intended to highlight such considerations.

While the results presented demonstrate the obvious advantages of the filament wound composite over metallic materials, the latter also reveal the advances made by fiber producers. Industrialists today must constantly take account of the rapid developments in carbon performances.

Computer aided design, finally, though not dealt with in this document as it is a field in which the equipment is gradually being implemented, is an extremely important subject for our Plant. It enables staff to be freed from the repetitive tasks and devote themselves more fully to structure optimization. It should be pointed out that equipment providing automatic transfer of elements from definition to production is gradually being set up. In particular, the winding parameters are stored on a magnetic medium immediately at the design stage, and this can be used directly to control the winding machines. This results in a reduction in labor, in cost and in the risk of error.

Currently, we consider that progress must be made in the field of automation during the design and justification stage, then during the fabrication stage.

In conclusion, we hope we have made it clear that our constant concern has been, in the design field, to find solutions taking account not only of product performance, but also quality and efficiency during the fabrication stage.

References :

- [1] TIMOSHENKO AND WOINOWSKI-KRIEGER - Theory of plates and shells.
(Second Edition) Mc Graw Hill Company - New York - 1959 - Page 435.
- [2] HILDEBRAND - Introduction to numerical Analysis
Mc Graw Hill Company - New York - 1956 - Pages 236 - 237.
- [3] J.P. DENOST - New Design concepts for filament wound pressure vessel with unequal openings.
Société Nationale Industrielle Aerospatiale - 1982 - AIAA (Cleveland).

CONCEPTION DES STRUCTURES DE PROPULSEUR BOBINÉES

par

J.P. DENOST

Chef de Programmes Structures Bobinées

AEROSPATIALE

St-Médard-en-Jalles

33165

FRANCE.

RESUME

Les méthodes de conception et de dimensionnement des structures de propulseur bobinées ont commencé à être développées dans notre Société au début des années 70. Depuis, ces méthodes ont évolué et ont ainsi permis d'obtenir des moyens de conception rapide et de vérification fine.

Le présent document aura pour objet de délimiter ces deux approches, de les critiquer et de montrer leur complémentarité. Elles feront l'objet de présentations détaillées afin de permettre au lecteur d'en comprendre les grandes règles et de tirer les enseignements qui lui permettront de les développer dans des domaines particuliers.

Cette partie à dominante théorique sera complétée par des considérations relatives aux matériaux, leurs mises en oeuvre, leurs performances et une description des grands principes de fabrication de ce type de structure.

NOTATIONS

A = aire d'une section droite du fil.

\vec{b} = $\vec{t} \wedge \vec{n}$.

\vec{b}_S = $\vec{t} \wedge \vec{n}_S$.

c = courbure de (Γ) en M ; $c > 0$.

C_1, C_2 = centres de courbure principaux de (S) en M .

D = $(1 + \rho^2)^{\frac{1}{2}}$

d = symbole de dérivation.

e = épaisseur du réservoir en M .

\vec{F} = action du mandrin sur le fil, par unité de longueur de celui-ci.

g = constante de gravitation terrestre.

H = projection orthogonale de M sur l'axe de révolution de (S) .

k = $\tan \Psi$.

L = distance axiale entre les deux ouvertures polaires du réservoir.

M = point courant de (Γ) et de (S) .

m = masse du réservoir.

\vec{n} = vecteur unitaire de la demi-normale principale positive de (Γ) en M .

N = nombre de fils coupés par un plan parallèle.

\vec{n}_S = vecteur unitaire de la demi-normale intérieure à (S) en M .

N_ϕ = valeur en M de l'effort interne de membrane dans la direction de \vec{t}_ϕ , par unité de longueur du parallèle ; pour la traction : $N_\phi > 0$.

N_θ = valeur en M de l'effort interne de membrane dans la direction de \vec{t}_θ , par unité de longueur de la méridienne ; pour la traction : $N_\theta > 0$.

O = origine du repère $(\vec{x}, \vec{y}, \vec{z})$; situé dans le plan de jonction entre le fond et la partie cylindrique.

p = valeur de la pression interne ; $p > 0$.

q = facteur de performance du réservoir ; $q = \frac{pV}{mg}$.

R_1, R_2 = rayons de courbure principaux de (S) en M ; $R_i = MC_i \cdot \vec{n}_S$ ($i = 1, 2$).

s = abscisse curviligne de M sur (Γ) orientée.

S = surface moyenne du réservoir ; surface de révolution dont la concavité de la méridienne est tournée vers l'axe de révolution.

- \vec{t} = vecteur unitaire de la demi-tangente positive de (Γ) en M ; $\vec{t} \cdot \vec{z} > 0$.
 T = valeur de la tension dans le fil ; $T > 0$.
 \vec{t}_ϕ = vecteur unitaire de la demi-tangente positive de la méridienne en M ; $\vec{t}_\phi \cdot \vec{z} > 0$.
 \vec{t}_θ = vecteur unitaire de la demi-tangente positive du parallèle en M orienté par \vec{z} .
 u = ρ' .
 v = $\frac{\rho}{\rho_0}$.
 V = volume intérieur du réservoir .
 x, y, z = coordonnées de M par rapport au repère général .
 $(\vec{x}, \vec{y}, \vec{z})$ = base orthonormée directe du repère général ; \vec{z} : porté par l'axe de révolution de (S) .
 α = mesure en radians de l'angle du couple de vecteurs (\vec{t}_ϕ, \vec{t}) ; si $(\vec{t}_\phi \wedge \vec{t}) \cdot \vec{n}_s > 0$: $0 < \alpha < \frac{\pi}{2}$.
 Γ = courbe représentée par le fil .
 θ = mesure en radians de l'angle du couple de vecteurs (\vec{x}, \vec{HM}) ; $\theta = \int_{M_0}^M \theta' dz$, θ' étant exprimé par la relation (36) .
 λ = $\vec{F} \cdot \vec{t}$.
 μ = $\vec{F} \cdot \vec{n}_s$.
 v = $\vec{F} \cdot \vec{b}_s$.
 ρ = HM .
 ρ_{F_1}, ρ_{F_2} = rayons des ouvertures polaires des deux fonds .
 σ_f = contrainte dans le fil ; $\sigma_f = \frac{T}{A}$.
 ϕ = mesure en radians de l'angle du couple de vecteurs $(\vec{z}, -\vec{n}_s)$; si $(\vec{n}_s \wedge \vec{z}) \cdot \vec{t}_\theta > 0$: $0 < \phi < \pi$.
 χ = titre volumique de fibre dans le composite .
 Ψ = mesure en radians de l'angle du couple de vecteurs (\vec{n}_s, \vec{n}) ; si $(\vec{n}_s \wedge \vec{n}) \cdot \vec{t} > 0$: $0 < \Psi < \frac{\pi}{2}$.

Notations particulières :

- $()'$ = symbole de dérivation par rapport à la variable z .
 o = indice affectant toutes grandeurs évaluées pour $z = 0$.

1. INTRODUCTION

La technologie du bobinage est utilisée depuis environ 25 ans pour réaliser les structures de propulseurs des différents programmes français.

Ces programmes ont été civils (DIAMANT) et militaires (MSBS, SSBS).

Cette technologie a essentiellement permis de remplacer le métal par le composite et ainsi de diminuer la masse inerte au profit de la portée du vecteur. De plus, le bobinage est une méthode de réalisation automatique qui assure simultanément rapidité, économie et qualité.

Les fibres imprégnées de résine ont évolué au cours du temps. Les premières structures ont été réalisées avec du fil de verre. Par la suite, sont apparus le Kevlar et plus récemment le Carbone. Chacune de ces évolutions a renforcé l'avantage du composite sur le métal.

Si les moyens de production mis en place ont rapidement évolué afin de permettre le déroulement des programmes militaires principalement, nos moyens de conception ont été perfectionnés de manière plus progressive.

Au début des années 60, la définition était obtenue par des méthodes où l'empirisme était en position dominante. La voie expérimentale permettait d'obtenir un produit répondant aux besoins ; quelques années se révélèrent nécessaires pour permettre aux compétences des Bureaux d'Etudes de s'exercer en ce domaine, en commençant d'établir des méthodes relativement simples vers la fin des années 60.

Le développement de l'Informatique en France, et plus tard l'apparition de programmes de calculs ont conduit progressivement aux méthodes de travail sophistiquées du milieu des années 70. Enfin, aujourd'hui l'accent est porté sur l'automatisation de la conception et de la définition (CAO) et récemment sur la liaison qui peut être faite entre la définition et la réalisation assistée par ordinateur (FAO). Toutefois, les méthodes dites "légères", adaptées pour répondre rapidement à des questions ne nécessitant pas immédiatement une grande précision et surtout permettant au potentiel humain de ne pas perdre la compréhension des phénomènes physiques, continuent d'être développées et utilisées.

Parallèlement, les moyens de calculs nécessitant des caractéristiques de plus en plus nombreuses, le concepteur a établi des programmes de caractérisation des composites bobinés. Ces programmes ont conduit à des travaux importants assurant une activité soutenue pour les Laboratoires de Matériaux et d'Essais.

L'objet principal de ce document sera de présenter les méthodes de conception et de justification des structures de propulseurs bobinés. L'analyse critique des méthodes dites "légères" et des moyens informatiques sera faite et montrera comment notre Société les utilise de manière complémentaire.

La partie la plus développée sera celle-ci, mais il nous est apparu inévitable de devoir consacrer des chapitres courts pour présenter, d'une part, comment en général les problèmes se posent, d'autre part, les méthodes de fabrication et de qualification expérimentale.

Enfin, revenant aux moyens de calculs, il sera nécessaire de développer quelques notions mathématiques qui seront condensées autant que possible afin de permettre au lecteur de comprendre, en espérant ne pas le lasser, l'objectif étant d'ouvrir à qui le souhaite quelques notions suffisantes lui permettant de développer les modèles adaptés à ses applications particulières.

2. POSITION DU PROBLEME

2.1 DESCRIPTION DE LA STRUCTURE

Dans le but de permettre une meilleure compréhension de ce qui suivra, une présentation des principaux sous-ensembles de la structure est nécessaire. La figure (1) représente une telle structure.

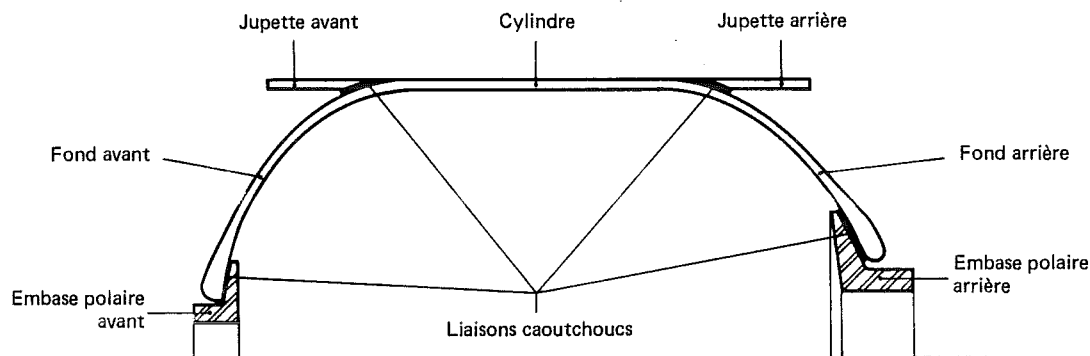


Figure 1

Cette figure permet de détailler :

- les deux jupettes qui sont deux cylindres courts, assurent la liaison de l'enveloppe de propulseur avec le reste du vecteur,
- le cylindre et les deux fonds qui sont réalisés par bobinage et dont nous présenterons plus loin les principes de conception et de justification,
- les deux embases polaires métalliques qui renforcent les ouvertures et assurent la liaison avec d'autres pièces (bouchon allumeur à l'avant, tuyère à l'arrière),
- des liaisons en caoutchouc entre réservoir et jupettes d'une part, et entre réservoir et embases polaires d'autre part.

Le réservoir (partie cylindrique et fonds) est donc réalisé par bobinage ; au cours de cette phase de fabrication on effectue deux types d'enroulements :

- le premier par bobinage dit "satellite" qui constitue les deux fonds et le cylindre, par une succession de boucles tangentes aux deux ouvertures,
- le deuxième par bobinage dit "circonférentiel" qui n'est déposé que sur la partie cylindrique de telle façon que les fils soient quasiment perpendiculaires aux génératrices.

2.2 PRINCIPALES SPECIFICATIONS

Les spécifications techniques d'un tel produit font l'objet d'un document détaillé et volumineux, nous retiendrons ici les principales.

2.2.1 TENUE AUX EFFORTS MECANIQUES

Les sollicitations mécaniques sont la pression interne exercée par la combustion de la poudre lors du fonctionnement de l'étage considéré, et des efforts de traction et flexion supportés principalement par les jupettes lors de la vie du vecteur.

De plus, des sollicitations thermiques doivent être prises en compte lors des phases propulsées.

Les règles de qualification associées à ces sollicitations sont telles que la structure à l'état neuf doit présenter un coefficient de sécurité : $K > 1,4$.

Par ailleurs, les différents sous-ensembles doivent rester dans le domaine élastique pour des charges égales à 1,15 fois les charges nominales. Cette dernière spécification est vérifiée expérimentalement pour chaque spécimen avant livraison au client.

2.2.2 VIEILLISSEMENT

Chaque spécimen fabriqué doit être capable d'assurer ses fonctions avec une probabilité supérieure à une valeur minimale lors de toute sa durée de vie opérationnelle.

2.2.3 GEOMETRIE

- Des spécifications géométriques sont imposées afin de :
- respecter des encombrements maximaux fixés à l'état de repos et lors du fonctionnement,
 - assurer des conditions d'interface avec le reste du vecteur.

2.2.4 CHARGEMENT EN POUDRE

L'intégrité structurale doit être assurée pendant la phase de chargement. En résumé, ceci se traduit par des sollicitations de température et de pression interne pendant une durée fixée.

2.3 TENUE A LA PRESSION INTERNE DE FONCTIONNEMENT

Dans ce document nous traiterons la conception et la justification d'une telle structure lors de la sollicitation qui, dans tous les cas, est la plus sévère : la pression interne due à la combustion de la poudre pendant le fonctionnement de l'étage considéré.

De plus, si de nombreux éléments sont contraints par l'effet de la pression interne, le sous-ensemble le plus critique dans le travail d'optimisation est constitué de la partie cylindrique et des deux fonds. C'est pourquoi, dans les paragraphes suivants, la conception et la justification de cette partie sera plus particulièrement détaillée.

Les problèmes liés aux jupettes ne seront pas traités du fait de leur masse faible et des notions classiques connues de tout Bureau d'Etude, que nous serions amenés à développer. Par contre, une courte présentation particulière sera consacrée au dessin de l'embase polaire arrière, celle-ci ayant parfois une masse telle que son optimisation est rendue nécessaire.

2.4 POSITION DU PROBLEME PARTICULIER AU BOBINAGE

La partie cylindrique bobinée s'étudie de manière très simple et il suffit de déterminer les épaisseurs respectives des deux enroulements la constituant, nécessaires pour assurer la tenue à la pression interne. La méthode de calcul sera présentée dans un paragraphe spécifique.

Les deux fonds posent le problème de conception de manière différente. En effet, il faut déterminer simultanément la forme de chaque fond et la trajectoire des fils sur celle-ci de telle façon que ces fonds soient réalisables et optimisés.

La figure ci-dessous illustre les notations présentées en début de document et permet de préciser comment le problème se pose.

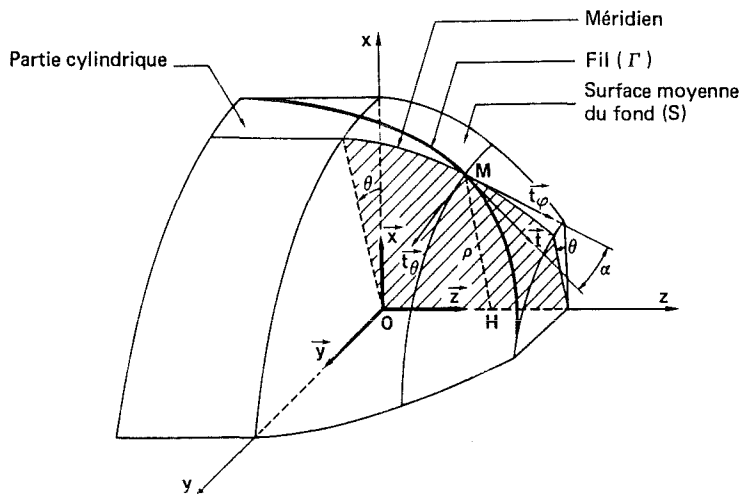


Figure 2

La forme du réservoir est définie par la fonction $\rho(z)$. La manière de déposer le fil au cours du bobinage, c'est-à-dire la ligne (Γ) est définie par la fonction $\alpha(z)$.

Le problème ainsi posé comporte donc deux fonctions inconnues. De ce fait, deux conditions faisant intervenir ces deux fonctions seront nécessaires. Dans les chapitres suivants il apparaîtra que ceci a conduit à développer différentes méthodes de conception.

3. CONCEPTION

Dans les méthodes de conception nous séparerons :

- la partie bobinée cylindrique,
- la partie bobinée sur les fonds.

Nous retiendrons le terme "méthode du filet" pour désigner globalement les notions théoriques qui seront développées ici. Dans le cadre de cette méthode nous considérerons que, en tout point, la structure bobinée ne présentera raideur et résistance que dans la direction des fils à l'exclusion de toute autre direction.

3.1 ANALYSE DE LA PARTIE CYLINDRIQUE

Compte tenu des notations nous pouvons écrire :

$$N_{\phi} = N_{\phi s} + N_{\phi c} , \quad (1)$$

$$N_{\theta} = N_{\theta s} + N_{\theta c} . \quad (2)$$

Avec :

$$N_{\phi} = \frac{PR}{2} ,$$

$$N_{\theta} = PR .$$

De plus, l'hypothèse de base de la méthode du filet entraîne :

$$N_{\phi c} = 0 . \quad (3)$$

La résultante de contrainte $N_{\theta c}$ s'exprime aisément par :

$$N_{\theta c} = \chi e_c \sigma_{fc} . \quad (4)$$

En ce qui concerne l'enroulement satellite il faut considérer la figure présentée ci-dessous :

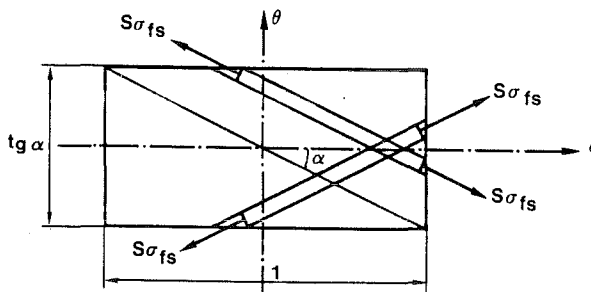


Figure 3

Compte tenu des notations il vient comme le montre cette figure :

$$N \operatorname{tg} \alpha \cdot S \sigma_{fs} \cos \alpha = N_{\phi s} \operatorname{tg} \alpha , \quad (5)$$

$$N \operatorname{tg} \alpha \cdot S \sigma_{fs} \sin \alpha = N_{\theta s} . \quad (6)$$

De plus, il est possible d'exprimer l'épaisseur de composite de l'enroulement satellite par :

$$e_s = N \frac{S}{\chi \cos \alpha} . \quad (7)$$

Les relations (5), (6) et (7) entraînent :

$$N_{\phi s} = \chi e_s \sigma_{fs} \cos^2 \alpha , \quad (8)$$

$$N_{\theta s} = \chi e_s \sigma_{fs} \sin^2 \alpha . \quad (9)$$

Les relations (1) et (2) conduisent en utilisant les expressions de $N_{\phi s}$, $N_{\theta s}$, $N_{\phi c}$, $N_{\theta c}$ à :

$$\frac{PR}{2} = \chi e_s \sigma_{fs} \cos^2 \alpha \quad (R = \rho_0) ,$$

$$PR = \chi e_s \sigma_{fs} \sin^2 \alpha + \chi e_c \sigma_{fc} .$$

Ces deux relations permettent d'obtenir les expressions des contraintes dans les fils des deux enroulements en partie cylindrique :

$$\sigma_{fs} = \frac{PR}{2 \chi e_s \cos^2 \alpha} , \quad (10)$$

$$\sigma_{fc} = \frac{PR}{\chi e_c} \left(1 - \frac{\operatorname{tg}^2 \alpha}{2} \right) . \quad (11)$$

Ces dernières relations sont très utilisées dans l'étude de la partie cylindrique des réservoirs de propulseur. Elles sont simples et permettent de définir rapidement les épaisseurs de composite nécessaires pour obtenir un niveau de contrainte imposé dans les fibres.

Remarques :

a - Si le bobinage circonférentiel est supprimé, on déduit aisément que l'angle de bobinage doit être tel que :

$$\operatorname{tg}^2 \alpha = 2 \quad \text{soit } \alpha = 54,7^\circ .$$

Il sera exposé ultérieurement que la valeur de l'angle de bobinage α en partie cylindrique impose les dimensions des ouvertures des fonds. De ce fait, pour préserver la liberté géométrique sur ce point, il est toujours nécessaire de réaliser un bobinage circonférentiel.

b - Si les fils appartenant aux deux types d'enroulement sont soumis au même niveau de contrainte on déduit aisément à l'aide de (10) et (11) :

$$\frac{e_c}{e_s} = 3 \cos^2 \alpha - 1 .$$

3.2 ANALYSE DES FONDS

3.2.1 EXPOSE DES PRINCIPES

Le problème de définition des épaisseurs en partie cylindrique a été étudié dans le paragraphe précédent. Il reste à définir la forme des fonds et la ligne de dépôt des fils. Il a été mis en évidence dans le paragraphe 2.4 que deux conditions sont nécessaires pour traiter le problème ainsi posé.

Trois voies seront détaillées. Leur présentation se succèdera de la même manière que leur utilisation chronologique s'est faite. Ceci permettra de mettre en évidence les limites de chacune de ces voies, les problèmes rencontrés concrètement et ce qui a justifié le passage à la méthode suivante.

3.2.2 CONCEPTION "ISOTENSOIDE"

Cette conception est fondée sur les deux conditions suivantes :

- les fils seuls équilibrent les efforts dus à la pression interne (Méthode du filet),
- la contrainte dans les fils est constante sur toute leur longueur.

3.2.2.1 EXPRESSION DE LA PREMIERE CONDITION

Les fonds n'étant constitués que du bobinage satellite, les relations (8) et (9) conduisent à :

$$\frac{N_\theta}{N_\phi} = \operatorname{tg}^2 \alpha . \quad (12)$$

De plus, il est supposé que le réservoir n'est soumis qu'à des sollicitations d'extension ; alors les expressions de N_θ et N_ϕ sont les suivantes (référence 1) :

$$N_\phi = \frac{PR_2}{2} , \quad (13)$$

$$N_\theta = \frac{PR_2}{2} \left(2 - \frac{R_2}{R_1} \right) . \quad (14)$$

Par ailleurs, il est aisé de démontrer :

$$R_1 = - \frac{(1 + \rho'^2)^{3/2}}{\rho''} , \quad (15)$$

$$R_2 = \rho \sqrt{1 + \rho'^2} . \quad (16)$$

Ainsi, l'expression finale de la première condition (méthode du filet) est :

$$2 - \frac{R_2}{R_1} = \operatorname{tg}^2 \alpha \quad \text{soit,}$$

$$2 + \frac{\rho \rho''}{1 + \rho'^2} = \operatorname{tg}^2 \alpha . \quad (17)$$

3.2.2.2 EXPRESSION DE LA DEUXIEME CONDITION

Cette deuxième condition impose que la contrainte dans le fil soit constante ; l'expression de cette contrainte se déduit de la relation (8).

$$\sigma_{fs} = \frac{N_\phi}{\chi e_s \cos^2 \alpha} . \quad (18)$$

Pour transformer cette expression sous une forme convenable il faut préalablement déterminer l'épaisseur locale de la paroi du réservoir.

La relation (7) permet d'écrire :

$$e_s = N \frac{S}{\chi \cos \alpha} , \text{ (en un point quelconque),}$$

$$e_{so} = N \frac{S}{\chi \cos \alpha_o} , \text{ (à la jonction entre l'un des fonds et le cylindre).}$$

De plus, on tient compte du fait que tous les fils qui coupent le parallèle à la jonction fond-cylindre coupent aussi le parallèle passant par le point considéré ; ceci se traduit par :

$$2 \pi \rho N = 2 \pi \rho_o N_o .$$

On obtient ainsi la relation qui exprime l'épaisseur locale :

$$e_s = e_{so} \frac{\rho_o \cos \alpha_o}{\rho \cos \alpha} . \quad (19)$$

D'où, à l'aide de (13), (18) et (20) :

$$\sigma_{fs} = \frac{\rho \rho^2}{2 \chi e_{so} \rho_o \cos \alpha_o \cos \alpha} \sqrt{1 + \rho'^2} . \quad (20)$$

Imposer que la contrainte dans le fil est constante consiste donc à écrire la deuxième condition de la manière suivante :

$$\rho^2 \frac{\sqrt{1 + \rho'^2}}{\cos \alpha} = K . \quad (21)$$

3.2.2.3 DETERMINATION DE LA MERIDIENNE ET DE LA LOI DE BOBINAGE

La méridienne du fond de surface (S) et la loi de bobinage sont respectivement définies par les fonctions $\rho(z)$ et $\alpha(z)$.

Ces deux fonctions sont solutions du système différentiel constitué des équations (17) et (21) rappelées ici :

$$2 + \frac{\rho \rho''}{1 + \rho'^2} = \operatorname{tg}^2 \alpha ,$$

$$\frac{\rho^2 \sqrt{1 + \rho'^2}}{\cos \alpha} = K .$$

Ces deux équations permettent tout d'abord de démontrer une relation simple.

La dérivation par rapport à z de l'équation (21) conduit après simplification à :

$$2 \rho' + \rho' \frac{\rho \rho''}{1 + \rho'^2} + \rho \operatorname{tg} \alpha \cdot \alpha' = 0 .$$

Tenant compte de l'expression de $\frac{\rho \rho''}{1 + \rho'^2}$ déduit de (17), il vient :

$$2 \rho' + \rho' (\operatorname{tg}^2 \alpha - 2) + \rho \operatorname{tg} \alpha \cdot \alpha' = 0 \text{ soit,}$$

$$\rho' \sin \alpha + \rho \cos \alpha \cdot \alpha' = 0 ,$$

$$\text{ou finalement : } \rho \sin \alpha = C^{\text{te}} . \quad (22)$$

Cette relation entre l'angle de bobinage et le rayon local est très simple et permet donc d'obtenir dans ce cas particulier (conception isotensoïde) la loi de bobinage lorsque le fond est défini géométriquement.

La relation (22), ceci sera démontré ultérieurement, est une propriété caractéristique des lignes géodésiques appartenant à une surface de révolution.

Ainsi, il a été montré que le fait de concevoir un fond de réservoir tel que les fils seuls équilibrent les efforts dus à la pression interne en étant sollicités par une contrainte constante entraîne que ces fils soient déposés suivant des géodésiques de la surface moyenne du réservoir.

Concernant la détermination de la forme géométrique de la ligne moyenne des fonds d'un réservoir, les développements mathématiques qui suivent permettent de préciser la fonction qui relie les coordonnées ρ et z . Les relations (17) et (21) après élimination de la variable α conduisent à :

$$3 + \frac{\rho \rho''}{1 + \rho'^2} = \frac{K^2}{\rho^4 (1 + \rho'^2)} . \quad (23)$$

Une autre forme peut se déduire :

$$(\rho^6)' (1 + \rho'^2) + \rho^6 (1 + \rho'^2)' = K^2 (\rho^2)' .$$

La forme intégrée de cette dernière relation s'écrit comme suit :

$$\rho^6 (1 + \rho'^2) = K^2 \rho^2 + C \quad (C = \text{constante d'intégration}).$$

La constante C peut être évaluée en écrivant la relation précédente pour $z = 0$.

$$\rho_o^6 = K^2 \rho_o^2 + C \quad (\rho_o' = 0).$$

Quelques manipulations mathématiques simples conduisent au résultat final :

$$z(u) = -\rho_o \int_1^v \frac{\cos \alpha_o \cdot t^3 dt}{\sqrt{(1-t^2) [\cos^2 \alpha_o \cdot t^2 (1+t^2) - \sin^2 \alpha_o]}}. \quad (24)$$

La relation (24) permet donc de connaître la forme de chacun des fonds. La relation (22) fixe la loi de bobinage.

3.2.2.4 MISE EN APPLICATION PRATIQUE

Un réservoir comporte deux fonds, donc deux plans de jonction cylindre/fond.

La géodésique sur un cylindre est une hélice, donc l'angle de bobinage α , constant, est le même à ces deux jonctions.

$$\alpha_{o1} = \alpha_{o2} = \alpha_o.$$

Aux ouvertures des deux fonds $\alpha = 90^\circ$.

La relation (22) entraîne immédiatement :

$$\rho_{F1} = \rho_{F2} = \rho_o \sin \alpha_o.$$

La première constatation est que la conception isotensoïde ne permet de réaliser que des réservoirs ayant des ouvertures polaires identiques.

De plus, la relation (17) montre que les méridiennes des fonds présentent un point d'inflexion pour α tel que :

$$\operatorname{tg}^2 \alpha = 2 \quad (\alpha \approx 54,7^\circ).$$

En pratique, les règles suivantes sont appliquées :

1. $\alpha_o < \alpha < 54,7^\circ$. La relation (24) est utilisée pour définir la forme des fonds.
2. $54,7^\circ < \alpha < 90^\circ$. La forme du fond est sphérique, son rayon est égal à la valeur prise par K_2 au point d'inflexion. La loi de bobinage est régie par la relation (22). La structure comporte un renfort métallique appelé embase polaire (figure 1). En conséquence la première condition (équation 12) n'est plus vérifiée et des méthodes de calculs plus compliquées sont nécessaires pour étudier le comportement de cette zone. Le point d'inflexion est choisi pour situer le début du renforcement métallique.

En conclusion du développement de cette première voie il convient de souligner que l'on ne peut réaliser que des réservoirs présentant des ouvertures égales. En pratique, pour des structures de propulseur, l'optimisation globale conduit systématiquement à une petite ouverture à l'avant afin de diminuer la masse du renfort métallique et à une grande ouverture à l'arrière du fait des dimensions de la tuyère.

En conséquence, cette voie ne peut être appliquée rigoureusement pour de telles structures. Par contre, elle présente l'avantage de permettre des réalisations simples et efficaces car la stabilité du fil est parfaite lors du bobinage et la contrainte dans le fil est constante. De ce fait, nous réalisons des petits réservoirs de caractérisation fondés sur ces principes.

3.2.3 CONCEPTION "PLANAIRE EQUILIBREE"

3.2.3.1 POSITION DU PROBLEME

Il a été démontré que la conception isotensoïde ne permettait pas de réaliser des structures bobinées répondant aux nécessités spécifiques des propulseurs.

De plus, les unités de production disposent de machines à bobiner particulièrement adaptées pour réaliser des dépôts de fil suivant une trajectoire contenue dans un plan. De ce fait, les bureaux d'études ont développé des méthodes de conception fondées sur les deux conditions nécessaires suivantes :

1. Les fils seuls équilibrent les efforts dus à la pression interne,
2. La trajectoire des fils est contenue dans un plan.

La figure ci-dessous décrit de manière simplifiée la configuration du fil et du mandrin.

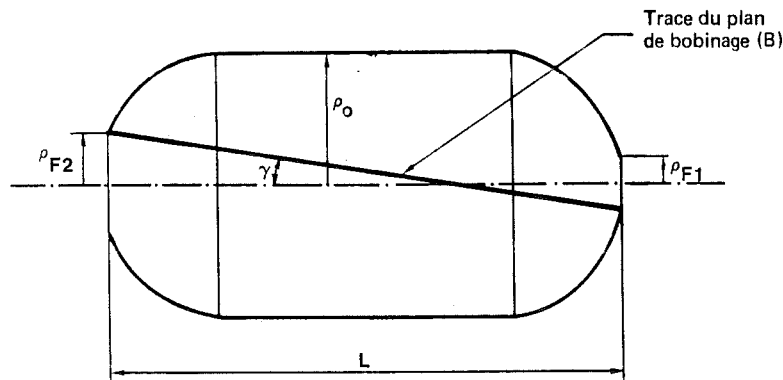


Figure 4

Il convient de noter que les formes des fonds et donc leurs profondeurs n'étant déterminées que lorsque le problème est résolu, la longueur de la partie cylindrique n'est connue qu'en fin de calcul. Par contre, l'angle définissant le plan dit "de bobinage" est déterminé par :

$$\operatorname{tg} \gamma = \frac{\rho F_1 + \rho F_2}{L}$$

(ρF_1 , ρF_2 , L sont des paramètres fixés au concepteur).

La première condition que doivent vérifier les grandeurs $\rho(z)$ et $\alpha(z)$ est toujours exprimée par la relation (17). La deuxième condition est obtenue en exprimant que la trajectoire du fil est planaire. Ceci fait l'objet du paragraphe suivant.

3.2.3.2 EXPRESSION DE LA DEUXIEME CONDITION

La figure ci-dessous résume les grandeurs et leurs représentations géométriques qui interviendront dans l'expression de la condition recherchée.

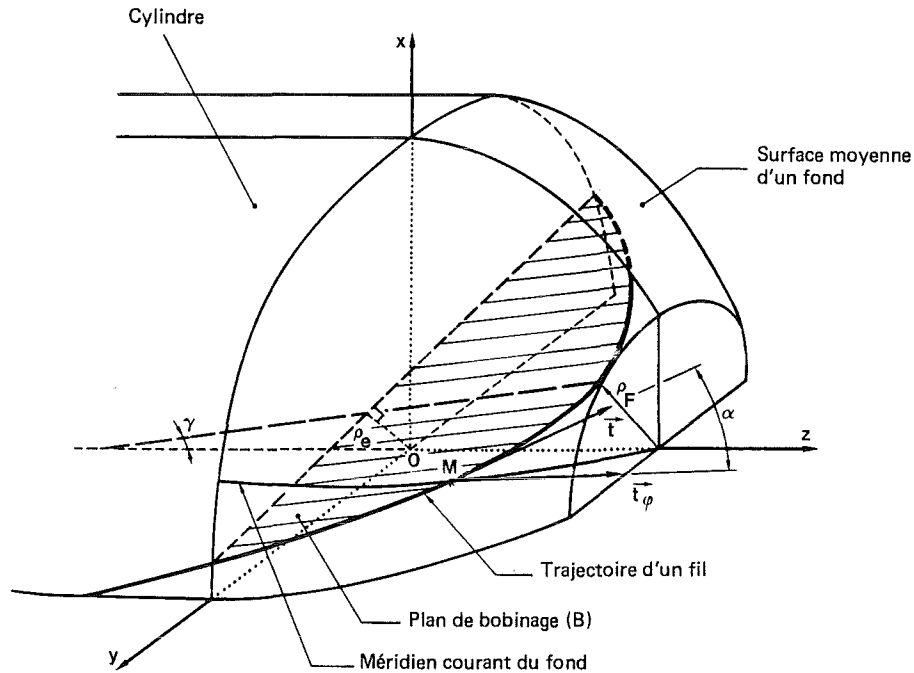


Figure 5

Des calculs longs, non détaillés ici, permettent d'obtenir l'expression de l'angle de bobinage α par :

$$\operatorname{tg}^2 \alpha = \frac{[\rho \rho' - (z \operatorname{tg} \gamma + \rho_e) \operatorname{tg} \gamma]^2 + (\operatorname{tg}^2 \gamma - \rho'^2) [\rho^2 - (z \operatorname{tg} \gamma + \rho_e)^2]}{(1 + \rho'^2) [\rho^2 - (z \operatorname{tg} \gamma + \rho_e)^2]} \quad (25)$$

Cette équation constitue avec l'équation (17) le système différentiel faisant intervenir $\rho(z)$ et $\alpha(z)$. L'élimination de α conduit à l'équation différentielle du second ordre de la fonction ρ :

$$[\rho \rho' - (z \operatorname{tg} \gamma + \rho_e) \operatorname{tg} \gamma]^2 = (2 - \operatorname{tg}^2 \gamma + 3 \rho'^2 + \rho \rho'') [\rho^2 - (z \operatorname{tg} \gamma + \rho_e)^2] \quad (26)$$

3.2.3.3 RESOLUTION NUMERIQUE

La méthode de Runge Kutta est employée pour intégrer numériquement ce type d'équation.

Afin d'utiliser cette méthode, l'équation (26) du second ordre est remplacée par le système différentiel du premier ordre suivant :

$$\rho' = u, \quad (27)$$

$$u' = \frac{1}{\rho} \left\{ \frac{[u \rho - (z \operatorname{tg} \gamma + \rho_e) \operatorname{tg} \gamma]^2}{\rho^2 - (z \operatorname{tg} \gamma + \rho_e)^2} - 3 u^2 - 2 + \operatorname{tg}^2 \gamma \right\} \quad (28)$$

Les deux fonctions ρ et u vérifient donc deux équations du type :

$$\begin{cases} \rho' = f_1(u, \rho, z), \\ u' = f_2(u, \rho, z). \end{cases}$$

Dans ces conditions, si les fonctions ρ et u ont des valeurs ρ_1 et u_1 pour $z = z_1$, les valeurs ρ_{1+1} et u_{1+1} pour $z = z_1 + \Delta z$ sont déterminées en réalisant la suite des calculs suivants (référence 2).

$$\begin{aligned}
 - \rho'_1{}^0 &= f_1(u_1, \rho_1, z_1), \\
 u'_1{}^0 &= f_2(u_1, \rho_1, z_1). \\
 - \rho'_1{}^1 &= f_1\left(u_1 + \frac{1}{2} u'_1{}^0 \Delta z, \rho_1 + \frac{1}{2} \rho'_1{}^0 \Delta z, z_1 + \frac{\Delta z}{2}\right), \\
 u'_1{}^1 &= f_2\left(u_1 + \frac{1}{2} u'_1{}^0 \Delta z, \rho_1 + \frac{1}{2} \rho'_1{}^0 \Delta z, z_1 + \frac{\Delta z}{2}\right). \\
 - \rho'_1{}^2 &= f_1\left(u_1 + \frac{1}{2} u'_1{}^1 \Delta z, \rho_1 + \frac{1}{2} \rho'_1{}^1 \Delta z, z_1 + \frac{\Delta z}{2}\right), \\
 u'_1{}^2 &= f_2\left(u_1 + \frac{1}{2} u'_1{}^1 \Delta z, \rho_1 + \frac{1}{2} \rho'_1{}^1 \Delta z, z_1 + \frac{\Delta z}{2}\right). \\
 - \rho'_1{}^3 &= f_1(u_1 + u'_1{}^2 \Delta z, \rho_1 + \rho'_1{}^2 \Delta z, z_1 + \Delta z), \\
 u'_1{}^3 &= f_2(u_1 + u'_1{}^2 \Delta z, \rho_1 + \rho'_1{}^2 \Delta z, z_1 + \Delta z). \\
 - \rho_{1+1} &= \rho_1 + \frac{\Delta z}{6} (\rho'_1{}^0 + 2 \rho'_1{}^1 + 2 \rho'_1{}^2 + \rho'_1{}^3), \\
 u_{1+1} &= u_1 + \frac{\Delta z}{6} (u'_1{}^0 + 2 u'_1{}^1 + 2 u'_1{}^2 + u'_1{}^3).
 \end{aligned} \tag{29}$$

Sachant que pour $z = 0$, $\rho = \rho_0$ et $u = \rho'_0 = 0$ le calcul peut être commencé et permet ensuite de déterminer ainsi une suite de valeurs discrètes des fonctions ρ et u , et de la fonction α à l'aide de l'équation (25).

La conception présentée étant fondée en particulier sur l'équation (17) la méridienne d'un fond présentera de même que pour la conception isotensoïde un point d'inflexion dès que l'angle de bobinage atteindra la valeur de $54,7^\circ$. Les règles de conception énoncées lors de la formulation isotensoïde seront encore appliquées en ce qui concerne la forme de la méridienne ; le bobinage sera par contre planaire au-delà du point d'inflexion, c'est-à-dire dans la zone du renfort polaire métallique.

En pratique, la forme de la méridienne et la loi de bobinage sont donc déterminées, par l'intégration numérique décrite précédemment, depuis les plans de jonctions fonds/cylindre jusqu'aux ouvertures ($\alpha = 90^\circ$).

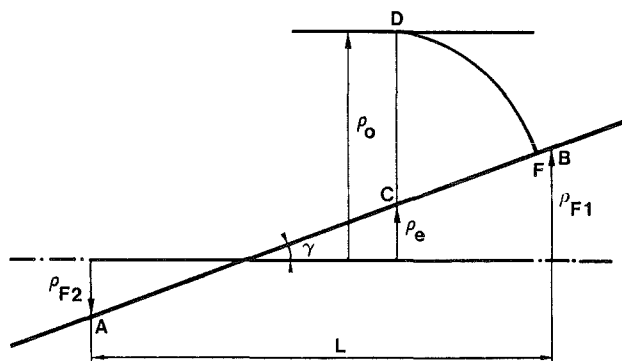


Figure 6

Toutefois, il faut noter que l'équation (28) fait intervenir la grandeur ρ_e qui positionne le plan de bobinage (figure 6) ; cette grandeur devra être déterminée pour chaque fond de façon à obtenir l'ouverture souhaitée. Cet aspect du problème est mis en évidence sur la figure ci-dessus.

Les grandeurs ρ_{F1} , ρ_{F2} , L étant connues, les points A et B et l'angle γ sont fixés.

S'imposer une valeur pour la grandeur ρ_e permet de placer, pour un fond, le point D qui représente le début de la méridienne pour le fond considéré (ρ_0 est connu).

L'intégration numérique permet de construire la méridienne jusqu'au point F où l'angle de bobinage prend la valeur de 90° ; ce point F n'est connu qu'en fin d'intégration du système (27), (28). Le problème ne sera résolu que lorsque le point F coïncidera avec le point B.

Il apparaît donc qu'il faudra procéder, pour chaque fond, à une recherche de la valeur ρ_e qui conduise à un point final coïncidant respectivement avec A ou B. Cette recherche se fait de manière itérative et, de plus, automatisée lorsque la méthode est programmée.

3.2.3.4 CONCLUSIONS SUR LA CONCEPTION "PLANAIRE EQUILIBREE"

Cette méthode présente l'avantage, d'une part, d'aboutir à une conception telle que le composite ne subit que des efforts qui sont équilibrés par la tension des fils, d'autre part de présenter une méthode de bobinage particulièrement bien adaptée à la cinématique de machines à bobiner simples et rapides dans leur fonctionnement.

Toutefois, l'expérience a montré que, pendant ou après la phase de bobinage, les fils peuvent, dans certains cas, glisser. Ceci se traduit par une position d'équilibre du fil différente de celle qui est prévue dans le dossier de définition du produit.

Ce phénomène, lorsqu'il est trop accentué, entraîne une diminution de la qualité de fabrication et une altération des performances de la structure.

Certains cas concrets ont conduit à prendre en compte ce phénomène de glissement dès la phase de conception ; ceci a abouti à l'élaboration d'une troisième méthode de conception de réservoirs à ouvertures polaires inégales (référence 3) ; celle-ci sera exposée dans les paragraphes suivants.

3.2.4 CONCEPTION A BOBINAGE EQUILIBRE ET STABILITE CONTROLEE

Le titre de ce paragraphe indique que cette conception prend en compte, d'une part l'équilibrage des forces dues à la pression interne, d'autre part, la stabilité du fil pendant ou après la phase de bobinage.

La mise en évidence des paramètres caractérisant cette stabilité fera l'objet du paragraphe suivant.

3.2.4.1 ANALYSE DE LA STABILITE DU FIL PENDANT LE BOBINAGE

Pendant la phase de bobinage, le fil est déposé sur le mandrin avec une tension T ; la figure 7 présente les grandeurs qui interviennent dans ce qui suit.

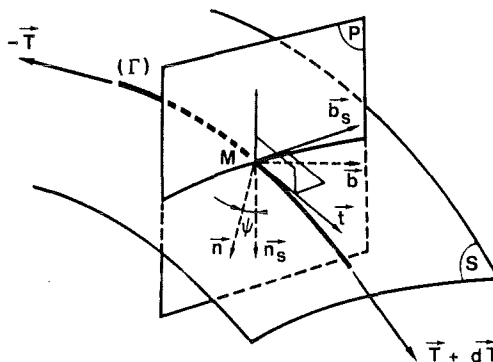


Figure 7

Le mandrin exerce sur le fil, par unité de longueur de celui-ci, une force \vec{F} qui peut s'écrire sous la forme :

$$\vec{F} = \lambda \vec{t} + \mu \vec{n}_s + \nu \vec{b}_s .$$

Il se démontre aisément, en mettant en équilibre un élément infiniment petit de fil, que les grandeurs λ , μ , ν ont les expressions suivantes :

$$\left\{ \begin{array}{l} \lambda = - \frac{dT}{ds} , \\ \mu = - Tc \cos \Psi , \\ \nu = - Tc \sin \Psi . \end{array} \right. \quad (30)$$

$$\mu = - Tc \cos \Psi , \quad (31)$$

$$\nu = - Tc \sin \Psi . \quad (32)$$

Sous l'effet de la tension T , le fil a tendance à glisser dans la direction du vecteur \vec{b}_s , par ailleurs, cette même tension "plaque" le fil sur le mandrin .

De ce fait, la tendance au glissement est caractérisée par la grandeur :

$$k = \left| \frac{\nu}{\mu} \right| = \left| \tan \Psi \right| . \quad (33)$$

Cette relation montre que l'angle Ψ est la grandeur qui caractérise la stabilité du bobinage ; en conséquence, dans la conception présentée ici, cet angle sera pris en compte pour exprimer la deuxième condition nécessaire pour déterminer $\rho(z)$ et $\alpha(z)$.

3.2.4.2 EXPRESSION DE $\tan \Psi$

L'expression de cette grandeur s'obtient de manière assez longue. Seuls, les principaux résultats intermédiaires seront successivement présentés.

Les composantes des vecteurs \vec{n}_s et \vec{t} dans le repère $(\vec{x}, \vec{y}, \vec{z})$ ont les expressions suivantes :

$$\vec{n}_s \left\{ \begin{array}{l} - \frac{\cos \theta}{D} , \\ - \frac{\sin \theta}{D} , \\ \frac{\rho'}{D} . \end{array} \right. \quad (34)$$

$$+ \frac{dt}{dz} \left\{ \begin{array}{l} \frac{\rho' \cos \alpha \cos \theta}{D} - \sin \alpha \cdot \sin \theta, \\ \frac{\rho' \cos \alpha \sin \theta}{D} + \sin \alpha \cdot \cos \theta, \\ \frac{\cos \alpha}{D} \end{array} \right. \quad (35)$$

Les expressions (35) ont été obtenues en tenant compte de la relation :

$$\frac{d\theta}{dz} = \frac{D \operatorname{tg} \alpha}{\rho} \quad (36)$$

Il est possible ensuite d'obtenir un vecteur parallèle à \vec{n} en calculant les composantes du vecteur $\frac{d\vec{t}}{dz}$:

$$\frac{d\vec{t}}{dz} \left\{ \begin{array}{l} \frac{\rho'' \cos \alpha \cos \theta}{D} - \frac{\rho' \alpha' \sin \alpha \cos \theta}{D} - \frac{\rho' \sin \alpha \sin \theta}{\rho} - \\ \alpha' \cos \alpha \sin \theta - \frac{\sin^2 \alpha \cos \theta}{\cos \alpha} \cdot \frac{D}{\rho} - \frac{\rho'^2 \rho''}{D^3} \cos \alpha \cdot \cos \theta, \\ \frac{\rho'' \cos \alpha \sin \theta}{D} - \frac{\rho' \alpha' \sin \alpha \sin \theta}{D} + \frac{\rho' \sin \alpha \cos \theta}{\rho} + \\ \alpha' \cos \alpha \cos \theta - \frac{\sin^2 \alpha \sin \theta}{\cos \alpha} \cdot \frac{D}{\rho} - \frac{\rho'^2 \rho''}{D^3} \cos \alpha \sin \theta, \\ - \frac{\alpha' \sin \alpha}{D} - \frac{\rho' \rho''}{D^3} \cos \alpha \end{array} \right. \quad (37)$$

L'expression de $\operatorname{tg} \Psi$ se déduit des relations (34) et (37) :

$$\operatorname{tg} \Psi = \frac{(\alpha' \rho \cos \alpha + \rho' \sin \alpha) (1 + \rho'^2)}{\rho \rho'' \cos^2 \alpha - (1 + \rho'^2) \sin^2 \alpha} \quad (38)$$

Remarque :

Une propriété caractéristique des courbes géodésiques d'une surface de révolution est que le vecteur normal à la surface et le vecteur normal principal à la courbe sont confondus en tout point.

Elles vérifient donc $\Psi = 0$.

La relation (38) indique donc : $\alpha' \rho \cos \alpha + \rho' \sin \alpha = 0$

Soit : $\rho \sin \alpha = C^{te}$

Ainsi est établie l'affirmation énoncée dans le paragraphe 3.2.2.3. Ceci montre donc bien que le fait de concevoir un réservoir dit "isotensolde" et concevoir ce même réservoir en déposant les fils suivant des lignes géodésiques est équivalent.

3.2.4.3 DETERMINATION DE LA GEOMETRIE ET DE LA LOI DE BOBINAGE

La première condition étant inchangée, le problème est résolu en intégrant le système différentiel suivant :

$$\left\{ \begin{array}{l} 2 + \frac{\rho \rho''}{1 + \rho'^2} = \operatorname{tg}^2 \alpha, \\ \frac{(\alpha' \rho \cos \alpha + \rho' \sin \alpha) (1 + \rho'^2)}{\rho \rho'' \cos^2 \alpha - (1 + \rho'^2) \sin^2 \alpha} = k \end{array} \right. \quad (39)$$

De plus, dans ce qui suit nous rechercherons des conceptions telles que la tendance des fils à glisser est constante sur toute leur longueur.

De même que précédemment, nous résolvons le système du premier ordre suivant par la méthode de Runge Kutta :

$$\left\{ \begin{array}{l} \rho' = u, \\ u' = \frac{1 + u^2}{\rho} (\operatorname{tg}^2 \alpha - 2), \\ \alpha' = \frac{1}{\rho \cos \alpha} (2 k \cos^2 \alpha + u \sin \alpha) \end{array} \right. \quad (40)$$

Le système suivant est résolu en utilisant des équations du même type que les relations (29) étendues à trois fonctions $f_1(u, \rho, \alpha)$, $f_2(u, \rho, \alpha)$, $f_3(u, \rho, \alpha)$.

La première équation du système (39) montre que cette conception entraîne de nouveau l'existence d'un point d'inflexion lorsque l'angle de bobinage atteint la valeur de $54,7^\circ$. Au-delà de ce point le fond a une forme sphérique, le rayon étant égal à la valeur du deuxième rayon de courbure en ce point et la ligne de dépôt du fil est géodésique assurant la continuité de l'angle de bobinage.

Enfin, l'angle θ nécessaire pour assurer le réglage de la machine à bobiner s'obtient numériquement à l'aide de la relation (36).

3.2.4.4 ETUDE DE LA PARTIE CYLINDRIQUE

La technique de bobinage avec une tendance au glissement constante peut être utilisée pour la partie cylindrique. Dans ce cas la relation (38) s'écrit :

$$-\frac{\alpha' \rho \cos \alpha}{\sin^2 \alpha} = k$$

Ainsi, en deux points M_1 et M_2 distants d'une longueur l , les angles de bobinage α_1 et α_2 vérifient :

$$\frac{1}{\sin \alpha_2} - \frac{1}{\sin \alpha_1} = \frac{kl}{\rho_0} \quad (41)$$

De même la variation de l'angle θ est obtenue en utilisant les relations (36) et (41) :

$$\theta_2 - \theta_1 = \frac{1}{k} \left\{ \log \left[\frac{kl}{\rho_0} + \frac{1}{\sin \alpha_1} + \sqrt{\left(\frac{kl}{\rho_0} + \frac{1}{\sin \alpha_1} \right)^2 - 1} \right] - \log \left[\frac{1}{\sin \alpha_1} + \frac{1}{\tan \alpha_1} \right] \right\} \quad (42)$$

3.2.4.5 APPLICATION DU BOBINAGE A TENDANCE AU GLISSEMENT CONSTANT

Lorsque le problème de concevoir un nouveau réservoir se pose, les grandeurs ρ_{F1} , ρ_{F2} et ρ_0 sont imposées. De plus, il est nécessaire de pouvoir se faire une opinion rapide sur la criticité des problèmes à résoudre. En effet, il faut pouvoir évaluer dans certains cas les risques technologiques et aussi être capable de prendre des décisions sur la nature du composite adapté au problème posé. Ceci a des conséquences techniques et évidemment une incidence sur le prix du produit vendu. Evidemment, ceci nécessite une première évaluation du problème n'exigeant pas une précision très fine.

C'est pourquoi la méthode présentée dans ces paragraphes et qui est employée dans nos fabrications industrielles, a été traitée de telle manière que quelques paramètres essentiels peuvent être évalués très rapidement.

A cet effet, nous présentons ci-dessous un diagramme commenté plus bas :

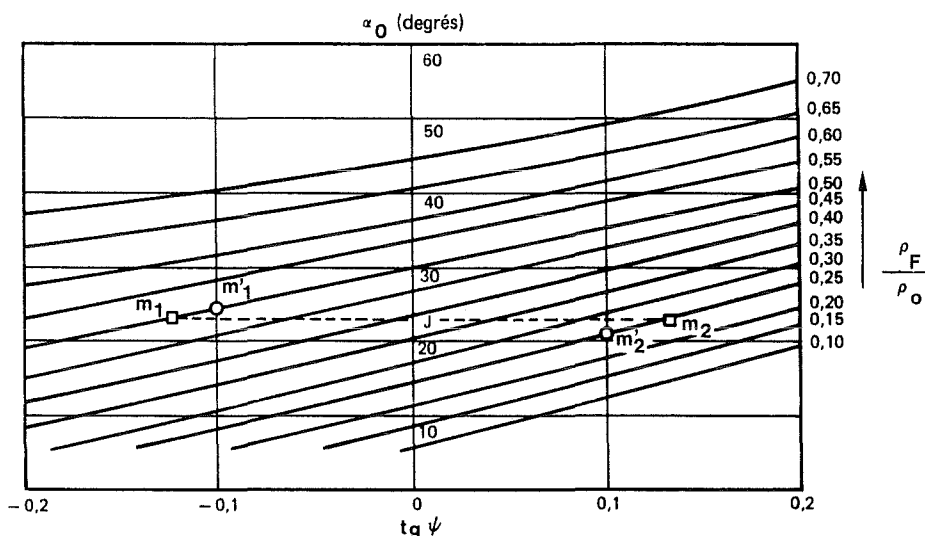


Figure 8

Ce diagramme relie les grandeurs :

- α_0 (angle de bobinage aux jonctions fond/cylindre),
- ρ_F / ρ_0 (ce que l'on appelle rapport d'ouverture),
- $\tan \psi$ (facteur de glissement).

Le tracé de ce diagramme a été obtenu par l'utilisation systématique du programme résolvant numériquement le système (40). Les lignes apparaissant sur la figure 8 ont pu ainsi être tracées point par point. L'exemple suivant permet de constater comment ce diagramme peut être utilisé.

Soit à réaliser un réservoir tel que :

$$\rho_{F1} / \rho_0 = 0,50 \quad (\text{fond arrière}) ,$$

$$\rho_{F2} / \rho_0 = 0,25 \quad (\text{fond avant}) .$$

Si une trajectoire hélicoïdale est utilisée pour déposer les fils sur le cylindre, les angles de bobinage aux deux jonctions fond/cylindre sont égaux. De plus, il sera admis que pour obtenir le bobinage le plus stable possible, il faudra procéder de telle sorte que les facteurs de glissement soient égaux sur les deux fonds. Dans ces conditions, les points m_1 et m_2 représentent donc les deux fonds sur le diagramme, celui-ci permettant alors d'obtenir :

$$\alpha_0 \approx 23^\circ ,$$

$$|\tan \psi| = 0,13 \text{ soit } \psi = 7,4^\circ .$$

Une autre possibilité consiste à choisir une loi de bobinage en partie cylindrique, qui présente une tendance au glissement. Dans ce cas, les angles de bobinage aux deux extrémités du cylindre peuvent être différents.

Alors, les points m'_1 et m'_2 obtenus toujours en égalant la tendance au glissement sur les deux fonds, représentent une nouvelle solution du problème.

Dans le cas présent, le facteur de glissement est diminué :

$$\operatorname{tg} \Psi = 0,10 \text{ soit } \Psi = 5,7^\circ .$$

La stabilité du bobinage sur les fonds a donc été améliorée. En lisant des valeurs des angles de bobinage aux jonctions fond/cylindre sur le diagramme il est aisé de calculer le facteur de glissement sur le cylindre à l'aide de la relation (41).

3.2.4.6 ETUDE DE LA CONTRAINTE DANS LES FILS

La relation (20) qui donne l'expression générale de la contrainte locale dans les fils peut s'écrire :

$$\sigma_{fs} = H \frac{\rho^2 \sqrt{1 + \rho'^2}}{\cos \alpha} ,$$

avec :

$$H = \frac{P}{2 \chi e_{so} \rho_o \cos \alpha_o} .$$

L'expression de $\frac{d \sigma_{fs}}{dz}$ est écrite ci-dessous :

$$\frac{d \sigma_{fs}}{dz} = H \left[\frac{2 \rho \rho' D}{\cos \alpha} + \frac{\rho^2 \rho' \rho''}{\cos \alpha \cdot D} + \rho^2 D \frac{\sin \alpha \cdot \alpha'}{\cos^2 \alpha} \right] .$$

La relation (17) permet d'éliminer ρ'' . Après simplification il vient :

$$\frac{d \sigma_{fs}}{dz} = - 2 \rho H \operatorname{tg} \alpha \cdot D \cdot \operatorname{tg} \Psi . \quad (43)$$

En utilisant le principe d'égaliser les tendances au glissement sur les deux fonds, il apparaît sur le diagramme de la figure 8 que :

- $\operatorname{tg} \Psi$ est négatif pour le fond ayant la grande ouverture (fond arrière),
- $\operatorname{tg} \Psi$ est positif pour le fond ayant la petite ouverture (fond avant).

Compte tenu de cette remarque, il découle donc de la relation (43) que la contrainte dans les fils augmente depuis la jonction fond/cylindre jusqu'au point d'inflexion pour le fond arrière et diminue pour le fond avant.

De ce fait, sans prendre en compte les phénomènes de flexion que les théories développées jusqu'à présent ne peuvent prendre en compte, il apparaît que le fond arrière devra toujours posséder une épaisseur supérieure à celle de l'autre fond pour tenir compte de la contrainte maximale atteinte au point d'inflexion.

3.3 CONCLUSION SUR LES METHODES DE CONCEPTION

Ces méthodes de conception présentées sont aujourd'hui en fonctionnement et font l'objet d'une utilisation quasi quotidienne. Elles sont utilisables en mettant en oeuvre des matériels et des logiciels simples. Les délais pour obtenir les résultats sont courts (de l'ordre de la journée). Les entrées et les sorties sont d'un faible volume.

Les résultats sont complets puisque l'on peut obtenir principalement :

- la géométrie d'ensemble,
- les masses et volume de l'enveloppe bobinée,
- les paramètres de bobinage des machines à bobiner,
- des paramètres permettant d'avoir un avis sur les difficultés de réalisation.

Toutefois, les hypothèses de ces méthodes sont telles qu'une vérification de la tenue de la structure aux spécifications doit être faite pour s'assurer, en particulier, que les surcontraintes locales sont admissibles.

De plus, les renforts métalliques doivent aussi faire l'objet de calculs que ne peuvent faire les méthodes décrites.

Le paragraphe suivant décrira les méthodes utilisées pour justifier de manière définitive la structure avant que des phases de réalisation irréversibles ne soient commencées.

4. JUSTIFICATION

4.1 PRINCIPES DES METHODES DE JUSTIFICATION

La méthode de travail consiste à utiliser un moyen de calcul fondé sur la technique des éléments finis (S.A.M.C.E.F. mis au point par le LTAS de l'Université de Liège).

L'objet n'étant pas de décrire la méthode des éléments finis nous énoncerons les grands phénomènes pris simultanément en compte pour assurer une étude du comportement de telles structures de la manière la plus réaliste possible :

- le comportement non linéaire géométrique lié au fait que la pression interne, à l'équilibre, ne s'exerce pas sur la géométrie initiale mais sur la géométrie déformée est nécessaire pour obtenir des déplacements et un état de contrainte correspondant à la réalité,

- l'anisotropie locale et variable suivant l'angle de bobinage, donc le point considéré de la structure, est un fait dont il faut tenir compte en créant des fichiers de données représentant les termes de la matrice de Hooke tout le long de la structure,
- des lois de comportement élasto-plastique sont nécessaires pour relier de manière réaliste les tenseurs de contraintes et de déformations des embases polaires,
- l'existence des jeux entre embases polaires, systèmes d'obturation et leurs liaisons ne peut être négligée et a conduit à développer des extensions du logiciel SAMCEF.

4.2 PRESENTATION DES PRINCIPAUX RESULTATS

Les résultats font l'objet de listings volumineux, nous extrairons de ceux-ci quelques planches représentatives.

1 - Contraintes dans les fils

Ces contraintes sont présentées sur des planches de type de la figure ci-dessous :

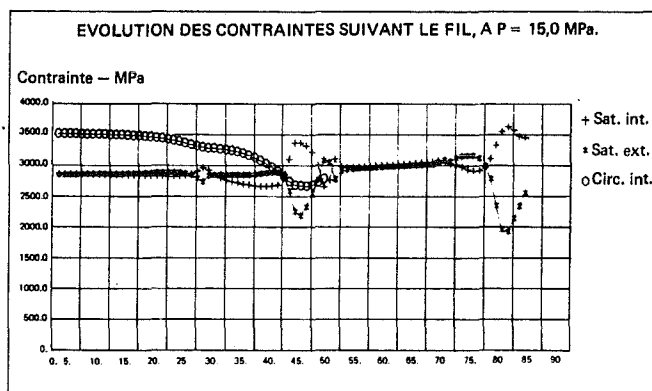


Figure 9

Cette figure indique l'évolution des contraintes depuis le milieu du cylindre jusqu'à l'ouverture d'un des deux fonds. Ces contraintes concernent les couches interne et externe de telle manière que les phénomènes locaux soient mis en évidence. On constate principalement une évolution sensiblement constante excepté :
 - à la jonction fond/cylindre,
 - dans une zone proche de l'ouverture.

Seule la méthode aux éléments finis peut fournir les valeurs maximales atteintes et justifier le renforcement qui avait été défini en se fondant sur les expériences passées.

2 - Contraintes dans les embases polaires

Plusieurs représentations ont été utilisées dans les années passées pour illustrer un état de contrainte bidimensionnel à partir de fichiers numériques fournissant un tenseur de contrainte par élément de la modélisation.

Actuellement il est retenu de fournir au concepteur des figures en couleur définissant par zone les niveaux atteints. Le type de figure est représenté ci-dessous :

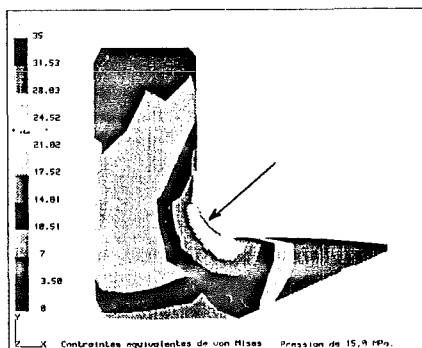


Figure 10

Ici est dessinée une coupe radiale d'une embase polaire avant (petite ouverture).

On constate sur cet exemple que la zone la plus sollicitée est située dans l'arrondi indiqué par la flèche.

De multiples résultats sont obtenus et font l'objet d'une analyse précise conduisant soit à des modifications, soit à une décision de donner accord pour effectuer la réalisation. Nous ne citerons que les principaux paramètres critiques pour la tenue de la structure :

- cisaillement entre couches du bobinage (possibilité récemment mise au point),
- cisaillement des lames de caoutchouc assurant la liaison bobinage/embases polaires,
- déformée générale de la structure pour juger de son encombrement.

4.3 ANALYSE CRITIQUE DES METHODES DE CONCEPTION ET DE JUSTIFICATION

Il est de règle dans notre Société de considérer que l'existence de ces deux méthodes est nécessaire. La première possède les qualités de rapidité, d'efficacité et la capacité de permettre à leurs utilisateurs de garder une connaissance intuitive en ce qui concerne l'influence des principaux paramètres sur les résultats obtenus. La deuxième, plus longue d'emploi, plus chère est seule adaptée pour permettre de tirer la conclusion de pouvoir fabriquer la structure.

C'est pourquoi il est nécessaire de préserver un équilibre entre l'utilisation de ces deux méthodes que nous considérons comme complémentaires.

5. CARACTERISATION DES MATERIAUX

Ce sujet mériterait à lui seul un document et une présentation particulière. Nous limiterons ici l'exposé à quelques grands principes ayant pour objet de mettre en évidence l'importance de cette caractérisation dans le domaine de production industrielle.

La caractérisation peut être décomposée en deux grandes catégories :

- travaux liés à la connaissance des propriétés dans le but de permettre au Bureau d'Etude de réaliser la justification du produit à fabriquer en ayant les renseignements les plus complets possibles concernant les caractéristiques des matériaux constituant le bobinage et le composite.

Par exemple, le Bureau de Calcul a besoin de lois de comportement liant les tenseurs de contraintes et déformations. Des essais particuliers sont nécessaires pour déterminer les termes de la matrice de Hooke si un comportement linéaire est considéré comme représentatif. Ce cas particulier, le plus simple qui puisse être choisi, nécessite toutefois la détermination de neuf coefficients.

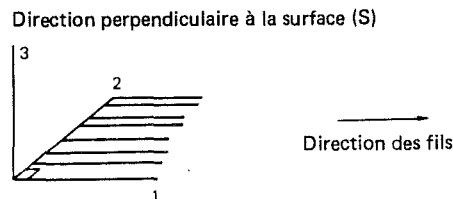


Figure 11

Les relations s'écrivent :

$$\begin{bmatrix} \sigma_{11} \\ \sigma_{22} \\ \sigma_{33} \\ \sigma_{12} \\ \sigma_{13} \\ \sigma_{23} \end{bmatrix} = \begin{bmatrix} H_{11} & H_{12} & H_{13} & 0 & 0 & 0 \\ & H_{22} & H_{23} & 0 & 0 & 0 \\ & & H_{33} & 0 & 0 & 0 \\ & \text{Sym} & & G_{12} & 0 & 0 \\ & & & & G_{13} & 0 \\ & & & & & G_{23} \end{bmatrix} \begin{bmatrix} \epsilon_{11} \\ \epsilon_{22} \\ \epsilon_{33} \\ \gamma_{12} \\ \gamma_{13} \\ \gamma_{23} \end{bmatrix} \quad (44)$$

D'autres méthodes, dans les années 70, partant des propriétés des fils et de la résine permettaient de déterminer les éléments de la relation (44). Alors la caractérisation des constituants était nécessaire.

Des lois spécifiques ont été parfois nécessaires lorsque le composite avait des relations (σ, ϵ) non linéaires (dégradation du composite, par microfracturation de la résine pendant la mise en pression interne).

Par ailleurs, en plus du composite, la présence de caoutchouc a nécessité des expérimentations permettant de relier la contrainte à la déformation. Des courbes du type suivant ont été utilisées :

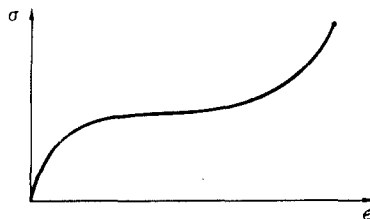


Figure 12

- La deuxième catégorie concerne la caractérisation nécessaire pour assurer la conformité du produit réalisé aux spécifications de réception des matériaux.

Les caractérisations sont multiples, nous ne détaillerons ici que ce qui est attaché au bobinage.

La fibre est achetée à des fabricants qui livrent la matière en quantités telles qu'elles appartiennent à un lot de leur fabrication. Avant utilisation pour fabrication d'une structure bobinée, des éprouvettes de conception semblable aux propulseurs sont réalisées à échelle réduite (diamètre 304 mm). Les éprouvettes sont soumises à rupture sous pression interne. Les valeurs obtenues permettent de décider si le matériau peut ou non être utilisé.

Des essais moins onéreux sont faits sur des mèches unidirectionnelles soumises à des efforts de traction. Toutefois, le premier type d'essai, plus cher, est plus représentatif des sollicitations biaxiales (méridien, parallèle) qui existent sur une structure réelle.

Des valeurs caractéristiques des performances des matériaux seront indiquées dans le paragraphe 8.

6. FABRICATION

Ce paragraphe sera consacré aux modes de fabrication de ce type de structure. Trois parties seront détaillées :

- a - description des machines à bobiner,
- b - description des principales phases de fabrication,
- c - commentaires particuliers sur la manière d'obtenir le composite bobiné.

6.1 DESCRIPTION DES MACHINES A BOBINER

Les machines à bobiner que nous utilisons sont de deux types, nous retiendrons les dénominations suivantes :

- machine satellite verticale,
- machine horizontale.

6.1.1 MACHINE SATELLITE VERTICALE

Le principe de fonctionnement d'une telle machine est représenté par la figure ci-dessous :

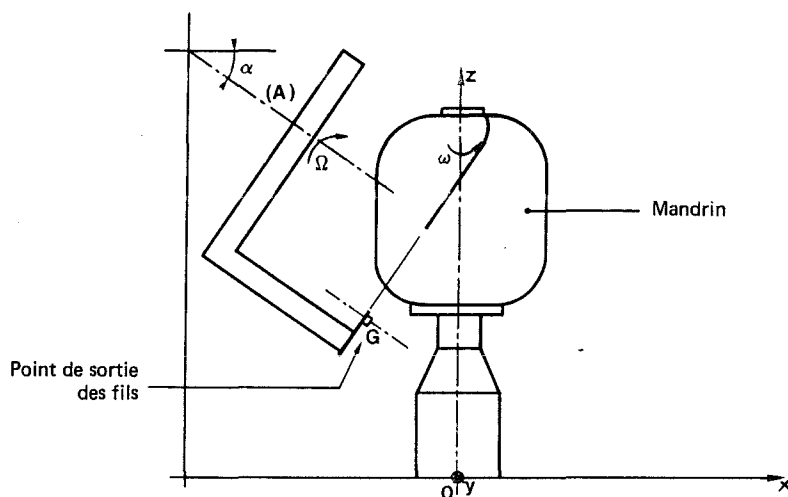


Figure 13

Le mandrin est fixé sur un support, l'axe étant vertical. Un bras tournant à une vitesse Ω supporte le cheminement des fils et comporte à son extrémité, un dispositif destiné à assurer la sortie de ceux-ci avant la dépose sur le mandrin.

Si le mandrin est immobile, les fils après plusieurs rotations du bras, seront déposés par superposition suivant une trajectoire planaire. C'est pourquoi une petite rotation du mandrin est nécessaire afin de provoquer un décalage de l'ensemble des fils (nappe) à l'issue d'un tour de rotation du bras. C'est ainsi que l'on assure le recouvrement du mandrin. Lorsque l'ensemble de ces décalages représente 360° , une couche du bobinage est constituée.

Le nombre de couches déposées est défini par l'épaisseur de composite nécessaire pour respecter les spécifications de tenue (paragraphe 3).

La configuration de certaines structures est telle que la stabilité du bobinage planaire n'est pas assurée. Pour résoudre ce problème, la technique du "bobinage planaire modifié" est utilisée. Ce type de bobinage est réalisé en faisant tourner le mandrin à une vitesse de rotation ω . La trajectoire de dépôt du fil n'est plus planaire. Lorsque le bras a fait un tour, la nappe ne se dépose plus à côté de la précédente dépose. Le rapport des vitesses ω et Ω est choisi de telle sorte que la juxtaposition puisse se produire. On obtient ainsi des bobinages étoilés.

Ce type de machine ne permet pas de respecter en toute rigueur les lois $\alpha(z)$ compatibles avec la forme du mandrin définie par $\rho(z)$. Toutefois, l'expérience montre qu'il est possible d'approcher les lois théoriques.

Par ailleurs, ces machines sont simples, rapides et fiables. De plus, elles existent et il convient de les utiliser. C'est pourquoi ce type de machine est encore très utilisé. Nous verrons ultérieurement qu'elles présentent toutefois des limitations en ce qui concerne le type de mise en oeuvre du composite au moment du bobinage.

6.1.2 MACHINE A BOBINER HORIZONTALE

Le principe de fonctionnement de telles machines est représenté par la figure ci-dessous :

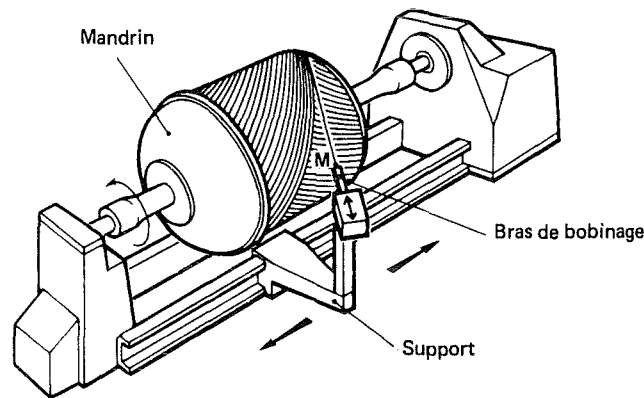


Figure 14

- Dans le cas le plus simple, les mouvements permettant de réaliser le dépôt de la nappe de fils sont :
- une rotation du mandrin,
 - un déplacement parallèle à la direction z du support,
 - un déplacement du bras de bobinage dans la direction y.

Donc, le point M symbolisant ici la tête de bobinage d'où sort la nappe de fils peut se déplacer de manière quelconque dans un plan parallèle à \vec{z} .

Des perfectionnements peuvent être apportés dans un domaine particulier pour améliorer la qualité du bobinage.

La nappe déposée est, en pratique, un ensemble de mèches qui elles-mêmes sont un ensemble de plusieurs milliers de filaments (la mèche est l'état du matériau livré par le fabricant). De ce fait, la nappe qui sort de la tête de bobinage (M) a une largeur qui, en général, est environ 20 mm. Pour diminuer la durée de cette phase de réalisation il est envisagé d'augmenter cette largeur jusqu'à environ 50 mm. Il est inévitable que la nappe n'est pas naturellement planaire entre le point M et le point de tangence avec le mandrin. Ce phénomène, s'il est trop accentué, peut provoquer une mauvaise qualité de bobinage. Afin d'y remédier, il est développé actuellement une tête de bobinage possédant des degrés de liberté de rotation autour du point M. Ces degrés de liberté seront programmés de même que les mouvements principaux décrits au début.

Ce type de machine permet de respecter parfaitement les lois de bobinage théoriques ($\alpha(z)$) définies au paragraphe 3. De plus, elles permettent, contrairement aux machines verticales, de bobiner les structures quelle que soit la mise en oeuvre du composite (paragraphe 6.3).

6.2 PRINCIPALES PHASES DE FABRICATION

La réalisation des structures de propulseur a pour objet de livrer au client une structure prête à être chargée de poudre et équipée de la tuyère avant de pouvoir devenir un étage propulsif prêt à être assemblé avec le reste du vecteur.

De ce fait, la réalisation se décompose comme suit :

- réalisation des pièces primaires (cadres et embases polaires),
- réalisation des protections thermiques internes assemblées aux embases polaires par drapage de caoutchouc dans des moules spécifiques. La vulcanisation est assurée par mise en étuve sous pression (autoclave),
- réalisation du mandrin par apport de sable et de liant dans des moules équipés des protections thermiques protégées. Après tassage du sable, celui-ci est durci par mise des moules en étuve,
- assemblage des différentes parties ainsi constituées afin d'obtenir le mandrin prêt au bobinage,
- fixation du mandrin sur la machine à bobiner et bobinage,
- polymérisation du composite en étuve (la réalisation des jupettes peut se faire pendant la phase de bobinage ou après la première polymérisation, dans ce dernier cas, un deuxième cycle de polymérisation est nécessaire),
- extraction du sable par adjonction d'eau tiède provoquant la désagrégation et l'évacuation du sable,
- usinage des jupettes, fixation des cadres de jupettes et opération de finition,
- contrôles géométriques et de zones critiques telles que les liaisons en particulier. Une phase importante du contrôle est le timbrage de la structure à une pression interne égale à 1.15 fois la pression maximale de fonctionnement.

Enfin intervient la livraison de la structure.

6.3 MISE EN OEUVRE DU COMPOSITE

Deux méthodes sont utilisées. Elles concernent la manière d'imprégner les mèches de fils avec la résine.

La première (méthode W) consiste à imprégner les mèches pendant la phase de bobinage immédiatement avant le dépôt des fils sur le mandrin. Nous l'appellerons technique WET.

La deuxième (méthode P) consiste à imprégner les mèches avant la phase de bobinage (parfois plusieurs mois), soumettre les fils imprégnés à un champ thermique pour provoquer un début de polymérisation et ensuite stocker ce produit sur des bobines en congélateurs à -18°C . Nous l'appellerons bobinage Prepreg.

Ces deux méthodes présentent naturellement des avantages et des inconvénients.

a - Méthode W

Le procédé est moins cher que la méthode P. Par contre la stabilité du fil pendant la phase de bobinage est parfois faible.

b - Méthode P

Ce procédé permet d'obtenir une meilleure stabilité pendant la phase de bobinage. Par contre, il entraîne une augmentation du coût de la structure du fait du temps supplémentaire nécessaire pour réaliser le Prepreg.

Une autre source de surcoût lié à l'amélioration de la qualité est le contrôle du produit avant son utilisation.

Enfin, il faut noter (paragraphe 3.2.4) que, dans certaines configurations le Prepreg est nécessaire pour pouvoir bobiner la structure.

7. QUALIFICATION EXPERIMENTALE

En dehors d'actions expérimentales destinées à caractériser les matériaux utilisés pour réaliser la structure, une nouvelle structure fait l'objet d'un essai destructif permettant de connaître la tenue ultime de l'objet.

Les jupettes sont soumises à des efforts mécaniques déterminés afin de représenter au mieux l'état de contrainte le plus sévère.

Le reste de la structure est soumis à un essai destructif, par application d'une pression interne générée par apport d'eau dans la capacité bobinée.

De plus, un effort mécanique appliqué sur la liaison arrière représente le délestage de poussée. La jupette avant est donc soumise à un effort de compression.

Ce type d'essai doit démontrer que la pression de rupture P_R est telle que :

$$P_R > K \times P_{MF} ,$$

(P_{MF} = pression maximale de fonctionnement) .

La structure est placée en position verticale dans une fosse. De nombreuses mesures sont effectuées afin de :

- permettre d'expliquer comment la rupture a été initiée,
- permettre au groupe calcul de comparer la prévision théorique à la réalité,
- donner au responsable du chargement de la poudre les conditions aux limites concernant la déformation de l'enveloppe bobinée.

Ces mesures sont réalisées à l'aide de capteurs de déplacements et de jauges de déformations.

Les zones particulièrement instrumentées sont :

- le milieu de la partie cylindrique pour déterminer la sollicitation dans l'enroulement circonferentiel,
- les liaisons jupettes/cylindre qui sont des zones de flexion,
- les zones du composite proche des embases polaires (zones de flexion),
- l'embase polaire arrière métallique toujours optimisée car lourde du fait de la grande ouverture.

Ces essais sont toujours longs du fait d'une instrumentation dense (250 voies de mesures pour les essais importants) et de la mise en oeuvre de moyens importants :

- moyens d'enregistrements nécessitant de raccorder chaque voie de mesure à un système d'acquisition de données,
- moyens mécaniques lourds afin de garantir le respect des règles de sécurité.

Enfin des enregistrements vidéo et par caméras rapides (≈ 3000 images/secondes) sont systématiquement faits, en couvrant au mieux l'intégralité de la structure, pour permettre après essai de revoir le déroulement de la rupture.

La Fosse d'essai a une hauteur d'environ 8 mètres et un diamètre d'environ 7 mètres.

La figure ci-dessous permet de préciser les notions rapidement évoquées dans ce paragraphe.

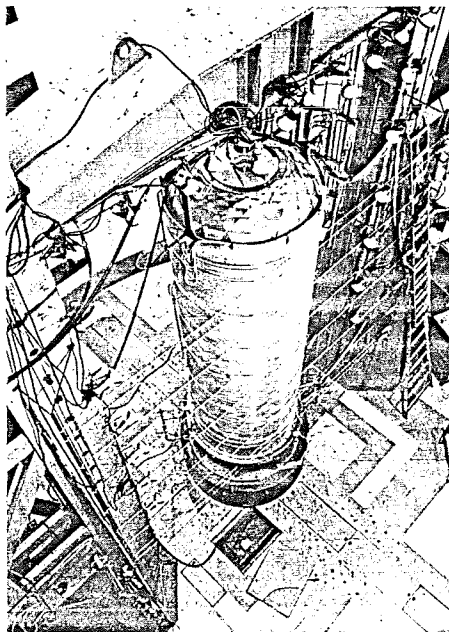


Figure 15

8. RESULTATS

Nous présenterons dans ce paragraphe quelques résultats permettant d'évaluer :

- les performances obtenues par bobinage comparées à quelques métaux,
- l'évolution des performances des produits bobinés,
- la performance spécifiquement attachée à la notion de structure de propulseur.

8.1 COMPARAISON COMPOSITE/METAL

Nous excluerons ici les performances pouvant être indiquées par les fournisseurs pour établir ce type de comparaison. En effet, les performances dépendent évidemment des qualités intrinsèques des matériaux, mais tout aussi fortement de l'objet (géométrie, sollicitations) et de la qualité de la mise en oeuvre déterminée par la mise au point de bonnes résines, associées à de bons cycles thermiques, la qualité du bobinage etc...

De ce fait, le composite bobiné évalué ici, l'aura été à l'aide de contraintes à rupture obtenues sur des éprouvettes connues et dont il a été discuté paragraphe 5.

De plus, les contraintes présentées sont obtenues en prenant en compte, non pas la section des fibres sèches, mais la section totale (fibre sèche + résine d'imprégnation).

Enfin, le paramètre retenu est σ / d (d = densité du composite).

Ainsi on obtient à ce jour :

MATERIAUX	σ / d
Composite verre	≈ 900
Composite Kevlar	≈ 1400
Composite Carbone (IM6 Hercules)	≈ 1600 à 1800
Acier	≈ 200
Alliage léger	≈ 170
Titane	≈ 220

σ = exprimé en MPa.

L'intérêt du composite est très important si l'on compare les valeurs du tableau ci-dessus.

De plus, on constate que les fibres successivement utilisées : verre, kevlar et carbone ont apporté des augmentations de performances sensibles. Sur ce point, il convient de faire apparaître la notion d'effet d'échelle.

On ne peut, l'expérience l'a montré, juger la performance uniquement sur les résultats obtenus sur éprouvettes de petites dimensions (diamètre ≈ 300 mm).

En effet, il a été constaté avec l'utilisation du verre et du kevlar une diminution significative des performances lorsque les dimensions de la structure augmentaient. Ce fait expérimental non expliqué par nos services Etudes est mis en évidence sur le diagramme ci-dessous :

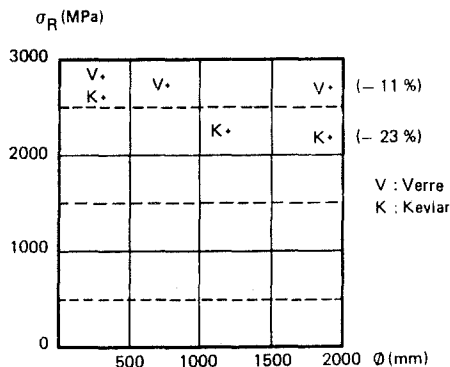


Figure 16

- Il est constaté donc respectivement :
- 23 % de diminution ($\phi = 300$ mm à $\phi = 2000$ mm) pour le kevlar,
 - 11 % de diminution ($\phi = 300$ mm à $\phi = 2000$ mm) pour le verre.

Ce phénomène a rendu beaucoup plus difficile l'obtention de définition respectant les spécifications lorsque ces matériaux étaient utilisés.

De plus, les performances constatées lors des essais préliminaires d'évaluation à petites échelles n'ayant pu être obtenues sur l'objet réel, la masse inerte de la structure a été augmentée.

En ce qui concerne la fibre carbone, ce phénomène semble ne pas exister aujourd'hui, ce qui augmente encore l'intérêt de ce nouveau matériau.

8.2 FACTEUR DE PERFORMANCE DES STRUCTURES DE PROPULSEURS

La grandeur suivante est fréquemment utilisée dans le monde des industriels réalisant de telles structures ; elle est définie comme suit :

$$q = \frac{pV}{mg}$$

p = Pression de rupture.

V = Volume interne.

m = Masse de la capacité bobinée.

g = Accélération terrestre.

Ce facteur a la dimension d'une longueur. Pour les pays utilisant le système métrique, elle est couramment exprimée en kilomètres.

Ce facteur est effectivement assez représentatif des critères que souhaitent respecter les fabricants.

En effet, q est d'autant plus grand que :

- p est grand (sans commentaire),
- V est grand, ce qui correspond au souhait de pouvoir transporter la masse de poudre la plus grande possible,
- m est petit, ce qui correspond à une masse inerte la plus petite possible.

L'augmentation de q représente donc bien le souci d'apporter, pour un étage, sa meilleure contribution à la portée du vecteur.

Toutefois, il convient de noter que la comparaison d'une structure à l'autre doit être faite en prenant garde au fait que la longueur totale est imposée au fabricant de structure.

Or, à qualité égale de réalisation une analyse rapide montre que, tout restant inchangé, augmenter la longueur entraîne une augmentation du facteur de performance.

Ces remarques étant exprimées, nous présentons toutefois, à titre indicatif, les meilleures performances obtenues par notre société en ce domaine.

Diamètre (mm)	1500	2000	1150
Matériaux	Verre	Kevlar	Carbone
q (km)	20	31	41

Le domaine des longueurs étant assez resserré, on peut donc clairement constater les progrès apportés par l'évolution des fibres commercialisées.

8.3 INFORMATIONS SUR L'EVOLUTION FUTURE

En ce qui concerne la fibre carbone, deux grands fabricants proposent des fibres de plus en plus performantes : l'Américain HERCULES et le Japonais TORAYCA.

En ce qui concerne HERCULES, après les fibres AS4 et AS6 cette société commercialise la fibre IM6 annoncée à :

$$\sigma_R = 5000 \text{ MPa (essai mèche)}$$

Une autre fibre existe et est encore peu commercialisée l'IM7 annoncée à :

$$\sigma_R = 5500 \text{ MPa (essai mèche)}$$

D'autres fibres au stade laboratoire laissent espérer des niveaux plus élevés.

En ce qui concerne TORAYCA, après la fibre T300 (classe AS4), cette société commercialise les fibres T800 et T800H qui sont respectivement comparables aux fibres IM6 et IM7.

Plus récemment, ce fabricant a annoncé la fibre T1000 à :

$$\sigma_R = 7000 \text{ MPa (essai mèche)}$$

On constate donc une évolution rapide des matériaux mis à la disposition des fabricants de structures bobinées. Ce fait rend d'autant plus difficiles certaines décisions, que, lorsqu'un programme commence, il faut toujours avoir à sa disposition les éléments qui permettent l'utilisation des meilleures fibres, celles-ci devant être constamment évaluées et qualifiées pour application industrielle.

9. CONCLUSION

L'expérience des années passées, en matière de conception et de justification, a été détaillée dans ce document (paragraphes 4 et 5). Il est important de noter que ces méthodes ont été développées pour répondre à des besoins bien précis concernant les structures de propulseurs, dont les grandes lignes ont été présentées dans le paragraphe 2.

Nous insistons, car ceci est l'image d'un effort permanent de notre groupe Etude, sur le fait que nous avons toujours voulu préserver la rapidité dans le domaine de la pure conception et la précision dans la justification.

Il convient aussi de faire apparaître le souci constant d'imaginer des conceptions permettant à notre groupe Production de fabriquer des structures de qualité à moindre coût. Les commentaires portant sur le choix WET ou Prepreg et sur les problèmes de stabilité de bobinage avaient pour but de mettre en lumière de telles considérations.

Si les résultats présentés montrent de manière évidente l'intérêt du composite bobiné par rapport aux matériaux métalliques, ceux-ci mettent aussi en évidence les progrès faits par les fabricants de fibres. Actuellement, les industriels doivent en permanence prendre en compte une évolution rapide des performances du carbone.

Enfin, la conception assistée par ordinateur, non traitée dans ce document car c'est un domaine dans lequel les moyens se mettent progressivement en place, est un sujet très important pour notre Etablissement. Il permet aux exécutants, d'être déchargés de travaux répétitifs pour mieux se consacrer à l'optimisation de la structure. Il faut signaler de plus que des moyens permettant le transfert automatique d'éléments de définition à la production commencent à se mettre en place. En particulier, dès la phase de conception les paramètres de bobinage sont stockés sur des supports magnétiques qui sont ensuite directement utilisables aux postes de commande des machines à bobiner. Ceci a pour effet de diminuer la main-d'oeuvre donc le coût, ainsi que les risques d'erreurs.

Actuellement, nous considérons donc que des progrès doivent être faits dans l'automatisation pendant la phase de conception - justification et pendant la phase de fabrication.

En conclusion, nous espérons avoir fait clairement apparaître que notre souci constant a été, en matière de conception, d'imaginer des solutions prenant en compte non seulement la performance du produit mais tout autant la qualité et l'efficacité pendant la phase de fabrication.

Références :

- [1] TIMOSHENKO AND WOINOWSKI-KRIEGER - Theory of plates and shells.
(Second Edition) Mc Graw Hill Company - New York - 1959 - Page 435.
- [2] HILDEBRAND - Introduction to numerical Analysis
Mc Graw Hill Company - New York - 1956 - Pages 236 - 237.
- [3] J.P. DENOST - New Design concepts for filament wound pressure vessel with unequal openings.
Société Nationale Industrielle Aérospatiale - 1982 - AIAA (Cleveland).

CONSIDERATIONS FOR DESIGNERS OF CASES
FOR SMALL SOLID PROPELLANT ROCKET MOTORS.

by: H. Badham Manager Rocket Motor Design & Development
G.P. Thorp Projects Manager
R.O. SUMMERFIELD
Kidderminster DY11 7RZ
Great Britain
(Operated by IMI Kynoch Limited
on behalf of Royal Ordnance plc).

Summary

When considering the initial design of the case or load bearing components for a solid propellant rocket motor a number of possible solutions may be apparent and many factors need consideration before the design of the individual components can be finalised.

The process of optimisation involves consideration of material properties, methods of manufacture, inspection and proof as well as interactions with other rocket motor and missile components. The various factors are considered and indications are given of the interactions to be taken into account.

This paper concentrates primarily on the design of metallic motor cases. Both homogeneous and non-homogeneous body structures are considered, the latter being fibre overwound metallic and strip laminate.

A relatively recent requirement is that for insensitive munitions and this factor is also discussed relative to body construction.

1. Introduction

The design of the hardware, that is the load bearing structure, of solid propellant rocket motors is dependent on many interacting factors arising from the requirements and the overall motor design. Consequently it is only possible to give concepts and guide lines and not precise design details. Only metallic structures are considered in this paper, composite structures being the subject of a separate paper.

In hardware design an important aid for the design of the more complex components is finite element stress analysis, a powerful tool allowing more optimum designs to be achieved and a reduction in testing. Comments on the use of this technique is included.

The main factors to be considered when designing hardware are the requirements, and the material and manufacturing methods: separate sections are developed to these aspects.

Rocket motor cases may be homogeneous or non-homogeneous structures and these are dealt with independently. Other components which are common to both types of cases are considered under the former. Two non-homogeneous case constructions are detailed, a composite overwound metallic and strip laminate the latter being an adhesively bonded structure.

A relatively recent requirement is for insensitive munitions and the final section of this paper is devoted to this topic.

2. Finite Element Stress Analysis

Finite element stress analysis is a powerful aid used extensively in rocket motor design for evaluating stresses and strains allowing the design of more optimised components which could require less testing.

The structure or continuum to be analysed is modelled as a set of elements of finite size connected only at points called nodes. Each node has specified freedoms of translation and rotation in response to the neighbouring elements or boundary conditions. The stresses are obtained from the field of nodal displacements together with the appropriate constitutive equations for the material properties.

Significant advances have been and are still being made in the basic computer stress analysis programmes, some programmes being very general and others having been developed for a specific industry. Two significant advances that have simplified stress analysis are programmes for element generation and the display of results.

However sophisticated these suites of programmes, in general they can only analyse a structure; they are design aids and cannot replace designers and stress analysts.

To optimise a component a design is first evolved usually based on a classical text book approach coupled with general design expertise. The stress analyst will then define the elements which from experience he considers best fit the component. The resultant analysis will show areas of high or low stress or strain. If it is considered that changes are necessary to the design then the designer and stress analyst will decide from previous experience the modifications to be made prior to carrying out a further analysis.

As programmes become simpler to use there is the temptation to design the ultimate component. When deciding whether a design is satisfactory the limitations of the programme, limitations imposed by machining accuracies and material properties and the possible advantages particularly in terms of mass must all be taken into account.

More specific comments on finite element stress analysis are included in the following sections.

Programmes

Many programmes exist for finite element stress analysis and it is essential to attempt to evaluate these to find the ones most suitable for the work required.

The use of any finite element programme requires a detailed knowledge of the capabilities of that programme and it is usually best to obtain a detailed understanding of one programme. However if, as is usual, a number of people in one organisation are involved in stress analysis different people may be involved with different programmes, thus allowing the 'best' one to be used for any particular application.

Programmes for rocket motor design should be able to deal with almost any stress problem featuring almost any geometry, complete anisotropy, various material constitutive formulations, regions of differing materials in the same body and thermal, pressure, acceleration or point loadings in combination. Both two and three dimensional problems should be handled and the analysis should not be limited to small strains or small deflections.

For general rocket motor analysis it could be advantageous for the programme to deal with isotropic materials having a Poisson's ratio of 0.5. Many programmes do not have this capability, the results becoming increasingly inaccurate as the value of 0.5 is approached. This limitation is probably because a formulation of the governing equations is required to deal with this special case.

A major finite element programme will offer about a hundred different element types ranging from those with very general applications such as brick elements to special elements exemplified by those that simulate a crack tip. The analysis tends to yield relatively inaccurate results if elements exhibit long, thin aspect ratios or corner angles near to zero or 180°. Usually these situations can be avoided but difficulties can be experienced with long, thin, adhesive layers in bonded structures.

The two elements most frequently used for the analysis of components are the quadrilateral with its degenerate form the triangle and the hexahedron with its degenerate form the triangular prism or tetrahedron.

The quadrilateral is used as a plane element in either plane strain or plane stress or as an axisymmetric element under axisymmetric loading. For many applications an adequate initial solution may be obtained by making an analysis using slight modifications to the geometry to bring it within the scope of this element. Applications include motor bodies, end rings and reasonably axisymmetric end closures in the axisymmetric mode.

The hexahedron is used as a solid brick element in a three dimensional analysis. A particular application would be a closure for a multi-nozzle motor or with non-symmetric features, and launch hooks.

Problem Idealisation

Idealisation is the process of representing a real body or structure in terms of its geometry, material properties, loading and constraint by a mathematical model that is amenable to analysis by the finite-element method. Very often, an insignificant modification to geometry, loading or support will result in a very great reduction in the computing and data preparation times. The term "insignificant" depends on behaviour under load and also on which aspect of the result is under investigation. On the other hand, the model must possess adequate freedom or flexibility for the results to reflect the essential features of the real situation. The idealisation process therefore requires judgement and experience. Application of the finite-element method is therefore not an exact science.

Finite element analysis should never be used uncritically or without insight. It is vital to ensure that the elements chosen do not lack a freedom that it is essential to take into account and that they are sufficiently numerous for the model not to be significantly too stiff. Finite-element models in general err on the side of being stiffer than the real item. Most finite-element analyses used in rocket motor design are applied to a geometry of a type that has been analysed previously and the expected behaviour is known. In the case of a problem that is new to the user, it is good policy to do an initial run with a coarse division into elements to determine the general behaviour. The solution should be examined with a view to understanding the deformation, shown by plotting the deformed shape, and the stress output. It is possible for a solution to appear feasible and yet be quite wrong, so further checks should be made. The solution should reflect the loads and constraints that were intended in the input and, in the case of a compound body, the material properties should be seen to be distributed as intended. It is usually a simple matter to check the load balance in at least one direction by ensuring that the reactions given in the solution are equal and opposite to the total load that was intended to be applied in that direction. This check should never be omitted. If further verification is desired, it may be possible to make a very rough approximation to the actual problem and apply simple engineering formulae. Having determined that the coarse solution is behaving correctly, a finer division into elements may be made, using the results of the coarse solution to concentrate the elements in regions in which any stress is changing relatively rapidly with position. The fineness of division into elements depends upon the accuracy required and is a matter of experience backed, if necessary, by trial.

Input

The parameters required to specify the component are:

- (i) Node numbers and co-ordinates. It is necessary to set up an ordered set of nodes before defining elements.
- (ii) Element types and topology. A set of nodes alone does not determine elements. It is necessary to specify which element types are in use and in what way they connect with the nodes to form the required model.
- (iii) Material properties. Every element must be given at least two material properties.
- (iv) Suppressions and constraints. It is necessary to stipulate which nodes have any freedom of movement suppressed and in what way. Nodes may be constrained to move by a particular amount in a particular direction or to relate their movements to those of other nodes. These constraints must be specified.
- (v) Load data. Elements that experience applied loads must be identified and the load types specified. Load types include body forces, differential thermal expansion, pressure applied to element faces and point forces applied to individual nodes.

Output

Programmes vary in their output, but stresses and nodal displacements are the fundamental quantities. At present, strains are not usually given, but programmes are continually being updated. Graphical output from which deformed plots may be obtained is virtually essential. Plots of stress contours are desirable, but not essential. Some programmes give stresses only at interior points of the elements, whereas others extrapolate out to the nodes, if required, and output nodal stresses. Since stresses are frequently at their maxima on boundaries, nodal stresses are required.

3. System Requirements

The main requirement in the design of any rocket motor is minimum mass and size consistent with the design requirements coupled usually with minimum cost, requirements which are not necessarily compatible.

The factors to be taken into account include,

- (i) The internal conditions of pressure, temperature, gas velocity and time,
- (ii) type of motor; integral, discrete or jettisonable,
- (iii) mechanical environments, bump, shock, vibration and acceleration, bending moments, shear forces and couples,
- (iv) natural environments, which may range from tropical to arctic, desert to saline, or high altitude to underwater,
- (v) induced environments, particularly aerodynamic heating during air carriage, if relevant, and flight,
- (vi) interface with the missile,
- (vii) insensitive munitions,
- (viii) safety factors.

The internal conditions in a rocket motor vary considerably from design to design, an indication of the range of the various parameters being as follows:-

(i)	pressure	2 to 25 MPa	:	30 to 3750 psi
(ii)	temperature	2500 to 3600°K	:	4500 to 6500 °R
(iii)	velocity	0 to 2500 m/s	:	0 to 8000 ft/s
(iv)	time	1 to 60 s		

In general rocket motor hardware is insulated from the hot gases to limit the temperature rise and ensure that the ambient temperature properties are virtually unaffected. Thus for the purposes of hardware design internal temperature and velocity can generally be ignored leaving pressure as the only relevant parameter and allowing components to be designed on their ambient temperature properties. Occasionally, however uninsulated components are used in which case heat transfer calculations have to be carried out and the properties evaluated at high temperatures.

The different types of motor are

- (i) integral, where the motor forms part of the load bearing structure, the case usually forming part of the outer skin,
- (ii) discrete, where the motor is housed within the missile and does not form part of the load bearing structure,
- (iii) jettisonable, where the motor is attached to the rear of the missile 'in tandem' or mounted at the side 'wrap round' and is jettisoned when burning is complete.

Integral motors are subjected to the full rigours of the mechanical, natural and induced environments while for the discrete motor many of the environments are alleviated. Tandem boosts form part of the missile structure being cantilevered from the dart while wrap round motors have mounting points on the side of the missile. The only alleviation for these motors compared to integral motors is in aerodynamic heating during flight. Most current motors are either integral or jettisonable.

While the type of motor will influence the environment to which it is subjected, for example, the vibration spectrum resulting from road transport will be different for the different types of motors, the design principles will be the same.

Other factors that will influence the environments are whether the missile is for use by the Army, Navy or Air Force.

The Technical Requirement should specify the full range of environments for the motor. The mechanical environments should be directly related to the motor and should require no interpretation. With the natural and induced environments it is essential to ensure that each is relevant, in some instances interpretation is necessary: this is particularly relevant to the effect of solar radiation and aerodynamic heating.

The interfaces with the remainder of the missile includes the motor attachment points and fittings for wings, launch hooks and cable conduits. While these are the missile contractor's responsibility to define they can have a significant effect on the design and these attachment features should be negotiable during development.

The requirement for insensitive munitions is becoming more and more important and is discussed in section 7.

The safety factors used for rocket motor structural components are low and can vary according to the type of load.

Different factors and definitions are used in different countries. The minimum values recommended in the UK are

- (i) 1.5 for the repeated loads such as bending moments and shear forces arising from vibration, shock and carried flight loads,
- (ii) 1.33 for pressure loads when failure would endanger personnel or the launch platforms,
- (iii) 1.25 for pressure loads in other instances:

for (ii) and (iii) the maximum pressure is defined as that pressure that will not be exceeded on more than 1 firing in 1000 with 95% confidence at the upper firing temperature. In all instances the weakest case is considered, that is, minimum thickness and minimum strength.

Limited experience with requirements for contractors outside the UK indicates that similar factors apply although definitions may vary.

To minimise the mass of the hardware components necessitates working as closely as possible to the appropriate safety factors.

4. Materials & Methods of Manufacture

Materials

The materials used for motor body manufacture can be divided into two groups, metallic and non-metallic. The metallic materials used are generally either steel or aluminium alloys while non-metallic materials take the form of plastic reinforced by fibres such as glass, carbon and aramid.

Table 1 gives typical properties for metallic and non-metallic materials with weight comparison factors for pressure and for simple beam bending. Dealing first with metallic materials, figures are given for two typical steel and two aluminium alloys plus one titanium alloy. Mass comparison factors for pressure loading show that similar masses are possible with steel and aluminium alloy using stress as the design criterion but lower masses are feasible with aluminium alloy when strain is the criterion. The factors also show a significant advantage for Titanium using stress as the criterion but on the basis of strain masses would be higher than for a steel component.

Now considering hoop bending as the criterion which is applicable to end closures then aluminium alloys are superior to steel or titanium whether the design criterion is stress or strain.

For motor bodies where the criterion is usually stress then similar masses can be achieved with light alloy or steel and other criteria have to be taken into account such as

- (i) the economic manufacturing thickness,
- (ii) internal volume
- (iii) the thickness to diameter ratio where a value less than 0.005 is considered undesirable on a damage criterion,
- (iv) aerodynamic heating or subsequent high temperature processing which could affect the strength of aluminium alloys,
- (v) possible stress corrosion with aluminium alloys which can be virtually eliminated by careful design in areas of changing section, for example, by the provision of large fillet radii,
- (vi) external attachments.

When considering aerodynamic heating it is necessary to consider the possible effect of this on the propellant as well as the case. If the conditions are such that significant propellant heating occurs either during carried flight on an aircraft or during missile flight, then this may be unacceptable as it could lead to high pressures necessitating a thicker case. Repeated excursions to high temperatures, as could occur during carried flight, could also significantly reduce propellant life. In either case it may be necessary to increase insulation to limit the temperature rise in the propellant. This could be done by external insulation which would also limit the temperature of the case.

Also included in table 1 are properties for fibre composite bodies these being based on information for filament wound structures. The figures for stress and modulus are hoop composite values for a balanced structure. Corresponding figures for an uniaxial structure would be approximately 50% higher. The weight comparison factors for the pressure loading case clearly show the mass advantages possible in the section of the body designed on pressure alone when using these materials. However many other factors need to be considered in particular the loss in internal volume; as composite structure design is the subject of a separate paper no further discussion of these structures will be attempted in this paper.

Two materials which are showing improved properties are (i) aluminium lithium alloys which are stated to have a 15% higher modulus and an 8% lower density making them particularly useful for components where stiffness is required. (ii) fibre reinforced aluminium which has increased strength and stiffness. Both materials require evaluation, the second in particular is expensive and is only likely to be useful for very special applications.

Manufacture

Steel motor cases have been made by the following processes

- (i) wrapping and welding sheet of the desired thickness,
- (ii) machining from forgings or extrusions,
- (iii) deep drawing to the required thickness and machining the ends,
- (iv) helically winding strip of the required thickness around a mandrel and welding along the helical butt joint,
- (v) flow forming,
- (vi) the strip laminate process,

but

method (i) is no longer used,

method (ii) can be costly in terms of wasted materials unless close tolerance forgings or extrusions are available; in addition, if a large amount of material has to be removed distortion may occur when machining,

method (iii) is well established although is more applicable to bodies with a low length to diameter ratio,

method (iv) suffers from the disadvantage that the poisson effect on winding a relatively thick strip causes bending of the strip across its width which can lead to difficulties when lining, while the external surface may not be aerodynamically smooth,

method (v) is now well developed and is being used for a range of motor bodies,

method (vi) is also well proven and is particularly applicable where the body length to diameter ratio exceeds four.

The strip laminate body is a bonded structure with additional design features to those for a homogeneous case. The construction and design are given in section 6. This method is particularly useful where insensitive munitions are required, this is discussed in section 7.

Aluminium alloy bodies have been made by processes (ii), (iii) and (v). As the strength of aluminium alloys is greater in the direction of grain flow, flow forming gives the higher strength in the hoop direction which is advantageous for a pressure vessel whereas other methods of manufacture give the higher strength in the longitudinal direction.

A further method of manufacture that has been used in the UK is a fibre reinforced metal case, this design is outlined in section 6.

The final method chosen will be influenced by external attachments and loading conditions. As an example wing roots could be welded to a simple body or the body, including wing roots, could be machined from an extrusion. Where attachments are required over a short length of the body then this section could be machined from an extrusion and welded to a simple tube prior to heat treatment. Whereas if small or lightly loaded attachments are required then these could be bonded to a simple tube.

Only detailed discussions and costing will allow the most effective method of manufacture to be determined.

For end closures and blast tubes the most common manufacturing method is forging and machining to obtain good grain flow and optimum properties. Precision casting, although not as good on grain flow, offers advantages in the reduced amount of machining and hence cost but additional inspection is necessary to ensure the high reliability necessary.

As closures and blast tubes have to be insulated the method of application of the insulation has to be considered when deciding the best manufacturing route. Rigid insulants are invariably used, these being filled, cured, resin systems. These insulants may be made separately and bonded into the component or may be moulded in situ. The former method involves close tolerance machining of both components prior to bonding under the application of heat and pressure. In this instance the hardware components can be finish machined prior to application of the insulation and a gap filling resin has to be used.

When the insulation is moulded in situ the metal blank should be as simple as possible, to allow it to seat in the mould tool, and final machining is carried out after moulding. With this method it is essential to ensure that there is no significant strain on the components during the moulding operation. This process is more applicable to aluminium than to steel components as the thermal coefficient of expansion of aluminium is greater than that of the insulant whereas that of steel tends to be lower. Thus on cool-down from the moulding temperature the aluminium tends to put the liner in compression whereas with steel there is a tendency for the liner to pull away although it is unlikely that a gap will develop.

5. Body Design - Homogeneous Metal Cases

For design purposes the motor body may be split into a number of sections as shown in fig 1 each of which reacts with adjacent parts or components.

The design of the individual parts are considered in the following sub sections:

Parallel section

The five factors that have to be taken into account when designing the parallel sections of the motor cases are

- (i) internal pressure,
- (ii) external pressure,
- (iii) attachments,
- (iv) loads imparted to body by the missile i.e. bending moments, shear forces and attachment loads,
- (v) stiffness requirements.

Excluding loads arising from attachments such as launcher hooks and wings the over-riding consideration is usually the internal pressure and for an initial estimate of thickness the simple formula for hoop stress in a thin walled pressure vessel is used. This will indicate the materials that should be considered for example for a small diameter or a low pressure motor an economic manufacturing thickness for steel may not be possible leading to a detailed consideration of light alloy.

It is then necessary to carry out a detailed check on the maximum principal stresses taking into account all loads and possible materials before the thickness can be finalised. The body is usually an axially symmetric structure and thus the principal stresses are in the hoop or axial direction depending on the load combination. As already stated the hoop stress when pressurised is often the design criterion; two other conditions that have occasionally governed the thickness are bending moments when unpressurised, which can result in buckling, and stiffness. The thickness determined for the body is usually consistent with that described as a thin wall structure. Occasionally this is not the case and the appropriate formulae then have to be applied.

For short length to diameter bodies theories suggest that the thickened end sections interact to reduce the maximum hoop stress, thus allowing thinner sections to be used. However for bodies with length to diameter ratios as low as 1 : 1 practical testing, including burst tests, does not indicate any significant effect from the end rings.

A particular case that requires more detailed investigation is that of underwater operation where the external pressure in the unpressurised condition could result in buckling of a body designed on the basis of internal pressure loads. The simplest approach is to design the thickness for the external pressure. But as buckling can be prevented by internal circumferential ribs this offers an alternative which can have a lower mass and provide a greater internal volume. This would lead to complications in lining and propellant filling but provided these can be overcome a lighter structure will result.

Attachment features such as launcher hooks and wing fixings require detailed consideration and could influence the choice of material, for example, aluminium alloy could be acceptable for wing fixings but steel could be necessary for launch hooks to withstand the mechanical environments. These features may be incorporated into the body in a number of ways, examples being,

- (i) the body including the attachment feature can be machined from a forging or extrusion,
- (ii) the section of the body incorporating the attachment features can be machined from a forging or extrusion which is then welded to the remainder of the tube, see fig 2a,
- (iii) the features can be incorporated into separate rings which can be bonded to or clamped onto a simple body as shown in figs 2b, 2c or 2d,
- (iv) individual features can be welded or bonded to a simple body.

Method (i) would be applicable to a body incorporating say wing ring fixings which extend over a high percentage of the length of the body and where the loads are too high for method (iv) to be used.

Method (ii) could be used for shorter attachment features; it has been used for wing fixings and launcher hooks.

Method (iii) is a simple method of attaching relatively short features but does result in local increases in diameter. To assemble the simple components, shown in fig 2b and 2c, necessitates the rings being passed along the tube. If this is not possible then the assembly shown in 2d could be used.

Method (iv), like method (iii), can result in considerable simplification of the body tube but bonding, in particular, is only suitable for lightly loaded components.

When launcher hooks or wing fixings are incorporated into a body as in methods (i) or (ii) local thickening of the tube is usually necessary to withstand the additional loads imposed. The optimum structure, that is one in which the loads result in a constant maximum stress in any radial location will vary in thickness. The thickness will be a maximum in the neighbourhood of the load and a minimum at a point farthest from the applied load taking into account the degree of machining and mass. In deriving the optimum thicknesses throughout the ring initial estimates are carried out based on the theory of curved beams followed by detailed stressing and modifications to the design until an acceptable solution is obtained.

End rings

The main function of the end rings is to provide attachments for the motor end closure and for the missile. The attachment features inevitably require these end rings to be thicker than the main body tube which, when a flush outside diameter is required, necessitates the inside diameter being smaller than that of the main tube.

The minimum inside diameter at one end of the tube at least will be governed by the charge manufacturing method. The two basic types of charges are cartridge loaded and case bonded. With a cartridge loaded charge the outside diameter must be slightly smaller than the inside diameter of the end ring hence the inside diameter should be similar to the inside diameter of the body lining to ensure minimum motor length. With a case bonded charge no such restriction exists; in this instance the diameter would be governed by manufacturing considerations such as core extraction and ease of propellant filling. In this instance ease of body lining is also an important criterion.

In addition to the pressure and missile loads the end rings must also withstand the bending moments imparted by the end closures so there is an interaction between the design of these components. The method of missile attachment required is also an important factor in the design of the end ring. Other factors such as access holes for igniter cables, safety and arming mechanisms have also to be taken into account.

Again it is necessary to carry out an initial design based on classical methods and experience followed by a detailed stress analysis and modification as necessary.

End closures

Three basic forms of end closure are possible

- (i) integral: where the closure and end closure/body are a continuous structure. In this instance there may be a small central hole to house an igniter or to ease some aspect of motor manufacture, see fig 3a,
- (ii) part integral: in this instance the outer part of the closure is integral with the end closure-body but the closure has a relatively large central hole, see fig 3b,
- (iii) separate: where the closure is mechanically attached to the end ring, as shown in fig 3c.

An integral closure will generally be the lighter for any given material and hence with back extrusions, forgings or for bodies with welded ends this type of closure can be used.

Part integral closures may be for nozzle or blast pipe attachment and are particularly relevant when no missile attachment is necessary.

However important criteria for the choice of closure will be body lining and charge manufacture as

- (i) the lining of relatively long motors with sheet material is usually simplified with access from both ends leading to the use of separate or part-integral closures,
- (ii) a cartridge loaded charge requires a separate closure at one end for loading,
- (iii) manufacture of a case bonded charge will necessitate a relatively large opening at one end for ease of propellant filling and core removal so that a part integral or separate closure is required at one end: at the other end an integral closure may be used for an HTPB charge but access greatly simplifies the manufacture of CDB charges so that part integral or separate closures are required.

For small diameter motors, that is up to about 150 mm, there will be little difference mass wise between separate and part integral closures and body manufacturing considerations become the criteria.

When using a cartridge loaded charge with an integral closure this closure could be at either end of the motor. However lining of the aft closure is a very critical operation and is more difficult if this is the integral closure at the end of a long tube. For this reason it is recommended that the forward closure should be the integral closure.

In general closures are designed so that motor pressure is on the concave side this generally resulting in a lighter closure and lower bending moments on the end ring. But single chamber designs have been successfully used with motor pressure on the convex side. This design concept generally arises from interface considerations.

The operation of a dual chamber motor with a single internal closure may require the closure to be designed to withstand the pressure in the two chambers independently. If there is a significant difference between the two operating pressures then consideration should be given to designing the closure such that the higher pressure operates on the concave side to reduce the effect of buckling.

The ideal shape for an end closure for a pressure vessel is a hemisphere but for maximum utilisation of a volume a flat plate is the optimum. However the latter is much heavier and imparts a significant bending moment into the end ring. In practise a compromise between these two extremes is sought. From experience it has been found that an end closure in the shape of an ellipsoid with a ratio of minor to major semi axes of 0.4 gives a good compromise between mass and volume.

Due to the deformation of an end closure under pressure loads and the bending moments imparted to the body the over-riding design criterion is usually strain rather than stress. As stiffness is proportional to thickness cubed a light alloy closure will generally result in a lower mass structure and consequently aluminium alloys are often used when separate closures are required.

Closures for multi-nozzle side vented motors usually require to be very stiff and require special consideration. It may be necessary to add ribs to the design to ensure the required stiffness.

Closure attachment

Many methods may be used for attaching end closures including

- (i) screwing the closure into the body, fig 4a,
- (ii) locating the closure in the body and holding it with a screwed ring, as in fig 4b,
- (iii) locating the closure in the body and holding it with a snap ring. An additional ring is located on the outside of the snap ring which is bolted to the closure: this holds the closure in place and traps the snap ring as shown in fig 4c,
- (iv) a lock wire in which a wire of suitable cross section, ductility and strength is passed through a slot in the end ring into mating grooves in the end ring and closure; fig 4d,
- (v) bolting the closure to the body, as shown in fig 4e.

Interface conditions may influence the decision, for example if an internal screw thread is required for attachment of the rest of the missile this could also be used for closure attachment (i) and (ii).

Method (i) is not recommended when 'O' seals are used as the 'O' seal has to rotate in relation to the end ring: with this method it is also very difficult to align the end closure and body radially as is often necessary.

With methods (i) and (ii) it is necessary to stop the screwed component from rotating under vibration, while with methods (ii), (iii) and (iv) a location feature is necessary if the end closure has to be located radially; method (v) gives a positive radial location.

For the lock wire method the wires deform as they are inserted. The wires have to be sized to ensure that any deformation does not result in binding making for difficulty in assembly or scrapping of components. A further design criterion is buckling of the wire as it is pushed into the slot. Withdrawal of the wire requires special consideration. For development motors this is possible by making the lock wire longer than necessary so that it protrudes from the motor allowing it to be withdrawn. An alternative method of withdrawing the wire would be to make the slot in the end ring wide enough to allow the insertion of a tool to push out the wire. This method of assembly, because of possible binding and pick up makes it more suitable for steel components than for light alloy although it should be applicable to a steel end ring and a light alloy closure.

Method (v) requires a thick flange on the body and is also more applicable to large diameter motors.

For a given outside diameter of end ring methods (iii) and (iv) will give the maximum inside diameter, while method (v) will give the smallest. Taking the different factors into account then method (iii) is that used mostly with aluminium alloys, while (iii) or (iv) are equally applicable for steel components.

Blast tubes

Blast tubes may be of two types

- (i) supersonic: where the choke is at the forward end so that the gas flow is supersonic throughout the tube while the pressure is relatively low
- (ii) subsonic: where the choke is at the aft end so that the gas flow is subsonic throughout the tube, but the pressure is relatively high.

Blast tubes require insulating, rigid insulants, that is, fibre filled resins, being the usual materials employed. The insulating liner may be manufactured separately, machined and then bonded into the structural component using a gap filling resin or it may be moulded directly into the structural component. In either case the maximum strain allowable in the liner has to be considered as well as the maximum stress in the structural component before the thickness of the latter can be determined.

For the supersonic tube with its lower internal pressure then the maximum stress in the structural component is likely to be the design criterion but for the subsonic tube with its higher internal pressure then strain is more likely to be the over-riding consideration. In either case, however, on small diameter tubes a thickness less than the minimum economic manufacturing thickness may be indicated in which case the lowest density material available should be used.

Blast tubes may be designed as separate components which are assembled to the end closure after manufacture or they may be integral with the closure. The latter allows a one piece end closure/blast tube liner which avoids a joint at the critical entry to the blast tube. This one piece construction is more applicable to small diameter motors and relatively short blast tubes because of the problems involved in the manufacture and handling of large components. Only a detailed consideration of manufacturing routes will allow the best solution to be determined for any particular application.

Nozzles

The majority of fixed nozzles, in use on current solid propellant rocket motors for tactical weapons, have three main components, these being:

- (i) the outer load bearing shell,
- (ii) the insulating liner
- (iii) the throat insert

Figure 5 shows two typical nozzle configurations.

It should be noted that under certain conditions it is possible to use a simplified structure, for example a single-piece steel nozzle or a throat insert in a steel shell without an insulating layer. Only a detailed knowledge of the motor and propellant parameters will enable the designer to assess the appropriate design.

The internal design of nozzles is dealt with in detail elsewhere and hence comments are made here in relation to the materials and method of manufacture of the outer load bearing shell only. The design, and materials used for the insulation and the throat section would result from knowledge of the propellant and ballistic requirements.

The outer load bearing shell is usually made of light alloy or steel but other materials such as fibre-reinforced plastics may be used. The shell can be designed as an integral part of either the motor end closure or the blast pipe or as an independent unit attached to the closure or blast pipe with appropriate sealing at the joint. Methods of attachment similar to those described for the closure to body attachments can be employed.

In addition to the pressure loads from the motor, the outer shell will have to withstand any loads specified in the Technical Requirement and possibly the loads imposed during manufacture, eg. pressure moulding of the insulation. Whenever possible the shell should be made in one piece although the expansion cone may be attached separately.

As with blast pipes, the insulation, and in some instances the throat section, can be moulded directly into the shell or bonded in separately. When 'in situ' moulding is used, the internal profile of the shell is designed to facilitate retention of the liner during firing. If a pre-fabricated liner is to be bonded into the shell, then a mechanical retention device will be required to ensure that the liner does not experience high tensional loads.

The high pressures associated with moulding 'in situ' will usually dictate the use of an over thick shell which can be subsequently machined to the sizes required by motor and missile loads. Care must be taken to ensure that the material does not self-relieve after machining, because as with the blast pipe, the strain capability of the material may well be the over-riding criterion.

If a reinforced plastic is used for the load bearing member, it is usually in the form of an over-wind onto the insulating layer, or in conjunction with a steel or aluminium alloy where the fibres can be used as a hoop over-wind in the expansion cone to reduce structural mass.

Sealing of joints

Pressure seals are necessary between mating surfaces of the various components of the pressure vessel. A common method is an 'O' seal which is usually located in a groove on an external diameter although where other considerations dictate a thick body attachment it may be placed in the inside diameter. Face seals have also been used.

With screwed joints it is possible to rely on some thread sealant but the 'O' seal is a more positive method with a proven life in excess of 15 years.

The materials used for 'O' seals are elastomeric in nature. The material must be chosen carefully to withstand the temperature extremes: the most suitable materials to withstand the low temperature for Army and Air Force use are silicone rubbers which remain flexible at low temperature. The precise size and grade depend on the diameter of the mating parts and the operating pressure of the motor. Manufacturers recommendations for these and the tolerances on 'O' ring grooves and the mating components should be followed.

All joints should be leak tested at a low pressure, say between 0.2 and 0.7 MPa, 30 and 100 psi. If an 'O' seal holds this pressure it will seal against normal motor operating pressure. One method of testing is to pressurise the motor and check for leaks. An alternative method which is used extensively is to use double 'O' seals, as shown in fig 6, and to leak test by applying pressure between them and checking for a pressure drop over a period of about two minutes. This is a severe test which detects very minute leaks because of the small volume of gas between the seals. After a successful test the leak test hole is plugged and sealed to give added protection should the inner seal fail although this plug itself cannot be leak tested. This technique is more expensive than a single 'O' seal as two grooves require machining and it is necessary to machine holes for the leak test itself. In addition each joint has to be tested individually but the ease of testing, as no account has to be taken of the effect of pressure on the internal components of the motors, is considered to warrant the additional expense.

The use of 'O' seals with a threaded component has the disadvantage that when assembling there is movement between the component and the 'O' seal and there is more likelihood of damage on assembly.

When designing the mating surfaces it is essential to ensure that there are no sharp corners which can damage the 'O' rings, in addition the minimum length of mating surface is desirable to assist

assembly and to ensure minimum movement of the 'O' seal in the compressed state.

Surface treatment

The majority of metallic materials need to be protected from the environmental conditions which could be encountered during service life. Although most external surfaces are painted, this is not usually enough to combat the effects of the elements such as salt spray, acid rain and prolonged exposure to hot-wet conditions as well as mechanical abrasions resulting from handling. Hence a number of plating and deposition procedures have been used on steel and aluminium components.

It is not the aim of this paper to discuss the details of individual processes, but more to highlight the need for surface protection to the design engineer and the considerations to be used in deciding upon the appropriate treatment.

For a number of years cadmium plating has been the most commonly used protection for steel surfaces and indeed this electroplating process is relatively simple, and hence low cost; it is also very effective in terms of corrosion resistance. However, the process with high strength steel can promote hydrogen embrittlement, it has a limited salt spray life and recent medical evidence has shown that cadmium is as toxic as mercury; thus its use is likely to be severely restricted in the future.

An alternative process is to employ an insoluble phosphate coating which protects by exclusion, whereas cadmium protects sacrificially. Phosphating needs to be supplemented by paint or an organic finish, but can be applied in very thin coating layers and hence is advantageous in regions of high dimensional accuracy.

Other options include ion vapour deposition of aluminium, mechanical plating by dipping using combinations of tin and zinc or cladding using aluminium and electroplating using tin and zinc. Short term protection of aluminium alloys is provided by anodising and sealing.

Some materials, in particular stainless steels and titanium can be left unprotected, although as part of the missile it is likely that they will be painted. Testing of unpainted bodies in stainless steel, which have been subjected to normal atmospheric conditions in the UK for up to 3 years has shown no detrimental effects.

Testing of Components

All structural components should undergo testing during both the development and production stages.

During development all components should be subjected to a routine pressure test. The component should be supported in a similar manner to that used in the final assembly so that loads are as representative as possible. For example, the body should have end closures reproducing as closely as possible those of the finished assembly while end closures should be held by similar retention devices to those used in the motor assembly. The pressure used should be higher than the maximum expected during motor firing: in the UK a value 12.1/2% above the maximum pressure as defined in section 3 is suggested and this pressure is usually held for 2 minutes.

In addition to routine testing it is also necessary to carry out additional limited testing to simulate other load conditions, using as appropriate the pressurised and unpressurised conditions, and tests to destruction to check that the appropriate safety factors are achieved.

Production components should be subjected to routine pressure testing in a similar manner to those for development: in addition an occasional test to destruction may also be carried out.

During assembly all joints should be leak tested using a pressure of between 0.2 and 0.7 MPa that is 30 and 100 psi for two minutes or longer depending upon the volume being pressurised. As mentioned in the section on sealing of joints the use of double 'O' seals allows a very searching test to be carried out. If it is not possible to use double seals it is then necessary to pressurise the motors and account must be taken of other components such as igniters and nozzle seals when fixing the leak test pressure.

6. Non Homogeneous Cases

Two non homogeneous body constructions have been developed in the UK these being fibre reinforced metallic and strip laminate. These are described in the following sub-sections:

Fibre-reinforced metallic rocket motor cases

In a rocket motor body the hoop loads are usually higher than the axial the ratio generally being 2:1. If the basic metal tube is designed to meet the axial loads and a material with higher specific strength is used to take the additional hoop loads, significant mass savings can be effected. Such a material must be easily applied to the external surface of the basic metal tube such that the resultant mass saving does not incur a cost penalty.

Wires and fibres can easily be hoop wound onto a cylindrical tube, but metal wires are unlikely to provide the additional specific strength and have hence been discounted. Fibres with high specific strength are glass, carbon and aramid. With the glass and carbon fibre, a resin matrix is required because of the relatively poor abrasion resistance and the need to transfer some stress between fibres. The use of a resin system, reduces winding speeds and increases the mass of the overwind. Aramid fibres, such as Kevlar, which is produced by Dupont, have greater abrasion resistance and nominal strength which is less dependent on fibre length, thus allowing the possibility of dry winding with the advantages of increased winding speeds and reduced mass.

For each design, the metal thickness, winding tension and fibre thickness need to be evaluated. The first of these is readily determined from the end loads and the material properties. The hoop loading will then determine the required overwinding by summing the capabilities of the two materials. The tension in the fibre during winding will induce a compressive stress in the metal tube without problems associated with fibre creep strain relaxation if it is maintained below 30% of the ultimate stress.

This winding tension can be particularly beneficial when an aluminium alloy tube is used; the reason being that the compressive strain accepted by the metal case raises the pressure at which permanent tensile hoop strain occurs.

More stringent design programmes have been developed, and analytical stress analyses for this type of case construction have been developed by Royal Ordnance Research and Development Centre.

Unlike other methods of case construction it has been found advantageous to ensure that failure occurs as a result of axial loads. This involves winding additional hoop layers which has little effect on mass due to the low density of the fibre. If there are significant bending loads, then the thickness required in the metal case may obviate the gains made by overwinding.

Typical masses for a 120 mm diameter cylindrical case with a length of 1 m and designed for a burst pressure of 40 MPa, without ends but with hoop: axial load ratio of 2:1 are:

Aluminium Alloy	$(0.055\text{GN/m}^2, 80\ 000\ \text{lbf/in}^2)$	4.33 kg
Maraging Steel	$(2.0\text{GN/m}^2, 290\ 000\ \text{lbf/in}^2)$	3.88 kg
Al. Alloy overwound		2.74 kg

The above figures indicate that a dry overwound aluminium alloy case provides a combined hoop stress of approximately 0.760GN/m^2 ($110\ 000\ \text{lbf/in}^2$) and a weight comparison figure of 0.50 for the simple stress consideration for the pressure loading case (Ref. Table 1).

Royal Ordnance have employed the system of fibre overwinding on an aluminium alloy case on one shoulder-launched rocket motor currently in service and a second which is about to go into production.

The combination of a fibre overwind on an aluminium alloy case has led to considerable mass and cost savings over the more conventional types of case manufacture. Where a maraging steel tube with a separate aluminium alloy nozzle shell was replaced by a one piece aluminium alloy case with an integral nozzle shell and a dry overwind there was a 30% mass saving and a 60% reduction in cost.

The work carried out to date has indicated that this method of construction can offer significant mass savings without incurring a cost penalty. The plant required is relatively simple and hence initial tooling costs are also kept to a minimum with the advantage that lightweight bodies can be produced very early during development.

Strip laminate motor bodies

The strip laminate body is a bonded structure manufactured from metallic strip. It was designed and developed at Royal Ordnance Summerfield and has been used for over 30 years for the manufacture of high strength steel bodies for solid propellant rocket motors.

Motors using this type of body have shown specific advantages in the field of insensitive munitions: this is discussed in section 7.

The basic manufacture of a rocket motor body by the strip laminate process is fairly simple, the operations being outlined below.

Steel strip is degreased, shot blasted and degreased again. It is then coated with a suitable adhesive which is gelled and the strip is coiled. The coated strip has a life of at least six months.

The steel strip is helically wound onto a heated mandrel so that there is a small gap between successive turns of the helix. Successive layers of strip are added until the desired thickness is obtained. Each layer is wound in the same direction but the helices are staggered.

After winding is complete the adhesive is partially cured and the tube is removed from the mandrel and cut to length. End fittings, and any other fittings which may be required, are bonded in place using a jig to ensure accuracy and the assembly is fully cured.

The finished motor body may be lined, painted and filled in exactly the same way as a body made by any other process.

Basically the equipment required consists of a strip preparation and coating plant, a winding machine which may be a converted lathe, a curing oven, and an assembly jig. The end fittings are assembled to the motor tube in the finish machined state and this applies also to any other fittings. This gives two of the advantages of the process, namely, a wide range of supply sources for the body fittings and a minimum of manufacturing scrap.

The process is capable of producing round straight tubes with combined bow and ovality of less than 10^{-4} on length and end squareness of less than 10^{-3} on diameter.

Providing strip is available then development bodies can be produced within 4 months.

Design

The principles of the construction are

- i) the hoop loads are taken by the layers of steel strip,
- ii) the longitudinal loads in the tube are transmitted by shear in the resin layers,
- iii) loads are transmitted from the tube to the end ring by shear in the resin layer.

The cross section of a three layer strip laminate tube and end rings including shear paths is shown in fig. 7.

Design considerations for the body are given below: the comments made in section 5 re end closures and closure attachments are equally relevant to strip laminate bodies.

Body tube

In most respects the mechanical properties of tubes made by the strip laminate process are identical to those of homogeneous tubes.

For the strength and rigidity of the tube the usual principles of design are applied, based on the total metal thickness of the tube wall, provided that the strip overlap pattern has been chosen so as to give adequate longitudinal shear strength between the layers. This would only be a problem if narrow strip was being considered. In general the length of shear path in the tube is about one and a half times the length of resin shear path in the end ring to tube bond, this being a consequence of the construction rather than a design criterion.

The number of layers used should not be less than three, to avoid distortion under pressure at adjacent strip edges and to obtain the maximum material strength, but may exceed this by any desired amount. However, it is advantageous to make the number of layers as small as possible, consistent with reasonable strip thickness, as the winding time is thus reduced.

The overlap pattern chosen depends on the number of layers of strip. For a three layer tube the pitch is simply one third of the helix. For a four layer tube a pitch of one quarter has been used successfully as have alternative pitches of half and five-eighths. An overlap pattern with alternate pitches of one-half and three-quarter strip widths has been successfully used on a thirteen-layer tube. Experience indicates that where the thickness demands a large number of layers of strip, then there should be at least four layers before the pattern repeats.

End rings

The end fittings, which may be in the form of attachment rings or complete closures, are provided with cylindrical extensions to provide the necessary bonding surface. These extensions may be designed to fit the strip-laminate tube internally or externally. Internal bonding has the advantages that a flush external diameter can be provided. If a flush internal diameter is required, however, external bonding must be used with a consequent local increase in external diameter. Centre rings or closures can also be provided to join two tubes of the same or differing diameters or thicknesses together. Fig. 7 shows examples of internally and externally bonded end fittings.

Care must be taken when designing an end joint to ensure that stress concentrations at the end of the bond are avoided so that no "peeling" effect is produced; this is particularly important with internally bonded fittings. Attention must also be paid to the effect of any bending moments which may be present in the end region; this effect normally takes the form of an additional shear stress, positive or negative according to the position in the end bond.

In general the end ring bond is designed to be stronger than the tube so that the body will fail in hoop.

Attachments

The end rings normally provide attachment locations for other missile items, forward and aft of the motor. Launcher feet or fin attachments can be incorporated into the end ring design or alternatively bonded directly onto the motor body. They may be attached as individual components bonded directly onto the tube or for more highly stressed components attached by means of a complete ring which can be bonded onto the body in the desired position, as shown in Fig 2b. Welding to strip laminate bodies is not possible without affecting the strength.

In the finished condition the strip laminate body can be painted to suit the particular missile requirements, in the same way as a conventional motor body.

Electrical continuity of the strip laminate motor body can be provided via appropriate application of silver loaded resin or by a variety of mechanical links.

Materials

Strip

Most of the experience gained to date with this technique has been based on the use of carbon steel strip, rolled and polish ground, having a design ultimate tensile strength of 2 GN/m^2 , $290\,000 \text{ lb.f/in}^2$. Recently stainless steel strip of equivalent strength has also been qualified, which obviously offers the additional advantage of increased resistance to corrosion.

Aluminium alloy strip, heat-treated to give an ultimate tensile strength of 0.54 GN/m^2 , $78\,000 \text{ lb.f/in}^2$, has also been successfully used and there is no theoretical limitation on the strip material provided that it possesses sufficient ductility to enable it to be wound successfully. Titanium alloys have also been employed. The material comparison shown in table 1 is applicable to strip laminate body tubes.

For cheapness it is desirable to use strip as wide and thick as possible as this reduces winding time. However if excessively wide strip is used difficulties due to lateral curvature and gap variations between successive turns of the helix arise. From practical experience the strip width should be less than the tube diameter. The ease of winding a tube of a given diameter will also influence the maximum thickness of the strip although in practise the design thickness is the over-riding criterion on smaller diameter tubes.

Many of the bodies produced have been between 125 and 200 mm diameter, 5 and 8 in, with wall thicknesses of 0.75 to 1 mm, 0.030 to 0.040 in. For these bodies strip 100 mm wide and 0.25 mm thick, 4 in wide and 0.010 in thick, has been used and has become a standard stock material. This strip has been used successfully for bodies up to 650 mm diameter with a thickness of 3.25 mm, 26 in diameter and 0.13 in thick, but wider thicker strip could be used on a production motor of this size to reduce winding time and cost. For motors significantly less than 125 mm diameter narrower and thinner strip would be used. However where the standard strip can be used it leads to rapid manufacture of bodies for initial development.

Adhesives

The adhesives used in strip laminate are based on epoxide resin chemistry this being the strongest practical system available for production use. Different epoxide systems are used for strip and end rings₂ because of the different methods of application but in either case resin strengths in excess of 30 MN/m^2 , 5000 lbf/in^2 are achieved.

Summary

The strip laminate process is applicable to a wide range of sizes of rocket motor tubes. The main characteristics of the tubes are:

- (i) high strength steels are used, typically having a UTS of 2 GN/m^2 , $290\,000 \text{ lbf/in}^2$,
- (ii) the mechanical properties are identical to those for a homogeneous steel tube in the same material,
- (iii) bow and ovality less than 10^{-4} on length,
- (iv) end squareness less than 10^{-3} on diameter.

In addition

- (i) changes to motor length can be easily made,
- (ii) prototype cases can be produced very quickly using stock size material,
- (iii) relatively simple manufacturing equipment is required,
- (iv) the ability of the tube to rapidly delaminate under conditions of thermo-mechanical attack attributes particularly favourable characteristics to this form of construction.

7 Insensitive Munitions

A relatively recent requirement for solid propellant rocket motors is that for insensitive munitions that is, ideally, no reaction when subjected to fragment attack and fuel fire.

Whilst the rocket motor is not the only sensitive component of a missile it does represent the largest single explosive component which makes it the most vulnerable particularly to fragment attack. Trials have been carried out in the UK in which rocket motors have been subjected to both environments. The results of these trials are given in the following sub-sections.

Fragment attack

Trials have been carried out on a range of propellants, extruded double base, (EDB), cast double base (CDB), composite modified CDB (CMCDB), elastomer modified CDB (EMCDB) and hydroxy terminated polybutadiene (HTPB) and case constructions, aluminium alloy and steel homogeneous construction, strip laminate (SL) and filament wound carbon fibre reinforced plastic (CFRP). A number of different trials have been carried out including attacks from 'in-service' rounds of ammunition which provide a fragment with a controlled velocity and direction and attacks using 105 mm pack howitzer shells electrically detonated at set distances from motors. Not all of the combinations were tested but in general there was sufficient read across amongst trials to show that the major influences which affect the way in which a solid propellant rocket motor will respond to fragment attack are:-

- i) the propellant
- ii) the motor temperature and
- iii) the motor case material and construction

Propellant

The physical properties of the propellant allied to its latent energy level dictate how it will respond when attacked.

A brittle propellant of the EDB and to some extent the CMCDDB type is extensively damaged when struck by a fragment. The propellant breaks into pieces which are easily ignited producing a large burning area which leads to a pressure build up and inevitably an explosion when retained in a strong case.

A more flexible propellant of the CDB, EMCDB and HTPB types generally remain intact on fragment attack. A hole is made in the propellant which ignites and, having a relatively small burning area results in a slower build up of pressure.

Motor temperature

The properties of some solid propellants vary with temperature, becoming more brittle on thermal cooldown and conversely more flexible as the temperature rises. Consequently, some propellants which are flexible at ambient can react like brittle propellants at low temperature and will be more vulnerable to fragment attack.

Motor case material and construction

Rocket motors using homogeneous cases whether of aluminium alloy or steel tend to explosion or pressure burst when subjected to fragment attack, although with lower velocity fragments the reaction of aluminium alloy cases may be reduced to burning only.

However the use of a strip laminate case reduces the effect significantly, in most instances only burning, or at low temperatures mild explosions, occurring.

Limited work with CFRP cases shows a similar reaction to strip laminate.

Fuel fire

When subjected to fuel fire or external heating the main parameter which affects the response of a rocket motor is the case. The auto-ignition temperature may affect the time at which the propellant ignites but the resultant effect once ignition occurs is similar.

The standard fuel fire test is to suspend the motor over a bath of burning fuel having a flame temperature of up to 1000°C. This test has been carried out on both homogeneous, strip laminate and CFRP motors.

Homogeneous structures invariably exploded when the propellant ignited while with strip laminate bodies the result was either propellant burning or at worst a mild pressure burst. The limited trials with a CFRP body tended to show marginally worse results than those with strip laminate bodies tending more towards the mild pressure burst.

Mechanism of motor vulnerability under fragment attack and fuel fireFragment attack

When a fragment penetrates a rocket motor case it usually punches a hole at the entry point and a somewhat larger hole at the exit.

If the fragment ignites and breaks up the propellant the burning area increases and the pressure within the motor will increase rapidly. Normally the nozzle, fragment entry and exit areas are insufficiently large to cater for this increased pressure, and high pressure failure, or even an explosion, will result.

With a strip laminate case, the area of damage at the fragment exit point is more extensive than it would be in a conventional motor case, due to the strip delamination effect. When the propellant ignites and the pressure increases the delamination of the strip continues, the pressure rise is restricted and the motor either burns out or at worst a mild explosion results, the latter usually being restricted to low temperature conditions with CDB propellants.

With a CFRP case extensive damage results to the fibre construction significantly weakening the body and allowing further delamination of the fibres as the pressure builds up again restricting the motor to burning or a mild explosion, again the latter appears to be restricted to low temperature conditions with CDB propellants.

Fuel fire attack

When a solid propellant rocket motor is heated externally, the propellant eventually reaches its self ignition temperature and normally an explosion results. This is due to the uncontrolled nature of the burning producing quantities of gas beyond that which the nozzle alone was designed to vent coupled with the fact that the case strength is almost unaffected at this time.

Whilst this is the mechanism of vulnerability associated with homogeneous motor cases which retain their strength above the self ignition temperature of the propellant, this is not so with the strip laminate and composite cases. When subjected to heat the resin used for bonding begins to lose strength at temperatures above 130°C, 270°F, and at 250°C, 480°C, it has virtually no strength remaining. Most CDB propellants ignite at approximately 180°C but, as the propellant temperature will lag behind that of the case, the resin temperature will be higher and its strength will be significantly reduced. At the instant of propellant ignition only a very low pressure is required to disrupt the motor case thus preventing a rapid pressure rise limiting the effect to one of a mild pressure burst.

Although the auto-ignition temperature for HTPB is higher than CDB the difference is not significant and similar results are obtained.

Summary

The trials carried out on existing propellants and cases indicates that the degree of insensitivity for existing rocket motor systems is dependent on both propellant type and case construction. A qualitative assessment of both factors shows that existing systems may be classified as follows in their reaction to fragment attack:

	Propellant	Case
Most sensitive	EDB & CMCDB CDB	Steel - homogeneous Al. alloy - homogeneous
Least sensitive	EMCDB & HTPB	SL & CFRP

When considering fuel fire only the case appears to have a significant effect, the classification falls generally into two groups

Most sensitive	Homogeneous cases
Least sensitive	Strip Laminate & CFRP

8. Discussion

The optimisation of the design of the hardware for a solid propellant rocket motor requires consideration of the technical requirement, mechanical and thermal environments and interfaces not only with the missile but with other components of the rocket motor.

For metallic structures while a number of materials could be used, cost alone has generally restricted those used to aluminium alloy or steel. The properties possible with these two materials are such that similar masses can be obtained for components designed on stress alone and other considerations such as economic manufacturing thickness, internal volume and method of manufacture become relevant in the choice. In general for low pressure and small diameter motors aluminium alloys would be used for the motor case while steel would be used for higher pressure and larger diameter motors. For components where strain could be the design parameter, such as end closures, then aluminium alloy is the preferred material as this results in a lighter structure.

The method of manufacture used must take into account the fact that a high reliability is required as component failure could result in injury to personnel or the launch platform. This necessitates a high standard of specification for the material and its manufacture. However improvements in both materials and manufacturing methods are continuously being made which can improve the choice available to the designer. As examples, castings have not been favoured for components other than those which are not highly stressed but improvements in techniques are making casting increasingly attractive; the use of flow forming has allowed high strength, maraging, steels to be used for body tubes and has resulted in a reduction in the economic manufacturing thickness and improvements in welding techniques have further simplified manufacture.

For body tubes two non-homogeneous constructions have been outlined. The fibre over-wrapped metal tube offers considerable potential for mass savings on long tubes when the main component of stress in the longitudinal direction results from pressure. However as the ratio of longitudinal to hoop stress increases due to missile loads the advantages of this system reduce. The second method of construction, strip laminate, has advantages in terms of simplicity and ease of manufacture and is also particularly applicable to longer tubes. The main advantage of this latter tube is for use in insensitive munitions.

The requirement for insensitive munitions could drive the design of future systems in terms of both propellant and case. The best metallic case construction demonstrated to date is the strip laminate which reduces the reaction of a motor under fragment attack and fuel fire to at worst a mild explosion. Fibre composite cases also significantly attenuate the effect being very similar to strip laminate. No tests have been carried out on the fibre over-wrapped case but this should be better than a homogeneous case although not necessarily as good as strip laminate and fibre composite.

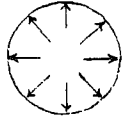

Rocket Motor Case Materials				Weight comparisons			
				Pressure loading		Hoop bending	
Material	Density	Stress	Modulus				
	ρ Kg/m ³	f GN/m ²	E GN/m ²	Stress ρ/f	Strain ρ/E	Stress ρ/\sqrt{f}	Strain ρ/\sqrt{E}
Steel	7850	1.40	200	1.00	1.00	1.00	1.00
Steel	7850	2.00	200	0.70	1.00	0.84	1.00
Al. alloy	2700	0.45	80	1.07	0.86	0.61	0.47
Al. alloy	2700	0.65	80	0.74	0.86	0.50	0.47
Titanium	4600	1.30	110	0.63	1.07	0.61	0.72
Glass 'S'	2040	1.04	35	0.35	1.49		
Carbon	1600	0.85	102	0.35	0.40		
Aramid	1440	0.95	58	0.24	0.64		

Table 1

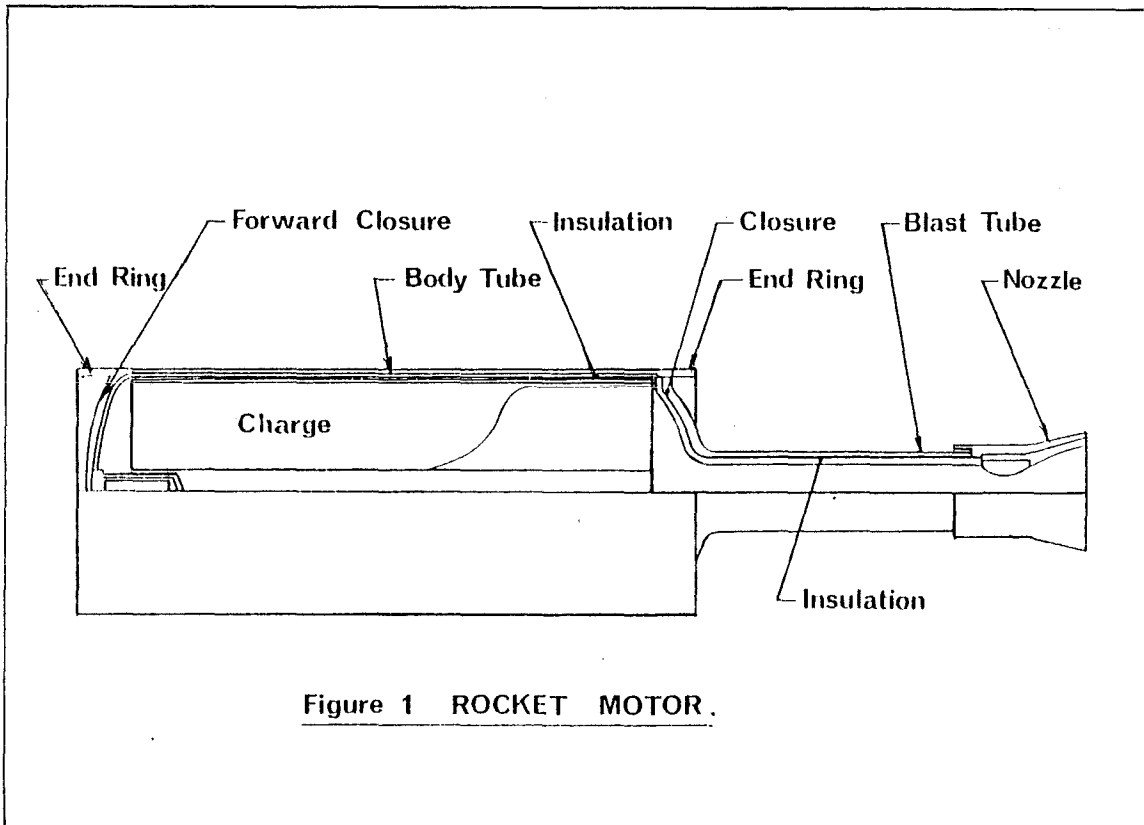


Figure 1 ROCKET MOTOR.

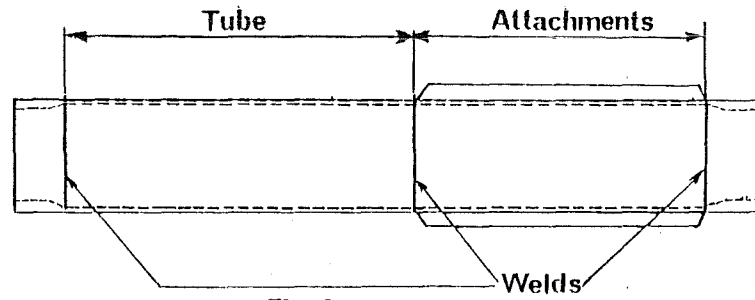


Fig 2 a
Machined & Welded

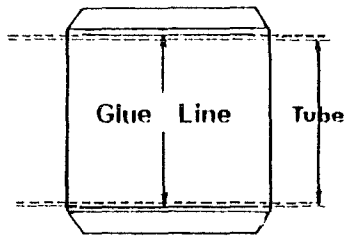


Fig 2 b
Bonded

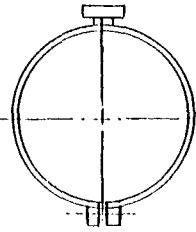


Fig 2 c

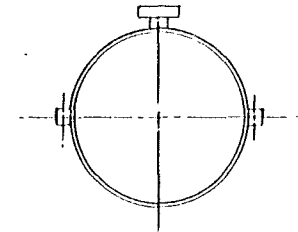


Fig 2 d

Clamped Attachments

END CLOSURE

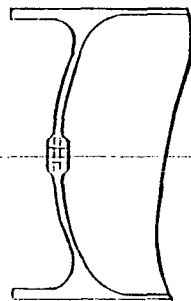


Fig 3 a
Integral



Fig 3 b
Part Integral

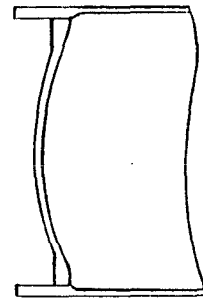


Fig 3 c
Separate

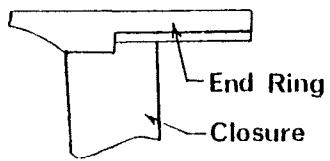


Fig 4a
Thread on Closure

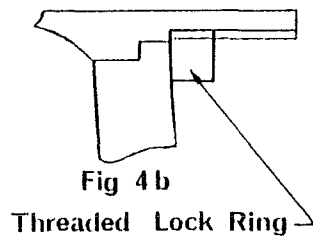


Fig 4b

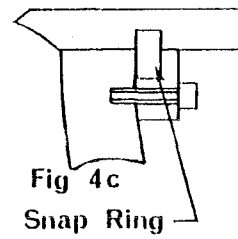
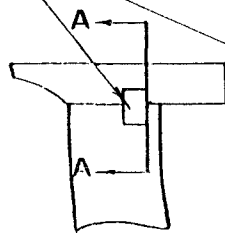


Fig 4c

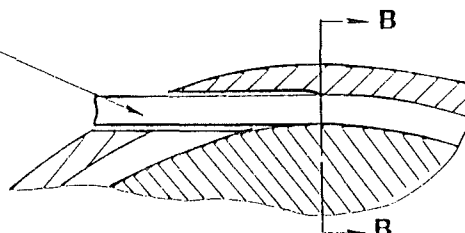
Snap Ring

CLOSURE ATTACHMENT.

Wire Assembled
Thro' Closure



Section B-B



Section A-A

Fig 4d
Lock Wire

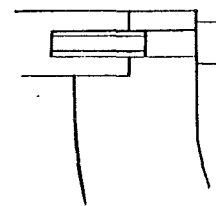


Fig 4e
Bolts

CLOSURE ATTACHMENT.

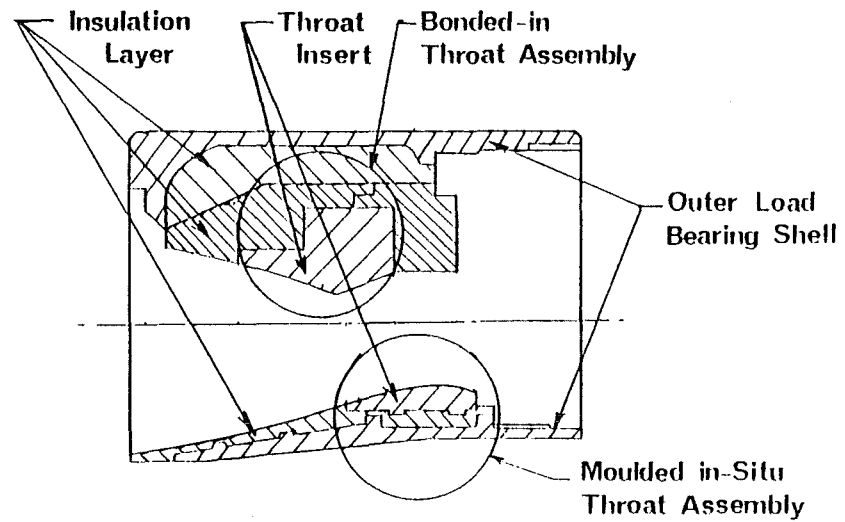


Figure 5 TYPICAL NOZZLE CONFIGURATIONS.

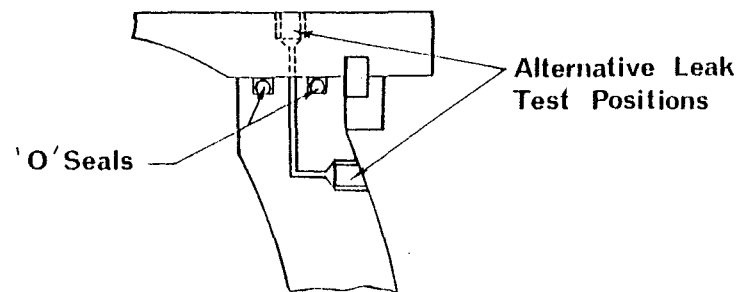
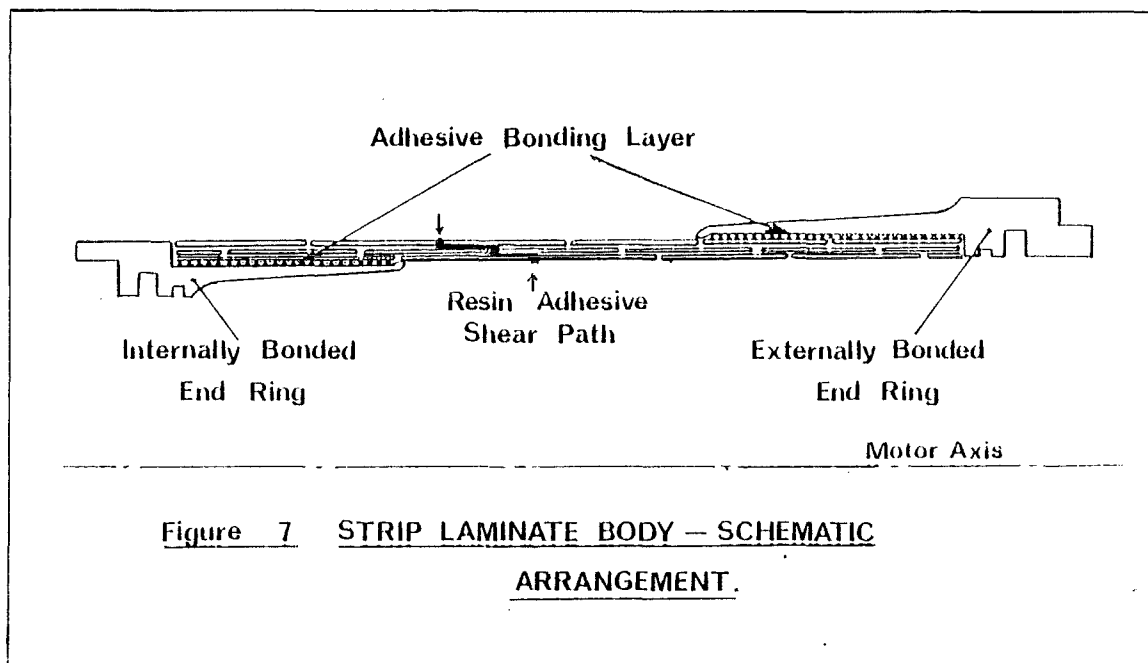


Figure 6 DOUBLE 'O' SEALS.



PROPELLANT GRAIN DESIGN

S. Scippa
 SNIA - BPD
 Defense and Space Division
 R & D Directorate
 Colleferro, Italy

SUMMARY

This lecture reports a general overview of the current methodologies used at SNIA BPD in designing solid rocket motor propellant grain. The Internal Ballistics aspect in grain design is emphasized. An overview of what are the general requirements (Thrust vs time curve, volumetric constraints, etc...), the available technologies (propellant types, manufacturing processes, etc..) and the methodology for the selection of the most appropriate one is presented. Then, the methods used for grain design are summarized. The lecture deals, in particular, with the methods for propellant formulation choice, design of internal geometry, propellant characterization (performances, internal ballistics, etc...).

An analysis of the predictability factors (various mechanisms that can affect the thrust curve, i.e.: erosive burning, hump factor, etc...), and how they can be taken into account for contingency planning is reported.

The experimental tests commonly used for grain design validation are summarized.

GRAIN DESIGN OVERALL PROCESS

The main aim of the solid propellant grain designer is to realize a propellant grain that will evolve consistent with the thrust-time curve required for the mission, taking into account other specified constraints (envelope, weight, etc...).

These requirements provide the basis for establishing the range of variability of the main parameters applicable to the grain design.

The main steps necessary for grain design are:

- evaluation of requirements
- preliminary design optimization
- propellant selection
- selection and design of grain configuration
- propellant characterization and tailoring
- analysis of the design

A typical flow-chart for propellant grain design is reported in fig. 1. Basically the approach is that suggested in ref. 1.

The grain design is not realized independently of other rocket motor components design: there is a necessary interconnection between grain design and other design areas (fig. 2).

The above mentioned steps in the grain design process are described more in detail in the following.

Evaluation of requirements

The requirements which define the basis for selection of grain geometry and propellant type originate from motor performances specification. They include:

- Ballistic performance Characteristics (Thrust, time, Total Impulse);
- Mission Requirements (Envelope, Weight, Environment-Reliability).

The specified ballistic performances shall be evaluated for selecting applicable grain configurations.

The envelope and weight constraints define the geometrical motor design parameters (length, diameter, chamber volume available for the propellant, nozzle length and exit diameter).

Also some environmental requirements (temperature range, ambient pressure, vibrations, etc...) must be taken into account, because they may strongly influence the grain design.

Preliminary design optimization

Some "dependent parameters" must be defined before the grain design process begins.

The most important are:

- Average Operating Pressure (\bar{P}), and the related MEOP
- Nozzle Throat Area (A_t) and Expansion Ratio (E)
- Volumetric Loading (V_l)

- Web Fraction (WF)
- Port-to-Throat Area Ratio (A_p/A_t)
- Length-to-Diameter Ratio (L/D)

In the preliminary design phase it is necessary to quickly and accurately evaluate the effects of these variables.

This study can be accomplished by solid rocket motor optimization computer programs (Ref. 2).

These programs receive inputs from the mission and ballistic requirements, with a fixed design criterion (maximum total impulse, minimum propellant weight or length).

All the designs that satisfy the requirements are compared and the motor that meets the optimization criterion is selected.

Propellant selection

During the preliminary design optimization, the required propellant properties are defined. Although the ballistic (burning rate (r), temperature sensitivity (T)) and performance properties (Specific Impulse (I_{sp}), Density (ρ)) of the propellant usually are dominant in the propellant selection, also the other characteristics (Mechanical Properties, Thermal and Storage Stability, Hazard Properties, Exhaust Products, Cost) must be taken into account.

Once the propellant requirements have been established, the list of the candidate formulations can be reduced to those that require a minimum tailoring.

- Several families of solid propellants have been developed, characterized and utilized at SNIA-BPD.

Among others they include:

- . Aluminized CTPB composites,
- . Aluminized HTPB composites,
- . Extruded double base.

For CTPB and HTPB propellants the Aluminum content ranges from 0.5 to 18 per cent and the solid loading (Aluminum plus Ammonium Perchlorate) reaches values up to 88 per cent.

Cast double base propellants were also studied and motor tested.

The development of new propellants is still under progress, mainly in the field of aluminized composites to obtain higher performances, burning rates over the actual range, reduced smoke compositions.

Selection and design of grain configuration

Configuration Selection. The grain configuration types most commonly used are:

- internal/external burning tube
- star
- wagon wheel
- dendrite
- slotted tube
- conocyl
- finocyl
- multiperforated

Combinations of these shapes can be used to satisfy some particular requirements (i.e. dual thrust levels).

The configuration can be selected on the basis of:

- output of preliminary design optimization analysis - (Ballistic constraints: WF, VI, L/D)
- thrust vs time shape
- processing technique
- structural integrity

The growth potential of the candidate solutions must be assessed.

Detailed grain design. Preliminary calculations and parametric grain geometry studies are sufficient to pre-dimension the grain.

Subsequent iterations typically are necessary for adjusting the grain dimensions to provide the required ballistic performances with an adequate margin of safety for the propellant structural integrity.

A variety of Computer Programs are routinely utilized for geometrical trade-offs (for example between sliver fraction and burning neutrality) and preliminary structural analysis, to ensure the designer of an optimum design.

Obviously, at the beginning, simplified schemes of the configuration are utilized in the analysis.

These Programs are described in the paragraph dealing with the analysis of the design.

In this phase of grain design, Water table experiments can be utilized for selection of grain profile.

A Water table facility exists at SNIA-BPD to analyze the internal flow field in a Rocket Motor Chamber.

Basically, the Water table simulates a 2-D flow of an inviscid gas with $\gamma=2$, by a free sur-

face flow over a horizontal surface.

An hydraulic analogy exists between the water depth and the gas pressure, so that pressure field in the gas flow can be determined by water depth measurements.

Pictures of the experimental facility are shown in fig. 20-21.

Typical applications are for analyzing:

- the effects caused by aerodynamic interaction between the axial port flow and radial slot flow;
- the flow pattern in the aft dome region for different propellant grain configurations;
- the effects of port sudden enlargement, with formation of recirculation zones and vortex shedding, for selecting the grain configuration that promotes smooth gas flow in any transition region with consequent reduced probability of stagnation pressure loss and vortex driven pressure oscillations.

Propellant characterization and tailoring

Having selected the propellant, it must be characterized completely, in order to define theoretically and/or experimentally its main properties (performance, internal ballistics, mechanical properties).

Then, these basic properties can be adjusted or tailored in a variety of ways to satisfy the specified requirements.

In the following, a short description of techniques utilized for Propellant Performance and Internal Ballistic Characterization is reported.

Propellant performance characterization. The propellant theoretical Specific Impulse, under the anticipated motor functioning condition (P, E), is evaluated by the NASA-Lewis Equilibrium Chemistry Computer Program.

The estimate of Delivered Isp is based on a theoretical Impulse reduced by efficiency and heat losses.

The methods utilized at SNIA BPD for predicting Delivered Specific Impulse are described in ref 3.

The experimental value of the Delivered Specific Impulse can be obtained only from the analysis of motor static firing tests results.

Scale testing of propellant by 2" motors shown that the measured Specific Impulse depends upon the motor size, and the difference between values measured in small and large motor is influenced also by aluminum content.

For this reason the small scale measured Isp is used only for correlations and propellants comparison, not for performance prediction.

Propellant Density can be calculated from the density of the ingredients, and generally coincides with values measured.

It is important, however, to calculate the density at the grain casting temperature in dimensioning the casting mandrel, otherwise a deficiency in propellant weight can result.

Internal ballistics characterization. Burning rate vs pressure and propellant temperature measurements are realized by:

- Crawford strand burners (useful for preliminary screening and process control)
- 2"/6" standard ballistic test motors

Standard Motors firing tests are also utilized to evaluate the propellant burning rate dispersion.

Scale-up of burning rate data for use in large motor analysis is based on correlations of similar motors data.

Analysis of the design

The above described steps of grain design procedure provide the starting points for detailed design analysis.

In this phase of grain design, detailed calculations are performed, with grain dimensions being subject to subsequent refinement.

Three main areas of analysis are involved:

- Combustion Geometry
- Internal Ballistics
- structural analysis

Combustion geometry. Computer Codes are utilized to calculate burning and wetted perimeters, surfaces and port areas, starting from grain initial profile.

These programs are either 2-D, 3-D or axisymmetric codes, and can be selected depending on the particular grain geometry.

The 2-D Computer Program (fig. 3) is an in-house developed code. It can analyze star or wagon wheel shapes, which are the most common 2-D cross-sections.

They can be described by a series of lines and arcs.

The cross-sectional perimeter at various stations along the grain is input, using the parameters defined in fig. 4.

The module assumes a linear change in perimeter and port area between stations analyzed (fig 5) and calculates surfaces and port areas history for selected increments of web burn-back and lengths along the grain.

An axisymmetric module (fig.3) developed by SNIA BPD, can be used for any grain which is symmetrical about the motor centerline.

The input is extremely simple.

A typical axisymmetric grain is shown in fig. 6.

The grain is described by inputting the R-Z coordinates shown in the figure, plus information as to whether a particular segment is a straight line or arc.

A series of R-Z coordinates is used to describe the motor case.

Surfaces and port areas are calculated using closed form analytical relationships.

The Program outputs the burning surface and port area vs web.

In the Original Version of the SPP (ref.4) the 3-D grain analysis is accomplished by a generalized 3-D grain design module (GD 3D).

An extensively revised version of this Program (fig.3) is at present utilized at SNIA BPD FOR 3-D combustion geometry analysis.

Some of the features of this code are described below.

Basically, the code simulates drafting techniques to obtain propellant surface and port areas vs web burn-back distance for virtually any grain design.

The motor case is assumed full of propellant initially.

Voids in the case are simulated by four basic figures (cones, cylinders, prisms, or spheres) that may overlay and/or protrude outside the case if needed; they are used to simulate the void as it is initially. The figures may be normal outburning figures, grain filled inburning figures, or nonburning figures, and may have rounded corners and edges if needed. The order of input can be important. Each figure may be placed in any orientation anywhere in space, inside or outside of the grain.

Ordinarily, a solid propellant is symmetric about the motor axis so that only one sector of the symmetry is analyzed.

The answers are then automatically adjusted for the whole motor.

Examples of the four solid figures used in the analysis are reported in fig. 7.

An example of the plotted output obtainable for a star-shaped grain is shown in fig. 8+13.

Segmented grains, such as are commonly used in large solid rocket boosters, require special attention to provide for fully or partially inhibited vertical slots. The nomenclature associated with a typical slotted grain design is shown in Fig. 14.

A slot face that is partially inhibited can be specified by superimposing two cylindrical disks that are identical except for radius. Each disk is an outward burning void, but the larger disk has a fully inhibited face. The growth of a void can be controlled by input of a bound. Either or both faces can be partially inhibited. An example of a slot with a partially inhibited aft face is shown in fig.14.

Internal ballistics. In the Internal Ballistic Computer Program developed by SNIA BPD, pressure and thrust histories are calculated considering the effect of mass addition, port area change, and burn rate variation under quasi-steady state flow conditions. The burn rate theory used is a modification of the Lenoir and Robillard theory. Erosive burning is considered to account for the significant effect of gas velocity and burn rate. The program has two erosive burning options: Modified and Standard Lenoir-Robillard Model. The program can calculate stagnation pressure losses from sudden contractions or expansion such as occur in segmented motors, utilizing standard relationships, with the correction for 2D and compressible flow effects.

Burning rate modifier tables may also be input and used in any element desired.

The governing gas dynamic differential equations are solved by a finite difference technique. The grain may, in accordance with the technique, be considered to be comprised of nodes or elements of finite length. Pressure, mass flow rate, Mach number, velocity, temperature, and web burned are determined at each node along the grain length for each time increment. The resulting thrust, pressure and thrust impulse, throat diameter, exit diameter, amount of propellant burned, thrust coefficient, and delivered specific impulse are determined for each time increment. Inputs to the code include: propellant properties; nozzle throat and exit diameter versus time; perimeter versus web; port area versus web and wetted perimeter versus web, which may be varied independently for each node. Inputs and outputs are illustrated in fig. 15.

Outputs include the fundamental quantities of pressure, thrust, and time. Appropriate quantities are integrated with time; these are thrust, pressure, and propellant weight.

Burn rate and other quantities useful in ballistic analysis are also included in the output.

Motor weight and center of gravity with time are optional output.

A block-diagram of the overall methodology for Ballistic Performance Prediction is shown in fig. 16.

Details of the methodology are reported in ref. 3.

This methodology can be utilized for calculation of:

- nominal performance
- performance dispersion (3σ)

The dispersion analysis must be realized, taking into account:

- propellant characteristics dispersion (density, temperature, burning rate, characteristic velocity)
- Thrust coefficient dispersion

- Throat erosion low variability
- mandrel misalignment
- case availability and other tolerances.

This, in order to verify in the worst case assumption (35), the compliance with motor technical specifications.

Structural analysis. The primary finite element code utilized at SNIA BPD is an Axisymmetric and Planar Structural Analysis code.

It is utilized with orthotropic, temperature dependent material properties.

Input to the program consists principally of:

- material properties (Modulus, Poisson's ratio, Coefficient of thermal expansion Vs temperature).
- geometric configuration, in the form of a finite element mesh.
- loading conditions (thermal, pressure, force, acceleration).

Program output consists of:

- Nodal points displacements
- Hoop stress/strain
- Radial stress/strain
- Axial stress/strain
- Shear stress/strain
- Max principal stress/strain
- Min stress/strain
- Max shear stress
- Angle of Max stress

In addition to the printed output, grid plots and isoplots are available.

PREDICTABILITY LIMITS

The basic predictability limits have to be analyzed for contingency planning in the mandrel design and to generate the performance envelope.

One of the most widely recognized factors that is not entirely predictable is the erosive burning.

Its effect on initial chamber pressure depends upon design characteristics, such as:

- Mass flux
- Port-to-throat area ratio
- Reference burning rate
- Complexity of grain geometry
- Binder system
- Chamber pressure

An analysis that will accurately predict erosive burning is fundamental to successful design analysis.

Such estimates are established from correlations of actual performance data of similar motors.

Examination of large motor data, indicated that in these motors erosive burning did not significantly affect the ballistic performance, limiting the port mass velocity.

For smaller motors, data have been analyzed to establish the nature of the erosive burning exponent (β), used in the Lenoir and Robillard burning rate theory.

These data indicated that the main parameters affecting β are:

- propellant formulation
- grain internal configuration

Correlations are used as a first estimate of the β to be used for a new motor design.

The SNIA BPD Internal Ballistic Computer Program has two erosive burning options:

- LENOIR-ROBILLARD MODEL

$$r = ap^n + \alpha \frac{G^{0.8}}{D_h^{0.2}} \exp(-\beta p r/G)$$

- MODIFIED LENOIR-ROBILLARD MODEL

$$r = ap^n + \alpha \frac{G^{0.8}}{f(D_h)} \exp(-\beta p r/G)$$

where $f(D_h) = 0.9 + 0.189 D_h (1 + 0.043 (D_h) (1 + 0.023 D_h))$.

The hydraulic diameter function attempts to compensate the above mentioned effect of motor scale on erosive burning.

In many motors, both large and small, the actual trace shapes are initially lower than theoretical, higher in the middle of burn, and lower again near web time.

At this phenomenon was given the name of BARF (Burning Anomaly Rate Factor) or HUMP. HUMP was found in the 1 m diameter Strap-on-Booster motors for ARIANE 3 and ARIANE 4 launchers (fig. 17-18).

It was also found in Thiokol, Aerojet, LPC motors (fig. 19).

The method of quantifying the HUMP phenomenon is to determine the correction factor that

must be applied to the burning rate low as a function of the web to correct the theoretical performance to the measured value.

The mechanisms that can cause the anomaly are not well understood. One possible cause is the motor filling process.

The anomaly occurs in a quite repeatable manner for a given motor-propellant combination. Its effect can be estimated based on correlations of similar motors data.

Based upon the frequency of occurrence of HUMP, particularly in large motors, the mandrel design should include the flexibility to counter it.

Other parameters which could affect mandrel design are:

- predictability of I_{sp}
- predictability of nozzle throat erosion
- predictability of stagnation pressure drop, due to sudden contractions or expansion in the port.

The predictability of I_{sp} is about 1%

The accuracy of predictability of throat erosion is about 20%.

The impact of stagnation pressure losses due to any flow anomaly is generally limited to the first burning seconds with consequent not serious effects on performances.

Analytical grain design modifications can be undertaken to counteract the effects of the assumed HUMP or I_{sp} prediction inaccuracy and quantify the potential mandrel changes.

These changes will be contained into the contingency planning.

MOTOR FIRING TEST

The experimental test commonly used for grain design validation and margins verification is the motor static firing test.

It can be realized utilizing the motor case real configuration or an heavy motor case.

Furthermore, it can be or not "dureis" (i.e.: the pressure, can be increased to verify the propellant integrity at the ignition).

Motor testing is done on static benches both in atmosphere and in vacuum when is needed.

The following facilities are available:

- . Static atmospheric benches, of usual type with head chamber pressure and thrust versus time standard measurements;
 - . Six components static bench, for booster motors up to 9.5 propellant tons;
 - . ISA vacuum test facility, whose characteristics are described in ref.5.
 - . A vertical static bench for Ariane boosters has been build up and successfully tested.
- From the analysis of the recorded pressure and thrust curves vs time, utilizing a computerized procedure set-up at SNIA-BPD (fig22), it is possible to obtain all the ballistic parameters, as:

- Burning Rate Scale Factor
- Hump Factor vs Web
- Erosive Burning Coefficient
- Average Characteristic Velocity
- Throat Area vs Time

The experimental traces, together with these data, can be compared with the theoretical values, calculated during the design phase, in order to:

- verify the compliance with motor technical specifications;
- verify the margins, taking into account the performance dispersion (3σ);
- identify if propellant grain design changes are necessary.

COMPARISON WITH EXPERIMENTAL RESULTS

The discussed grain design and internal ballistics analysis procedure has been applied to:

- solid rocket motors for military application
- solid rocket boost motors

The main characteristics of several SNIA BPD motors are reported in table 1. The numbers after the propellant binder identification indicate in the order the Aluminum and binder per cent.

Motors of very different propellant Aluminum content, dimensions and nozzle expansion ratios are included and constitute an acceptable base for testing a grain design and a performance prediction methodology.

The good agreement between predicted and delivered performance is confirmed by internal ballistic analysis results shown in fig.23-37 where computed traces are compared with experimental traces envelopes (ref. 6-7).

CONCLUDING REMARKS

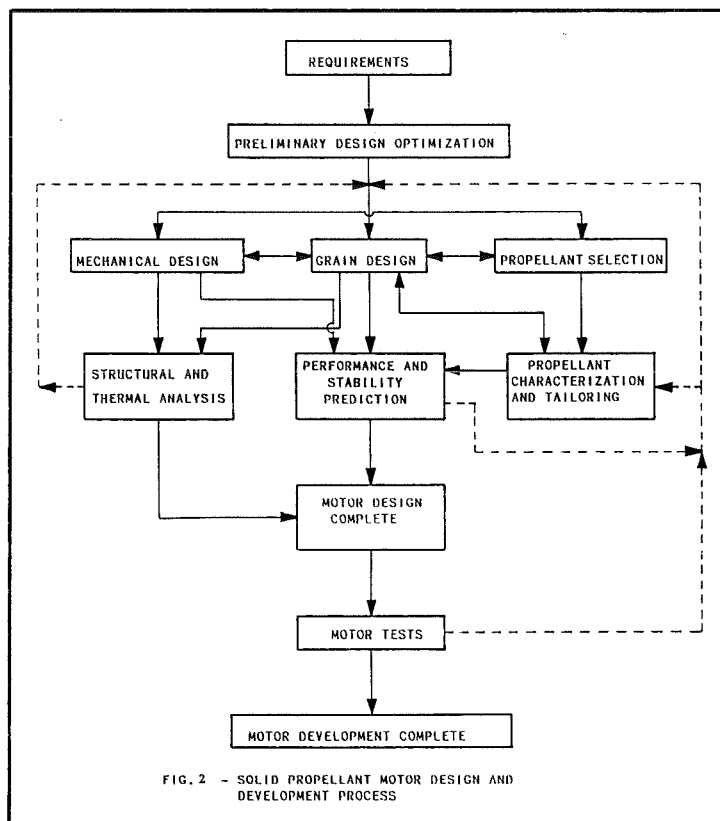
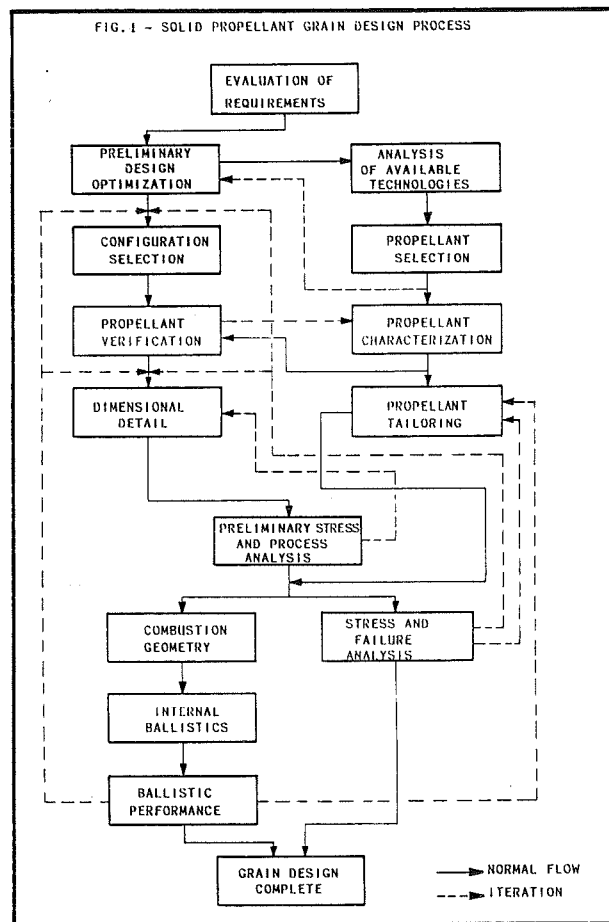
An attempt has been made in this paper to report a general review of the current methodologies used at SNIA BPD in the area of design solid rocket motor propellant grains.

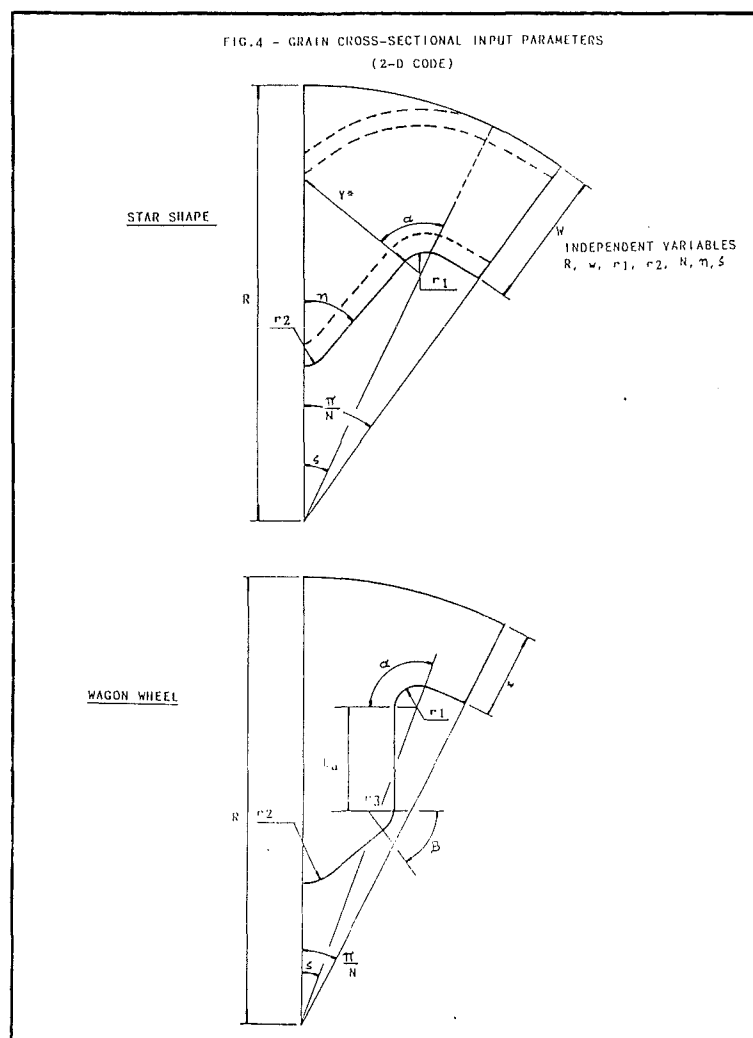
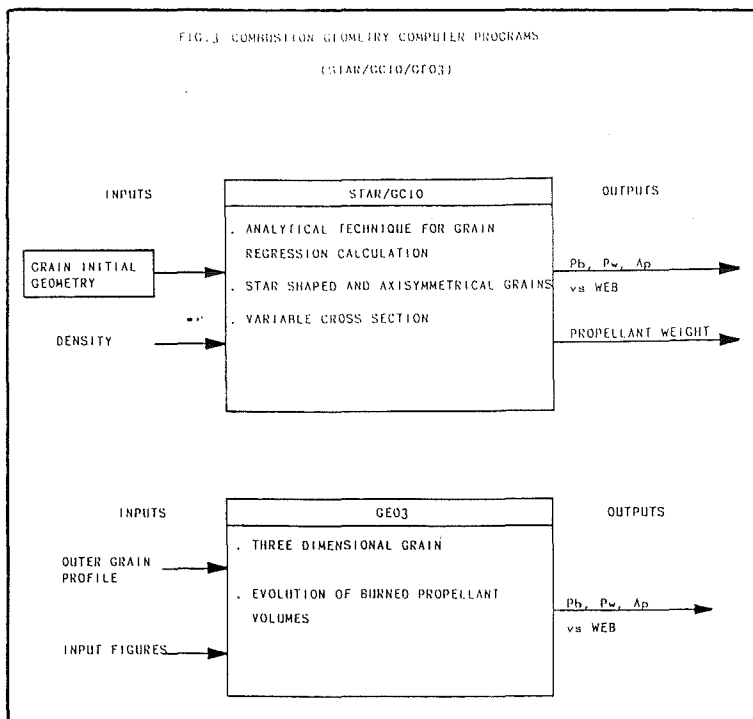
Examples have been used to demonstrate the existence of a consistent data base for grain design (and, more generally, performance prediction) methodology validation.

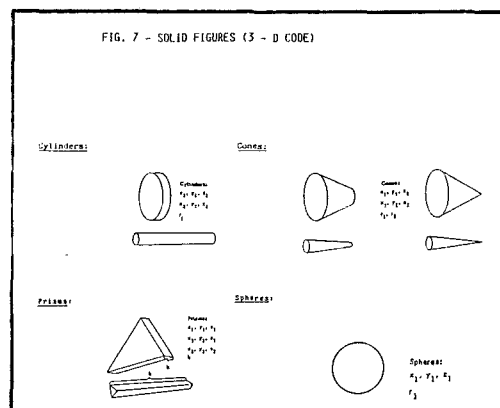
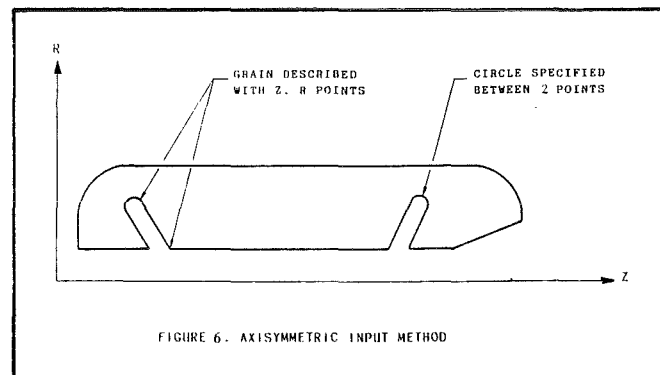
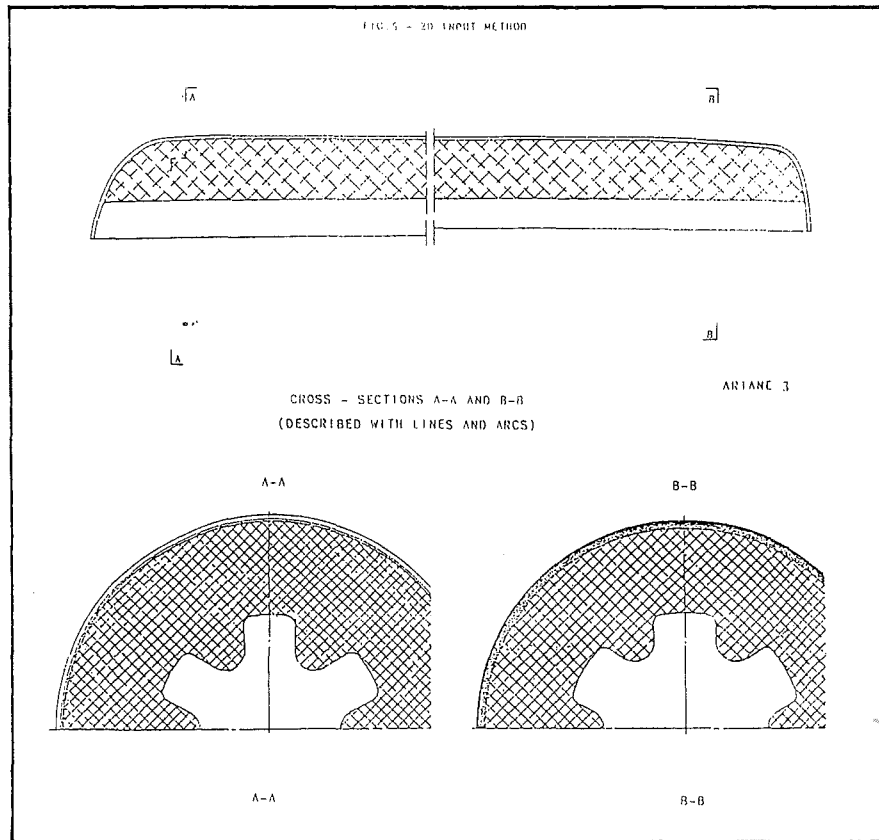
At present, several improvements in the described methodology are in progress. Particularly, efforts are devoted in the area of Computer Automated Design (CAD) to aid the analyst to procedure and analyze virtually any grain geometry with high accuracy and low time expense.

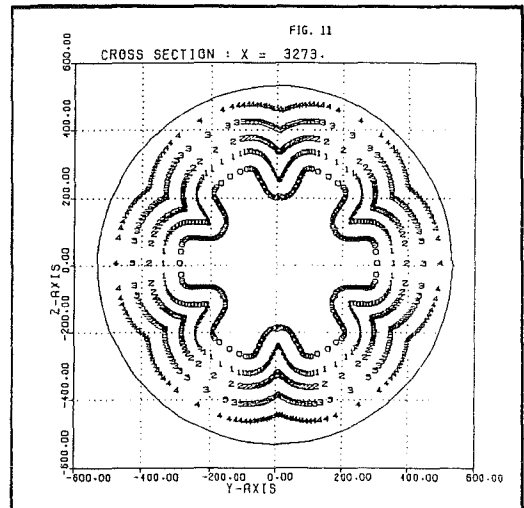
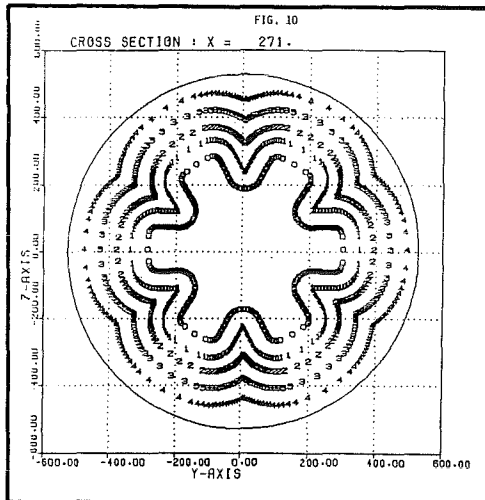
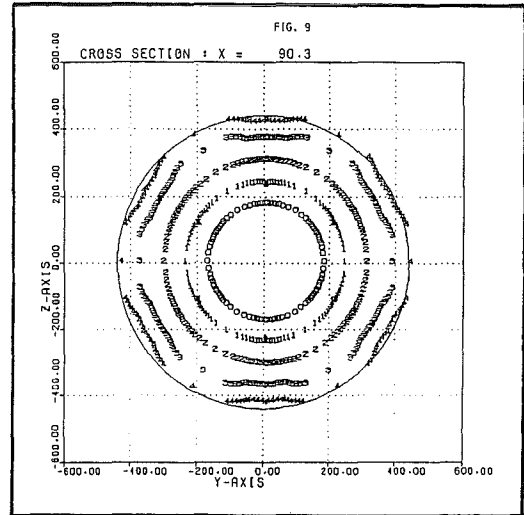
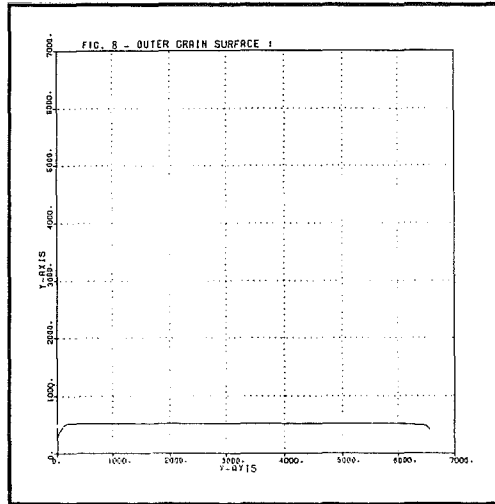
REFERENCES

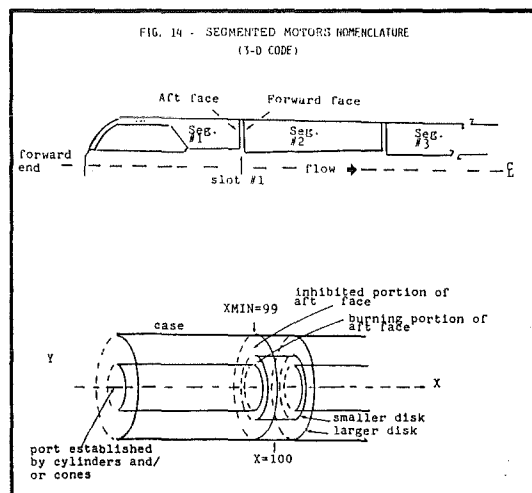
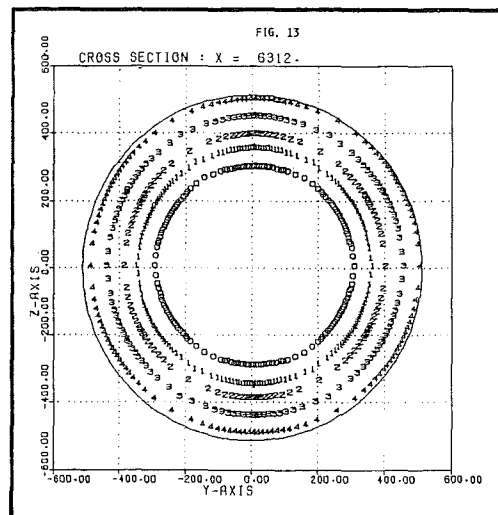
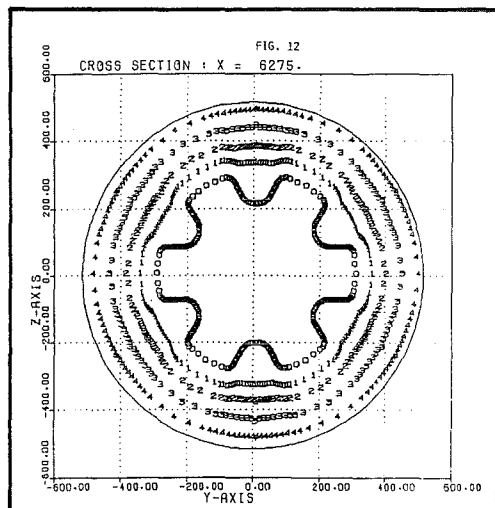
1. Brooks, W.T.: "Solid Propellant Grain Design and Internal Ballistics", Nasa SP-8076, Lewis Research Center, Cleveland, Ohio, March 1972.
2. Haymes, W.G., et al.: "Solid Rocket Motor Design Automation Technology", AGARD CP-259, July 1979.
3. Various, "Performance of Rocket Motors with metallized Propellants", AGARD AR-230, September 1986.
4. Nickerson, G.R., et al.: "A Computer Program for the Prediction of Solid Propellant Rocket Motor Performance". AFRPL-TR-75-36. July 1975.
5. Solfanelli, G, et al.: "A New Simulated Altitude Facility for Space Motor Tests", Paper No 82-11G9, AIAA/SAE/ASME 18th Joint Propulsion Conference, Cleveland, Ohio, June 1982.
6. De Amicis, R., et al.: "Performance Prediction of Apogee Boost Motors and Correlation with Vacuum Firing Tests and Flight Results", Paper No. 79-1296, AIAA/SAE/ASME 15th Joint Propulsion Conference, Las Vegas, Nevada, June 1979.
7. Mura, M. and Vari, E.: "Ariane 3 European Launcher Strap-on Booster Development, Qualification and Flight", AIAA/ASME/SAE/ASEE 21st Joint Propulsion Conference, Monterey, California, July 1985.











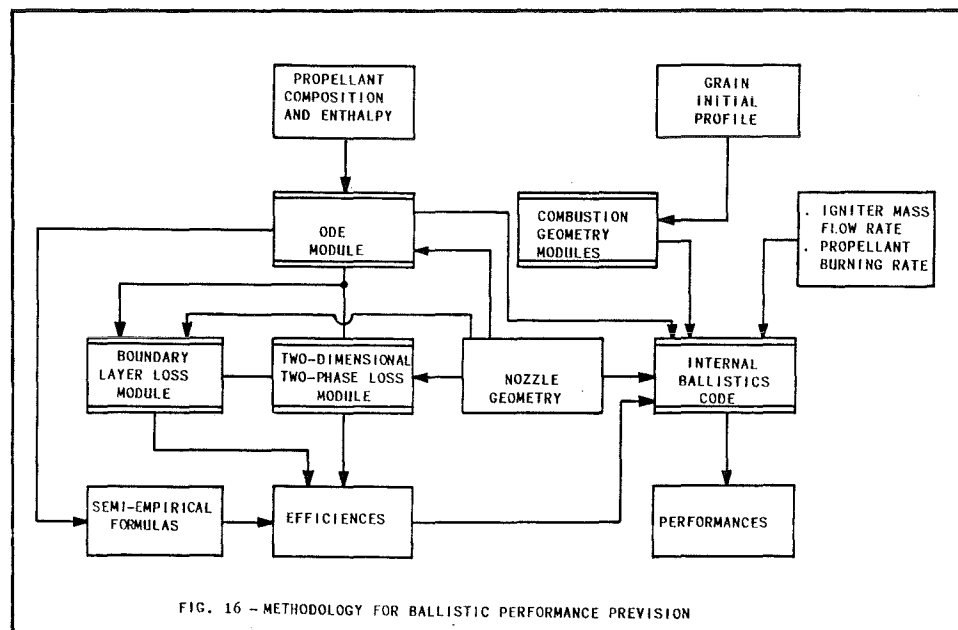
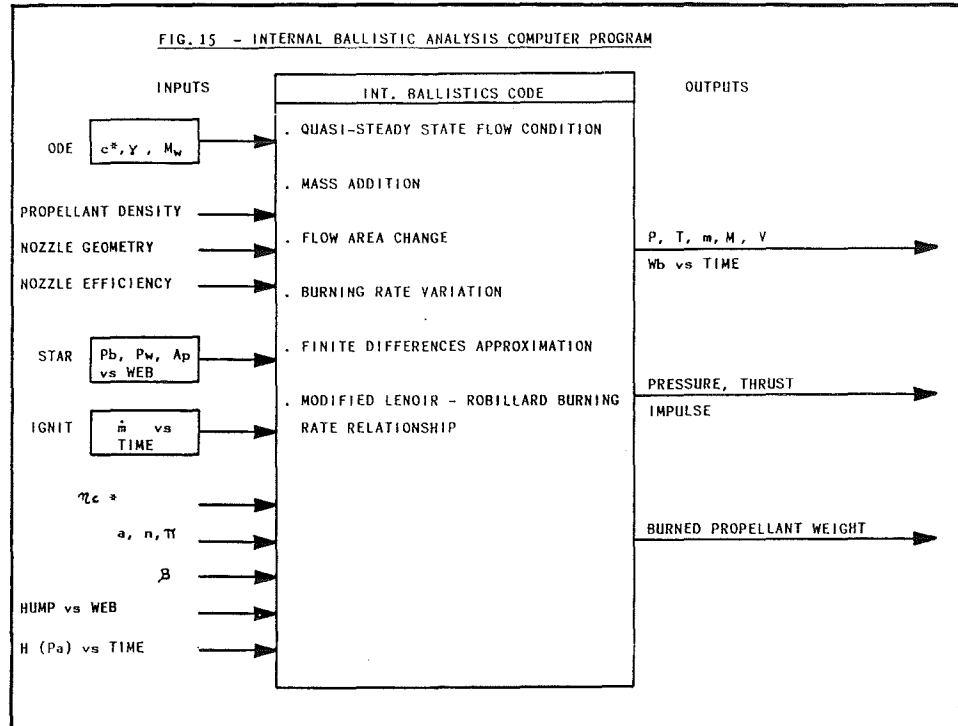


FIG. 17 - ARIANE 3 STRAP-ON-BOOSTER AVERAGE HUMP FACTOR

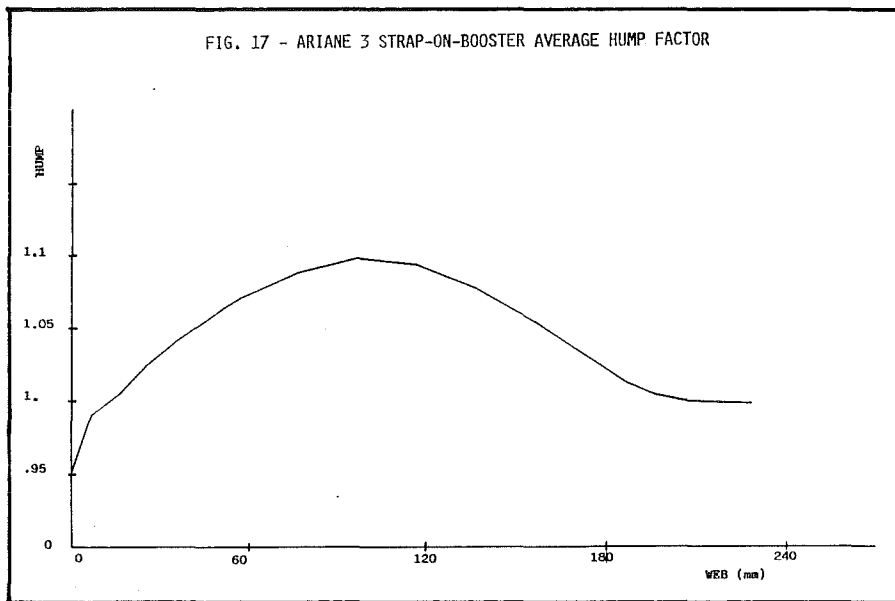


FIG. 18 - ARIANE 3 STRAP - ON - BOOSTER BALLISTIC PERFORMANCES

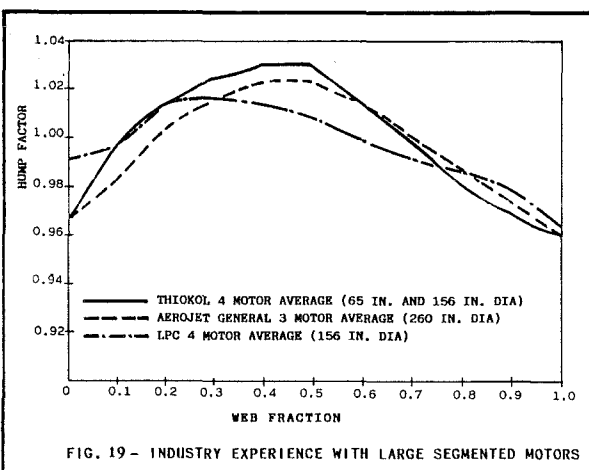
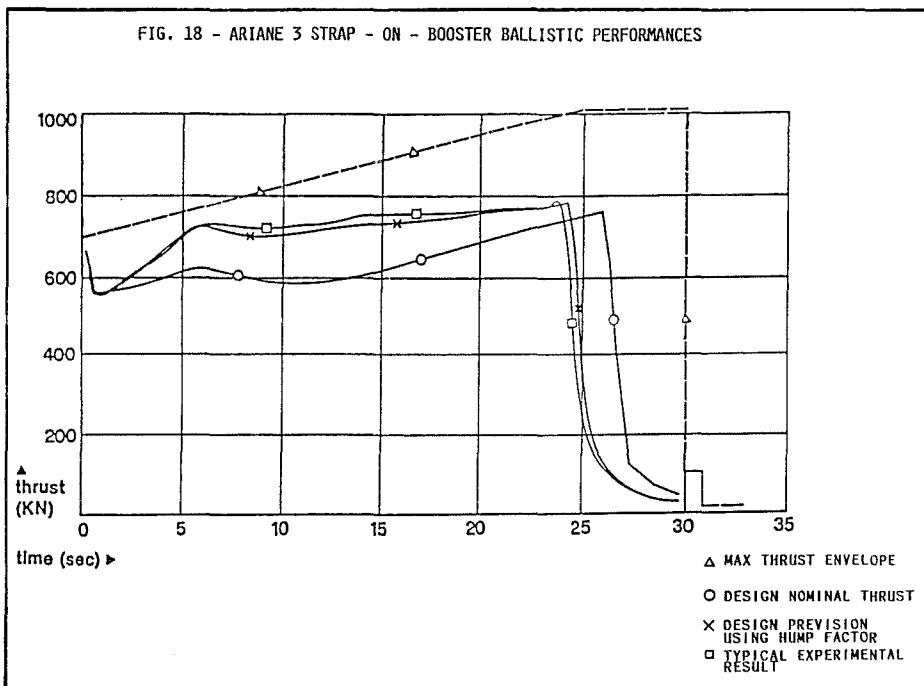


FIG. 19 - INDUSTRY EXPERIENCE WITH LARGE SEGMENTED MOTORS

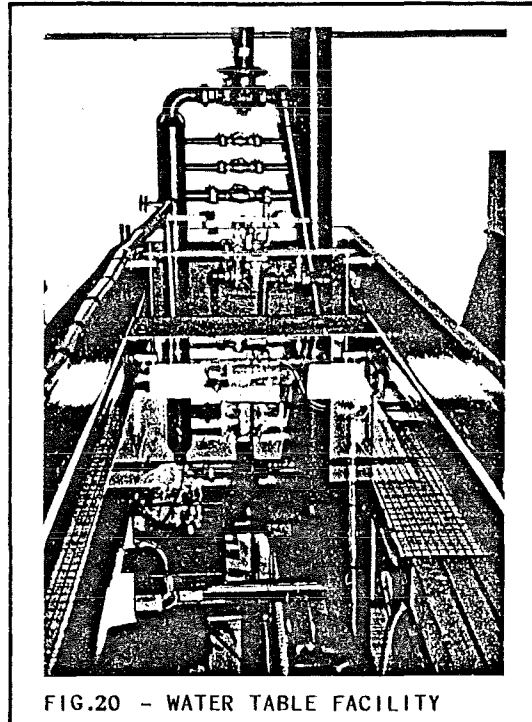


FIG.20 - WATER TABLE FACILITY

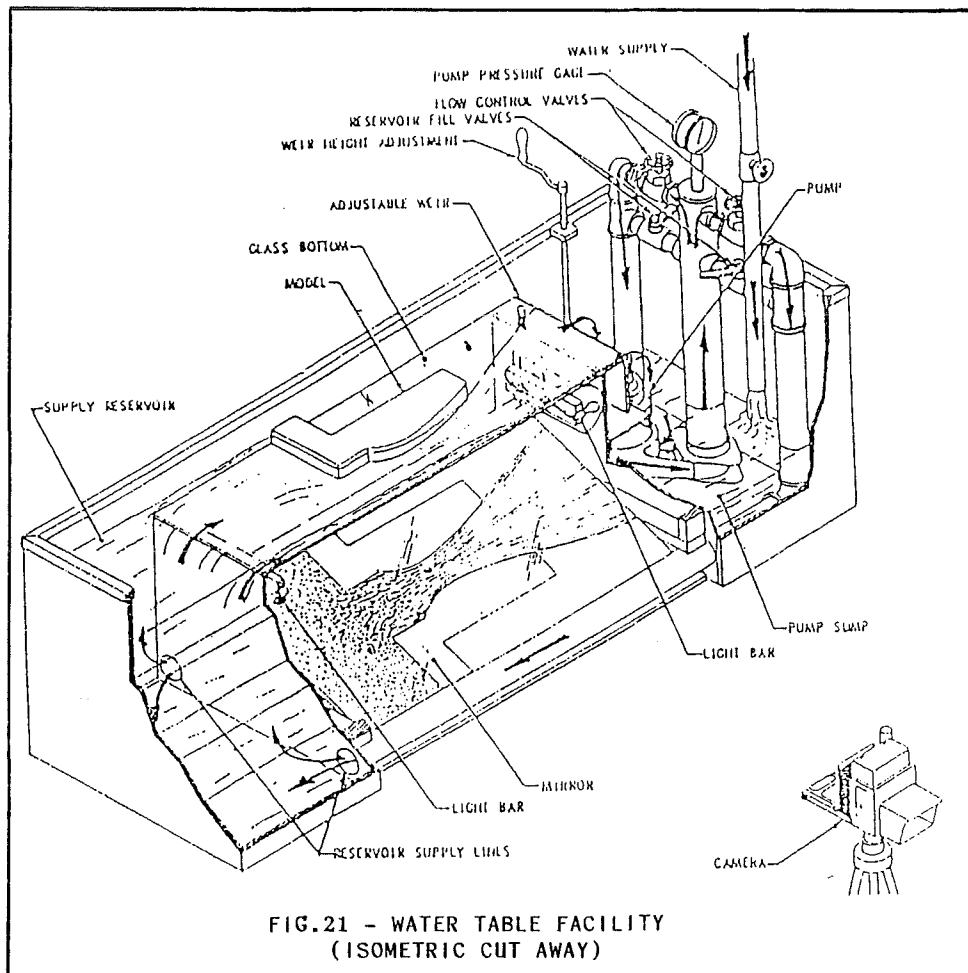
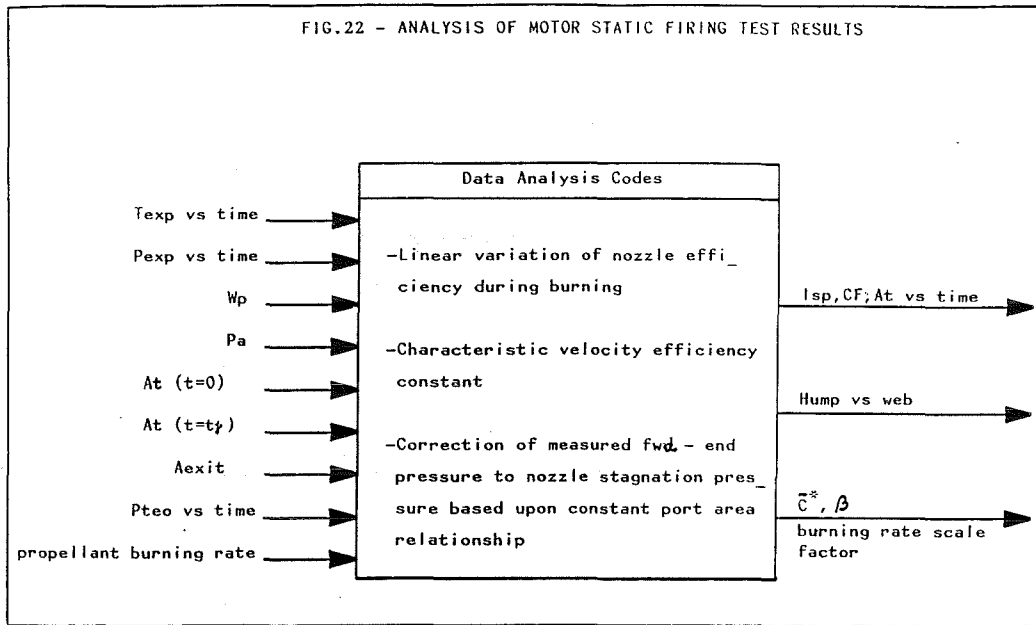


FIG.21 - WATER TABLE FACILITY
(ISOMETRIC CUT AWAY)

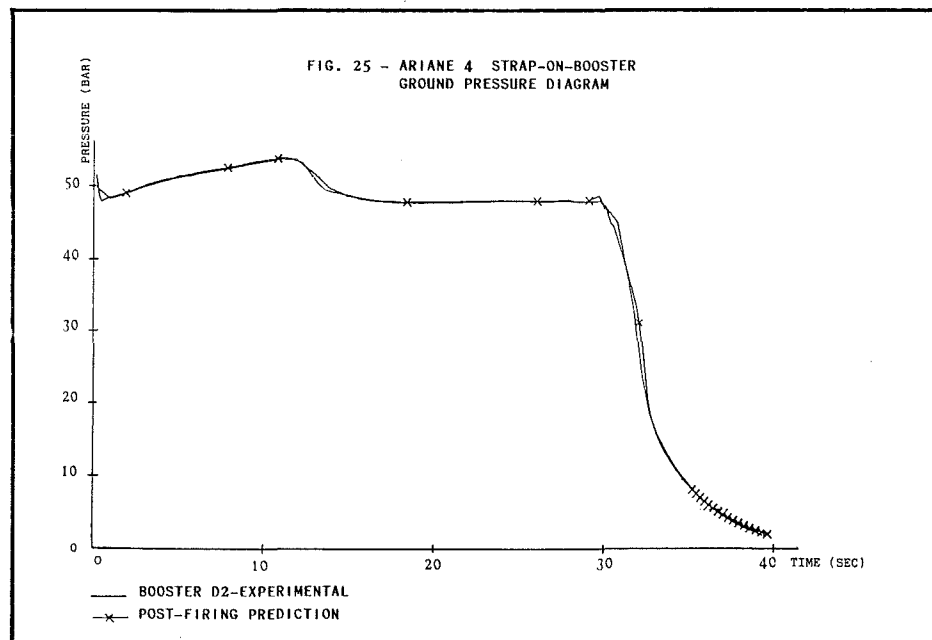
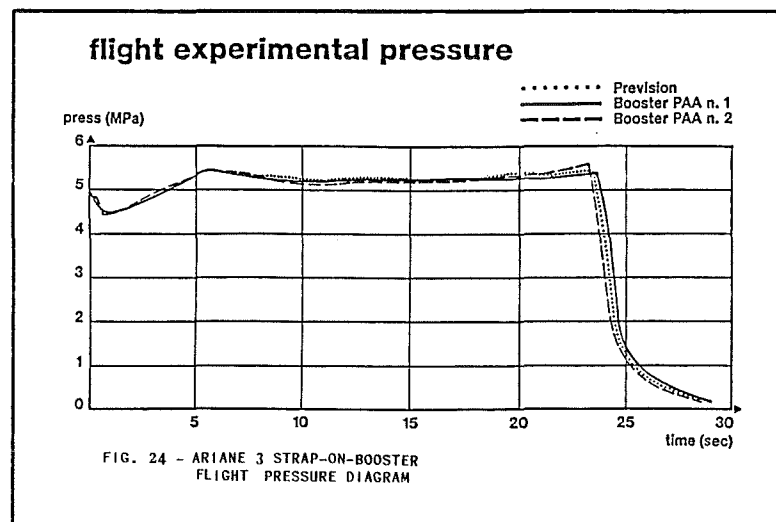
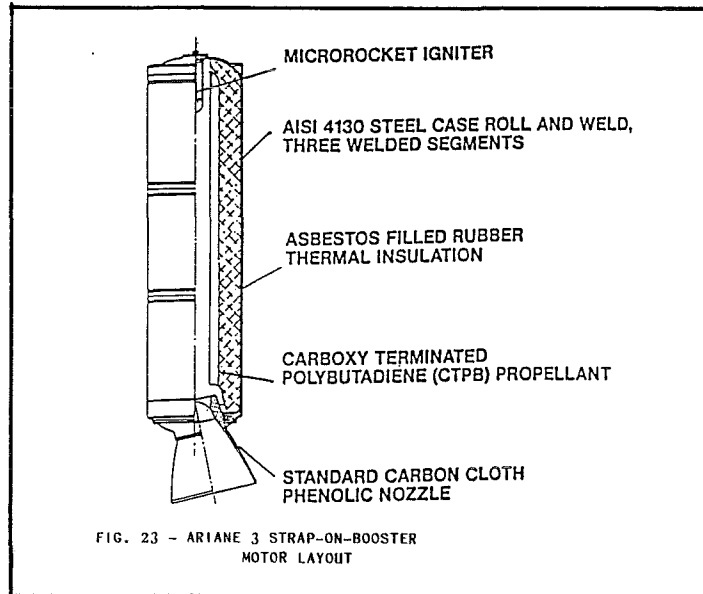
FIG.22 - ANALYSIS OF MOTOR STATIC FIRING TEST RESULTS

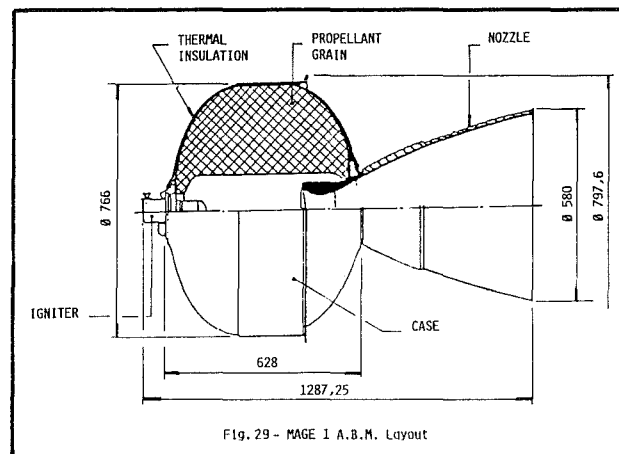
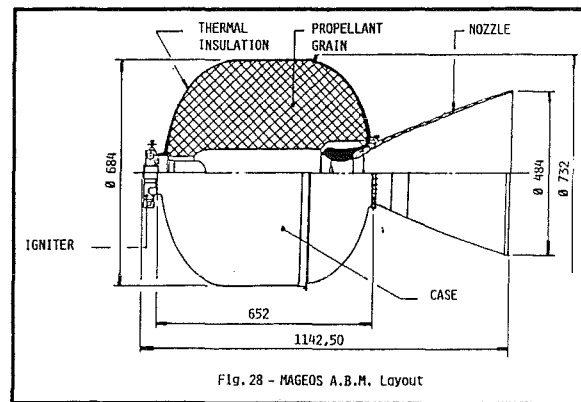
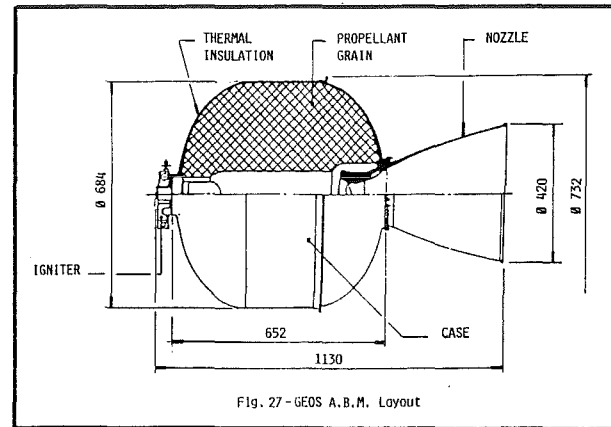
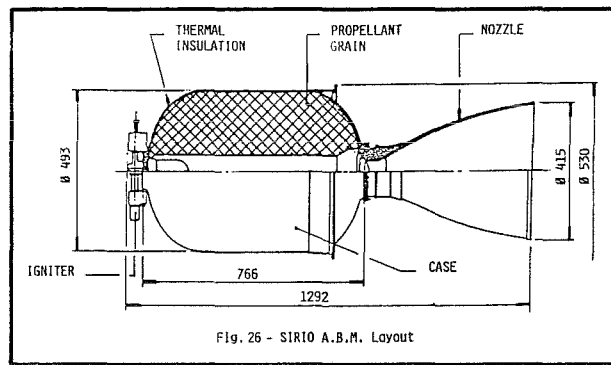


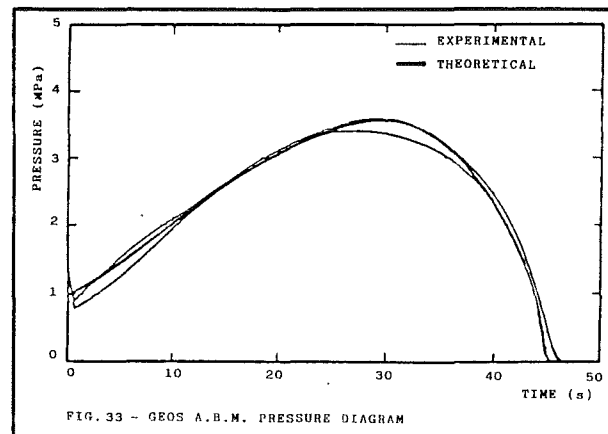
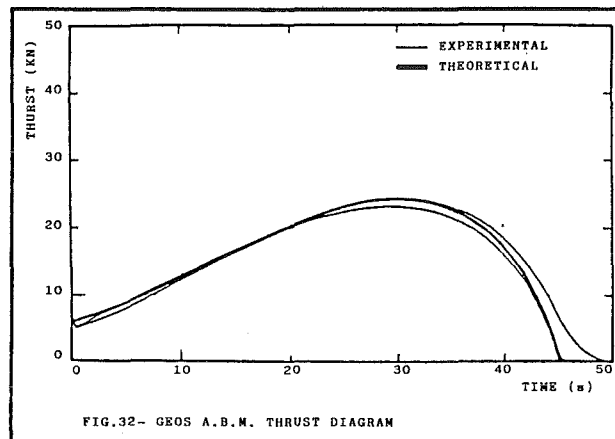
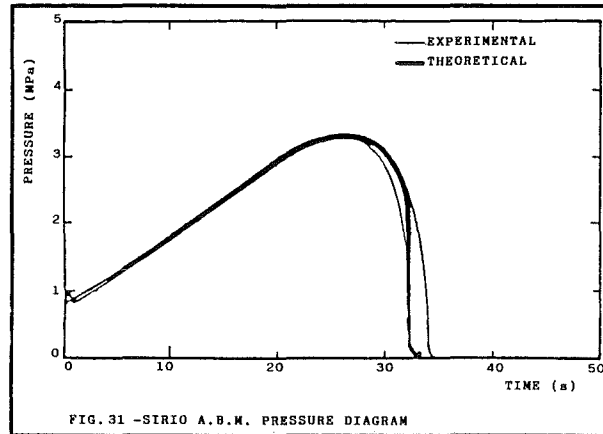
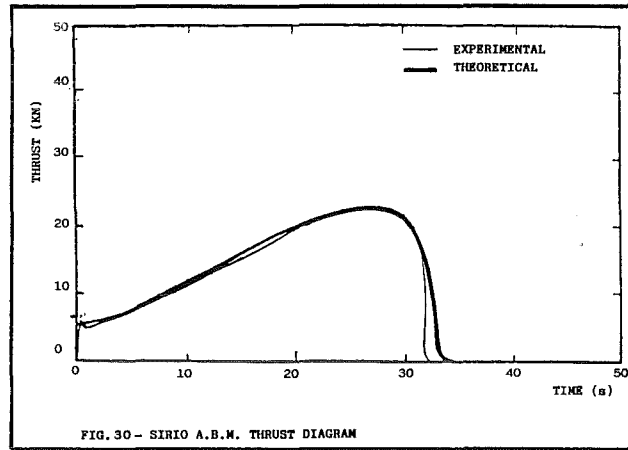
MOTOR	PROPELLANT	PROPELLANT W T (K g)	L (m)	D (m)	NOZZLE EXP. RATIO	STATE	APPLICATION
ARIANE III ULLAGES	CTPB 5-14	from 11 to 14	0,3	0,23		Production	Stage Separation
	CTPB 16-14						
	CTPB or HTPB						
M1		56	1,3	0,20	5,8	Production	Military
SIRIO	CTPB 10-14	176	1,29	0,493	35	Production	Apogee
GEOS	CTPB 10-14	269	1,13	0,684	37	Production	Apogee
MAGE FAMILY	CTPB 16-12	from 250 to 490	1,29	0,766	65	Production	Apogee
IRIS	HTPB 18-13	1575		1,3	60	Static Tested	Perigee
ARIANE III BOOSTER	CTPB 16-13	7350	6,5	1,08	8	Production	Strap-on Booster
ARIANE IV BOOSTER	HTPB 10-14	9500	8,5	1,08	8	Qualified	Strap-on Booster
AL - SR	CTPB 10-14	550	1,3	0,63	8		Technological
M2	CTPB 15-13	178	2,6	0,28	7	Static Tested	Military
M3	DOUBLE. BASE	21	2,0	.12	5,2	Production	Military
M4	"	4	1.	.08	7.8	Production	Military

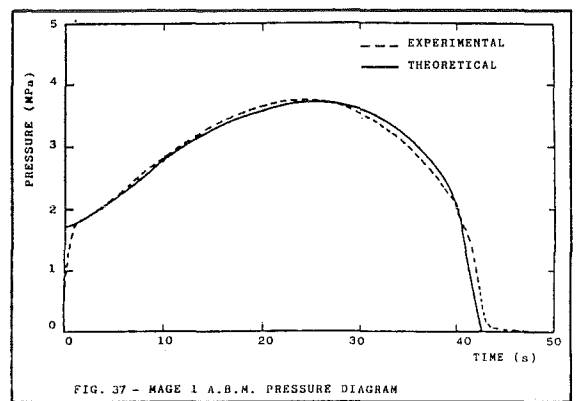
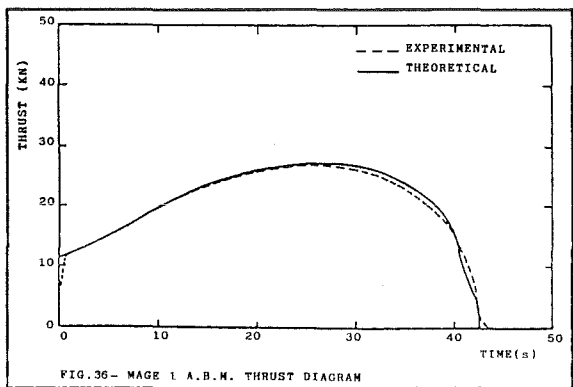
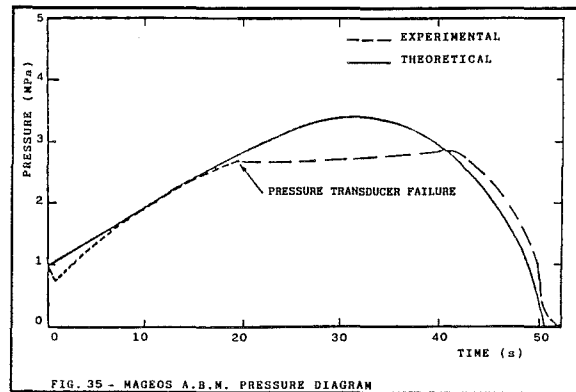
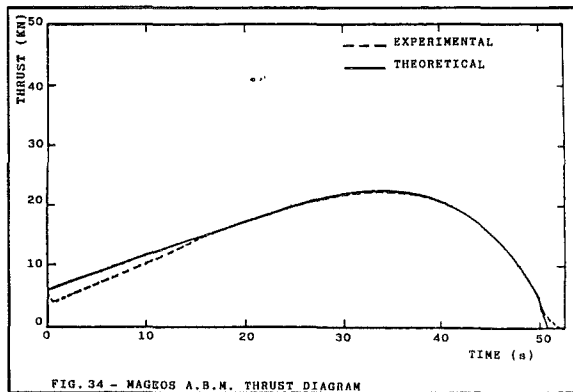
MAIN CHARACTERISTIC OF SEVERAL SNIA-BPD MOTORS

TABLE 1









SOLID PROPELLANT GRAIN DESIGN

Bernard ZELLER

SNPE - Direction Technique Autopropulsion
 Centre de Recherches du Bouchet, BP N° 2, 91710 VERT LE PETIT - FRANCE

ABSTRACT

To design a solid propellant grain is to conceive and to define a grain which satisfies various requirements. This paper describes the methods and procedures which are used today in France to design propellant grains. It describes and analyses :

- the various types of grain and the various families of propellant which are available and used today,
- the detailed requirements that a solid propellant grain must satisfy,
- the methods which are used to precisely define the propellant, the architecture and the configuration of the grain, and more specifically the methods used in order to ensure required ballistic performances though maintaining structural integrity of the grain (which is submitted to mechanical loads all along its life,)
- an overview on a method of solid propellant grain reliability assessment.

Lastly, the improvements needed in the area of grain design analysis and the related technical breakthroughs are briefly presented.

1. INTRODUCTION

During the last twenty years, requirements on performances, reliability and cost of solid propellant rocket motors (and also on schedules and cost of developments) have become more and more stringent. Consequently it had a direct effect on solid propellant grain design methods and procedures and on development program contents.

The need for improved performances is the consequence of the need for longer ranges, higher velocities and more powerful payloads. The improvement of reliability originates from the need for higher availability of weapon systems, for lower malfunction probability and for longer service life. A decrease of duration and cost of development program directly reduces program total cost.

During the same period of time, energetic, kinetic, mechanical and aging propellant properties have also been largely improved. Furthermore, the power of scientific computers has greatly increased and the use of micro-computers has widely spread within the project managers community.

Due to the pressure of competition (tactical missiles, space launchers) or to technical/political reasons (strategic missiles), the time assigned to designers for performing grain preliminary design * has considerably decreased.

It seems appropriate, to present a synthesis of the various methods used today for designing solid propellant grains, within the larger frame of solid propellant rocket motors design.

Design of propellant grains involves vast knowledges and numerous techniques. It is due to the nature of propellants, the geometry and architecture of propellant grains and to their operation modes in rocket motors.

* Result of preliminary design is a first propellant grain definition which generally demonstrates how initial requirements may almost totally be satisfied. Additional modifications of the grain, involving often the use of large computer codes, are needed in order to establish final design.

Grains are made of solid propellant put into a given configuration during manufacture ; their surface is generally locally restricted or inhibited (to prevent ignition and combustion) by a flame resistant, adhesive material. Other parts of the grain may be bonded by a liner to the motor case (case-bonded grains).

Weights of propellant grains range from just a few grams to several metric tons, chamber pressures from a few tenths to more than thirty MegaPascal (MPa), operating times from a few milliseconds to a few minutes.

Manufacture, fielding, storage and operation of a propellant grain (within a rocket motor) involve numerous phenomena related to chemistry, thermodynamics, geometry, combustion, fluid dynamics, mechanics of continuous media, etc... In the present paper, it is not possible to comprehensively analyse all the aspects of grain design which precisely defines a propellant grain which can be industrially manufactured and which must satisfy requirements on storage and operation in various conditions. A selection has therefore been made in the potential content of this paper. It is assumed that the reader is familiar with the basic knowledge of solid propulsion (see (1) and (2)). Since a wide variety of solid propellant grain configurations is available, it is not possible to analyse them in details. Consequently, this paper is mainly focused on design of case-bonded solid propellant grains used for tactical and strategic missiles. There is no in depth discussion on free standing grains (although much of the material developed hereafter could be used for such grains), on nozzleless grains mainly used for initial boost of ramrockets, on grains containing imbedded metal wires for local increase of propellant burning rate, and also on clusters of stick propellant used in very short action time rockets.

Main points discussed include :

- a description of various types of grain and associated propellants (including french terminology),
- an analysis of requirements for solid propellant grains,
- a review of mechanical and ballistic design methods used today in France (the description of related three-dimensional computer codes and of a rapid grain preliminary design method are emphasized),
- a method of assessing propellant grain reliability and a description of associated tests.

In the conclusion, one tries to point out the main areas wherein improvements on the present state of the art are needed either in the knowledge of the phenomena or in the analytical and numerical tools which are necessary to design satisfactory high performance/low cost propellant grains.

2. DESCRIPTION OF GRAIN GEOMETRIES AND ASSOCIATED PROPELLANTS

In this section, various types of grain configurations and of propellants are presented, and also general principles on configuration and propellant selection.

21. Grain configurations

There are two main types of grain architecture : free standing grains and case-bonded grains. Grains of the first type are introduced into rocket motor cases (cartridge-loaded) after manufacture. Grains of the second type are bonded to the motor case during the casting (or injection) and curing steps of the propellant grain manufacturing process (figure 1)

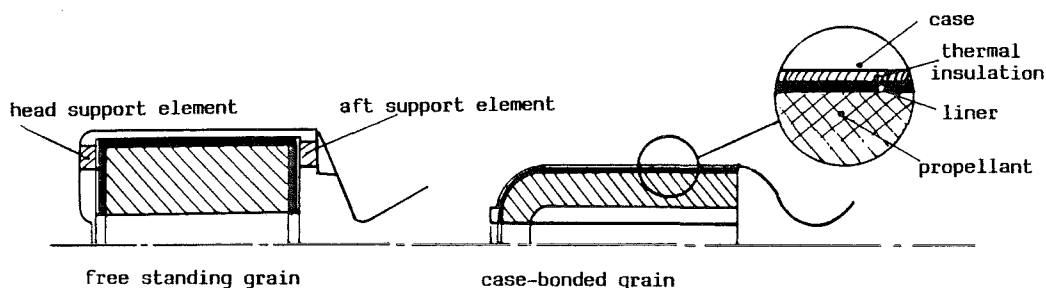


Figure 1

There is not a single, well defined, procedure for selecting a free standing grain architecture or a case-bonded grain architecture for a given rocket motor, except when one of these two architectures is obviously most appropriate for a specific reason. Nevertheless, case-bonded grains generally give higher performances than free standing grains for equal available volumes. However free standing grains are largely wide-spread because this type of architecture may present significant advantages, for instance from the point of view of cost and of overall industrial management. Today, one can yet notice a trend towards case-bonded architectures due to the demand for higher performances.

211. Configurations of case-bonded grains

When propellant grains have an outer diameter larger than 500 mm or a weight of more than 300 kg, they are almost always case-bonded. High performance, middle-sized (outer diameter between 100 mm and 500 mm, weight between 10 and 300 kg) are case-bonded, but free standing middle-sized grains are very common. For small rocket motors, free standing grains are generally used.

Case-bonded grains generally have a central port ; the outer surface of the grain is bonded by a liner (and a thermal insulation) to the motor case. During firing, combustion of the propellant is initiated on the internal surface of the central port and proceeds radially towards the case (and to a certain extent longitudinally depending on the exact geometry). Exact grain geometry is obtained during manufacture of the grain either by direct casting in the case around the mandrel or by machining the port after casting and curing have been completed.

- Axisymmetric configurations

. AXIL Axisymmetric grain with annular slots. The slots are circular : their axis is the same as the grain axis. They are located all along the central port (Figure 2).

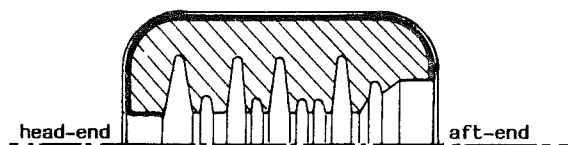


Figure 2 : AXIL configuration

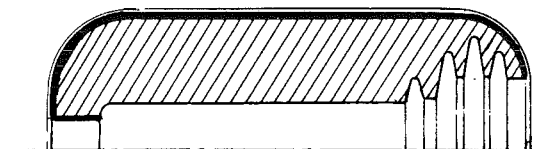


Figure 3 : AXAR configuration

. AXAR Axisymmetric grain with annular slots. This configuration is similar to AXIL, except that the slots are located near the aft-end of the central port (Figure 3).

. CONO CYL (Contraction of cone and cylinder). Axisymmetric grain with annular slots. The tips of the annular slots are inclined towards grain head-end so that a part of the grain is cone-shaped (Figure 4).

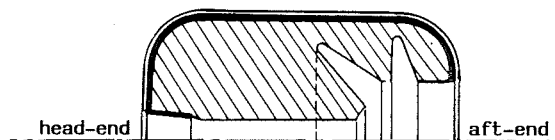


Figure 4 : CONO CYL configuration

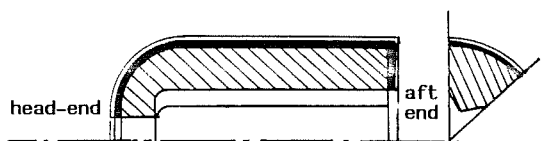


Figure 5 : Star configuration

- Cylindrical configurations

. STAR The cross section of the central port has the shape of a n points star. The contour of the star is constant along the axis (In some cases it may be slightly evolving for manufacture practicality) (Figure 5).

. WAGON WHEEL The cross section of the central port looks like a wagon wheel (Figure 6). Numerous parent configurations exist like dendrite, anchor and dogbone configurations.

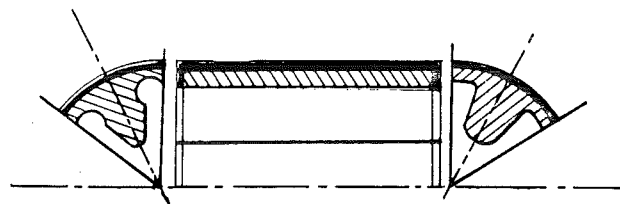


Figure 6 : Wagon wheel

Other configurations may be obtained by combination of some of the above described configurations. For instance bipropellant star configuration (to eliminate sliver), or AXAR configuration having a stress-relieving annular slot in the head-end area. Full head-end web grains are also used. Simpler configurations such as internal-burning tube are commonly used ; the ends are usually unrestricted to function as a burning-surface control ; they may also be partially restricted.

Three-dimensional geometries

Above described configurations are considered as one or two-dimensional, though of course being actually three-dimensional. They are either axisymmetric or cylindrical, with, often, an order n symmetry. It is therefore not too difficult to calculate burning area versus web burned or stress-strain field. Today, three-dimensional configurations are getting more and more popular among the designers community ; they are also much more difficult to design. Most of these configurations are referred to as "finocyl", which is a contraction of fin and cylinder. The fins may be located either at head-end or at aft-end of the grain (and sometimes at both ends) ; they merge into a central cylindrical port. They may have the shape of slots, which simplifies the geometry (Figure 7).



Figure 7 : FINOCYL configuration
(slots and tube)

Often, for stress relieving, there are annular slots. These configurations require three-dimensional analysis for calculating burning area versus web burned as well as stress-strain field or gas flow inside the central port.

- End-burning grains

End-burning configuration is not well adapted to case-bonded architecture because of problems of structural integrity. However it is possible to manufacture such case-bonded grains using stress-relieving grain support and retention systems which allow thermal shrinkage due to propellant cooling after curing though permitting pressure to equilibrate during firing.

212. Configurations of free standing grains

Free standing grains are generally smaller than case-bonded grains. Because they are not bonded to the case wall, except sometimes locally, they allow configurations which cannot be obtained with case-bonded grains (for instance internal-external burning tube).

Final checking of the grains is easier than in the case of case-bonded grains. They are loaded into the motor case during final assembly of the rocket motor. Various support systems may be used to ensure proper operation during firing. During missile service life, it is often possible, if necessary, to replace the grain independently of other motor components.

- Cylindrical configurations

Star, wagon wheel, tube configurations similar to those above described may be found for free standing grains. Grain ends are generally simpler : they are plane and may be restricted or not.

- Configurations with evolving port cross section

To reach high volume loading fractions for free standing grains a configuration was developed : the cross section of the central port is right circular in the forward section and becomes progressively star-shaped in the aft section of the grain (Figure 8). In France, this configuration is referred to as "trompette" (trumpet), though it has not much of the shape of a trumpet.

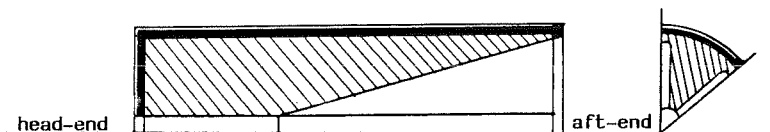


Figure 8 : TRUMPET configuration

- End-burning grains

The orientation of burning is totally in the longitudinal direction. This configuration is wide-spread because gas generation rate is almost constant, volumetric loading fraction is high and grain manufacture is easy. Side and head faces are restricted. Burning times are long and thrust levels are low or moderate. Thermal insulation and inhibitor play an important role respectively to protect the chamber walls from the continuous exposure to hot gas and to restrict the combustion to the desired area. They also generate pyrolysis gaseous products during firing which must be taken into account in the total amount of gas generated by the grain. They are used mainly for the sustaining phase of the flight of some missiles.

213. General principles for selection of grain configuration

A practical procedure for selecting the couple configuration/propellant is discussed at section 4. Hereafter only basic principles are discussed.

For selection of grain configuration, the main factors which are taken into account are :

- volume available for the propellant grain,
- grain length to diameter ratio (L/D),
- grain diameter to web thickness ratio (D/e),
- thrust versus time curve : it gives a good idea of what should be the burning area versus web burned curve (neutral, regressive, progressive, dual-level),
- volumetric loading fraction. It can be estimated from required total impulse and actual specific impulse of available propellants,
- critical loads (thermal cycles, pressure rise at ignition, acceleration, internal flow)
- manufacture practicality, which depends on case geometry (some grain configurations are more or less easy to obtain)
- fabrication cost : it can be the critical factor for selecting a given configuration.

There is no definite procedure to select grain configuration in order to satisfy a set of requirements, because there are often several technical solutions to the propulsion problem.

Practically, there are some general trends in selecting configurations, based on the shape of the burning area versus web burned curve (which is qualitatively close to the thrust versus time curve). Table 1 summarizes these trends.

Burning area neutrality	Grain configuration	Remarks and comments
GOOD NEUTRALITY (LESS THAN 15 % RELATIVE CHANGE IN BURNING AREA)	WAGON WHEEL DENDRITE	Short burning times (≤ 3 s), low volumetric loading fraction
	TRUMPET TUBE AND SLOTS	A constant burning area versus web burned is obtained by progressive cylinder zone and degressive slots or trumpet zone
	AXIL	Case-bonded grain, $L/D \leq 1$ for third stage of strategic missiles
	FINOCYL AXAR CONOCYL	Case-bonded grains, $2 \leq L/D \leq 4$ for first and second stages of strategic missiles
	TUBE (end faces may be restricted)	Volumetric loading fraction less than 0.8
	BI PROPELLANT STAR	Two different propellants. Internal propellant has a higher burning rate than external propellant by a factor of about 2. It is a costly configuration requiring long manufacture cycles (two curing stages). But neutrality is kept, even for high volumetric fraction, and sliver are eliminated.
	END-BURNING	Long burning times, low or moderate thrust
	Remark : the lower the volumetric loading fraction, the better the neutrality. A constant burning area can be accurately obtained by adding axisymmetric slots in the central port or by restricting specific propellants surfaces. It raises grain cost because it requires additional phases during grain manufacture.	
DUAL LEVEL	TRUMPET SLOTTED TUBE AXAR BI PROPELLANT STAR END-BURNING (with annular slots in the aft-end face)	The ratio of the two levels can be adjusted by varying the geometry of the aft-end section Volumetric fraction may reach 0.88. L/D may reach 10 Adjusted by number and geometry of the annular slots Adjusted by the geometry of the stars and propellant burning rates Adjusted by the geometry of the annular slot(s) (boost with radial burning, sustain with end-burning)
PROGRESSIVE	TUBE (right circular port section) STAR	The most common is the grain with restricted faces With restricted end faces ; slivers induce long tail-off
REGRESSIVE	TUBE WITH INTERNAL EXTERNAL BURNING STAR WITH INTERNAL- EXTERNAL BURNING END-BURNING WITH TAPERED AFT-END	Unrestricted end faces and low to moderate L/D ratio Long burning time, low to moderate thrust

Table 1 : burning area neutrality versus grain configuration

CONFIGURATION	VOLUMETRIC LOADING FRACTION	WEB THICKNESS	BURNING AREA	BURNING AREA NEUTRALITY	SLIVER FRACTION	WEB FRACTION	COMMENTS
STAR	0.75-0.90	intermediate	intermediate	good	5-10 %	3.5-5.5	Case-bonded and free standing grains
TRUMPET	0.88-0.95	large	intermediate	excellent	0 %	> 2	Free standing grains
SLOTTED TUBE	0.75-0.85	large	large	good	0 %	≈ 3	Case-bonded grains
WAGON WHEEL	0.5-0.7	small	very large	excellent	5-10 %	6-12	Free standing and case-bonded grains
FINOCYL	0.85-0.95	large	large	good to excellent	0 %	2-3	Mainly case-bonded grains high L/D
AXIL	0.88-0.93	intermediate	large	excellent	5 %	3	Case-bonded grains L/D ≈ 1
AXAR	0.88-0.95	large	large	good to excellent	0 %	2-3	Case-bonded grains high L/D
STAR (with full head-end web)	0.75-0.85	intermediate	intermediate	good	5-10 %	3	Case-bonded grains
BI-PROPELLANT STAR	0.9	large	intermediate	excellent	< 5 %	2.5-3	Case-bonded grains
END-BURNING GRAINS	0.98-1	very large	small	excellent	0 %	1	Low thrust

Table 2 : main characteristics of common grain configurations

Table 2 presents main characteristics of commonly encountered grain configurations. It allows to aid to select a configuration.

22. Propellant selection

There are several solid propellant families which differ from their ingredients, their manufacturing processes and their ability to be processed into certain configurations.

22.1. Propellant families

In France, five families of propellant are commonly manufactured and used :

- solventless extruded double-base propellants (SD), the main ingredients of which are nitrocellulose and nitroglycerine. Configuration is obtained by extrusion through a die having the desired shape. Outer diameter is limited to about 300 mm. Additional grain machining may be performed.
- cast double base propellants (EPICTETE)* ; the ingredients are similar or parents to those of SD propellants ; they are obtained by casting a mixture of nitroglycerine and triacetin into a mold containing nitrocellulose based casting powder.
- composite cast double base propellants, which are derived from Epictete propellants by addition of hexogen, octogen, or ammonium perchlorate and possibly nitroglycerin, in the casting powder (3,4).
- composite propellants based on a non energetic polymeric binder and on ammonium perchlorate, which may also contain aluminum powder.
- high energy propellants based on an energetic binder highly plasticized by a liquid nitric ester, on hexogen or octogen, which may contain ammonium perchlorate and aluminum (3,4).

* trade mark

There is a terminology commonly used in France for the three preceding propellant families. It is based on the following principles :
the name of a propellant is made of a prefix, one consonant, and a suffix.

The prefix gives some information on the binder :

NITRA	energetic binder (usually containing nitric esters)
BUTA	binder based on carboxy or hydroxy terminated polybutadiene
ISO	binder based on polyurethane

Central letter indicates the nature of the main energetic filler

L	ammonium perchlorate
M	octogen (HMX) or hexogen (RDX)
P	potassium perchlorate

Suffix indicates the nature of the metallic fuel

ANE	aluminum
ABE	beryllium
AZE	zirconium
ITE	no metal added.

The three above mentioned propellant families include the following main propellants :

- Nitramite* E : nitrocellulose/nitroglycerine binder filled with RDX ou HMX. E reminds that this family of propellants is obtained through a process very similar to the one used for manufacturing Epictète propellants.
- Isolite* : polyurethane binder and ammonium perchlorate
- Isolane* : polyurethane binder, ammonium perchlorate and aluminum
- Butalite* : polybutadiene binder and ammonium perchlorate
- Butalane* : polybutadiene binder, ammonium perchlorate and aluminum
- Nitramite* G : elastomeric binder, plasticized with a mixture of liquid nitric esters, and filled with RDX or HMX and possibly some ammonium perchlorate. Letter G reminds that the manufacturing process is the slurry cast (global) process.
- Nitralane* : elastomeric binder plasticized with a liquid nitric ester, and filled with HMX, ammonium perchlorate and aluminum.

Besides main ingredients, propellants may contain several other ingredients, generally at low contents, used as stabilizers, afterburning suppressants, combustion instabilities suppressants, burning rate modifiers. One of the important task of propellant designers is to find a practical way (fillers particle size, burning rate modifier, ...) to control burning rate, which is a key factor in designing solid propellant grains.

222. Propellant selection

Selection of a propellant for designing a given grain is based on numerous criteria and, here again, there is no strict procedure for selecting a given composition. The type of architecture (case-bonded or free standing), energy and burning rate criteria, structural integrity considerations, smokelessness and safety considerations, may lead towards a given propellant family. Each of the propellant families covers a certain range of properties, and it is necessary that the properties of the selected propellant allow to design and manufacture a grain satisfying all the requirements. Table 3 summarizes some properties of the main propellant families. The information presented is very succinct and would need more thorough development. However, it allows, in combination with tables 1 and 2, a first approach in the selection of the couple configuration/propellant which is detailed at section 43.

* trade mark

Propellant	Maximum delivered specific impulse in standard conditions (70/1)	Maximum density (kg/dm ³)	Range of burning rates at 7 MPa (or at the plateau) (mm/s)	Pressure exponent	Temperature coefficient	Architecture	Primary secondary smokelessness	Hazard classification * Card Gap test (number of cards)	Sensitivity to electrostatic discharge	Manufacturing cost	Ingredients cost
Extruded Double base SD	225 s	1.65	5 - 40 (plateau)	≈ 0	very low	free standing	primary and secondary	1.3 / 110	no	low	low
Cast double base EPICTHTE	215 s	1.60	4 - 22 (plateau)	≈ 0	very low	free standing	primary and secondary	1.3 / 100	no	high	low
Cast composite modified double base NITRAMITE E	230 s	1.70	3 - 28 (plateau)	0-0.2	low	free standing and case-bonded	primary and secondary	1.3 / 150	no	high	moderate (RDX)
Non aluminized composite polybutadiene propellant BUTALITE	240 s	1.73	4 - 60	0.3-0.5	low to moderate	free standing and case-bonded	primary	1.3 / 0	no	moderate	low
Aluminized composite polybutadiene propellant BUTALANE	245 s	1.86	5.5 - 80	0.2-0.5	low to moderate	free standing and case-bonded	smoky	1.3 / 0	often	moderate	low
Non aluminized cross-linked double base NITRAMITE G	245 s (with AP)	1.79	10 - 25	0.45-0.6	moderate	case-bonded	primary (and secondary without AP)	1.3 / 180	no	moderate	moderate (RDX)
	235 s (without AP)	1.75	5 - 10					180			fairly high (HMX)
Aluminized cross-linked double base XLDB or NEPE NITRALANE	254 s	1.86	9 - 25	0.5-0.7	moderate	case-bonded	smoky	1.3 / 180	no	moderate	fairly high (HMX)

* according to French regulations

- Notes : AP : ammonium perchlorate

Card Gap Test is French Gap Test

Table 3 : main characteristics of common propellants

3. REQUIREMENTS ON SOLID PROPELLANT GRAINS

This section addresses technical requirements propellant grains must meet. Requirements are settled as the consequence of an agreement between rocket motor designer and propellant grain designer. They must be clear, complete and consistent, so that the propellant grain designer may precisely define the grain and eventually build the corresponding engineering development program.

Requirements are divided into requirements related to functional specifications, requirements related to operational specifications and interface requirements. They are detailed hereafter.

31. Requirements related to functional specifications

311. Main internal ballistics requirements

Average, minimum and peak values of chamber pressure, thrust, total impulse, burning times, must be specified within the full operating temperature range. Envelopes of thrust versus time or mass flow rate versus time curves may also be specified.

312. Special requirements

Other requirements are necessary to the designer in order to define a satisfactory propellant grain :

- maximum weight of propellant grain
- maximum weight of total inert (thermal insulation, liner and restrictor)
- maximum axial and transverse acceleration undergone by the propellant grain during operation of the rocket motor
- rocket spin rate (for instance for unguided rockets)
- dispersions on pressure, thrust, total impulse, burning time have to be specified. Depending on the corresponding requirements, manufacturing process and control operations may be strongly affected and thus the cost of the grain as well.
- plume characteristics (emission and transmission in the visible, infrared, electromagnetic wavelengths range).

32. Requirements related to operational specifications

Depending on environmental conditions, definition of the propellant grain may be significantly affected. Such conditions must therefore be well defined in order to be correctly taken into account during grain structural design phase.

321. Long term storage

Desired maximum shelf-life, related temperature cycles and storage conditions must be defined. Particular conditions (relative humidity, salty atmospheres ...) which could directly affect propellant grain behavior must be specified.

322. Thermal environmental conditions

The nature and number of thermal cycles undergone by missiles (for instance during operational flights for airborne missiles) must be defined. Generally they are the limiting factors for structural grain design because very low temperatures may be encountered.

323. Acceleration, handling and transportation

- Acceleration before and during rocket motor operation :
longitudinal acceleration undergone by the rocket motor must be specified, as well as radial acceleration due to rocket spin.

- Handling and transportation : dynamic loadings such as shocks and vibrations encountered during handling (drops) and transportation must also be specified.

324. Reliability

A level of reliability is more and more commonly required. It is essential to define in which conditions it has to be satisfied. The principle of a method of reliability assessment is discussed at section 5.

325. Maintainability

The content and the planning of missiles surveillance, inspection, and maintenance must be defined, as far as they may have an effect on rocket motor environmental conditions.

326. Safety and vulnerability

These requirements are related to safety and survivability of persons and materials. They are not yet often taken directly into account during grain design analysis. They may induce an a priori selection of a type of propellant (e.g. a non detonable propellant or a propellant having a large critical detonation diameter) or, during engineering development, the performance of safety and vulnerability tests.

33. Interface specifications

Close environment plays an important role on grain behavior during its life and operation. It is often prescribed by the rocket motor designer. The grain designer must take special care that its definition is complete.

331. Case geometry and properties

A blue print of the case, or at least, its geometry (length, diameter, configuration of head- and aft-ends) are mandatory in order to perform grain preliminary design analysis. Physical and mechanical characteristics of the case have a direct effect on structural and ballistic design :

- type of case (metal, filament winding/resin, ...)
- thermal expansion coefficient,
- hoop and longitudinal strains as function of internal pressure,
- maximum allowable peak pressure (depending on ultimate elastic elongation of case material),
- maximum temperature allowable at case wall at the end of motor firing.

332. Thermal insulations

Nature and geometry of thermal insulations (specially for case-bonded grains) must be known in order to settle grain definition, either on a ballistic point of view (case wall surfaces subjected to high temperature combustion products), or on a structural point of view (configuration of stress relieving flaps and boots). Thermal diffusivity, specific heat capacity and mechanical properties data must also be available.

333. Support system

In the case of free standing grains, the support elements ensure that combustion gas may flow between the grain and the case wall during pressurization due to ignition. The support system must be well determined so that prediction of grain operation may be possible at any temperature.

334. Nozzle

The characteristics of the nozzle have a dramatic effect on practical ballistic performance of a rocket motor. The following characteristics are of particular interest to the grain designer :

- number and orientation of the nozzles (the angle between nozzle center line and rocket motor center line must be known),
- degree of nozzle submergence,
- erosion of the nozzle (diameter evolution) versus operation time at throat and exit planes,
- angle of the exit cone (or a dimensioned sketch, in the case of a contoured nozzle),
- failure pressure of the frangible closure disk (it allows to define ignition system and to control pressurization at ignition),
- dimensions of the blast pipe (between chamber and nozzle), when existing ; it affects rocket motor efficiency.

335. Ignition system

The conditions of propellant grain ignition depend on its configuration (location, volume, design),

- pressure at the end of ignition,
- pressurization rate (which affects structural integrity during firing).

Minimum and maximum values of delivered pressure and pressurization rate must be accurately known because they are important factors governing grain structural integrity. An envelope of ignition pressure versus time is of interest for this task.

4. BALLISTIC AND STRUCTURAL GRAIN DESIGN METHODS

41. Input

In order to design a propellant grain, two types of data are needed :

- technical specifications ; the preceding section gives an almost complete list of these specifications. They are the reduction of functional, operational and interface requirements that must be satisfied in order that the rocket motor fulfill its assigned mission.

- a data bank on propellants, liners, inhibitors and thermal insulations : it allows the grain designer to have at his disposal, quickly and with a low probability of error, chemical, physical, kinetical, mechanical, thermodynamical, etc... characteristics of the various candidate materials which may be used in a rocket motor. The values of these characteristics will be used as input data in analytical and computational design tools.

42. Procedure

When performing a solid propellant grain design analysis, two levels of design accuracy has to be distinguished :

- First level, it is the level of preliminary design analysis. The tools used at this level must be simple and friendly enough to be operated by propellant grain project managers themselves. They usually are small computer codes based on analytical models, or even graphs which give very simply the first results.

In any case, the method involves four main stages :

- . selection of a couple propellant/configuration,
- . definition of grain geometry satisfying internal ballistic and structural integrity (versus temperature cycles related loads) requirements,
- . approximate assessment of erosive burning and potential combustion instabilities,
- . assessment of grain structural integrity during pressure rise at ignition.

The method is iterative : depending on the results obtained at the third or fourth stage, it allows to start again at second stage or even at first stage if it appears that the first definition needs strong modifications.

For a few years, grain designers have been requested to quickly provide fairly precise preliminary design analysis for a given project. In order to satisfy this request a computer aided grain preliminary design analysis method (M.I.D.A.P*) has been developed in France. This method is discussed in details at section 45.

- Second level, it is the level of grain final design. The tools required for this task are more sophisticated. They are operated by grain design experts. They are mainly finite differences or finite elements computer codes based on two or three-dimensional models of physical phenomena related to internal ballistics, fluid dynamics, continuous media structural analysis, etc.... They allow accurate calculations and therefore optimization of the grain final definition.

* M.I.D.A.P. : Méthode Informatisée de Définition des Avant-Projets

The principle of the method is parent to the one developed for preliminary design analysis, but it starts from the final result of this analysis, that is to say : the geometry and the propellant selected at the end of the preliminary design analysis.

Starting from this geometry, the evolution of grain burning surface area versus web burned is accurately calculated. Taking into account propellant properties, one obtains the evolution of chamber pressure versus time $P(t)$, and thrust versus time $F(t)$. If necessary, the effect of erosive burning has to be taken into consideration at this stage. The results must then be compared with corresponding requirements (maximum pressure, combustion time, total impulse, ...). Afterwards structural safety factor (related to thermal cycles and pressure rise loads) has to be assessed with the aid of advanced structural analysis computer codes.

If the results are satisfactory, design is correct and the propellant grain definition is accepted for starting engineering development. If they are not, grain definition must be modified so as to increase safety factor in grain critical area. Additional structural analysis must be performed in order to check the benefits of geometry modification. Evolution of burning area versus web burned, pressure, and thrust versus time must also be checked so that the ballistic requirements remain satisfied. It may happen that, after these modifications, some of the requirements no longer be satisfied. In this event, selection of the couple propellant/geometry has to be changed, or, if there is no other possibility, modification of some requirements has to be considered, in connection with the rocket motor designer.

43. Ballistic design analysis

431. Basic equations

Basic equation of solid propellant rocket motor internal ballistics are :

$P = \frac{P \cdot S \cdot V_c}{C_D \cdot A_t} \quad (I)$	<p>P chamber pressure</p> <p>ρ propellant mass density</p> <p>S propellant grain burning area</p> <p>V_c propellant burning rate</p> <p>C_D propellant discharge coefficient</p> <p>A_t nozzle throat area</p>
$V_c = f(P), \text{ often } aP^n \quad (II)$	<p>a burning rate coefficient</p> <p>n burning rate pressure exponent</p>
$F = P \cdot C_F \cdot A_t \quad (III)$	<p>F motor thrust (specific impulse multiplied by propellant weight flow rate)</p> <p>C_F nozzle thrust coefficient.</p>

A quick examination of the basic solid propulsion equations indicates the effects of various parameters on motor operation and therefore on motor and propellant grain design :

- . evolution of burning area versus web burned is directly connected to pressure evolution versus time,
- . sensitivity of burning rate to factors like propellant initial temperature, rocket motor acceleration, chamber pressure, gas flow, will have an effect on motor operation,
- . ρ and C_D which are specific of a propellant may be considered for propellant selection,
- . initial values, and possible evolutions during firing, of A_t and C_F , which are directly related to nozzle definition (and also, regarding C_F , to propellant nature), must be accurately known.

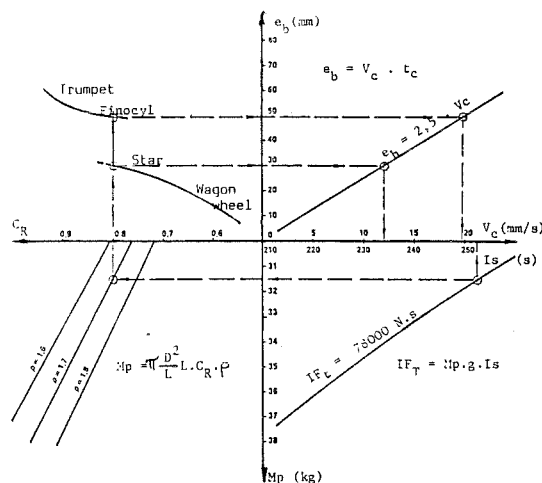
In the following sections, the series of stages encountered in ballistic design analysis is described.

432. Selection of a geometry associated with a propellant

This important part of design work has been approached at section 2 but only through a semi-quantitative analysis. In the present section, it is quantitatively treated using a simple method which yet preserves designer's judgment.

Selection is performed with the aid of charts and graphs like the one presented at figure 9. The example of this figure illustrates the logical method used, which permanently takes into account technical requirements, properties of actual propellants and characteristics of wide-spread actual grain configurations.

Figure 9 : Graph
for aiding in initial
selection of couple
propellant/geometry



The steps are :

- calculation of propellant mass (M_p), given total impulse (I_{ft}) and standard delivered specific impulse (I_{sms}) (for an expansion ratio of 70/1 and an optimum expansion ratio nozzle) measured for the propellant likely to be selected. This first calculation is iterative, for, the value of I_{sms} has to be corrected so as to be representative of the average conditions of motor operation :

- . average chamber pressure (P_c) estimated from the specified maximum pressure
- . nozzle expansion ratio \mathcal{E} depending on maximum allowable nozzle exit cone diameter

$$\mathcal{E} = \frac{A_s}{A_t} \quad A_s \text{ is limited by the specification on maximum diameter of nozzle exit cone}$$

$$A_t \text{ equals } \frac{M_p}{P \cdot C_D \cdot t_c}, \text{ where } t_c \text{ is specified}$$

- assessment of volumetric loading fraction (C_R) required to obtain specified total impulse, given the mass density of the propellant likely to be selected and the volume available for the propellant grain.

- selection of grain configurations. For each family of grain configuration, an empirical maximum volumetric loading fraction has been determined. Thus, given the volumetric fraction required, one or several configurations can be selected. Other criteria, like processing practicality, difficulty of structural analysis, propellant web thickness, have also to be taken into consideration.

- definition of propellant burning rate V_c : $V_c = \frac{e_b}{t_c}$

- verification of consistency between specific impulse, density, and burning rate (at the average chamber pressure).

This approach must be completed by an accurate calculation of nozzle throat diameter generating a maximum pressure lower than that required by the specifications. This step requires a precise definition of grain geometry in order to calculate burning area evolution which is needed for the determination of A_t :

$$A_t = \frac{\rho \cdot S \cdot V_c}{C_D \cdot P_{\max}}$$

On figure 9, the various steps of the method can be represented by the path from A to B, then to C and D, or to C' and D'.

433. Calculation of propellant grain burning area

Accurate prediction of chamber pressure evolution versus time depends on accurate calculation of propellant burning area versus web burned. Computational tools which are commonly used belong to two families : one for "two-dimensional" configurations, the other for three-dimensional configurations. Actual grain configurations are three-dimensional, but in numerous cases their geometry is defined by only two coordinates (r, θ) or (r, z) ; in that case, configurations are said to be two-dimensional.

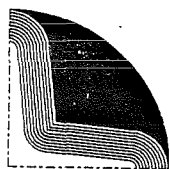


Figure 10 : GEOTOIL code

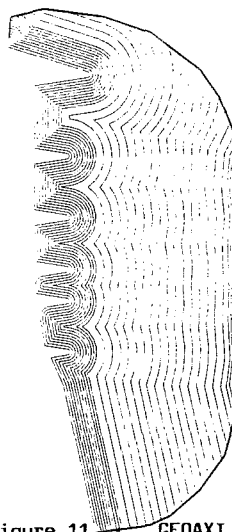


Figure 11 : GEOAXI code

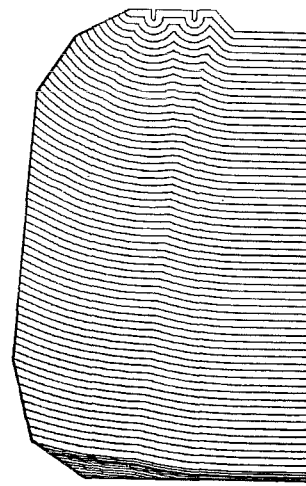


Figure 12 : GEOFAR code

Burning area evolutions

- two-dimensional geometries burning area computer codes

These codes predict the evolution of burning area of propellant grain of following configurations :

- . cylindrical grains (constant port area section), for instance starshaped grains, (GEOTOIL code, figure 10).
- . axisymmetric grains (grains presenting a symmetry of revolution with respect to motor center line for instance Axil, Axar, Conocyl configurations (GEOAXI code, figure 11).
- . end-burning grains having one (or several) axisymmetric slots in the aft-end face (GEOFAR code, figure 12).

- a three-dimensional geometries burning area computer code

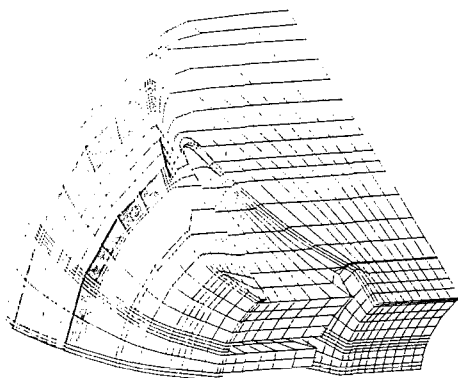


Figure 13 : volumetric grid of aft zone of a finocyl grain (symmetry number = 6) for the calculation of burning evolution.

Generation of the grid can only be performed by skilled experts who know where a denser grid is required for better accuracy. Results are given as data listings. Visualization of the results is possible by processing data. Figure 14 shows three stages of burning area evolution of the grain partially represented on figure 13. Complete performance of such a calculation requires about eight manhours (mainly devoted to grid generation and data input). Actual central processor unit computing time on a VAX 11/750 computer is about ten minutes.

The code, named FRONT, allows the calculation of burning area of finocyl grains having possibly axisymmetric slots. These grains generally present an order n symmetry about the motor axis. Burning area versus web burned is therefore calculated only in a $2\pi/n$ angle sector. Performing a calculation requires grid generation in the grain initial volume. A balance must be found on the number of elements between accuracy and computer C.P.U. time. Performing the calculation on a $2\pi/n$ sector reduces computing time for equal accuracy. The initial volume grid of the aft-end (only zone to be three-dimensional) of a finocyl-shaped grain presenting an order n symmetry is displayed on figure 13.

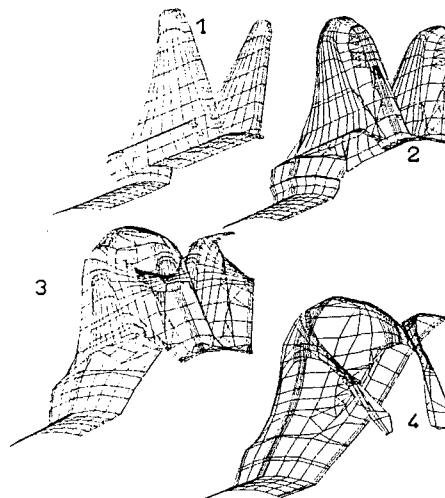


Figure 14 : several stages of a finocyl grain burning area evolution

- a simplified code for slots and tube configurations

Grain presenting the configuration of slotted tubes are three-dimensional, but a more thorough analysis of burning area evolution shows that three zones may be distinguished (see figure 15) :

- . zones A and C are two-dimensional.
- . zone B is three-dimensional.

Surface area of zone B is less than 10 % of total surface area. A parametric study previously performed on that kind of configurations has given results which allow to approximate fairly well the evolution of zone B burning area. Associated with algorithms of GEOAXI (zone A) and GEOTOIL (zone C), these results have led to the code GEOFIN which is accurate enough for preliminary design of that type of grains.

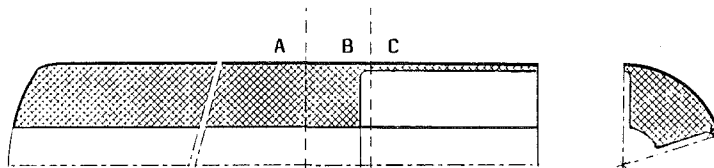


Figure 15 : Partition of a slotted tube into three zones for a simplified calculation of burning area evolution

434. Propellants burning rates

Burning rate is one of the major propellant characteristics. It is measured on standard ballistic evaluation motors and it is stored in the data bank mentioned earlier (section 41). It is sensitive to several factors :

- pressure. In the pressure range in which rocket motors operate, a de Saint Robert's burning rate law ($V = ap^n$) is generally preferred. It is also possible to directly use plots of actually measured burning rates versus pressure. The lower the pressure exponent, the more stable the rocket motor internal ballistics.

- temperature. Environmental and use conditions of rocket motors may correspond to a wide temperature range. It is therefore necessary to know burning rate sensitivity to initial propellant temperature. It is generally expressed at a given burning surface to throat area ratio, K , as a coefficient π_K defined by :

$$\pi_K = \frac{1}{V_c} \left(\frac{\partial V_c}{\partial \theta} \right)_K$$

where θ is propellant temperature.

- acceleration. Propellant burning rate is sensitive to acceleration, but it is taken into account only when it is more than 10 g.

- manufacturing process. "Hump" effect is the result of change in burning rate as a function of web burned (enhancement of burning rate in radially burning grains in the zone between central port and motor case walls). It is related to manufacturing process. Empirical correlations, drawn from experience, are generally applied to take account of this phenomenon in ballistic design.

- internal flow. Combustion products interact with propellant combustion phenomena and may locally change burning rate law which is no longer the one expected. Because of the significant effect of this phenomenon, it is discussed in more details in the following section.

Burning rate laws, evolution of burning surface versus web burned, and basic internal ballistics equations provide pressure versus time and thrust versus time evolutions. In the simple case where internal flow do not significantly interact with burning rate, equations (I) and (II) of section 431, combined with $V_c = de/dt$, lead to a differential equation which is numerically solved and which provides web burned versus time $e(t)$, burning area versus time $S(t)$, pressure versus time $P(t)$ and thrust versus time $F(t)$.

435. Effect of internal flows

It is often assumed that flow velocity in central port exit plane is low enough so that it can be neglected in internal ballistics analysis. It is then assumed that flow is accelerated only in the convergence zone of the nozzle so that it reaches sound velocity at nozzle throat. In fact this assumption is not satisfactory because flow calculations demonstrate that velocities of the order of 100 to 150 m/s are observed in port exit plane after complete ignition and pressurization. Depending on grain configuration and on propellant properties, two types of phenomenon may be generated :

- a pressure drop between forward and aft-end of the central port
- a local increase of propellant burning rate due to erosive burning.

Criteria for occurrence of non desired phenomena

When performing a ballistic design analysis, one has to quickly assess the magnitude of the phenomena connected with internal flow. Table 4 summarizes the knowledge empirically acquired in this field as the result of numerous solid propellant grain design analysis. This table involves a factor J, which is defined as :

$$J = \frac{K_p}{K}$$

- . $K_p : S'/A_c$
- . $K : S/A_t$
- . A_c : area of a given cross section of central port
- . S' : propellant burning area up-stream the above cross section
- . S : propellant grain burning area
- . A_t : nozzle throat area

J	Nature and intensity of phenomena due to internal flow
< 0,2	no abnormal effect
~ 0,25	<ul style="list-style-type: none"> . pressure drop in the central port must be estimated in order to accurately calculate maximum pressure . no erosive burning
~ 0,33	<ul style="list-style-type: none"> . pressure drop must be taken into account . erosive burning occurs for low burning rate (< 10 mm/s at 7 MPa) propellants, or at a very high operating pressure
~ 0,5	<ul style="list-style-type: none"> . pressure drop is high and may induce propellant grain failure . erosive burning occurs for all types of propellant
> 0,6	<ul style="list-style-type: none"> . propellant grains do not function, except nozzleless grains

Table 4 : Effect of factor J on nature and intensity of phenomena due to internal flow inside a propellant grain

Pressure drop

Pressure drop is related to a decrease of pressure from grain head-end to grain aft-end. It induces an increase of head-end pressure at the first phase of motor firing, and therefore maximum pressure generally increases. Pressure drops are generally due :

- to energy losses inside the flow and to phenomena occurring at the interface of flow and propellant surface or to sharp changes of port section or of flow direction,
- to side injections from burning propellant walls.

One of the critical steps in rocket motor operation therefore occurs just after ignition when port sections (through which combustion gas must flow) are minimum. Average pressure drops values encountered are of the order of 0.1 MPa between head and aft-end. In some cases, for special configurations, pressure drops of more than 1 MPa have been observed.

A gaseous flow is fully characterized by the knowledge of local velocities and pressures. Computer codes have been developed in order to know such characteristics. They are named PROCNE 2 and PROCNE 3 (depending whether geometry is respectively two or three-dimensional). They allow :

- to describe unsteady phases during pressure rise at ignition,
 - to know steady flow just after ignition, in the whole cavity and in nozzle convergence section.
- In order to use these codes, one has to generate a grid of the combustion chamber. Order n symmetry (when existing) is taken into account so as to reduce the analysis to a sector of $2\pi/n$ (n = symmetry number). Figure 16 presents an exemple of grid created inside the cavity of a finocyl propellant grain having a symmetry number of sixteen. Results may be, presented either as gas velocity or pressure contours lines in various cavity sections figures 17, 18) or as curves representing for instance gas velocity as a function of radial distance to central axis (figure 19) in central port cross section.

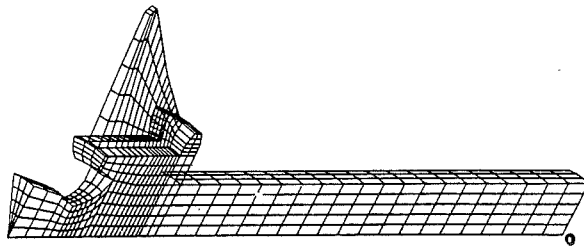


Figure 16 : Three-dimensional flow inside rocket motors; grid of central cavity

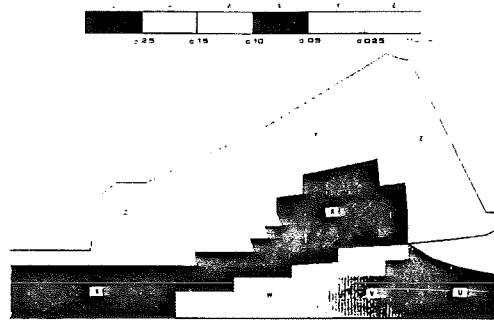


Figure 17 : Flow inside rocket motors : velocity field

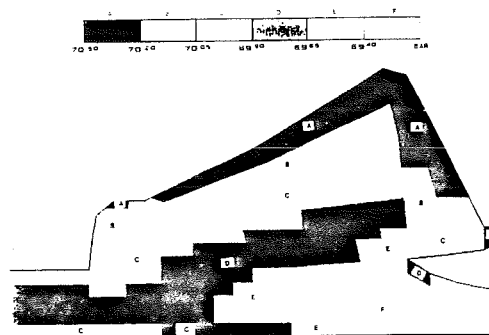


Figure 18 : Flow inside rocket motors : pressure field

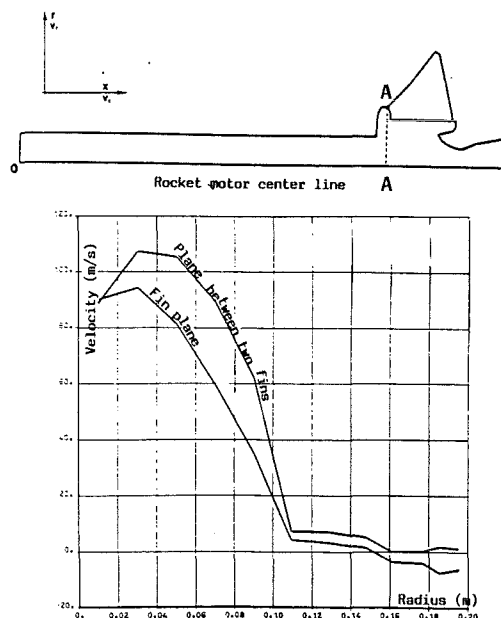


Figure 19 : radial distribution of flow velocities in plane AA inside grain central cavity

$$V_e = V_0 \left[1 + \alpha (G - G_0) \right]$$

- V_e is burning rate with erosive burning
 V_0 is burning rate without erosive burning
 G is mass flow rate unit in the given port cross section
 G_0 is mass flow rate unit threshold (beyond which erosive burning occurs).

COMBEROS code is used systematically in preliminary ballistic design analysis. It implies that grain geometry be described by the cross section contour perimeter evolution along grain axis. Erosive burning is calculated in several cross sections of the central port according to local flow characteristics (static pressure P and local mass flow rate G) and to above erosive burning law. Ignition phase is simulated as an unsteady phenomenon; time steps range from 1 to 5 ms. A complete motor firing may be simulated, using a steady state model and time steps generally ranging from 0.05 to 0.1 s (figure 20). A more comprehensive investigation of erosive burning in propellant grains, though keeping a one dimensional geometry assumption, may be performed with the aid of PROCNE 1 computer code (8).

436. Combustion instabilities

Grain design must incorporate an assessment of combustion stability during motor firing. The phenomenon of combustion instability may occur when perturbations excite oscillation modes of the chamber cavity. Interaction with combustion, flow, particles, nozzle, etc, may induce either an increase or a decrease of the phenomenon. When it increases, pressure vibrations and pressure increase may consequently be driven to an unacceptable level. In order to assess combustion stability, a two steps procedure is followed (9).

Pressure inside combustion chamber cavity is assumed to be :

$$\frac{P'}{P_0} = \sum_{i=1}^n e^{\alpha_i t} e^{j \omega_i t} \psi_i(M)$$

- P_0 : average chamber pressure
 P' : instantaneous pressure at point M
 ω_i : pulsation of mode of rank i and of frequency f_i
 ψ_i : spatial form of mode of rank i
 M : point in grain cavity
 α_i : damping coefficient (when $\alpha_i < 0$), or gain factor (when $\alpha_i > 0$) of the mode of rank i

First step of the analysis consists in calculating the various acoustical modes which are specific of the grain cavity. A finite element two-dimensional computer code, named VASAX, is used. Example of two dimensional grid and corresponding results are presented respectively on figures 21 and 22 (the rank of the mode is 3).

Erosive burning

Enhancement of propellant burning rate due to tangential gas flow (compared to propellant burning rate without tangential flow) is known as erosive burning. It occurs when propellant burning surface is subjected to a high velocity combustion gas flow parallel to it. The phenomenon is due to an increase of heat transfer from the flame zone to the propellant surface. There are numerous physical models to explain and to quantify this phenomenon (6,7). Practically, a simple computer code (COMBEROS), based on a monodimensional flow model, allows to calculate head-end and aft-end pressure evolution in a grain experiencing erosive burning. Erosive burning rate law selected for the model is :

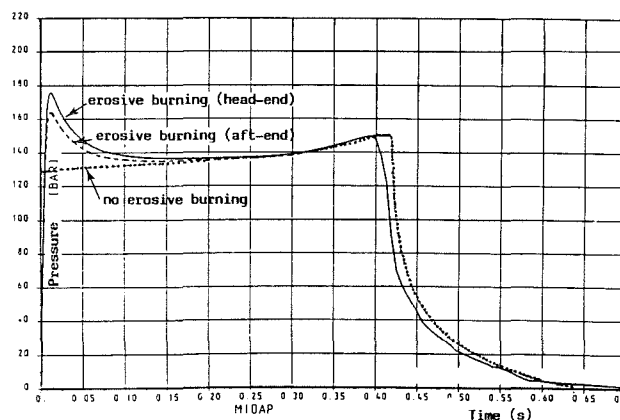


Figure 20 : pressure versus time with, or without, erosive burning

Figure 21 : Combustion instabilities :
grid of a motor cavity for calculation
of acoustical modes

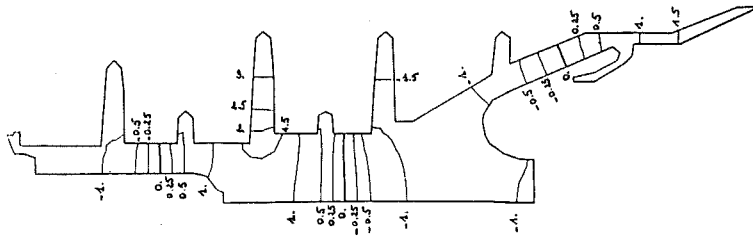
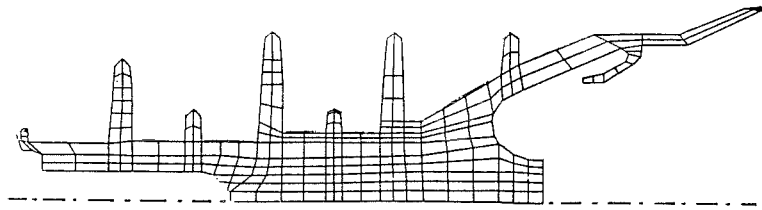


Figure 22 : Combustion instabilities :
pressure contour lines

Second step of the analysis consists in calculating the values of α . These calculations need not only the results of the first step but also data describing propellant response to pressure, effect of condensed particles, etc... . Computer code AVER is used.

Depending on the value of α (equal to the algebraic sum of the various gain and damping factors), it is possible to conclude on the grain propensity to experience combustion instabilities : for a mode of frequency f_i , a value of α_i larger than 0.1 f_i indicates that there is a significant probability that combustion instability may occur. Grain configuration (or propellant) has to be modified.

44. Structural design analysis

441. Principles of structural design analysis

Various loads are imposed to propellant grains all along their lifetime, from their manufacture until motor firing. These loads depend not only on rocket motor own characteristics but also on manufacturing conditions (temperature), environmental and operation conditions. Various factors affect loads imposed to a grain (specially a case-bonded grain) :

- curing temperature,
- acceleration of gravity,
- type and number of thermal cycles undergone during storage and transportation (for instance captive flights for airborne missiles),
- acceleration during boost phase,
- pressurization during grain ignition.

The goal of structural design analysis is to calculate a safety factor defined as :

$$K = C/S$$

where C is propellant (or bond) structural capability (allowable), and S is a functional related to stress/strain induced in the propellant grain region undergoing the more severe loads (margin of safety may be defined as $C - S$ or $C/S - 1$). In order to compare them, C and S must be of the same physical nature.

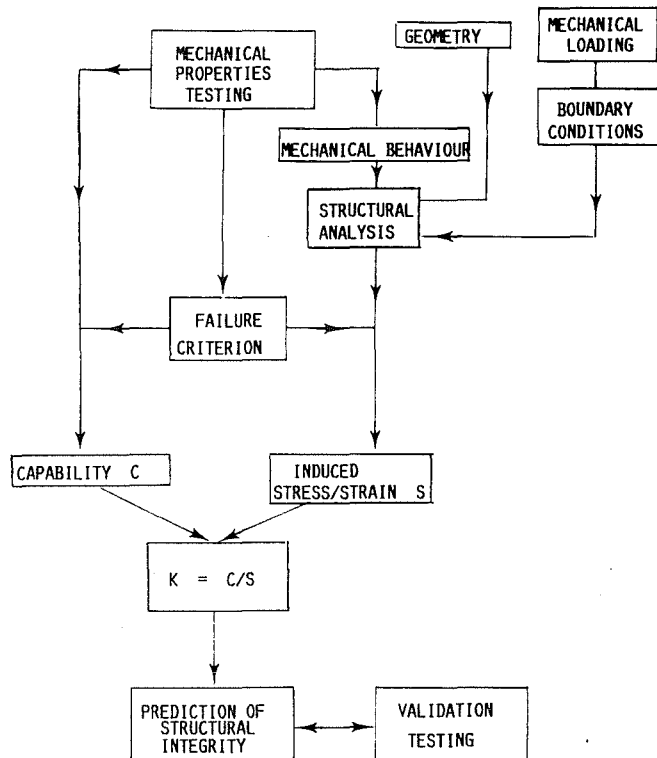
Safety factor must be and stay, until the end of motor firing, higher than 1 during rocket motor lifetime. According to this definition, it is assumed that grain cracking or propellant/liner debonding induce significant modifications of rocket motor internal ballistics having consequences ranging from failure of missile mission to rocket motor explosion. It is assumed that failure at the most stressed (strained) point does not depend on stress (strain) gradient in the surrounding region.

If the safety factor calculated for a given propellant grain and given imposed loads is lower than a required value, grain has to be redesigned until a satisfactory safety factor is obtained.

Assessment of capability variations (due to manufacturing process, to material reproducibility, to mechanical testing, to aging ...) and of induced stress/strain variations (due to uncertainties on boundary conditions, on imposed loads, on stress/strain determination methods) allows as a result of a probabilistic analysis to estimate reliability of a series of propellant grains of a given definition. This subject is discussed at section 5.

The procedure followed in order to predict safety factors comprises two major aspects : it must define how to assess propellant and propellant-liner bond structural capabilities on one hand, and how to determine induced stress/strain in various loading conditions encountered by the grain, on the other hand (Figure 23).

Propellant and propellant-liner bond capabilities are determined by performing various mechanical tests and require a failure criterion which is defined as the critical value (at failure) of a functional related to the state of stress (or strain) of propellant or bond.



Determination of induced stress/strain involves a structural analysis requiring input data such as geometry, boundary conditions (e.g. case displacement), propellant and bond mechanical behavior.

Results are expressed using the same functional selected for failure criterion so that they may be directly compared to propellant and bond capabilities. Experimental validation of the procedure has to be performed, either on the propellant grain itself or on subscale analogs, whenever new elements, such as uncommon grain configurations, new propellants, new bonding systems, have to be considered in safety factor assessment.

Figure 23 : procedure for predicting grain structural integrity

442. Assessment of structural capabilities and of mechanical behavior

Propellant or propellant-liner bond capability is maximum mechanical loading which can be imposed to the propellant or to the bond until failure occurs. Capability is determined by performing tensile testing on various specimens. Effect of main parameters is thus obtained (10) :

- loading rate (which are very different when thermal cooling or pressurization at ignition have to be simulated),
- temperature,
- surrounding pressure (when simulating ignition pressurization).

Evolution of tensile properties (tangential modulus E , propellant maximum stress σ_m and corresponding strain ϵ_m , bond normal stress σ_n and shear stress τ) versus loading rate and temperature provide corresponding master curves. These curves can be obtained because the materials behavior is such that the principle of time-temperature equivalence may apply ; they involve shift factors of W.L.F theory (11).

Figure 24 summarizes the various steps of the experimental work which has to be performed in order to eventually provide master curves for a given propellant and bond : evolution of E , σ_m , ϵ_m , σ_n , τ versus reduced time t/a_T (t is the reciprocal of loading rate - or specimen loading time, a is the shift factor related to the test temperature T).

When mechanical behavior, for a given loading rate and a given temperature, has to be determined, reduced time t/a_T is calculated which, using master curves, simply provides the requested data.

The effect of pressure on propellant capability has to be known in high loading rate conditions (which correspond to ignition times in propellant grains). Pressure main effect is to delay occurrence of vacuum holes (dewetting) and to limit their extension in the propellant around energetic fillers (such as ammonium perchlorate or octogen). Tensile testing at several constant strain rates under several pressures allow to quantify this effect for given propellants. They generally display an improvement of mechanical properties (ranging from + 50 % to + 100 % on maximum stress and corresponding strain, in the case of Butalanes -CTPB or HTPB aluminized propellants) which is taken into account in solid propellant grain structural design when ignition pressurization is the design limiting loading condition.

The whole experimental work performed on this subject has led to the conclusion that propellants behavior is (see for instance 12, 13, 14) :

- viscoelastic (experimental evidence originates from relaxation study),
- non linear (but assumed to be linear for small deformations),
- incompressible (Poisson's ratio ν is very closed to 0.5) until dewetting is significant enough so that volume variation occurs during tensile testing.

The functional which expresses propellant capabilities is discussed at section 444.

DETERMINATION
OF $\log \sigma_r$
VERSUS T

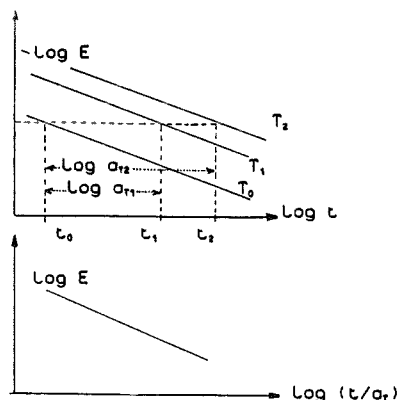


Figure 24 : how to obtain and to use master curves

443. Determination of induced stress/strain field

Determination of induced stress/strain field in the propellant grain requires the knowledge of :

- geometry on which loads are imposed,
- boundary conditions which describe imposed loads,
- propellant and propellant-liner bond behavior.

In most of the cases, geometry is three-dimensional, loads are static, dynamic or thermally induced ; propellant behaviour is viscoelastic, non linear. Loads which are the limiting factors in structural grain design are generally :

- thermally induced, in the case of grains for tactical missiles (low temperature cycling),
- pressurization induced, in the case of grains for large ballistic missiles (stored in almost isothermal conditions).

At the preliminary design phase, expected maximum value of stress/strain induced in the grain is quickly assessed using analytical expressions. For instance, in the case of fairly simple internally perforated grains, following expressions are commonly used :

$$\epsilon = 2 \alpha \cdot \Delta T \cdot K_T \cdot C \cdot (b/a)^2 \quad \text{for a thermally induced strain.}$$

ϵ is equivalent strain at grain innerbore surface,

α is propellant thermal expansion coefficient (assumed to be at least an order of magnitude higher than case material thermal expansion coefficient),

ΔT is difference between cure temperature and temperature at which induced strain has to be estimated (ΔT may be as large as 100 °C),

K_T and C are corrective coefficients taking into account respectively central port exact geometry and end effects,

b and a are respectively grain outer and inner radii

In the case of a pressurization induced strain,

$$\epsilon = k \cdot \epsilon_{0s} \cdot \beta \cdot K_T \cdot C \cdot (b/a)^2$$

ϵ_{0s} is hoop strain of the empty case submitted to ignition maximum pressure,

β takes into account case stiffness increase due to propellant grain,

k is an empirical coefficient.

These values of ϵ are input data for a first assessment of grain safety factor.

Final design phase involves extensive use of computational methods based on finite element techniques applied to grain stress/strain field analysis.

The procedure comprises three stages :

- Determination of induced stress/strain field

The material is assumed to have a linear behavior.

The incompressibility is treated using Hermann's reformulation (15)

The assumption that propellant is incompressible is justified by the fact that, even when severe loads are imposed to the grain, the regions, wherein vacuum holes may occur (because of high propellant elongation) and therefore wherein propellant is no more incompressible, represent only a small percentage of grain total volume. Stress/strain field therefore results from the incompressible behavior of almost all the propellant grain. Any structural analysis which does not take into account Hermann's reformulation and which is based on the assumption that Poisson's ratio is closed to 0.5 (slightly less) may fail, in certain conditions (for instance poor accuracy of computer calculation), to correctly predict stress/strain field and thus may lead to an erroneous value of the safety factor.

Mechanical load, which determines boundary conditions, is expressed either as prescribed displacement or as prescribed strengths at the nodal points of surface elements. Several computer structural analysis codes may be used for this stage of the analysis : PALEST and PROVISC for two-dimensional geometries, CAMILLE for three-dimensional geometries. CAMILLE has the main following characteristics :

- finite element method,
- HERMANN'S reformulation,
- quadratic elements with 20 nodal points,
- quadratic skin pseudo-elements with 8 nodal points, in order to accurately predict stress (or strain) at the surface of the grain where maximum stress (or strain) very often occurs. The use of skin pseudo-elements improves accuracy because it reduces the uncertainties connected with extrapolations which are needed to calculate maximum stress (strain) when there are no skin pseudo-elements.

Prediction accuracy depends also on the grid network generated for representing grain volume. The number of nodal points is limited because of computer power and computer time limitations. A typical grid network may contain 7000 nodes and 1000 elements.

Exemples of grid networks generated for structural analysis of two-dimensional and three-dimensional grain geometries are shown on figures 25 and 26.

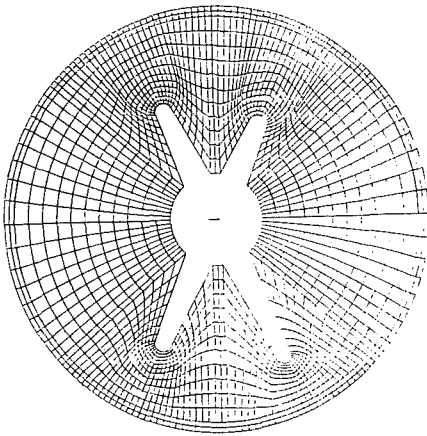


Figure 25 : Exemple of two-dimensional grid network

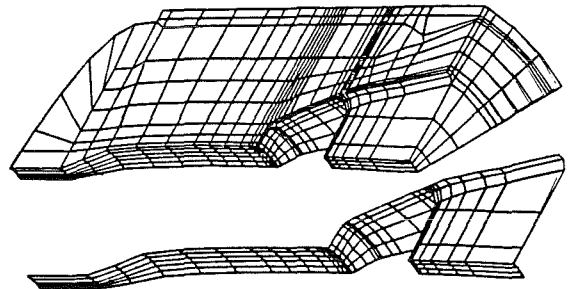


Figure 26 : Exemple of three-dimensional grid network

- Post-processing analysis. Propellant behavior is assumed to be linear and incompressible. Regions of the grain where stresses (strains) are maximum are identified. Figure 27 gives an exemple of equivalent stress contour lines (where equivalent stress has a given value) in a three-dimensional grain. In this exemple, maximum stress occurs at the forward slot-bore junction.

- Determination of stress in the region experiencing the most severe induced loads. Starting from above results, stress calculation is refined in the most loaded region : a viscoelastic non linear behavior is assumed in the case of thermally induced stress (strain) ; an elastic non linear behavior is assumed in the case of ignition pressurization induced stress.

. thermally induced stress. The structural analysis code is V.E.N.L. (16). It provides, at any moment of an imposed thermal cycle, the values of principal stresses in the propellant (σ_1^{th} , σ_2^{th} , σ_3^{th}). The numerical method is incremental with respect to the time. It consists in calculating stresses at a given time t from the values observed at time $t - \Delta t$. For this purpose, effect of thermal cycles are assumed to be successive infinitesimal strains with simultaneous relaxation of the stresses observed at the preceding time. This code is commonly used for grain engineering design analysis and simultaneously improved by comparison with actual grain structural behavior.

TIME = 0.10000E+01
CONTOURS OF EFF. STRESS (V-M)
MIN= 0.152E+00 IN ELEMENT 451
MAX= 0.186E+02 IN ELEMENT 358

CONTOUR VALUES
A = 4.00E+00
B = 7.00E+00
C = 1.00E+01
D = 1.30E+01
E = 1.60E+01

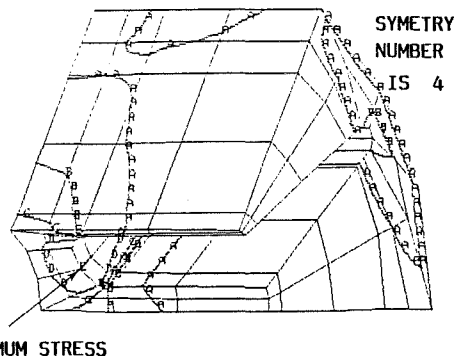


Figure 27 : contour lines of equivalent stress in a finocyl grain

. pressurization induced stress. The corresponding structural analysis codes require propellant master curves and data describing pressurization (pressure rise time, final pressure, temperature). They provide magnitudes of principal stresses (σ_{1p} , σ_{2p} , σ_{3p}) corresponding to maximum pressure.

Often, structural analysis of a propellant grain, which is fired after having experienced thermal cooldown, has to be performed. Corresponding maximum principal stresses results from the addition of thermally induced stresses and pressurization induced stresses as far as principal directions are identical (which is generally the case on grain external surfaces where most stressed areas are often located).

444. Determination of structural safety factor

At the stage of preliminary design analysis, simple analytical formulas provide magnitude of strain either due to thermal loading or due to pressure rise (see section 443). In both cases, propellant capability is obtained from the master maximum strain curves at t/a_T corresponding to the loading conditions. So a first assessment of safety factor is :

$$K = \frac{\mathcal{E} \text{ (due to thermal loading or pressure rise loading)}}{e_m \text{ (at } t/a_T \text{ corresponding to the loading conditions)}}$$

Propellant capability (section 442) is related to uniaxial tensile tests ; it is represented by maximum stress (σ_m) or maximum strain (e_m). Induced stress (strain) (section 443) is the result of a stress (strain) analysis ; it is expressed as principal stresses (σ_1 , σ_2 , σ_3) (strains, \mathcal{E}_1 , \mathcal{E}_2 , \mathcal{E}_3) in the most severely stressed (strained) region of the grain.

In order to be able to directly compare capability and induced stress (strain), failure criteria are needed (17). They are based on an equivalence between principal stresses and an equivalent uniaxial stress defined by :

$$\text{- Von Mises criterion : } \sigma_o = \left[(\sigma_1 - \sigma_2)^2 + (\sigma_2 - \sigma_3)^2 + (\sigma_3 - \sigma_1)^2 \right]^{1/2} / \sqrt{3}$$

or

$$\text{- Stassi criterion : } \sigma_o = \left[(\sigma_1 + \sigma_2 + \sigma_3) + \left[(\sigma_1 + \sigma_2 + \sigma_3)^2 + b \left[(\sigma_1 - \sigma_2)^2 + (\sigma_2 - \sigma_3)^2 + (\sigma_3 - \sigma_1)^2 \right] \right]^{1/2} \right] / c$$

a, b, c are coefficients which generally depend on the propellant, but do not depend on strain rate and temperature. When $\sigma_o = \sigma_m$, the combined STASSI-VON MISES criterion defines a failure surface (of revolution), in principal reduced stress space, which is coaxial to the hydrostatic axis ($\sigma_1 = \sigma_2 = \sigma_3$) (figure 28).

Depending on the magnitude of $\sigma_1, \sigma_2, \sigma_3$, STASSI criterion, or VON MISES criterion is used. STASSI criterion is represented by a paraboloidal surface coaxial to the hydrostatic axis. It is mainly used in the first octant ($\sigma_1 > 0, \sigma_2 > 0, \sigma_3 > 0$) which generally corresponds to thermally induced stresses.

VON MISES criterion is represented by a right cylinder coaxial to the hydrostatic axis (and to the STASSI paraboloid). It is mainly used in the eighth octant ($\sigma_1 < 0, \sigma_2 < 0, \sigma_3 < 0$). This state of stress corresponds to pressurization at propellant grain ignition (for an operating pressure of 7 MPa, pressure induces negative stresses in the propellant, which are much larger than any other stress). The two surfaces define two regions : internal region represents states of stress which do not involve propellant grain failure ; surface and external region represent states of stress involving failure. The parameters defining these surfaces (a, b, c) are obtained experimentally, for each kind of propellant, by performing tensile tests under various pressures and at several temperatures and strain rates.

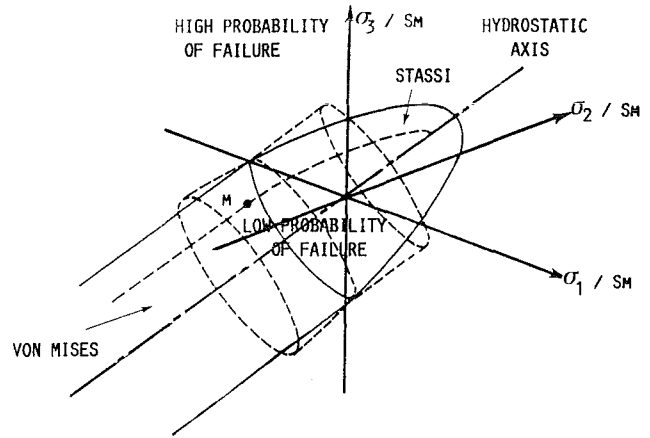


Figure 28 : Failure surfaces based on combined STASSI/VON MISES criterion in principal stress space

Propellant grain safety factor is then defined as the ratio of maximum stress obtained in a uniaxial tensile test (performed at a strain rate and at a temperature identical to those encountered in the grain) to uniaxial maximum stress (obtained either from STASSI criterion or VON MISES criterion, depending on the type of stresses encountered in the most stressed region of the grain) equivalent to the maximum three-dimensional state of stress calculated in the propellant grain :

$$K_{\sigma} = \frac{\sigma_m (t/a_T)}{\sigma_0 \text{ (Stassi or Von Mises)}}$$

Safety factor may also be defined as :

$$K_{\epsilon} = \frac{\epsilon_m (t/a_T)}{\epsilon_0 \text{ (Stassi or Von Mises)}}$$

ϵ_0 is the ratio of uniaxial equivalent stress to modulus, $\epsilon_0 = \frac{\sigma_0}{E}$

In the above described definitions of safety factor, it is assumed that the propellant has not been damaged before experiencing the imposed load. In fact, most of the time, the propellant of a rocket motor is subjected to a series of mechanical loadings (for instance thermal loads due to temperature cycles) which damage it. Several investigations have been performed on this subject, either for general purpose (18), or more specifically on solid propellants (19, 20). The method consists to define damage D as :

$$D = \sum_i t_i / t_{Ri}$$

t_i represents time during which stress i (strain i) is imposed to the propellant, and t_{Ri} represents failure time when stress i (strain i) is imposed.

As defined, and after validation, damage D is equal to 0 when propellant has not yet been subjected to loads ; it is equal to 1 when failure occurs. The method therefore consists to decompose mechanical loads undergone by the propellant during its life into elementary loads and then to compare at every moment elementary load to propellant capability. Use of experimental results from relaxation tests, creep tests, or various tensile tests allow to assess damage law for propellants.

The simplest form of damage law used for propellants (creep failure law is $\sigma_F \cdot t_R^{1/m} = \frac{1}{D_0}$, , σ_F = stress, t_R = time to failure, m = empirical exponent obtained from creep tests) is :

$$D = D_0 \left[\int_0^t \sigma_0^m d \tau / a_T \right]^{1/m}$$

σ_0 is uniaxial equivalent stress based on STASSI-VON MISES failure criterion ; m and D_0 are obtained from experimental tests and a is the temperature shift factor of time/temperature equivalence.

This cumulative damage method may be applied to the grain entire life including final firing. It is yet mainly used for grains subjected to thermal cycles before firing, i.e. grains for tactical missile rocket motors.

Safety factor based on damage is then defined as :

$$K = 1 / D$$

Other definitions and prediction methods of safety factors are available. A comprehensive analysis of most of them was recently performed (21).

In the case of propellant/liner bonds, the problem is different because of the presence at the interface of two different materials (propellant and liner). The states of stress/strain are different on the two sides of the interface. Only the strength applied to the unit interface is continuous. Its components are : a strength σ_n perpendicular to the interface, and a shear strength τ . Safety factor is defined by comparing magnitude of induced interface strength (σ_n , τ) to magnitude of strength at failure observed (at same strain rate and temperature) on a propellant/liner bond specimen.

Most of the time propellant/liner bonds are designed so that failure occur in the propellant near the interface. If, in addition, propellant of this zone has the same properties as bulk propellant, safety factor is then determined as first described, so that :

$$K_{\text{bond}} = \min. \left[K_{\text{strength at bond}}, K_{\text{propellant}} \right]$$

45. Computer aided preliminary design of propellant grains

451. General description

As mentioned at section 42, there is an increasing pressure to have, as early as the preliminary design phase, quick and rather accurate results defining propellant grain. Moreover, further changes in technical requirements have to be easily taken into account. A computer code allowing to satisfy these needs is now on service. It is named MIDAP (22) and it involves, today, around 20,000 statements in its newest version. Figure 29 presents the general architecture of the code. Each type of grain configuration (star-shaped, slotted tube, axisymmetric, finocyl, ..) is individually treated inside the code. The procedure for any of these configurations is the one which is generally followed to perform propellant grain preliminary design analysis (it is described in section 42). The architecture of the code is modular so that any addition of new module or any improvement of an existing module may be very simply worked out

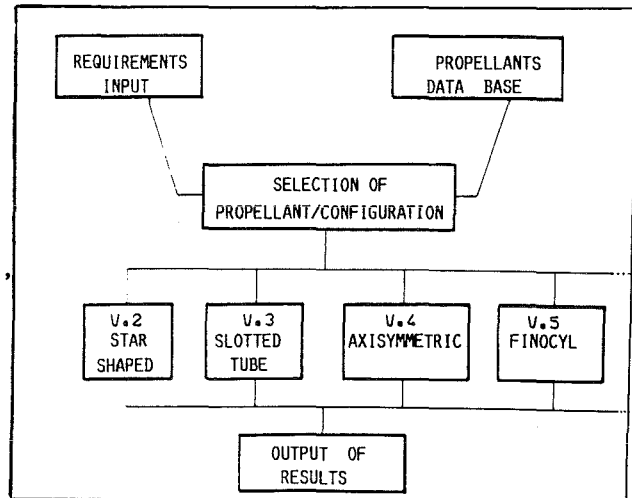


Figure 29 : general structure of preliminary design analysis computer code

Runs are controlled by the user from the graphic terminal. C.P.U. time is negligible as compared to time spent by the user performing the design analysis.

The process is iterative and, besides the input of technical specifications, the user has only to answer yes or no to the option which is proposed on the screen. Results are presented either as tables or as curves. The block diagram presented in figure 30 emphasizes the rôle of propellant/configuration selection, which allows to provide several possibilities, ranked according to a given set of criteria. The selection of propellant/configuration depends :

- on one hand, on technical requirements (total impulse, burning time, etc...),
- on the other hand, on semi quantitative requirements related for instance to manufacturing process practicality, industrial and economical aspects, etc...

Due to the dual nature of the criteria, an expert system was selected and implemented for this critical stage of preliminary design analysis.

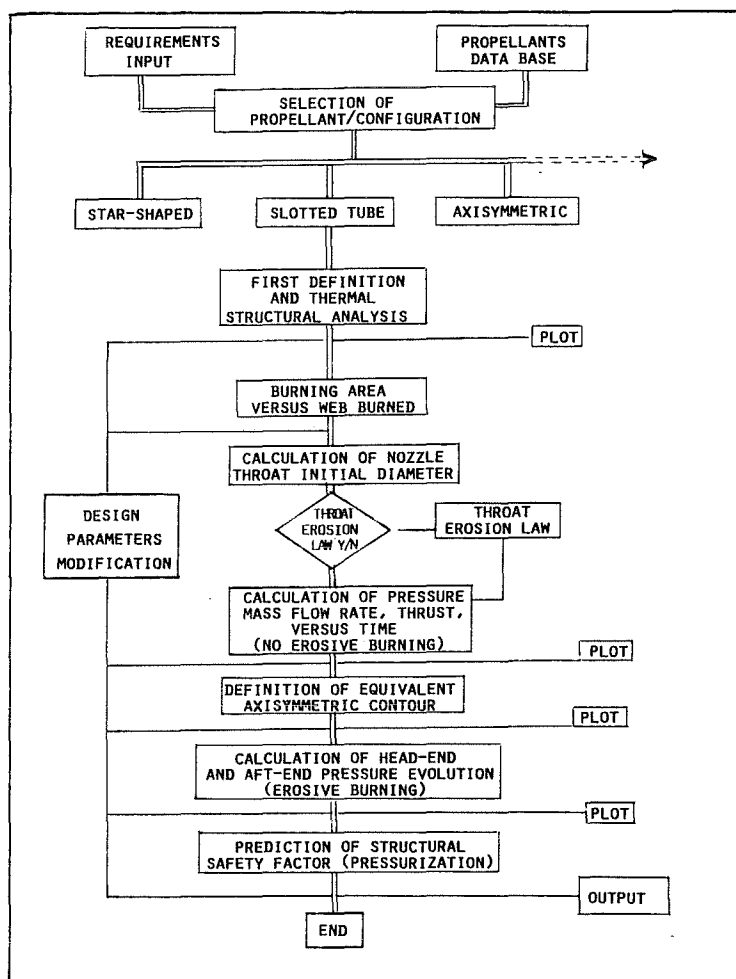


Figure 30 : detailed flow chart of slotted tube propellant grain preliminary computational design

The successive steps of the analysis are :

- First definition of the grain and thermal structural analysis

This definition meets various requirements, the priorities of which are ranked as follows :

- 1) structural integrity (for thermally induced strains) corresponding to a safety factor higher than 2,
- 2) maximum operating pressure,
- 3) total impulse,
- 4) evolution of pressure versus time,
- 5) burning time.

The structural analysis is based on data obtained from regression analysis of stress/strain field determination results, performed with the aid of three-dimensional computer codes (e.g. CAMILLE, section 443) on various selected slotted tube geometries.

- Burning area evolution

This task is performed by dividing the grain into three parts as described at section 433. A simplified version of GEOFIN is used in this preliminary design phase.

452. Description of the code

All the branches of the code have the same basic structure. The slotted tube branch is detailed hereafter.

On flow chart of figure 30, the main stages of the analysis appear.

Two possibilities are provided to the user :

- design of a case-bonded (or free-standing) grain meeting technical requirements,
- for a given rocket motor, calculation of motor operation (pressure versus time, thrust versus time, etc...).

In the case of slotted tube configurations, geometrical characteristics which are taken into account for design analysis are:

- cylindrical motor case, presenting possibly thermal insulation over-thickness in the aft-end zone (slotted zone)
- plane grain aft-end zone (slotted zone)
- cylindrical central port, slot walls may be parallel or not, (star-shaped),
- possibility of a tapered port in grain aft zone (in order to limit erosive burning effects).

. Determination of nozzle throat initial diameter

It is the minimum throat diameter value consistent with the specification on maximum acceptable pressure.

. Determination of pressure, mass flow rate and thrust evolutions versus time

In a first approach, erosive burning is not taken into account. The calculations provide expansion ratio, and thus nozzle optimum expansion ratio and exit diameter. Nozzle exit diameter is then compared to corresponding requirement. Afterwards, ratios K (burning area to nozzle throat area) and J (burning area to central port cross section) are calculated. If needed, a tapered zone is designed in the grain slots region so as to meet a criterion on J (maximum permitted value). Burning area versus time is then calculated again.

. Definition of equivalent axisymmetric longitudinal port contour

It is based on equal flow rates in any port cross section for actual (three-dimensional) and equivalent (two-dimensional axisymmetric) contours. It allows a simplified analysis of erosive burning which is taken into account at the following stage.

. Calculation of head-end and aft-end pressure evolution

At this stage erosive burning is taken into account. The module provides pressure evolution inside grain central port, as well as peak pressure at ignition and pressure rise time.

. Prediction of safety factor related to ignition pressurization

Preliminary structural design analysis is performed, as described at section 433.

5. PROPELLANT GRAIN RELIABILITY

Reliability is probability that a system fulfill a required mission in given conditions and during a given period of time. Reliability must be considered :

- at design phase ; the system must be designed so that its reliability will meet the requirement,
- at realization phase ; it must be demonstrated that reliability requirement has been met.

Reliability of a solid propellant rocket motor results from the reliabilities of constitutive elements, like case, thermal insulation, igniter, nozzle, propellant grain, etc... Grain reliability has several components ; but main components are ballistic and structural reliability. In the case of case-bonded grains, past experience and analysis performed according to F.M.E.C.A (Failure Modes, Effects, and Criticality Analysis) have demonstrated that structural reliability is the most important component of overall grain reliability.

There are two possible approaches in assessing propellant grain reliability : an analytical approach and an experimental approach ; both of them are complementary.

51. Analytical approach

It is performed according to F.M.E.C.A. method (23). It consists in :

- listing the functions the propellant grain must fulfill,
- describing failure modes,
- assessing probability of failure occurrence for each mode,
- validating assessments by comparing with overtests and analogs experimental results.

As mentioned above, this method has emphasized structural component of case-bonded grains reliability. This aspect is therefore discussed hereafter. A comprehensive description of the methods used in propellant grains structural reliability assessment would need extensive discussion because of the complexity of phenomena and analytical tools which are involved. Consequently, the following section provides only an idea of the principles governing structural reliability assessment.

Safety factors are considered at section 4 as having known values : propellant grain failure occurs when $K = C/S = 1$. K is structural safety factor, C is capability and S is induced stress/strain. In fact, most of the parameters involved in safety factor prediction are randomly distributed and their statistical distribution law is not always well known.

These parameters are related to :

- | | | |
|--|---|--|
| <ul style="list-style-type: none"> - grain geometry - boundary conditions - propellant and bond behavior - capability - failure criterion | } | <p>which define induced stress/strain field</p> <p>which may take aging into account</p> |
|--|---|--|

When designing a case-bonded grain, the distribution law of the parameters defining grains and imposed loads has to be known, so that the distribution law of C and S be known. It is then possible to determine minimum safety factor ensuring required reliability. In a second stage, taking into account variations due to manufacture (and possibly to aging), it is possible to define a mean safety factor (higher than the preceding one) that must be the objective at design phase. Grains, designed so as to meet this requirement on K, have the desired reliability at a high confidence level.

For a given propellant grain, variations of capability and induced stresses (strains) are due :

- to errors in test measurements of propellant and bond mechanical properties,
- to the probabilistic nature of loads imposed to the grain before, and during firing,
- to uncertainties related to structural models and to failure criteria determination.

Let \bar{C} and \bar{S} be the mean values respectively of capability and of induced equivalent stress (strain) and CV_C and CV_S corresponding deviation factors (which are assumed to be independant of the mean value), then $K = \bar{C}/\bar{S}$, and it can be demonstrated that probability that grain failure does not occur is :

$$\text{Prob } (C > S) = \varphi \left[\frac{\bar{K} - 1}{(\bar{K}^2 CV_C^2 + CV_S^2)^{1/2}} \right]$$

where φ is the repartition function of normal distribution law ($N(0,1)$). C and S are generally assumed not to be correlated (which is not correct but acceptable). It is possible, however, to take a correlation into account if it is clearly demonstrated.

Minimum safety factor, K_{\min} , ensuring required reliability F is then obtained by determining the value of K_{\min} which satisfies the relationship :

$$\varphi \left[\frac{K_{\min} - 1}{(K_{\min}^2 CV_C^2 + CV_S^2)^{1/2}} \right] = F$$

Taking into account variations due to manufacture, deviation of safety factor is assessed. It is then possible to calculate a value of safety factor which is the objective of structural design analysis : it ensures that grains accordingly designed have a given probability of meeting reliability requirement.

52. Experimental approach

Safety margin is $C-S$. There is a discrepancy between actual margin of safety $(C-S)_R$ and predicted margin of safety $(C-S)_C$, due to the use of an approximate model. It is possible to write :

$(C-S)_R = (C-S)_C + \xi$, where ξ is assumed to obey a normal distribution law. ξ mean value, m_ξ , represents the shift of the model. Deviation σ_ξ represents variations of this shift. m_ξ and σ_ξ must be assessed by performing significant experimental tests. There are two possibilities : either overtests or test on grain analogs.

521. Overtests

The first method consists to assume that ξ obey a given normal distribution law and to use overtests results in order to refine this distribution law : it is the Bayesian method (24). Grain overtests are tests which have a moderate probability (much higher than in a normal motor firing or temperature cycling) that failure does occur. Much information is thus obtained on grain reliability. Overtests are defined by changing thermal cycles applied to the grain (colder temperature, larger cycles number) or firing conditions (reduced nozzle throat diameter) compared to normal conditions.

The most interesting information is obtained when overtests performance does not induce propellant or bond failure : a more accurate definition of ξ distribution law may thus be proposed. Overtests best definition is however always difficult to establish.

522. Tests on grain analogs

A second method to quantify the shift of the model consists in performing loading tests on analogs such as the one represented in figure 31 (25)

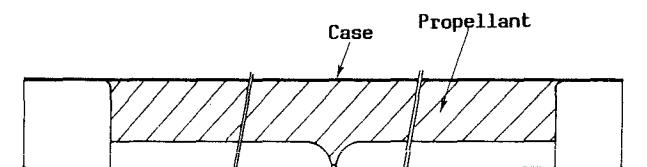


Figure 31 : Analog grain for assessment of propellant grain structural reliability

This analog grain definition has the following characteristics :

- configuration is simple enough so that analogs may be easily manufactured at low cost,
- two-dimensional geometry induces low cost computational structural analysis,
- ratio of maximum stress (strain) to mean stress (strain) induced in the analog is of the same order of magnitude as the one encountered in actual grains,
- maximum induced stress (strain) can be easily adjusted by simply modifying analog manufacture tooling.

The main drawback is that the analog is not ... the grain itself, which involves that propellant, liner and bond are not exactly the same, and are not in the same surrounding conditions, as those constitutive of the actual grain.

Mechanical testing consists in loading a given number of analogs in identical conditions until failure occur. Analysis of failure results and deviations yields the shift ξ between actual margin of safety and predicted margin of safety. It is then assumed that the shift observed on the analogs is equal to the shift existing in actual grains.

These set of complementary theoretical and experimental methods, that must still be improved, allow to assess structural reliability of case-bonded solid propellant grains.

6. CONCLUSIONS

The discussion, outlined in the present paper, on solid propellant grain design methods presently used in France, emphasizes the significant improvements obtained in this area during the last twenty years. Phenomena, which were not well understood, or which could not be considered (because of their complexity) in ballistic and structural description of rocket motor operation, are now taken into account. It is the result, on one hand, of a better understanding of physical phenomena or of material behavior, and, on the other hand, of the recent possibility of modelling these complex phenomena due to the dramatic improvement of both computational methods and computers performances. More specifically, the three-dimensional aspect of phenomena is more and more commonly treated. These improvements were naturally transposed into the more accurate design tools. Besides, preliminary computational design analysis of propellant grain can now be performed, not only by grain design experts, but also directly by project managers. It involves shorter response times and lower probabilities of error.

However the situation is far from being fixed. It is continuously evolving because of two types of factors : needs are still growing, techniques and methods improve. Needs, which appeared during the last twenty years, are growing : more accurate and quicker responses (though maintaining an acceptable cost) to propellant grain design requirements are requested. New needs also appear, or will appear ; they are related to requirements which, until now, are not (or are not well) taken into account during design phase : corresponding physical phenomena are not well understood ; corresponding expression of specifications is difficult or is now considered as being of secondary importance. These are requirements related to safety, vulnerability, plume characteristics, and grain industrial cost.

During the next ten years, it can be anticipated that grain design methods will therefore evolve in two directions. A better account of physical phenomena complexity will be taken in the dimensioning computational tools (three-dimensional aspects, more realistic mechanical behavior of propellant and propellant-liner bond, two phases and turbulence aspects of flow inside grain central cavity, etc...). Research work, now performed on better understanding of phenomena involved in safety, vulnerability and plume characteristics, will affect, on one hand, nature and expression of requirements in these fields and, on the other hand, the advent of methods for dimensioning propellant grains with respect to these new requirements.

Performing the entire set of tasks above described requires a close collaboration of theoreticians and experimenters who must coordinate their energies to consistently and continuously improve grain design methods.

REFERENCES

- (1) Jean BOISSON. La propulsion par fusée
Ecole Nationale Supérieure de Techniques Avancées. tome 1 (1972)
- (2) J. DARDARE, J. MERIGUET, L. VAILHE. Réacteurs-Fusées
Ecole Nationale Supérieure de l'Aéronautique et de l'Espace, tome 1 (1981)
- (3) Alain DAVENAS. Amélioration des propriétés balistiques et des propriétés mécaniques tout temps des propergols sans fumée.
AGARD PEP 53rd meeting, OSLO (Norvège), avril 1979
- (4) René COUTURIER. Propergols sans fumée contenant des nitramines
AGARD CP n° 391 (Confidentiel OTAN), janvier 1986
- (5) Guy DELANNOY, Bernard LOUBERE. A physical method for predicting thrust imbalance of solid rocket motor pairs for a satellites launcher (to be published)
AIAA/ASEE/SAE/ASME 23rd Joint Propulsion Conference, SAN DIEGO (1987)
- (6) Jean-Claude GODON. Modélisation de la combustion normale et érosive des propergols composites. Thèse Université de Paris 6 (1983)

- (7) M. K. RAZDAN, K. K. KUO. Erosive burning of solid propellants. Fundamentals of solid propellant combustion, Progress in Astronautics and Aeronautics, Vol 90, p 515-598 (1984)
- (8) Guy DELANNOY. Prediction of antitank solid propellant rockets internal ballistics. AIAA-84-1355 AIAA/SAE/ASME 20th Joint Propulsion Conference, CINCINNATI (1984)
- (9) Alain PHILIPPE, Paul TCHEPIDJIAN. Prediction of longitudinal combustion instabilities in axisymmetrical propellant grains. AIAA-84-1358 AIAA/SAE/ASME 20th Joint Propulsion Conference, CINCINNATI (1984)
- (10) Bernard GONDOUIN. Fiabilité des ensembles propulsifs à propergol solide. Engins Balistiques et Spatiaux à Propergol Solide. A.D.E.R.A (1985)
- (11) M. L. WILLIAMS, R. F. LANDEL, J. D. FERRY. The temperature dependence of relaxation mechanisms in amorphous polymers and other glass-forming liquid J.A.C.S., 77, 3701 (1955)
- (12) R. J. FARRIS. Development of solid rocket propellant nonlinear viscoelastic constitutive theory. AFRPL-TR-75-20 (1975)
- (13) E. C. FRANCIS et al. Propellant nonlinear constitutive theory extension. Preliminary results. AFRPL-TR-83-034 (1983)
- (14) Jean-Noël LHUILLIER et al. Tenue mécanique et fiabilité des chargements à propergol solide. Sciences et Techniques de l'Armement 52, p 11-144 (1978)
- (15) L. R. HERRMANN. Elasticity equations for incompressible and nearly incompressible materials by variational theorem AIAA Journal, vol 3, p 1896-1900 (1965)
- (16) G. MEILI, G. DUBROCA, M. PASQUIER, J. THEPENIER. Etude mécanique de chargements moulés-collés en propergol double base composite par une méthode viscoélastique non-linéaire Propellants, Explosives, Pyrotechnics, 7, p 78-84 (1982)
- (17) N. W. TSCHOEGL. Failure surfaces in principal stress space Polymer Science Symposium 32, p 239-267 (1971)
- (18) M. A. MINER. Cumulative damage in fatigue J. Appl. Mech., Trans. ASME, Series E, Vol 67 (1945)
- (19) K. W. BILLS Jr et Al. A cumulative damage concept for propellant-liner bonds in solid rocket motors J. Spacecraft, 3, 3 (1966)
- (20) R. A. SCHAPERY. A micromechanics model for nonlinear viscoelastic behavior of particle-reinforced rubber with distributed damage MM-4867-86-1, AD-A165728, (1986)
- (21) D. T. WANG, R.N. SHEARLY. A review of solid propellant grain structural margin of safety prediction methods, AIAA-86-1415 AIAA/ASME/SAE/ASEE 22nd Joint Propulsion Conference, HUNTSVILLE (1986)
- (22) G. URHIG, B. DUCOURNEAU, P. LIESA. Computer aided design of propellant grains for solid rocket motors (to be published) AIAA/ASEE/SAE/ASME 23rd Joint Propulsion Conference, SAN DIEGO (1987)
- (23) L'analyse des modes de défaillance, des effets et des probabilités. Cahiers de sécurité de l'Union des Industries Chimiques Cahier n° 4, Paris (1981)
- (24) Michel QUIDOT. Méthodes d'incorporation de résultats d'essais à la mesure de la fiabilité. Note technique interne n° 98-77-CRB SNPE (1977)
- (25) Jean THEPENIER, Hugues MENEZ-COUTENCEAU, Bernard GONDOUIN Reliability of solid propellant grain : mechanical analog motor design and testing (to be published) AIAA/ASEE/SAE/ASME 23rd Joint Propulsion Conference, SAN DIEGO (1987)

THANKS. The author thanks Bernard GONDOUIN, Roland LUCAS and Bernard PLANTIF who actively participated in writing this paper of AGARD LS 150 Lecture Series, and Francine VANDEVYVER who typed it.

State of the Art of Solid Propellant Rocket Motor Grain Design in the United States

Durwood I. Thrasher
Structural Analyst
United States Air Force Rocket Propulsion Laboratory
Edwards Air Force Base, California, USA

SUMMARY

This paper begins with a brief discussion of the basic ground rules and overall considerations in solid rocket motor design. This discussion includes ballistic design considerations, grain features related to ballistic design and their purposes, primary factors which determine stress and strain levels, and design approaches for avoiding structural weak points. The major section of the paper deals with solid rocket motor propellant grain structural integrity assurance, including materials characterization, structural analysis, and structural capability verification. The topics addressed include viscoelastic material behavior and the requisite thermomechanical characterization testing and analysis approaches; failure criteria and the appropriate testing approaches; experimental structural methods, including in-situ stress and strain measurement technology; and service life considerations. This section of the paper also addresses remaining unresolved problems and summarizes some of the more important ongoing work in the area.

INTRODUCTION

The purpose of a rocket motor or engine is to provide the propulsive force for a missile or other aerospace vehicle. Solid rocket motors are generally used for applications which require relatively low cost, long service or shelf life, mechanical simplicity, and a predetermined thrust level. The solid rocket motor is somewhat more limited in performance than the liquid rocket engine and is less easily operated in a controllable thrust mode. The typical solid rocket motor has fewer parts (and far fewer moving parts) than the typical liquid rocket engine, which leads to a fundamental difference between the design and testing of solid rocket motors and of liquid rocket engines. Liquid rocket engines can be designed and tested to a much larger extent at the basic component (e.g. injectors, pumps, valves) level, and the reliable operation of individual components can be verified prior to their end use by component testing and by all-up testing of complete engine assemblies. However, a solid rocket motor is essentially a one-shot proposition. Despite the advent of reusable motor cases, a complete rocket motor is used only once, and cannot be pre-tested in full operation. As a result, individual rocket motor reliability must be assured by assuring the structural integrity of entire populations of motors on an en-masse basis. Heavy reliance on engineering design and design verification processes is unavoidable. Other consequences of this situation are a strong reliance on past experience and a largely evolutionary (rather than revolutionary) technology development process.

The design of solid rocket motor propellant grains is in many ways an exercise in the art of compromise. Solid propellants are developed, selected and employed (in most instances) more on the basis of intrinsic ballistic performance than for their ability to provide structural integrity in a rocket motor. Solid propellants lack many of the basic desirable properties for a structural material - reproducible mechanical behavior, for instance - yet they must withstand severe mechanical loading without structural failure to actually deliver the desired ballistic performance. The structural design of rocket motors is necessarily concerned with making such materials perform satisfactorily as structures, rather than with selecting optimum structural materials. Solid propellant grain design must be discussed with this necessary process of compromise in mind.

The design process will be discussed in terms of the two basic design areas: ballistic design and structural design.

BALLISTIC DESIGN

The overall design considerations for the internal ballistic design of a rocket motor include the physical constraints on the motor, the total impulse requirement, and the environmental limits which must be met. These requirements are all ultimately defined by the mission (booster, space propulsion, tactical missile, etc.) requirements. Physical constraints on the motor include length, diameter, total volume, weight or mass fraction, and center of gravity location. An air-launched motor, for example, requires a large aspect ratio (typically, $L/D \sim 10$) to reduce drag in flight by minimizing the frontal area of the missile, while a motor used for space propulsion will usually have a more spherical shape (typically, $L/D \sim 1$) for better volumetric efficiency. In the case of multi-stage missiles, the individual motors' shapes and sizes are dictated by complex tradeoffs between individual stage performance and overall propulsion system performance. Most motors must be designed for a nearly constant center of gravity location. Since motors are always designed as part of a missile or vehicle, there are typically physical constraints in the form of critical interface dimensions which must be maintained.

A motor must be designed for storage and operation within specific temperature and humidity limits. Table 1 outlines the typical environmental requirements for the different types of motors.

Motors may be subject to other environmental factors which could require special grain design features or special design of other components to isolate the grain from the environment. For example, many motors are designed with "weather seals" to protect the propellant grain from environmental conditions such as external moisture, pressure, or vacuum.

The primary motor design requirement, of course, is delivery of a specified total impulse. Usually other ballistic performance parameters must be met as well. Typically the designer must meet constraints on the following ballistic parameters: motor action time, peak pressure, peak-to-average

pressure ratio, peak ignition-transient pressure, and ignition time. Action time, peak pressure, and ignition time are also required to meet maximum variability requirements over the operating temperature range.

TABLE 1. TYPICAL ENVIRONMENTAL REQUIREMENTS

		<u>Booster</u>	<u>Space</u>	<u>Air Launch</u>
Storage Temperature (F):	Minimum	40	40	-65
	Maximum	90	100	140
Operating Temperature (F):	Minimum	40	40	-45
	Maximum	140	100	140
Relative Humidity (%):	Minimum	50	(Vacuum)	20
	Maximum	85	85	95

The first design decision which must be made is selection of the propellant. The primary considerations here are the required ballistic performance parameters discussed above. The propellant properties used to select the propellant include specific impulse, burn-rate characteristics, density, hazards classification (i.e., Class I or Class III), and exhaust product requirements (e.g., minimum smoke, reduced smoke, or none). These requirements will guide the preliminary propellant selection. Typically, there will be no existing propellant formulation which exactly meets all of the ballistic requirements with the mechanical properties which a new motor design requires. Usually a slightly higher performance is required, or the motor design requires a slightly higher structural capability. One of the early processes in the development of a new motor is a propellant tailoring effort to achieve the necessary ballistic and mechanical properties. Over the years, continual growth in the capabilities of solid propellants has occurred through this tailoring to meet motor requirements, as well as through more intensive development programs to introduce new binders, oxidizers, and energetic ingredients. In the United States, this growth process has led to the successive replacement of older polyurethane binders by various new polybutadiene binders in most solid rocket applications; increases in the propellant solids loading from the 80 percent level to 90 percent and greater; the development of composite-modified double base propellants, and (very recently) the advent of nitrate-ester plasticized propellants for high-energy applications.

Some of the traditional methods of tailoring propellant to control the base burning rate and other burn-rate characteristics include changing the oxidizer particle size and/or the solids loading, adding a burn-rate catalyst or changing the level of catalyst, and changing the heat of combustion of the binder. All of these modifications to an existing formulation have the potential of modifying the propellant's structural properties or affecting its aging stability.

Once the propellant has been selected, the overall design of the propellant grain begins. A first consideration is the basic grain geometry. Figure 1 shows a "generic" solid propellant rocket motor which illustrates most of the common geometric features of a propellant grain. (While the insulation and liner are parts of the propellant grain, and the motor case has a profound relationship with the grain structural behavior, discussion of these will be left until later.) To illustrate some terminology, the grain configuration shown in Figure 1 is basically a "finocyl" (derived from "fin" and "cylinder") grain with a single radial slot. The primary purpose of the features just mentioned is to obtain a nearly neutral relationship between burning surface area and burn distance as the propellant grain burns. In the absence of the other geometric features, the circular cylindrical bore or port of the motor would rapidly increase in area; in other words, it would have a highly "progressive" burning characteristic.

In most motor applications, the progressive characteristic of a "pure" internal burning circular-port grain would be undesirable for the following reasons:

- (1) The efficiency of combustion would be low during most of the burn (efficiency increases with pressure).
- (2) Nozzle operation would be degraded because the fixed area ratio of the nozzle would result in overexpansion or underexpansion over most of the motor duration.
- (3) The high pressure at the end of the burn would require a heavy case to provide the necessary pressure vessel strength.
- (4) The resulting progressive thrust history would produce a variable acceleration during the burn, which is usually undesirable. (In fact, a moderately regressive thrust history would be required for a constant acceleration, depending on the payload being propelled by the motor.)

A highly regressive grain geometry would be undesirable for the same reasons. In order to achieve a high volumetric loading in the motor, the designer must therefore incorporate some initial burning surface in the motor in the early stages of the grain burnback while reducing the net burning surface later in the burnback. A feature such as the radial slot in Figure 1 accomplishes this purpose. Consider the aft face (i.e., the face on the nozzle side) of the radial slot. Once the bottom of the slot has "burned out" (reached the case insulation), the area of the slot face decreases with increasing burn distance. At the same time, the burnback of the slot face toward the nozzle end reduces the length of the burning surface of the circular bore. The same interaction occurs between the forward face of the slot and the circular port section forward of the slot. In effect, once the bottom of the slot has burned to the wall of the case, the two slot faces are equivalent to the burning surfaces at the ends of a simple uninhibited cylindrical grain. Also note that the shape of the propellant within the dome

region provides a regressive influence on the surface area evolution. While the fin region in the aft end of the motor has a much more complicated geometry, it provides a regressive contribution to the surface area evolution in the same way as the radial slot. Note that the radial slot has a progressive area evolution until the first burnout occurs; this is probably true of the fins as well. Besides initial surface-adding features such as slots and fins, the designer frequently applies the inverse approach: eliminating initial burning surface through the addition of inhibitors or restrictors (pieces of rubber insulation) to selected surfaces to change the burning pattern of the grain. Depending on its placement, an inhibitor may influence only the initial burning pattern or produce a drastically different surface evolution throughout the motor operation.

It may be clear at this point that achieving a smooth surface area evolution and approximate neutrality in the grain at the same time is very difficult to do; most motor grain designs do have peaks and valleys in their pressure traces due to local burnout of some grain features and complex interactions of the surface features as they burn back.

Sutton and Ross⁽¹⁾ have an excellent discussion of grain geometry and burnback. They also cover the quantitative aspects of rocket motor sizing and the analysis required to calculate internal pressures based on the usual power law burning rate/pressure relationship and the internal gas dynamics of the motor chamber.

In practice, the internal ballistics analysis is usually done using computer codes such as the Solids Performance Program (SPP)⁽²⁾. This program (discussed more extensively in Ref. 2) has two- and three-dimensional burnback models coupled with a one-dimensional nonequilibrium internal ballistic model, and is capable of accounting for erosive burning and nozzle throat erosion. The Solid Rocket Motor Design and Optimization Program (SRMDOP)⁽³⁾ uses a pattern-search technique to adjust geometric parameters of a motor to provide a specified thrust-time trace, to optimize the motor's total impulse to weight ratio, or to minimize the motor's weight.

The case insulation is typically a filled rubber material; typical fillers are silica and Kevlar[®] fibers. (A major development in rubber insulation within the past 10 years is the nearly total disappearance of asbestos-filled rubber because of the health problems produced by asbestos.) Particularly in air-launched rocket motors, hard materials such as silica-filled phenolic are sometimes used as case insulators. Design of the case insulation is primarily based on thermal considerations. The insulation withstands the high heat fluxes from the chamber gases by charring and ablation. Once the insulation material has been selected, the required thickness is determined by the time of exposure; greater thickness may be required in areas of high gas velocity. In the motor of Figure 1, only a very thin layer of insulation is needed in the mid-grain area, while the insulation must be substantially thicker under those grain features that burn out early in the motor operation, such as the radial slot and the aft-end fin tips. While the aft dome insulation could be "scalloped" to provide thickened insulation only where it's needed, this is rarely done in practice because of the added manufacturing complexity.

The above discussion provides a qualitative overview of the ballistic and some other nonstructural facets of designing solid propellant grains. We now turn our attention to the structural aspects of propellant grain design.

STRUCTURAL DESIGN

The structurally important features of a typical case-bonded solid rocket motor propellant grain are shown in Figure 1. Structurally, a solid rocket motor consists of:

- (1) the solid propellant grain itself;
- (2) the liner (or, in some systems, a "powder imbedment layer"), whose primary purpose is to provide an adhesive bond between the propellant grain and the case insulation;
- (3) the case insulation, which provides thermal protection to the case from combustion products and also structurally supports the propellant grain within the motor case.

Any of these structural elements may become the weakest link in the propellant grain structure.

The primary structural design concern with the insulation is generally the strength of the bond between the insulation and the case. Generally the propellant does not inherently bond well to the insulation; this problem is solved by using a liner which is formulated to both bond well to the insulator and to provide a good bond with the propellant when the propellant is cast and cured against it. Usually the liner uses the same polymer as the propellant itself, and is only partially cured before casting the propellant, so that a strong chemical bond is obtained upon propellant cure.

The motor case itself, while not considered a part of the propellant grain, structurally interacts with the propellant grain to various degrees under different loading conditions. In general, composite motor cases produce substantially larger stresses and strains in rocket motors under pressure loads for fully case-bonded grains than do metal cases because of the larger dome deflections. While the nozzle and the igniter are indispensable parts of the rocket motor, they will not be addressed in the present discussion.

The propellant grain must withstand a series of structural loads throughout the service life of the rocket motor; normally the final structural load is that imposed by motor operation (firing). The loads applied to the motor include thermal loads, acceleration loads, vibration loads, and ignition pressurization.

The primary thermal load on the propellant grain occurs under a simple uniform-temperature "thermal soak." At any temperature which differs from the motor's natural reference state ("stress free temperature"), the grain is subjected to stresses and strains produced by differential thermal expansion of the propellant grain and case materials. Since the propellant grain materials typically have thermal coefficients of linear expansion that are an order of magnitude greater than that of the usual case materials, relatively large strains are induced in motors at low temperatures. Tensile stresses at the propellant/liner/insulation bondline can also become quite large. The motor's stress free temperature corresponds to a temperature near its cure temperature, but is usually somewhat higher due to shrinkage of the propellant during the cure process. The stress free temperature can be altered by curing the motor under high pressure.

Additional thermal loads are produced by transient temperature loading conditions such as aeroheating, aerocooling, or rapid changes in the environmental storage temperature. ("Rapid" is a relative term; a large motor may require many days to reach thermal equilibrium.) In aeroheating during air-carry of an air-launched motor, the case temperature increases rapidly while most of the propellant grain remains at the original temperature. The temperature gradient produces a sudden thermal expansion of the case which results in tensile stress at the bondline and a tensile bore strain. These transient thermal stresses and strains are ordinarily rather small perturbations of the stresses and strains produced by thermal soak loads. However, aeroheat loading of a cold motor can produce propellant/liner/insulation bond stresses that exceed the bond strength because of the decrease in bond strength as the bondline warms up.

Acceleration loads include the long-term gravity load (often referred to as the "slump" loading condition) during motor storage. While this load is relatively small, the stresses and strains are additive to those produced by the thermal storage load. The change in grain shape, or slump, produced by the gravity load can produce significant changes in internal ballistics.

Additional acceleration loads include the air-carry acceleration loads imposed on air-launched missile motors by aircraft maneuvering, and vibration and shock loads imposed during ground handling and flight conditions. Upper stage motors and space propulsion motors are subjected to acceleration loads during booster operation, and all motors are subjected to in-flight acceleration during the motor operation.

The ignition pressurization load is the ultimate test of the motor's structural integrity. The case deformations under pressurization produce distortional strains in the propellant grain, resulting in tensile strains at the motor's inner bore surface and shearing stresses at the propellant/liner/insulation bondline. The pressurization loading is typically applied to a motor that is already under stress and strain due to thermal load (possibly including aeroheat) and is typically accompanied by axial acceleration.

The structural response of the propellant grain to all of the loading conditions described above is highly dependent on the grain configuration. Two geometric parameters often used to describe the propellant grain geometry are the web fraction $(b-a)/b$ and the length-to-diameter ratio $L/D=L/2b$ (see Figure 2). These basic geometric parameters apply specifically to a right-circular-cylinder geometry with free surfaces at the ends of the propellant grain, but have at least conceptual equivalents for any motor geometry. Results of closed form solutions for simple geometries^(4,5) provide some insights into the effects of the motor geometric parameters. Increasing either the web fraction or the L/D will result in an increase in bond stress and bore strain under any of the usual loading conditions. The stresses and strains become extremely sensitive to the web fraction for high volumetric loading. More specifically, bond stresses in an infinitely long grain are approximately proportional to the quantity $[b^2/(b^2-a^2)]$, while bore strains are approximately proportional to the square of the same quantity. The stresses and strains are reduced in short grains but are essentially the same as those in an infinitely long grain once L/D exceeds a value of 10. For a rigid motor case, bonding the grain ends to the case domes essentially makes the grain length infinite.

In real motors, the highest stresses usually occur at discontinuities such as the grain bondline termination point, and the highest strains occur on the bore surface either in the middle of a long circular section or at discontinuities in the geometry (such as the forward termination of the fins in Figure 1). The designer's task is to assure that the stresses and strains at these critical locations in the motor are within acceptable bounds; meeting this objective constrains the designer's options in designing the grain geometry to meet ballistic requirements, and sometimes requires special features in the grain design in addition to those incorporated for purely ballistic reasons. In actual practice, the ballistic design and the structural design are often done by two (or more) different specialists. It then becomes the task of the "structural designer" to modify the "ballistic designer's" design to produce a grain design with structural integrity, without significantly changing the motor's ballistic characteristics. To accomplish this, the designer concentrates on the critical areas of the motor: the free surfaces and the bondline.

Consider a motor configuration like that in Figure 1, but without the radial slot. A high strain area is located near the center of the long circular portion of the bore; due to strain concentration, the region where the fin bottoms intersect the bore surface may have an even higher strain. One option the designer has for reducing these strains is to incorporate a stress relief flap (sometimes called a boot) as shown in Figure 1. This reduces the effective L/D of the motor, producing lower bore strains and lower bond stresses in most areas of the motor. The flap has the additional advantage of drastically reducing the bond stresses at the bondline termination in that end of the motor, so that the critically stressed region is moved to the vicinity of the flap termination or "hinge." The crack-like singularity in the flap is buried in the rubber insulation, which is normally far tougher than the propellant or liner. By thickening the insulation at the flap termination in a smooth contour, the designer can reduce the stresses at the bondline to an acceptable level. Note, however, that the use of flaps carries the penalty of an increase in inert weight and a loss of propellant.

Since the motor of Figure 1 has the radial slot, the flap shown would have little value because the stresses in that end of the motor are already reduced by the radial slot. The radial slot also accomplishes the same effective length reduction as the flap. In this case, the structural penalty is a highly-strained region at the bottom of the radial slot, and a substantial amount of propellant would be lost if the designer incorporated the radial slot for stress and strain relief. Because of the profound effect on the motor ballistics, such a slot would rarely be incorporated for structural reasons. However, the structural designer might alter the location of the slot (or its width or depth) to gain some structural advantages at the penalty of slightly altering the pressure trace.

Returning to the aft end of the motor, the designer might find it necessary to increase the width of the fins to reduce the strain concentration at the intersection with the bore or the strain at the fin tips. Once again, a penalty of propellant loss would be paid, and the pressure trace would be altered somewhat. The substitution of an elliptical or approximately elliptical contour for a semicircular contour in the fin bottoms can substantially reduce the strains at the critical fin regions with virtually no propellant loss, but may increase the cost of building the tooling. Similar considerations apply at the bottom of the radial slot. Occasionally, the designer may incorporate a flap (e.g., in the aft end of the motor of Figure 1) to reduce the strains in a fin region of a motor. A secondary consideration in the structural design of fins or radial slots is the locally higher bond stresses which occur when the fin or slot closely approaches the bondline; slight modifications of the slot or fin geometry may be needed to reduce these stress concentrations.

For long motors, an option that is sometimes used is the stress-relieving liner (SRL). The SRL is a special built-up insulation assembly which allows the grain to pull away from the case under thermal load and is designed to vent chamber pressure into the area between the case and the propellant-to-SRL bond(6).

The long-term trends in recent years that affect the structural design of propellant grains have not been trends in basic grain design approaches. Instead, the important trends have been:

(1) the steady growth in propellant strain capability; (2) the increased application of composite cases and (3) the increased application of pressure cure.

STRUCTURAL INTEGRITY ASSURANCE

The above discussion of rocket motor structural design was conducted without specific reference to details of the mechanical behavior of the materials involved or the methodology required to assess stresses and strains in a particular motor design. The following discussion introduces these details and shows how structural integrity assurance is provided for solid rocket motors.

Materials Characterization

The primary materials in a solid propellant grain (propellant, liner, and insulation) are basically nearly-incompressible, rubber-like materials, and this basic property must be recognized in dealing with the materials on a structural basis. All of these materials have bulk moduli of compressibility of 200,000 psi or greater in the virgin (undamaged) state. A typical undamaged solid propellant contains on the order of one percent or fewer voids on a volume basis. However, the mechanical behavior of these materials (particularly the solid propellant) is tremendously sensitive to mechanical damage, and the materials are easily damaged by applied loads. The primary result of such damage is the appearance of porosity and binder-to-particle dewetting, which is manifested as dilatation under tensile or mixed loading conditions and as initial compressibility under compressive loads.

Mechanically, the propellant and the other grain materials respond as viscoelastic materials, but show strong strain level dependence and other nonlinear characteristics; hence they are not strictly treatable as linear viscoelastic materials. Complex mechanical behavior noted in propellants includes a degree of thermorheological complexity and a nonlinear response to combined straining and cooling or heating. Another nonlinear characteristic of propellant is an ability to reheal following damage. Application of these materials to extreme ranges of temperature and strain rate, as well as strain levels that range from near-zero to the vicinity of 100 percent, leads to more than a little difficulty in characterizing and analyzing them as engineering materials.

The following discussion concentrates on the propellant itself; however, most of the information applies equally to typical insulations and liners. In point of fact, the mechanical characterization of insulation and liner materials is almost totally ignored in most motor development programs; assumed properties are usually used for these materials in structural analyses.

Routine laboratory characterization of solid propellants consists of constant strain rate testing, constant strain level testing, and constant load testing. These are discussed separately below.

Constant strain rate testing is primarily done for the determination of failure properties and for manufacturing quality-control purposes. The stress-strain curve shown in Figure 3 illustrates the mechanical parameters measured in the typical uniaxial constant strain rate laboratory test. The initial or tangent modulus of elasticity, E_0 , is primarily used as a quality-control parameter rather than as an engineering mechanical response quantity (instead, the relaxation modulus, discussed below, is used to determine the modulus for stress analysis). The maximum stress, σ_m , is used to define the stress allowable for the propellant, while the strain at maximum stress, ϵ_m , is used to define the strain allowable. In more recent years, there has been a trend toward using the rupture strain to determine allowable strain, and to use the "corrected" or "true" stress (stress multiplied by the quantity $(1+\epsilon)$ to correct for the reduction in area under strain) in calculating σ_m and ϵ_m . Opinion on the validity of these approaches is divided, however. Typically, the data obtained from constant strain rate tests is transformed into master curves of σ_m and ϵ_m versus reduced strain rate or reduced time to

failure using techniques similar to those discussed below for stress relaxation data.

Two types of constant strain level tests are commonly employed to characterize propellants: the stress relaxation test and the strain endurance test.

The stress relaxation test is the primary source of data used to establish the viscoelastic response (relaxation modulus) of the propellant for structural analysis. Typically the stress relaxation test is run at strain levels of three to five percent, but higher and lower values are sometimes used. The relaxation test is conducted over a range of temperatures (typically between -65°F and 110°F, although wider ranges are sometimes used). The temperatures and test durations are selected so that the data from different tests overlap, allowing a master curve to be established for the stress relaxation modulus as a function of reduced time t/a_T . This procedure, known as "shifting," simultaneously establishes the time-temperature superposition function, a_T , also known as the shift factor or shift function.

A typical propellant master curve is shown in Figure 4; the inset graph shows the variation of a_T with temperature. When both the relaxation modulus and the reduced time are plotted on log-log coordinates, as in Figure 4, the shifting can be performed graphically. Since the shift factor is conventionally defined as equal to unity at 77°F ("room temperature"), the 77°F relaxation curve is held stationary while other curves are shifted to the left ($a_T > 1$) or right ($a_T < 1$) to obtain a smooth curve. The resulting shift function is, of course, purely empirical. Other approaches to shifting the relaxation data include constraining the a_T function to fit the theoretical Williams-Landel-Ferry (WLF) relationship,

$$\log a_T = -C_1(T-T_0)/(C_2+T-T_0) \quad (1)$$

where T_0 is the reference temperature (i.e., the temperature for which $a_T=1$). Actually, Eq (1) is a conveniently transformed version of the more basic WLF relationship,

$$\log a_T = -C_1'(T-T_s)/(C_2'+T-T_s) \quad (2)$$

where T_s is a temperature which is approximately 50°C above the glass transition temperature and C_1' , C_2' are the "universal" WLF coefficients⁽⁷⁾. The glass transition temperature determined by shifting relaxation modulus data usually agrees fairly well with that determined from thermal expansion tests. (At a fundamental level, the glass transition point and the time-temperature superposition principle are both closely related through the concept of free volume.)⁽⁷⁾

Another relationship sometimes used is the Schapery power law function^(5,8),

$$a_T = \left[(T_0+C)/(T+C) \right]^m \quad (3)$$

where C and m are constants determined by fitting the data. Generally, the constant C is close to the glass transition temperature. Several mathematical representations are used for the relaxation modulus itself, including an exponential series (the Prony series)^(8,9) and several variations of the power law^(9,10).

The strain endurance test is a test to determine the level of strain at which the propellant has "unlimited" endurance. There are several versions of this test in use. A representative technique involves holding samples at several strain levels for a specified period (typically two weeks), and reporting the strain endurance value as the strain level at (and below) which all samples survive. A slightly more sophisticated (and preferable) version of this test requires periodic examination of the samples so that their failure times can be determined. Instead of a single "endurance" value, this procedure provides a curve of strain level versus time to failure such as shown in Figure 5.

The only constant load test generally used for solid propellants is the stress endurance test. This test is similar to the strain endurance test; however, each sample is subjected to a constant force (using a simple pendant weight) instead of a constant strain level. The stress endurance test provides a curve of stress level versus time to failure such as shown in Figure 6.

The laboratory tests described above are usually performed under uniaxial loading; however, they are occasionally performed under biaxial loading as well. In such cases, the tendency is usually to "calibrate" the relationship between biaxial behavior and uniaxial behavior rather than to perform a complete biaxial characterization. Generally, replicate samples are tested to account for experimental and material variability.

In addition to the routine testing described above, special tests that are frequently performed on propellant grain materials include fracture testing (typically using cracked biaxial sheet samples or notched uniaxial tensile specimens), constant strain rate tests with dilatometry, pressurized constant strain rate tests, and "similitude tests" consisting of low-rate prestraining of the specimen followed by a high rate test to failure. The latter test is intended to simulate the loading history of propellant in a rocket motor fired under low temperature thermal soak conditions and is used as a source of failure data for this loading condition. Occasionally, the "similitude test" is used to establish modulus values for analysis input⁽⁸⁾. Another frequently-measured special property is the dynamic modulus. Generally, the real and imaginary components (or, equivalently, the real component and the tangent of the phase angle between the excitation and the response) are determined using any of several test methods and reported in the form of master curves (i.e., as functions of the reduced frequency ωa_T).

Two additional mechanical response properties needed for completeness of the propellant characterization are the bulk modulus of compressibility and the thermal coefficient of linear expansion (TCLE). The bulk modulus is usually measured by applying fluid pressure to a small cube-shaped specimen

and measuring the compression with linear displacement transducers. There are several techniques for measuring TCLE; one of the more commonly used methods is the quartz-tube dilatometer test, in which the sample is heated in a quartz tube and the linear expansion is measured with a displacement transducer.

Bondline strength evaluation entails another battery of laboratory tests. Several variations of the peel test (e.g., 90-degree peel, 180-degree peel) are used to qualitatively assess bondline strength, but are not used to establish strength for analysis purposes. Instead, a multitude of special-purpose bondline samples are used by various companies and government agencies to determine the bondline strength. To obtain uniform bond stress distribution, the bondline specimens typically incorporate a miniature version of the motor stress relief flap, formed by cutting a slit into the edge of the insulation portion of the bondline specimen. These samples are often pulled at an angle to simulate the combined tension/shear stress field in a motor. High rate bondline tests are typically done under pressure, again to better simulate actual motor conditions.

Structural Analysis Practices

The overall structural analysis process is depicted in Figure 7. As shown in Figure 7, the structural analyst must, in principle, make a series of basic decisions about the analysis approach to use in a particular situation.

The first set of decisions involves translating the overall design considerations into more concrete analysis input data. These decisions are fairly straightforward; the important structural loads are fairly consistent from one motor application to another, and the motor geometry is usually predefined by the motor designers. The material properties must be selected based on analysis of available laboratory data or (often, unfortunately) assumed where actual data are missing. The material properties consist of the response properties (e.g., modulus and Poisson's ratio) and the failure properties (stress and strain allowables). The response properties are used directly in the structural analysis model, while the failure properties are applied when using the structural analysis results to calculate the margins of safety for various failure modes. As indicated in Figure 7, all propellant grain material properties are affected by chemical-structural aging, which must be considered in the service life determination process. The selection of response and failure properties is, of course, interdependent with the selection of analytical treatment and failure theories.

A primary decision the analyst must make is the selection of analytical treatment for the propellant grain materials. As shown, the analyst may choose to regard the propellant grain materials as elastic, (either linear or nonlinear), linear viscoelastic, or nonlinear viscoelastic. While the propellant grain materials in fact behave as nonlinear viscoelastic materials, in practice they are rarely modeled in strict accordance with even linear viscoelastic theory in actual structural analyses. This is the case for a number of reasons, but primarily because no existing theory seems to fully explain propellant mechanical behavior. The analyst, faced with theoretical shortcomings regardless of his choice, usually opts for the simplest theoretical treatment, i.e., linear elasticity. In order to accommodate the viscoelastic behavior of the materials, however, the analyst uses a "quasi-viscoelastic" approach which involves the use of an effective modulus. The effective elastic modulus is conceptually based on the linear viscoelastic evolution of stress through the Boltzmann superposition integral⁽⁹⁾, given (for a simple uniaxial strain history) by

$$\sigma = \int_0^{\xi} [E_r(\xi - \xi')] \dot{\epsilon} d\xi' \quad (4)$$

where $[E_r(t)]$ is the relaxation modulus function, $\dot{\epsilon}$ is the strain rate as a function of time, and ξ is the reduced time. For an isothermal loading process, the reduced time is given by

$$\xi = t/a_T \quad (5)$$

where a_T is the time-temperature superposition factor discussed earlier. For a nonisothermal loading history, the Moreland-Lee Hypothesis⁽⁹⁾ is generally adopted, so that

$$\xi = \int_0^t (1/a_T) dt \quad (6)$$

The instantaneous effective modulus is simply the instantaneous secant modulus,

$$E_{eff}(t) = \sigma(t)/\epsilon(t) \quad (7)$$

where $\sigma(t)$ is given by the superposition integral, Eq. (4). It can be shown that for a linear viscoelastic material, the effective moduli for two strain histories that are exactly proportional to each other are exactly the same. If the strains everywhere within a given material in the motor are proportional to a particular normalized strain history (i.e., if the strains are affine), then the response can be represented by a single effective modulus value throughout the material at any instant of time. The effective modulus is therefore dependent on the "shape" of the strain history, rather than upon the absolute strain level^(5,10).

Note that these equations imply exact knowledge of the strain history (and in the case of non-isothermal loading, the temperature history) for the particular rocket motor being analyzed. Generally the analyst cannot predict the exact thermal or strain history in advance, so rather gross approximations must be made in the loading history. In actual practice, the typical method for calculating the effective modulus is to replace the strain history $\epsilon(t)$ with a simple step function at $t=0$ and to determine the effective modulus at a time, t , which is characteristic of the problem. For motor ignition, for instance, t would be equal to the duration of the ignition transient. The effective modulus is then simply equal to the relaxation modulus at time t . While this method is crude, it is often defended on the basis that the actual load history is not known accurately enough to warrant more exact techniques.

A frequent practice of structural analysts for treating the effective modulus is to use an order-of-magnitude approximation for the propellant modulus in the structural model, then to scale the resulting stresses and strains according to the actual modulus later on. Sometimes "unit loads" (e.g., a pressure of one psi or a temperature change of one degree) are used in such analyses and the results are scaled according to the actual load. Provided such effects as case-grain structural interaction are effectively constant, this procedure is valid for linear analyses. This "unit analysis" approach is a most useful way of coping with the analyst's typical dilemma; the results are needed "now," but the propellant is still being tailored.

The structural analysis proper is carried out primarily by finite element computer codes, although the older approximate techniques based on closed-form elastic solutions (made more practical by the availability of programmable calculators and desk-top microcomputers) are sometimes used for preliminary analyses⁽⁵⁾. Two major advancements in elastic finite element analysis for rocket motor propellant grains were the introduction of the Herrmann reformulation for finite elements in the mid-1960's⁽¹¹⁾ and the introduction of isoparametric curved-sided finite elements in the early 1970's^(12,13). These two features are necessary for efficient and accurate modeling of propellant grains.

A typical finite element model of an axisymmetric propellant grain contained in a composite motor case is shown in Figure 8. Note the concentration of elements in the critical regions near the stress relief flaps at each end of the motor to obtain precise modeling in these locations. Elements are also concentrated in the bondline region to capture stress gradients and through the thickness of the case to obtain accurate modeling of the case bending stiffness. This particular finite element model used Herrmann-reformulated quadratic-displacement (linear strain) isoparametric elements for the propellant, liner, and insulation; on the order of four times as many elements would be required to achieve the same accuracy with linear-displacement (constant strain) elements. The loads are applied to the finite element model as boundary conditions (e.g., internal pressure, and loads such as nozzle ejection load due to pressure), or as distributed body forces (e.g., acceleration and thermal loads).

In more complicated grain geometries (such as that of Figure 1) a three-dimensional (3D) finite element model would be used; however, 3D finite element analysis is avoided whenever possible because of the tremendous increase in modeling complexity and computer time consumption that results. The recent introduction of interactive computer-graphics aided finite element modeling codes such as PATRAN-G[®] has greatly increased the efficiency of the motor structural analyst in model generation. Using an interactive computer-graphics modeling code greatly reduces geometry and connectivity errors in the initial modeling and allows rapid "debugging" of a model once it's generated.

The results of the finite element analysis are stresses and strains at the element nodal points or at "integration points" within the element. The stress and strain values at the most severely stressed/strained locations in the motor are used to calculate margins of safety for the motor. The procedure of locating the highly stressed/strained areas can be greatly aided by interactive computer-graphics postprocessing of the finite element code results.

As shown in Figure 7, the analyst must make yet another basic decision before calculating a margin of safety for a motor failure mode. This decision is the selection of a failure theory to apply to the motor failure mode. In general, three primary propellant grain failure modes should be addressed⁽⁹⁾: fracture (cohesive or adhesive); excessive deformation; and autoignition. These failure modes will be addressed individually.

Cohesive fracture of propellant grain materials is traditionally considered to fall into two regions of behavior⁽⁹⁾, as shown in Figure 9. The conceptual approach recognizes that propellant and other materials inherently contain numerous microscopic flaws. The stress required to propagate a flaw increases as the flaw size decreases; when the flaw size becomes small enough (c_{cr} in Figure 9) the failure becomes dominated by the ultimate strength of the propellant, and classical failure criteria may be applied over "Region I." If the initial flaw size is larger than c_{cr} (i.e., in "Region II"), then fracture mechanics must be applied instead.

For the most part, current analysis practice regards propellant grain failure modes as "Region I" failure modes, and classical failure theories are applied. No global failure criteria (in the sense of a failure surface in maximum principal stress or maximum principal strain space) have been successfully applied to solid propellant grain materials, probably due to the inability to accurately calculate stress and strain under realistic loading conditions. However, simple failure criteria have been found to work satisfactorily under specific conditions; for instance, the maximum principal strain failure criterion is usually successful for defining failure at a free surface of the propellant grain away from material interfaces. The maximum principal stress failure criterion has been successfully applied to bondlines under thermal and gravity loads. Under ignition pressurization, the maximum deviatoric stress and the maximum octahedral shear stress criteria have been successfully used for bondline failure modes.

In applying the above failure criteria, the effects of time and temperature are as important as in determining the effective modulus. As mentioned earlier, the results of constant-rate laboratory tests are generally reduced to master curves of stress or strain as a function of reduced strain rate, (ϵa_T), or reduced time to failure, ($\epsilon_m / \epsilon a_T$). Typical master curves of constant rate uniaxial failure data are shown schematically in Figure 10. To determine the appropriate failure stress or strain value, the analyst would use the appropriate reduced strain rate for the applied load used in the structural analysis. For a maximum principal stress or maximum principal strain failure criterion, the data from the master curves would be used directly; for other criteria, the failure stress or strain can be calculated from the uniaxial values. For instance, the deviatoric stress at failure would be given by

$$\sigma_{f,dev} = \sigma_1 - \sigma_h = \sigma_1 - (\sigma_1 + \sigma_2 + \sigma_3)/3 = 2 \sigma_1/3 \quad (8)$$

where σ_1 is the axial stress and σ_2, σ_3 are the transverse stress components (the transverse components

being zero for uniaxial stress). For a test done under superimposed pressure the term $(-p)$ would be added to all the stress components, so that

$$(\sigma_{f,dev})_{pressurized} = 2 \sigma_1/3 - p. \quad (9)$$

Note that a sufficiently large value of σ_1 will result in a positive (tensile) value of $\sigma_{f,dev}$ under pressure, even though the maximum principal stress would be negative. It is this property of the deviatoric stress that makes it a useful failure criterion for propellant grain failure under ignition pressurization loads.

A different approach to the treatment of constant strain rate failure data is based on cross-plotting the stress and strain failure curves, eliminating the reduced strain rate variable. A plot of $\log(\text{stress})$ versus strain, such as Figure 11, is known as a stress-strain failure envelope (often referred to as the "Smith failure envelope," after its originator, Thor Smith⁽¹⁴⁾). For some propellants, the stress-strain failure envelope has been shown to coalesce data from a variety of laboratory tests, including constant-rate uniaxial and biaxial tests, strain endurance tests, and stress endurance tests. When such results are obtained, the failure envelope can be very useful as a tool for selecting failure criteria. For example, a very high loading rate would produce failure near the upper limits of stress on the failure envelope. Examination of Figure 11 shows that the failure stress is relatively constant in this region, though the failure strain varies greatly. One would expect that a stress-based failure criterion would work best in this situation. On the other hand, an intermediate loading rate might produce a stress-strain trajectory that crosses the failure boundary at the "knee" of the curve, and a very low loading rate trajectory would cross the failure boundary near the strain endurance limit (low-stress end of the curve). These regions of the failure envelope show a much better definition of failure strain than of failure stress; a strain-based failure criterion would appear to be the choice for these conditions.

As suggested earlier, superimposed pressure does affect the failure properties (as well as the response properties) of propellant grain materials. This is usually seen as an increase in the stress capability of the propellant, while the strain capability may increase or decrease slightly; Figure 12 shows the effects of pressure on constant rate behavior of a typical propellant. For the failure envelope, the pressure effects are usually accounted for by considering the deviatoric stress (both pressurized and unpressurized) as the stress parameter. When this is done, the pressure effect is manifested as an upward shift of the failure envelope. Typical analysis practice is to either use pressurized failure test data directly or to use a correction factor based on limited pressurized testing. The same procedures are used to account for pressure effects on bondline failure data. For consistency, of course, the analyst must account for the pressure effect on the modulus values used in the finite element analysis. (It should be noted here that this treatment is at variance with the basic work which has been done with polymers, in which the effect of pressure is treated as a shift in the time variable, similar to that produced by temperature changes and again related to the concept of free volume⁽¹⁵⁾).

As indicated in Figure 7, another failure theory often used is linear cumulative damage⁽⁹⁾. This failure theory is based on the concept that damage to propellant under constant load is proportional to the time under load. For a particular sample subjected to a stress σ

$$D = t/t_f \quad (10)$$

where D is the damage, t is the time under load, and t_f is the time to failure under the stress σ . The damage varies from zero to 1.0; a damage of 1.0 implies failure. The primary characterization data for cumulative damage is the stress endurance test (Figure 6). As is evident in Figure 6, considerable scatter is found in the time to failure at a particular stress; this data scatter must be taken into account through a probability distribution function. The relationship used to calculate damage accumulation for arbitrary stress and temperature histories⁽⁹⁾ is

$$D = [1/(P t_0 (\sigma_{ot} - C)^B)] \int_0^t [(\sigma_t - C)^B / a_T] dt' \quad (11)$$

where t_0 , σ_{ot} , C , and B are constants obtained from the stress endurance data, $\sigma_{t'}$ is the stress history as a function of time, P is the probability distribution function, and a_T is the time-temperature superposition function which will be a time-dependent variable unless the temperature is constant. For propellants, the stress vs time-to-failure relationship is a simple power law relationship (a straight line in Figure 6), so that the constant C is typically zero.

Typical practice in the United States for reporting propellant grain structural analysis results is to report the margin of safety relative to a minimum required factor of safety, based on an allowable value of the failure criterion parameter (e.g., maximum principal stress); the latter is usually based on the failure data but is adjusted to reflect aging, data scatter (i.e., pure experimental error in laboratory test results), sampling bias (e.g., carton-to-motor bias) and variability (i.e., actual batch-to-batch or motor-to-motor variation in propellant properties). When scatter or variability adjustments are made to allowables, the typical practice is to use the "lower-three-sigma" (i.e., three standard deviations below the mean) value. The basis for these adjustments is direct laboratory measurements where possible, but very often is simply past experience. The typical practice is not to adjust the modulus for variability or scatter; instead, mean experimental values are used (possibly adjusted for experimental bias or aging). By definition, then,

$$MS = [ALLOWABLE / (REQUIREMENT \times FS)] - 1 \quad (12)$$

where MS is the margin of safety, FS is the imposed minimum factor of safety, "ALLOWABLE" is the allowable value of the failure criterion parameter, and "REQUIREMENT" is the corresponding value of this parameter determined from the structural analysis.

When linear cumulative damage is used, the margin of safety (for a factor of safety of 1.0) is given by

$$MS = (1/D) - 1 \quad (13)$$

Fracture mechanics is rarely used in the routine initial design analysis of rocket motors in the United States. It is more often applied in analyses done during the investigation of motor failures, but even in such applications its use is still rather exceptional. When fracture mechanics is used, the two classical approaches (strain energy release rate and stress intensity factor) are used with approximately equal frequency. Some of the reasons for the infrequent use of fracture mechanics in routine propellant grain analysis are the inability to calculate motor stresses with sufficient accuracy, the rarity of known flaws in motors (other than motors rejected for use), and the lack of workable analysis techniques for crack pressurization and propagation in burning propellant.

Excessive grain deflection can be a problem in several different situations. One of the most interesting is the nozzleless rocket motor⁽¹⁶⁾. In the nozzleless rocket, the aft end of the propellant grain provides a sonic port which effectively replaces the usual hardware nozzle. The nozzleless motor usually has a drastic pressure drop from the head end of the propellant grain to the aft end, resulting in large shear stresses and bore deflections that significantly affect the flow field in the motor. Typically, the grain deflects inward at the aft end, increasing the pressure drop compared to that produced by an undeflected geometry. Since the resulting ballistic/structural interaction is highly nonlinear, the problem has to date only been solved approximately⁽¹⁶⁾. Essentially the same problem can be encountered in motors with nozzles when the port-to-throat ratio is close to one. Deflections under pressure loads can have a discernable impact on ballistics in most motors⁽³⁾. Long-term slump response of a propellant grain under storage loads can also produce excessive deformations which can cause ballistic problems. These potential problems should be addressed in motor structural analyses. In practice, however, they are relegated to such a low priority that they are usually not performed for most motors. Since the concept of margin of safety does not directly apply to such analyses, margins are normally not calculated for grain deflections. Autoignition could result from causes not usually considered by the structural analyst (e.g., static discharge or high environmental temperatures) but could also result from internal heating of the propellant under vibration loading. Autoignition typically requires an induction time as well as an excitation such as temperature; assessment of the likelihood of grain failure through autoignition is normally based on empirical treatment of laboratory data⁽⁹⁾.

Structural Capability Verification

It may be obvious from the foregoing discussion that structural analysis results are frequently in need of verification. Such verification is the role of the experimental structural methods used in rocket motor structural integrity evaluation. The primary experimental structural methods used for rocket motors are motor instrumentation and motor structural overtest.

Rocket motor instrumentation available for propellant grain structural integrity evaluation includes case strain gages (which are routinely used in motor firings), internal in-situ stress and strain gages, and embedded thermocouples. The use of in-situ instrumentation in rocket motor propellant grains has a long history⁽¹⁷⁾. Because of the expense and checkered success record of such instrumentation, however, its use has been somewhat rare. Recent improvements in transducer stability and accuracy, however, have led to increased use of motor stress and strain instrumentation for motor structural capability verification.

Figure 13 shows a normal stress transducer designed for use as an embedded gage to measure stress at the bondline of a rocket motor. In use, such transducers are usually embedded in the case insulation or mounted against the insulation, with a layer of liner between the stress transducer and the propellant. The usual practice is to select areas where stress gradients are expected to be small. While it would be more desirable to measure stresses in more critical locations, better results are obtained in low-gradient locations; also, the chance of inducing spurious motor failures is reduced by selecting low-gradient locations.

Figure 14 shows a typical clip strain gage, used to measure surface strains in a rocket motor. Other devices, such as linear displacement transducers, are often used to measure grain deformations. Dynamic deformations of propellant grains are often measured using accelerometers.

To verify the safety margins of a rocket motor directly, the motor (preferably with in-situ instrumentation installed) must be subjected to either an overtest to failure or a margin limit test. The margin limit test is defined as a test in which the structural load (usually temperature or pressure) is applied in excess of the design condition, but at a level lower than that required to reduce the calculated margin of safety to zero. If a motor successfully passes such a test (statistical considerations aside), the test provides assurance that the motor has a minimum margin of safety near the calculated value when subjected to the design load. The overtest, of course, provides a more definite validation of the margin of safety; it also has the advantage of verifying the critical motor failure mode. While either test could conceivably involve a live firing of the rocket motor, more information may be gained by using a cold gas or liquid pressurization to simulate a firing⁽¹⁸⁾.

In practice, the margin limit test is more commonly used. One reason for this is that a valuable motor asset is thus saved for other possible uses. Another reason is that a conservatively-designed motor may be nearly impossible to fail without destroying the validity of the test as a margin of safety verification. For instance, cooldown to failure may require cooling the motor to temperatures below the glass transition temperature of the propellant. In any case, drastic departures from the design condition may result in spurious motor failure modes.

Another useful tool for aiding in verifying the structural capability of motors once the design and

manufacturing procedures have been established is motor dissection⁽¹⁸⁾. Propellant and bondline specimens from dissected motor samples are the only direct assurance that the laboratory data on material properties is truly representative of the actual materials in the rocket motor. The results of motor dissection frequently show the presence of property gradients and other variations from "laboratory" test articles that must be taken into account for an accurate structural integrity assessment⁽¹⁹⁾.

Structural test vehicles or analog motors (with or without in-situ instrumentation) are sometimes used in the structural integrity verification process. Structural tests of these devices provide an indirect check on material properties and structural analysis procedures since they are more like the actual motor than are simpler laboratory samples.

Service Life Analysis

The goals of rocket motor design do not end at assuring the initial structural integrity and performance of the rocket motor. The designer must assure that the motor has the potential to survive for the intended service life. Typical service life goals are from 5 to 20 years; furthermore, the system user requires anywhere from 2 to 5 years' "visibility" (i.e., warning) of the impending end of the service life of any group of motors in order to prepare for motor replacement.

The techniques used for service life analysis and service life assurance vary, depending largely upon the cost of individual motors. For tactical motor systems, there are typically large numbers of rocket motor assets available for this purpose, and the cost of each unit is relatively small. Under these conditions, testing of many individual motors for service life assurance is practical, and the emphasis in current service life assurance programs for tactical motors is primarily on test firings of aged (either in the field or in controlled storage) motors. However, the trend of developing technology is to place more emphasis on temperature-accelerated aging and accelerated damage of motors, motor dissection, and motor structural overtesting^(19, 20). A greater emphasis is being placed on the role of structural analysis and cumulative damage analysis as well.

For larger and more expensive motors with a smaller total population, the emphasis is on analysis, laboratory testing and analog motor testing. The basic premise is that the motor service life is limited by the degradation in structural integrity with age. In the ideal service life assurance program, initial structural overtests of full-scale production motors are used to define the actual motor failure modes. The overtests thus provide the focus for material property testing on aged grain materials and for structural analysis updates, as well as validation of the original structural analysis models. Analog test devices designed to duplicate the critical motor regions provide additional failure data without the cost of testing full-scale motors. Material property tests are performed according to carefully planned time-phased, multilevel test matrices based on chemical-structural aging considerations. Maximum use is made of temperature-accelerated aging techniques and dissected motor propellant grain material samples^(18, 21). In actual programs, however, the full ideal service life assurance program is often somewhat curtailed.

UNRESOLVED PROBLEMS

The primary unresolved problems in propellant grain design were alluded to in the foregoing discussion. The two problems of greatest concern are the current inability to model the nonlinear aspects of solid propellant behavior in routine structural analysis, and the inability to successfully employ fracture mechanics in routine structural analysis. Government-sponsored work is being conducted in both areas, and in the long term, satisfactory solutions to both should become available.

The area of greatest impact is that of nonlinear propellant behavior. Work on nonlinear mechanical constitutive theories for propellant grain materials under Air Force sponsorship has proceeded intermittently for more than 10 years^(8, 22, 23). Some results from the most recent completed effort⁽⁸⁾ will provide insight into the magnitude of some aspects of propellant nonlinear behavior.

The linear viscoelastic techniques discussed above were carefully applied to a variety of loading conditions, using a Prony series representation of the relaxation modulus⁽⁸⁾. The success of the linear viscoelastic techniques in predicting the stress response to different constant strain rate loading histories varied with the strain rate. When a slightly more complex loading history (a dual-rate history) was attempted, the results were as shown in Figure 15. Notice that the stress was overpredicted by more than 50 percent at the end of the higher-rate segment of the loading history. Under a more complex loading history with some cyclic content (as well as creep at zero load during some portions of the strain history), the linear viscoelastic prediction (Figure 16) was in error more than 100 percent over significant portions of the history.

Part of the nonlinear response of the propellant is a manifestation of damage. This is illustrated in Figures 17 and 18. These figures are "hysteresis plots," or stress-strain curves for a sample subjected to a sawtooth strain history consisting of a constant strain rate loading process, followed immediately by a constant-rate unloading process to the zero-stress point, whereupon the sample was allowed to creep under zero load. After a period of "rehealing" time, the entire process was repeated. Figure 17 shows the results for "zero" rehealing time. While the stress response of Figure 17 shows that the sample had not fully recovered to its original length, the more significant aspect of the response on the second loading is the characteristic "s-shaped" stress-strain curve. This "s" shape is considered to be characteristic of damage. A closely-related characteristic is the tendency to return to the "virgin curve" as the previous maximum strain level is approached⁽²³⁾. To further complicate matters, these damage-induced phenomena tend to slowly disappear if the propellant is allowed to "heal" in a stress free condition for a time. As shown in Figure 18, less than a day of "healing" time produces a significant degree of recovery of the original behavior. After 30 days of healing time, essentially all traces of damage typically will have disappeared. For identical first and second

loadings, the response characteristics of the "virgin" hysteresis loop appear to be recovered in the following order: (1) unloading response; (2) strain at zero stress; (3) maximum stress; (4) loading response. The first two recovery phenomena may possibly be explainable by linear viscoelasticity; however, the damage phenomenon itself and the second two recovery phenomena are definitely recognized as nonlinear behavior.

Another nonlinear phenomenon is exhibited when propellant is subjected to combined straining and cooling(9). As shown in Figure 19, linear viscoelastic analysis drastically underpredicts the stress response of propellant under these conditions.

The recently completed Air Force sponsored research contract on nonlinear constitutive theories for solid propellant(8) resulted in significant improvements in stress prediction capability for isothermal loads; of five candidate constitutive laws investigated, three were developed to the point of being able to predict stresses for the load histories of Figures 14 and 15 to within 10 percent of the measured values. However, combined straining and cooling and response under pressure were not directly addressed. A follow-on contract now in the early stages will continue the constitutive law development to cover these loading conditions; in addition, humidity will be incorporated into the constitutive law as a constitutive variable. One of the more challenging aspects of the follow-on contract will be incorporating the constitutive law into a finite element code so that it can be assessed by comparing predicted responses with measured responses in instrumented motor tests.

REFERENCES

1. Sutton, G. P. and Ross, D. M., Rocket Propulsion Elements, 4th ed., New York, John Wiley and Sons, Inc., 1976, pp 354-382.
2. Lamberty, J. T., United Technologies Corp., Chemical Systems Division, "A Report on the Grain Design and Internal Ballistic Module of the Improved Solids Performance Program," 19th AIAA Aerospace Sciences Meeting, St Louis Mo., Jan. 1981 (AIAA Paper 81-0034).
3. Sforzini, R. H., "Automated Approach to Design of Solid Rockets," J. Spacecraft, Vol. 18, No. 3, May 1981, pp 200-205.
4. Williams, M. L., Blatz, P. J., and Schapery, R. A., California Institute of Technology, "Fundamental Studies Relating to Systems Analysis of Solid Propellants," Final Report, GALCIT 101, Feb. 1961.
5. Leighton, R. A., Air Force Rocket Propulsion Laboratory, "Quick-Look Structural Analysis Techniques for Solid Rocket Propellant Grains," 1982, AFRPL-TR-81-80.
6. Fullbright, J. L., Rockwell International Corp., Rocketdyne-McGregor Div., "Stress Relieving Liners for Air-Launched Tactical Rocket Motors," 13th AIAA/SAE Joint Propulsion Conference, Orlando, Fla., Jul. 1977 (AIAA Paper 77-827).
7. Ferry, J. D., Viscoelastic Properties of Polymers, 2nd ed., New York, John Wiley and Sons, Inc., 1970, p. 318.
8. Francis, E. C. et al, United Technologies Corp., Chemical Systems Division "Solid Propellant Nonlinear Constitutive Theory Extension," 1984, Air Force Rocket Propulsion Laboratory Report AFRPL-TR-83-071.
9. Noel, J.S., Rockwell International Corp., Rocketdyne-McGregor Div., "Solid Propellant Grain Structural Integrity Analysis," 1973, NASA SP-8073.
10. Thrasher, D. I. and Corbett, E. C., Air Force Rocket Propulsion Laboratory, "An Analysis of a Solid Propellant Transient Viscoelastic Response under Motor Ignition Conditions," 1982, AFRPL-TR-81-55.
11. Herrmann, L. R., and Toms, R. M., "A Reformulation of the Elastic Field Equation, in Terms of Displacements, Valid for all Admissible Values of Poisson's Ratio," J. Applied Mechanics, Trans. ASME, Vol. 86, pp 140-141, 1964.
12. Zienkiewicz, O. C., The Finite Element Method in Engineering Sciences, 2nd Ed., New York, NY, McGraw-Hill, Inc., 1971.
13. Hofmeister, L. D., Isoparametric Finite Element Analysis for Solid Rocket Motors, Computers and Structures, Vol. 3, Nov. 1973, p. 1369-1376.
14. Smith, T. L., "Characterization by a Time and Temperature Independent Failure Envelope, J. Polymer Science, Part A, Vol. 1, No. 12, Dec. 1963, pp 3597-3615.
15. Fillers, R.W., and Tschoegel, N.W., "The Effect of Pressure on the Mechanical Properties of Polymers," Trans. Soc. Rheol., Vol. 21, No. 1, 1977, pp 51-100.
16. Procinsky, I.M., and McHale, C.A., "Nozzleless Boosters for Integral-Rocket-Ramjet Missile Systems," J. Spacecraft, Vol. 18, No. 3, May 1981, pp 193-213.
17. Danieu, D. J., and Ruggles, V. L., Thiokol Chemical Corp., "Minuteman STV Stress Analysis and Testing," 1974, Air Force Rocket Propulsion Laboratory Report AFRPL-TR-74-27.

18. Neely, R. B., TRW Systems Group, and Veit, P. W., Aerojet Solid Propulsion Co., "Solid Rocket Motor Grain Design Verification Through Cold Gas Pressurization and Motor Dissection," AIAA/SAE Joint Propulsion Conference, San Diego, Ca., Oct. 1974 (AIAA Paper 74-1202).
19. Thrasher, D. I., and Hildreth, J. H., "Structural Service Life Estimate for a Reduced Smoke Rocket Motor," J. Spacecraft, Vol. 19, No. 6, Nov. 1982, pp 564-570.
20. Svob, G. J., and Bills, K. W., "Predictive Surveillance Technique for Air-Launched Rocket Motors," J. Spacecraft, Vol. 21, No. 2, Mar. 1984, pp 162-167.
21. Kelley, F. N., and Trout, J. L., Air Force Rocket Propulsion Laboratory, "Elements of Solid Rocket Service Life Prediction," 8th AIAA/SAE Joint Propulsion Conference, New Orleans, La., Nov. 1972 (AIAA Paper 72-1085).
22. Quinlan, M. H., "Materials with Variable Bonding," Arch. Rational Mech. Anal., Vol. 67, 1978, pp 165-181.
23. Quinlan, M. H., Air Force Rocket Propulsion Laboratory, "An Application of the Theory of Materials with Variable Bonding to Solid Propellant," 1979, AFRPL-TR-78-37.

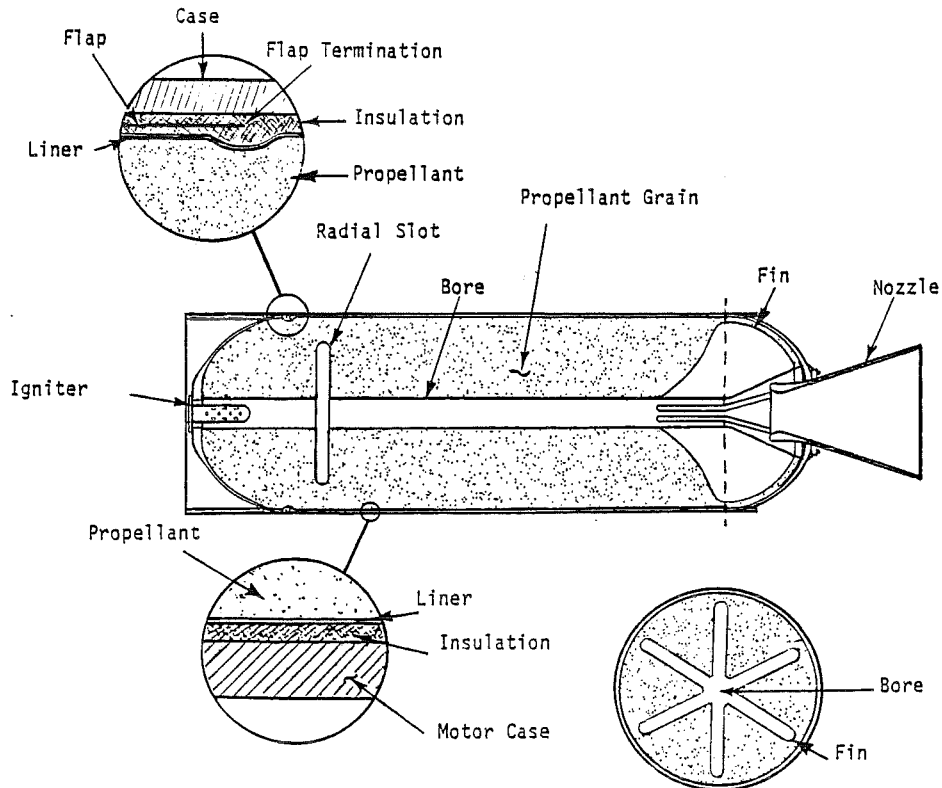


Figure 1. Generic Solid Propellant Rocket Motor

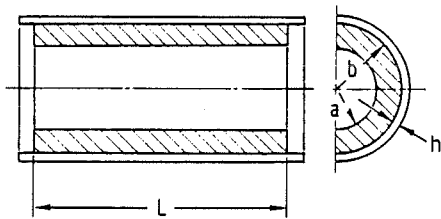


Figure 2. Basic Geometry Parameters

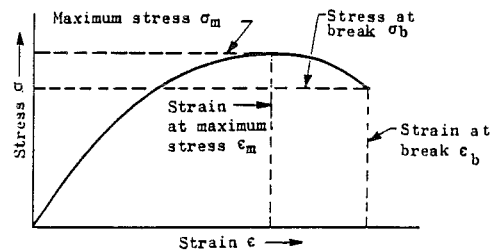


Figure 3. Uniaxial Stress-Strain Behavior at Constant Strain Rate

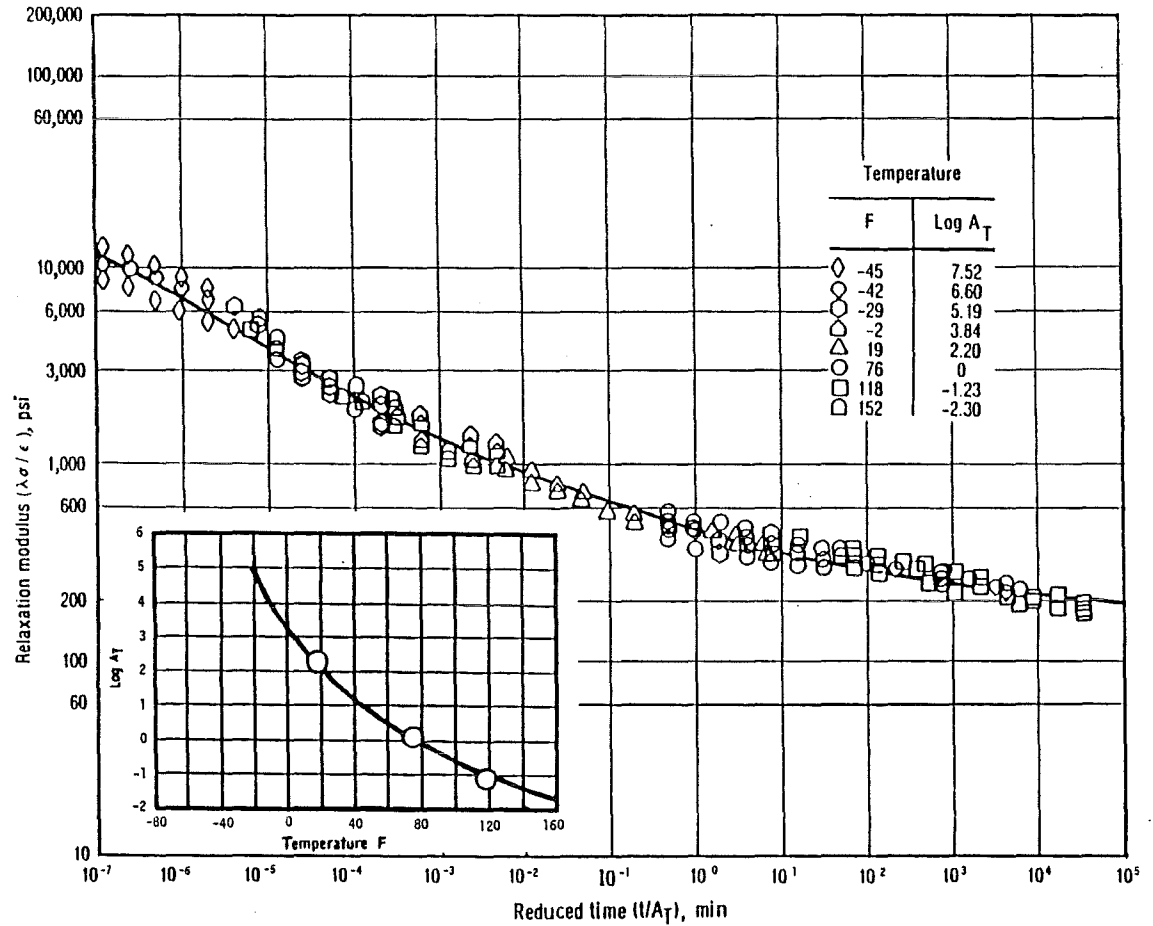


Figure 4. Stress Relaxation Modulus Master Curve for a Typical Solid Propellant

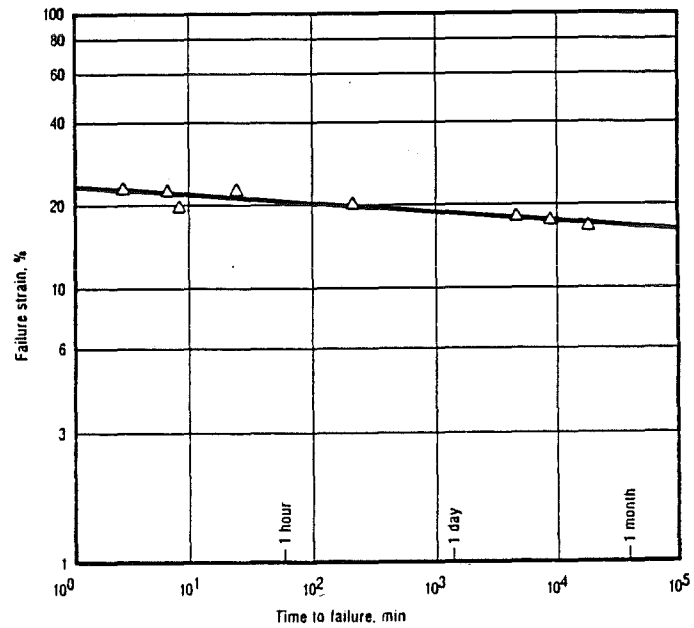


Figure 5. Strain Endurance Data for a Typical Solid Propellant

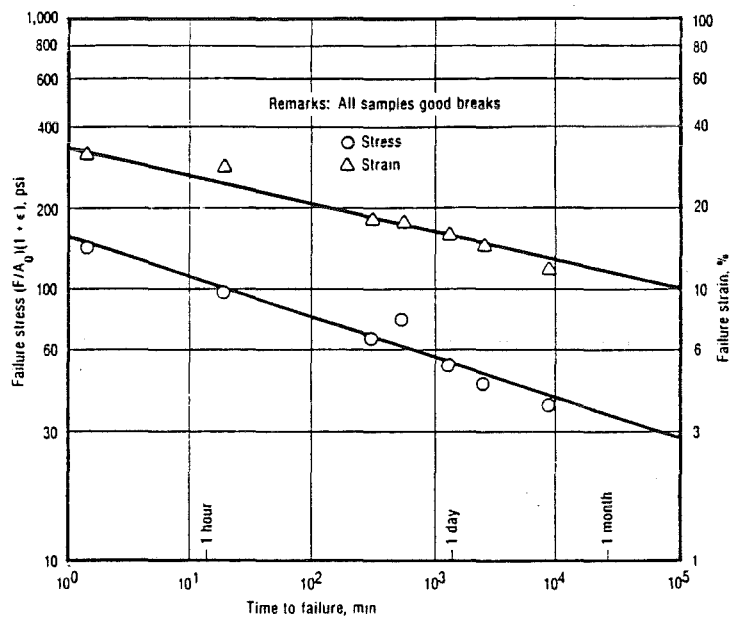


Figure 6. Stress Endurance Data for a Typical Solid Propellant

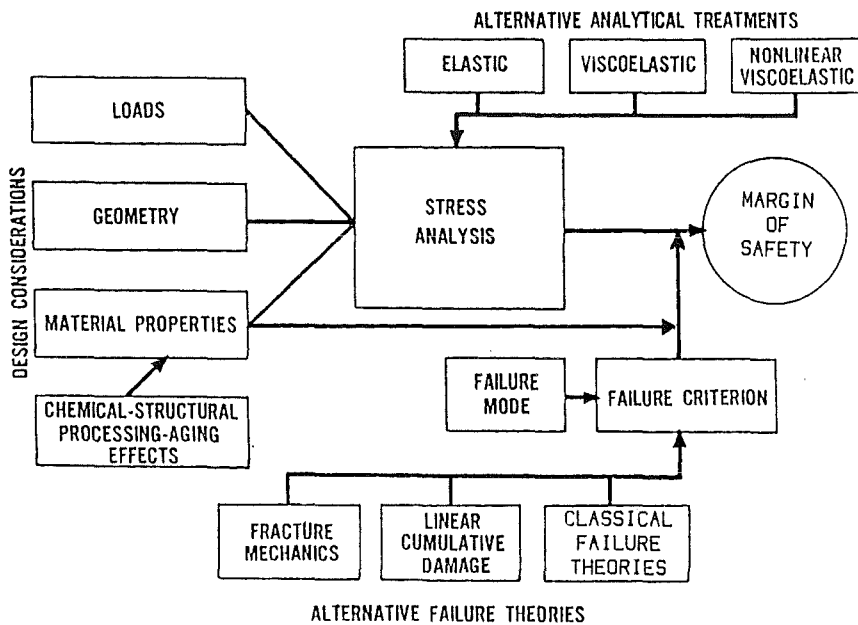


Figure 7. The Structural Analysis Process

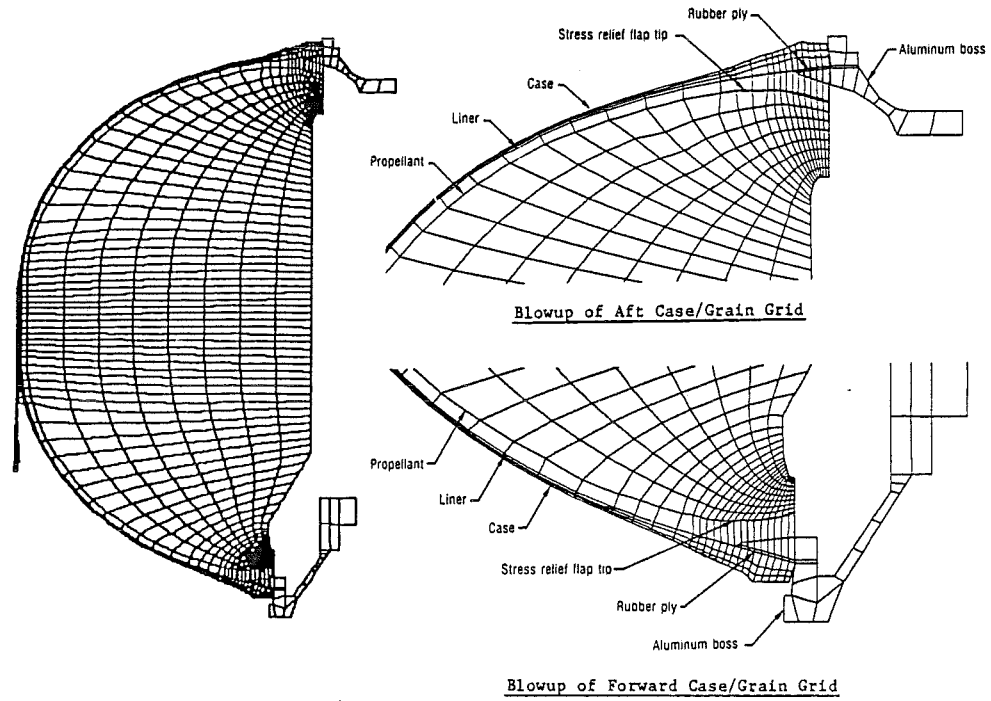


Figure 8. Typical Finite Element Model (Composite-Case Motor)

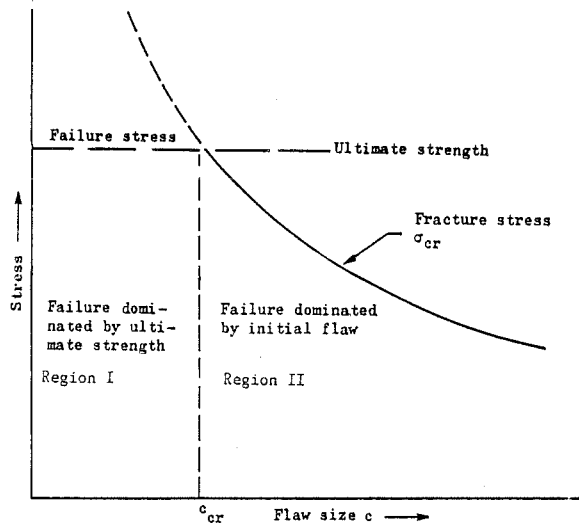


Figure 9. Conceptual Relation Between Flaw Size and Type of Failure

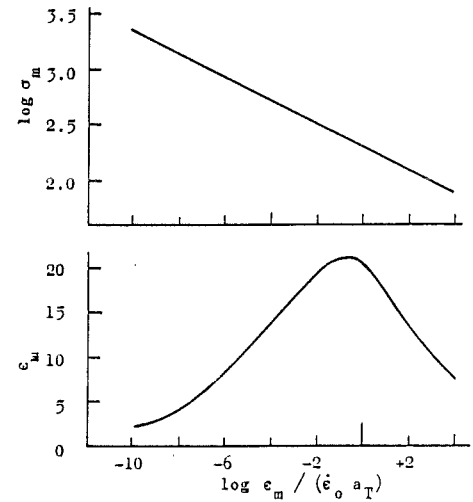


Figure 10. Constant-Rate Failure Data Master Curves (Schematic)

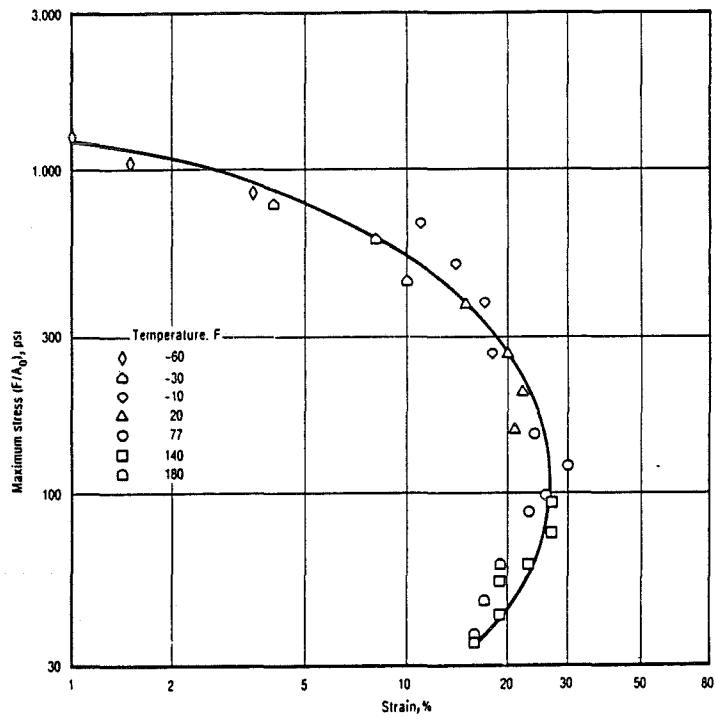


Figure 11. Stress-Strain Failure Envelope for a Typical Propellant

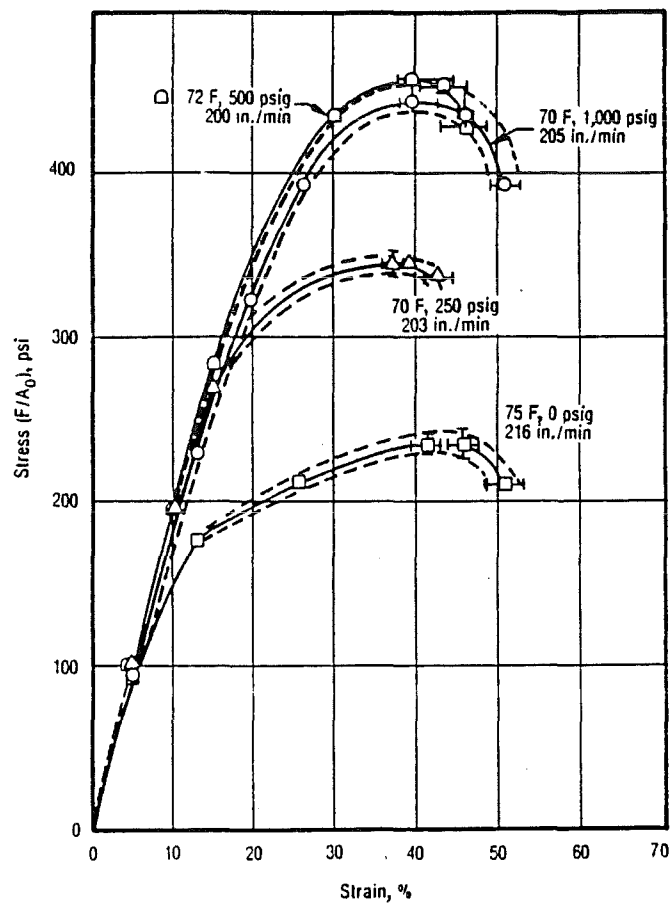


Figure 12. Effect of Superimposed Pressure on Uniaxial Sample Stress at Constant Strain Rate

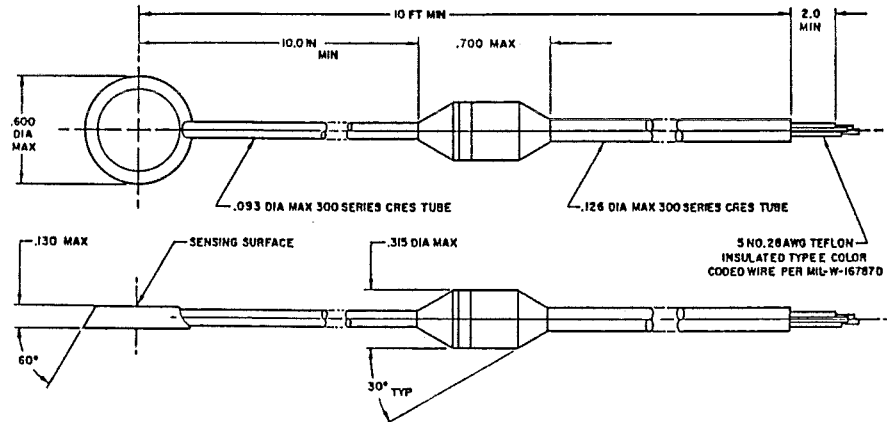


Figure 13. Normal Stress Transducer

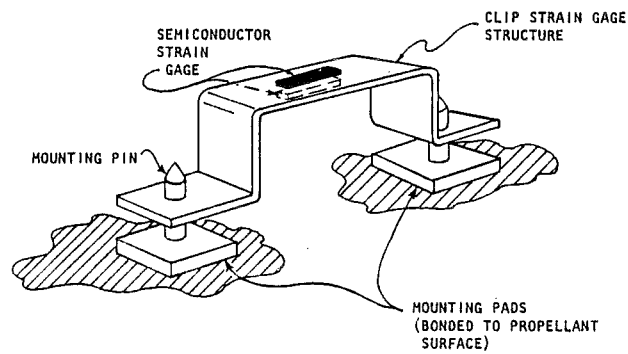


Figure 14. Clip Strain Gage

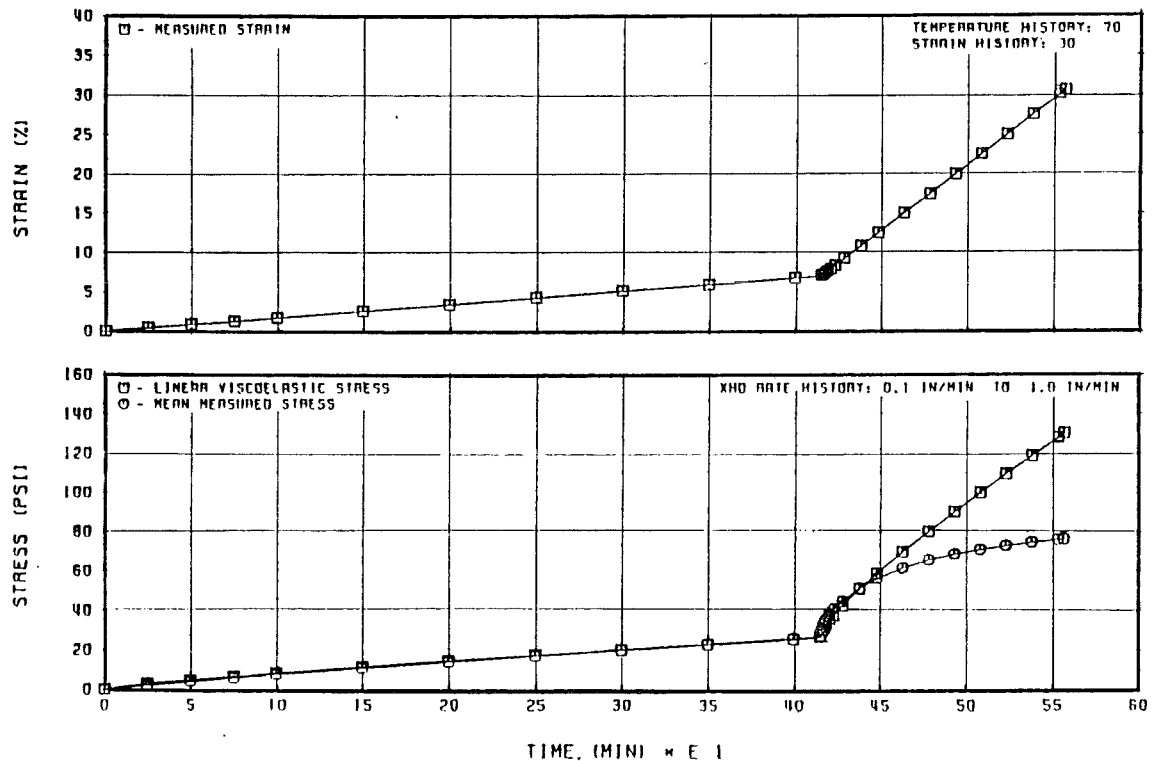


Figure 15. Linear Viscoelastic Stress Prediction Compared to Measured Stress (Two-Rate Strain History)

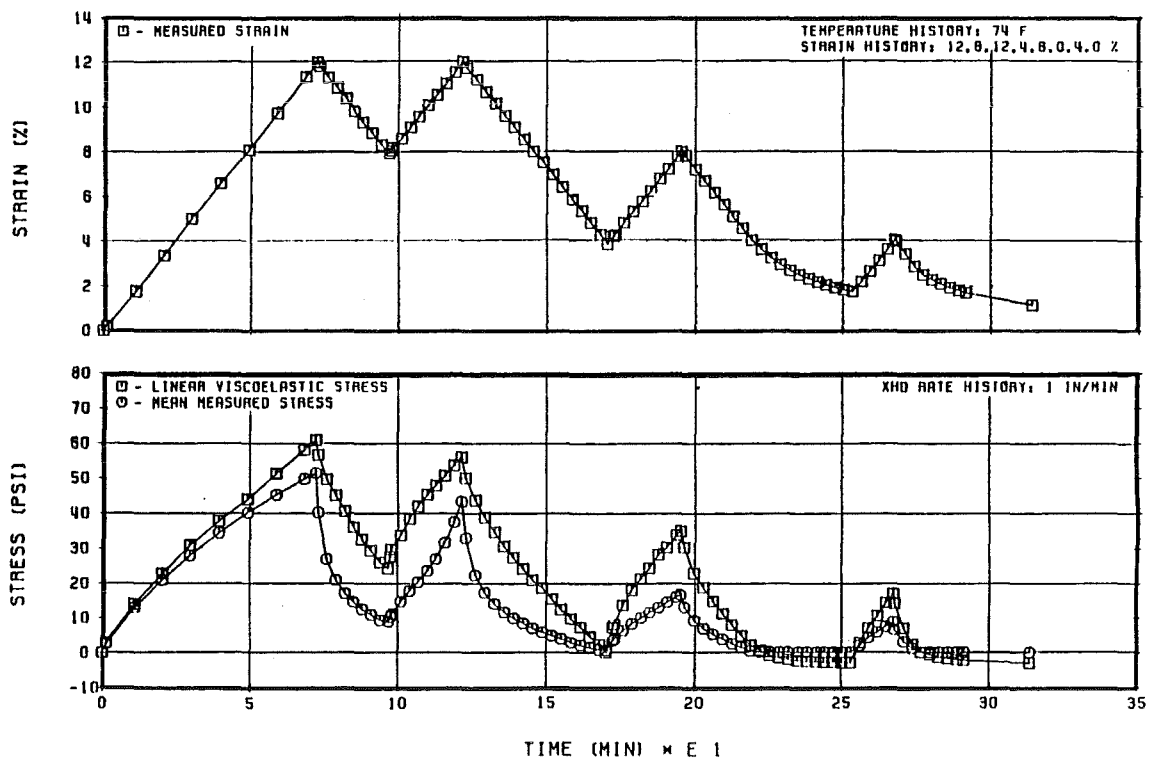


Figure 16. Linear Viscoelastic Stress Prediction Compared to Measured Stress (Complex Strain History)

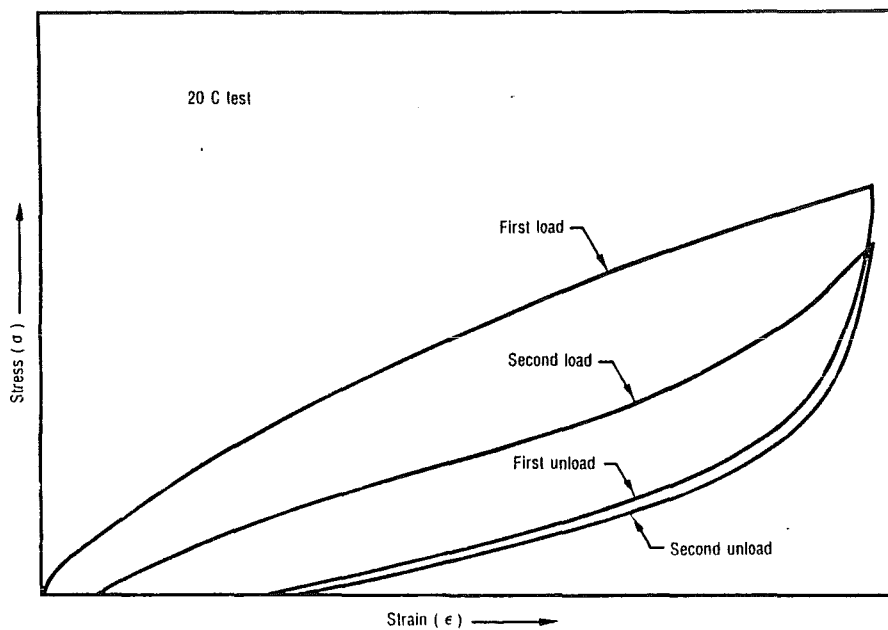


Figure 17. Load-Unload Curves with Zero Healing Time

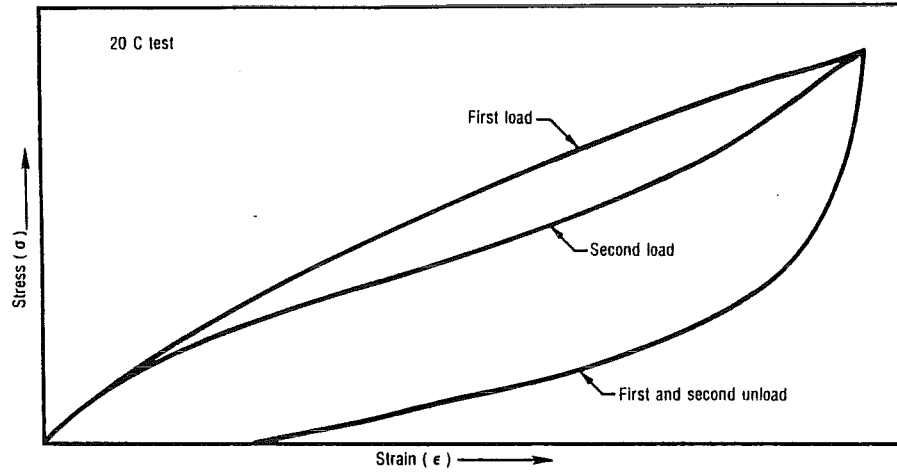


Figure 18. Load-Unload Curves with 1000 Minutes' Healing Time

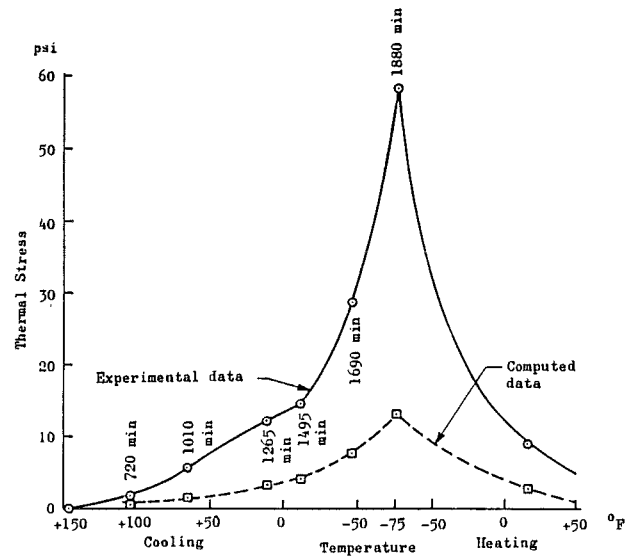


Figure 19. Stress Response Under Combined Straining and Cooling

DESIGN AND ANALYSIS OF SOLID ROCKET MOTOR INTERNAL INSULATION

by

Mr A.Truchot
Agence Spatiale Européenne
Division STS-AR
8-10, rue Mario Nikis
75738 Paris Cedex 15
France

ABSTRACT

The main purpose of internal insulation is to protect the motor case from the thermal environment of propellant combustion products. Several secondary objectives must also be met. Internal insulation must bond to propellant and case, transmit case strain into propellant and sometimes seal the case.

In the first step, the general process of internal insulation design is presented : evaluation of thermal environment, selection of material, thermal and structural analyses. For each phase the different analysis methods are described : aerodynamic, thermal, and structural.

To conclude the presentation, the different phases of internal insulation fabrication are presented : elastomer formulation, fabrication of parts and integration into the motor case.

1. - INTRODUCTION

The main purpose of internal insulation is to protect the motor case from the thermal environment of combustion products. The following objectives must also be met :

- . bonding to propellant and case
- . inhibition of certain propellant grain surfaces
- . transmission of case strain into propellant
- . tightness of the case for composite chambers.

The case insulation integrity must be maintained during the life expectancy of the motor. The elastomers used must maintain their properties during aging and environmental conditions.

2. - DESIGN OF INTERNAL INSULATION

The general configuration of a motor case loaded with propellant is presented in figure 1. The internal insulation is located between the propellant and the case. The internal profile of the insulation is sized so that the maximum quantity of propellant can be introduced into the structure. The stress relief flaps, which are represented in the forward and aft domes, are used to prevent case deformations due to internal pressure from inducing excess stresses in the internal insulation or propellant.

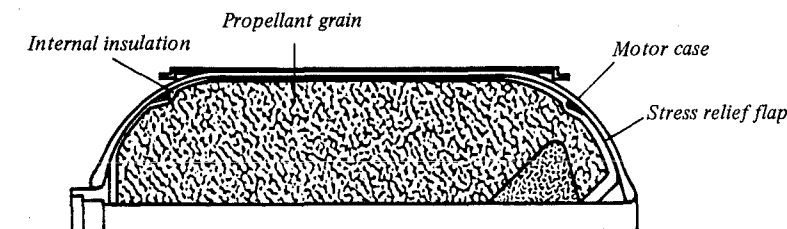


Fig. 1 - GENERAL CONFIGURATION OF INTERNAL INSULATION

The general process of the internal insulation design is presented in figure 2. This process involves four steps.

Evaluation of thermal environment

In the preliminary phase an evaluation of the thermal environment is required. The design of internal insulation depends on parameters such as combustion pressure, duration, internal flow fields, combustion geometry, and type of propellant.

Selection of material

The selection of the material is based on its thermal and mechanical properties.

Thermal analysis

This step calculates the thickness of insulation on each point of the internal profile of the case.

Mechanical analysis

A mechanical analysis of the motor case loaded with propellant, subjected to loads such as thermal gradients or internal pressure, is required in order to verify the structural behavior of internal insulation. This step allows to refine the stress relief flaps design.

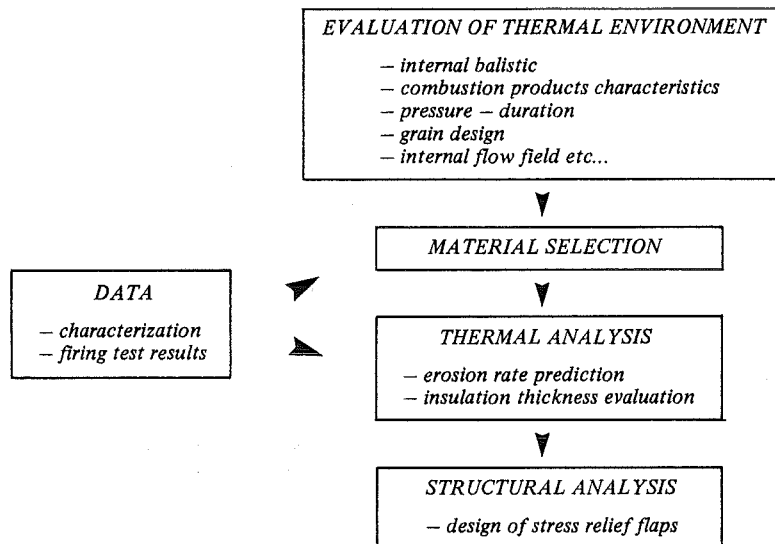


Fig. 2 - DESIGN PROCESS

2.1. Thermal environment evaluation

The insulation thickness is a function of exposure time of each point of the internal profile of the case. For this reason the design of internal insulation is greatly dependant on the combustion geometry. Thus in the example presented in figure 3, the insulation thickness varies from 14 to 1 millimeter, depending on the exposure time of each point.

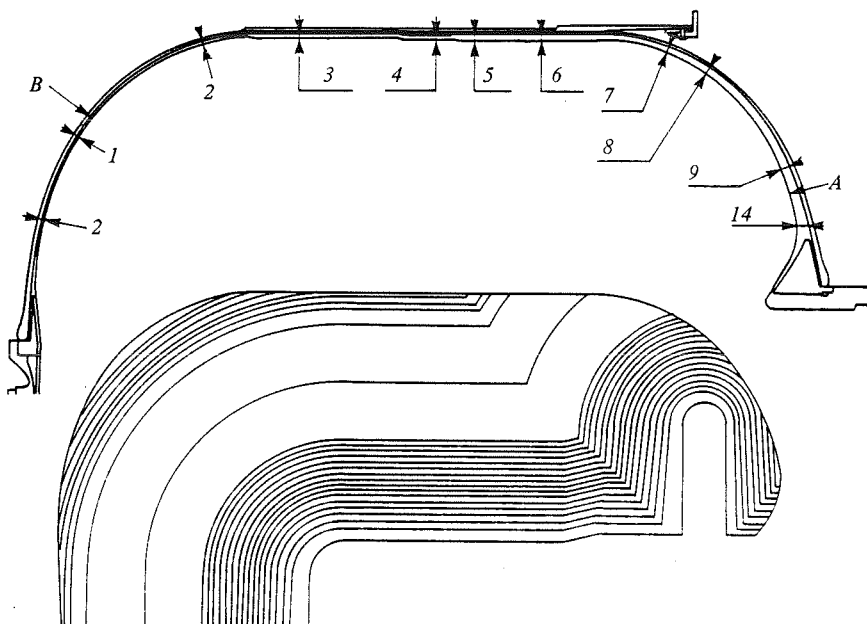


Fig. 3 - EFFECT OF GRAIN DESIGN ON INTERNAL INSULATION THICKNESS

The erosion rate of internal insulation increases with the gas velocity. Thus for external nozzles, the aft dome erosion rate is greater due to the increase of gas velocity near the wall. A decrease in rubber thickness is possible with submerged nozzles, because the gas velocity near the aft dome is significantly lower.

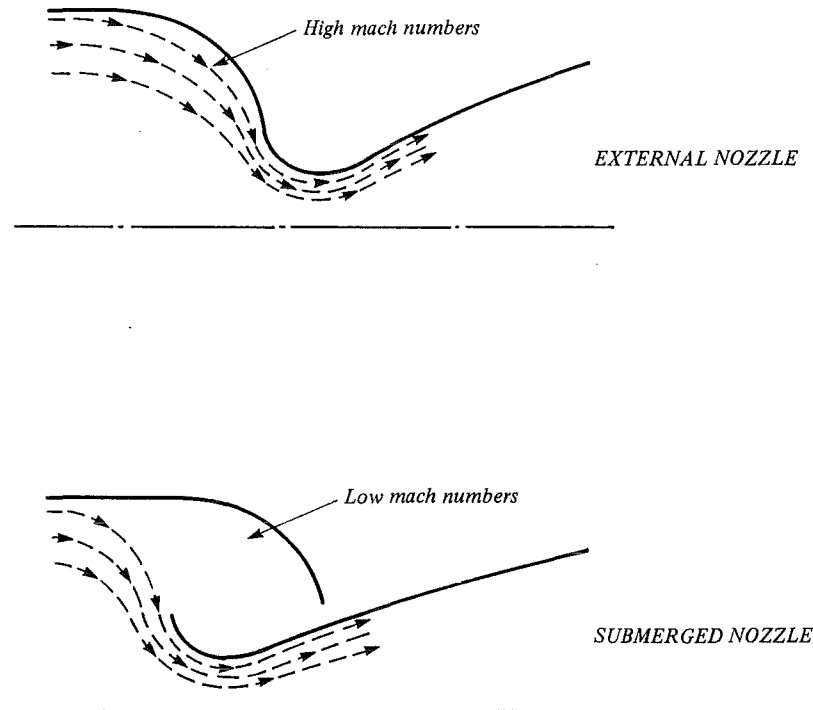


Fig. 4 - EFFECT OF NOZZLE CONFIGURATION ON INTERNAL INSULATION DESIGN

The design of internal insulation is also a function of propellant grain design. Thus for finocyl grains, the internal flow is greater in front of the slots, creating a non symmetric erosion of internal insulation.

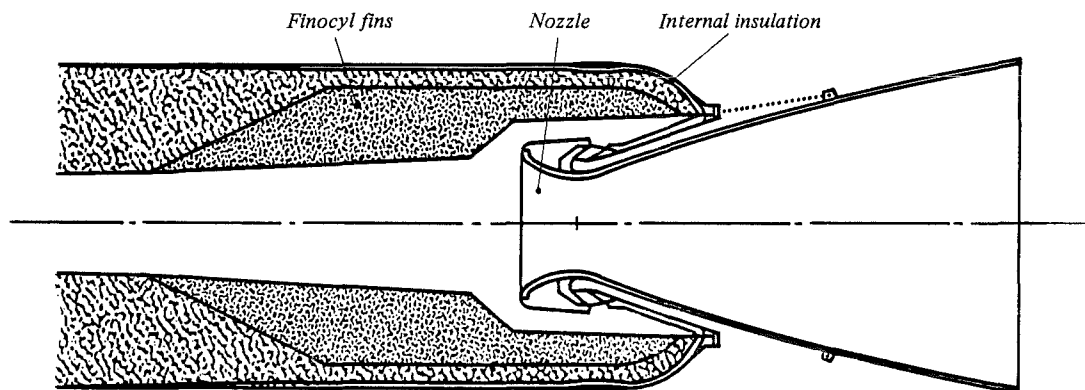


Fig. 5 - FINOCYL GRAIN

These two examples illustrate the importance of an accurate evaluation of the internal flow field inside the motor case. For this purpose, two or three dimensionnal analyses are used to calculate gas velocity in the motor. The results of a typical analysis are presented in figure 6. This analysis uses a method of singularity assuming an irrotational and ideal gas.

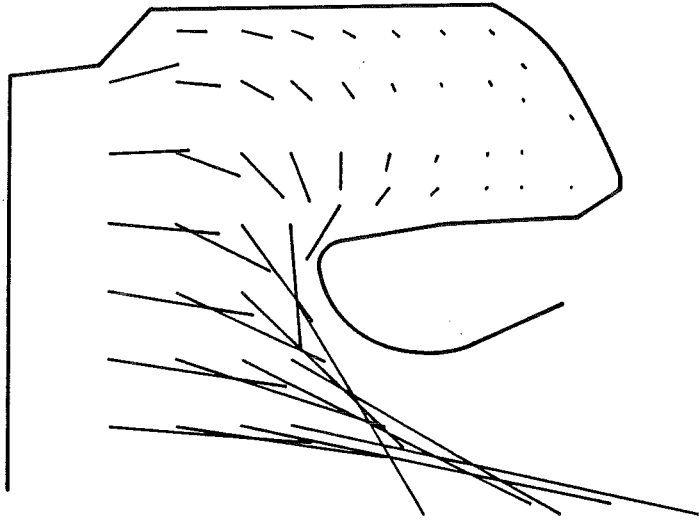


Fig. 6 - 3D INTERNAL FLOW FIELD ANALYSIS

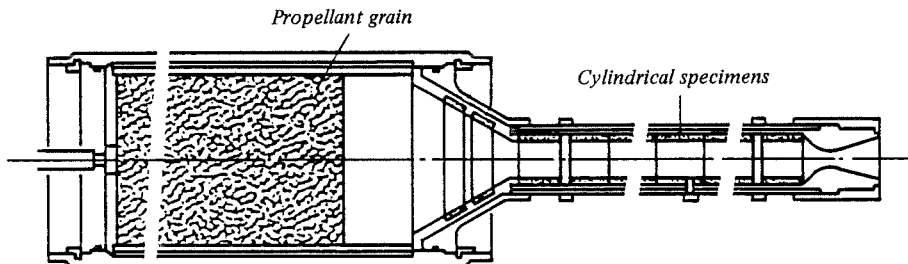
2.2. Material selection

The selection of rubber is based on thermal and mechanical properties. Thermal properties are based on laboratory characterizations and firing tests results. The mechanical properties are a measurement of the material behavior in response to applied tensile and shear forces. Testing of bonding to the propellant and the case is also required.

a) Thermal properties :

The thermal diffusivity of a rubber can be measured by tests performed in laboratory. However this sort of testing is limited in temperature by the chemical decomposition of rubber, which occurs at approximately 300°C. The response of rubber to a heat flux can be evaluated by tests using oxyacetylene torch or plasma arc. These tests are not representative of the ablation process by hot gases and firing test are required to evaluate ablation as a function of propellant gas velocity.

Preliminary firing tests are performed at a reduced scale, in order to investigate a large number of specimens at a low cost. Later fullscale tests are performed. Two examples of test motor are presented in figure 7. The first one evaluating specimens with constant gas velocity and the second one with variable gas velocity.



First case : constant velocity gas

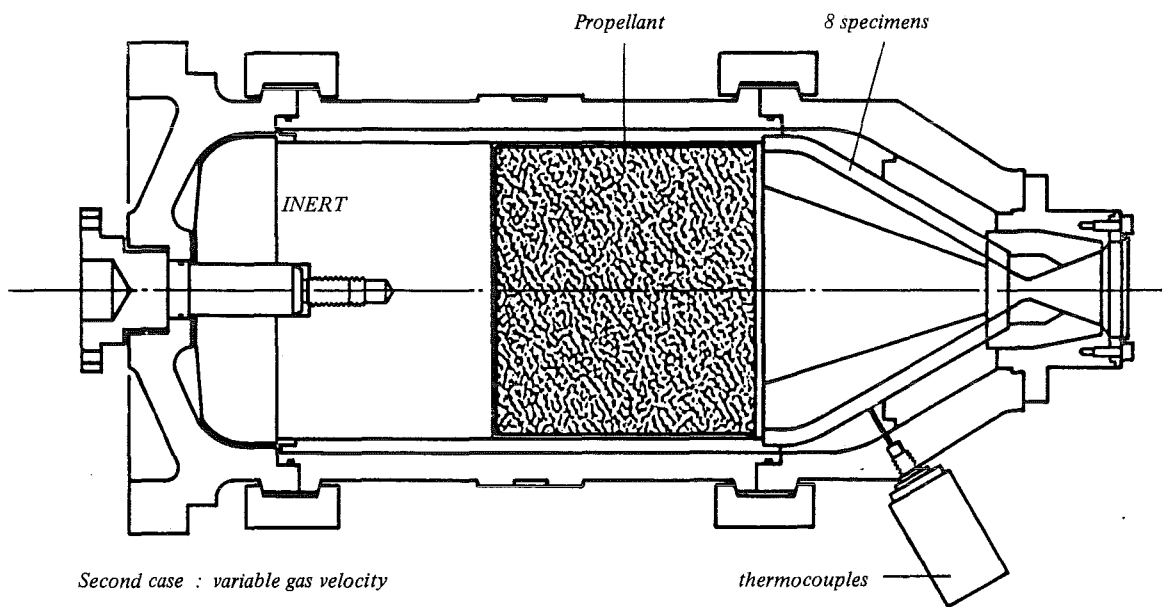


Fig. 7 - SUBSCALE FIRING TESTS SCREENING OF MATERIALS

These tests obviously present limitations and can not replace fullscale tests, but they permit evaluation of many specimens at a low cost, with different test conditions.

b) Mechanical properties :

The mechanical response of an elastomeric material to applied forces is measured by tensile or shear specimens. Typical specimen geometries and measured stress-strain curves are presented in figure 8 and 9.

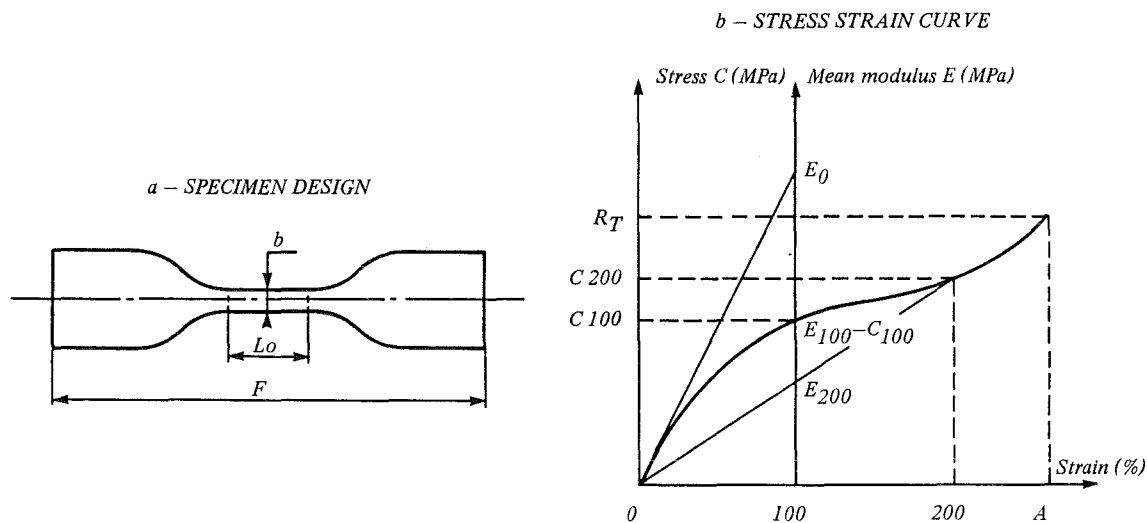


Fig. 8 - TENSILE TEST

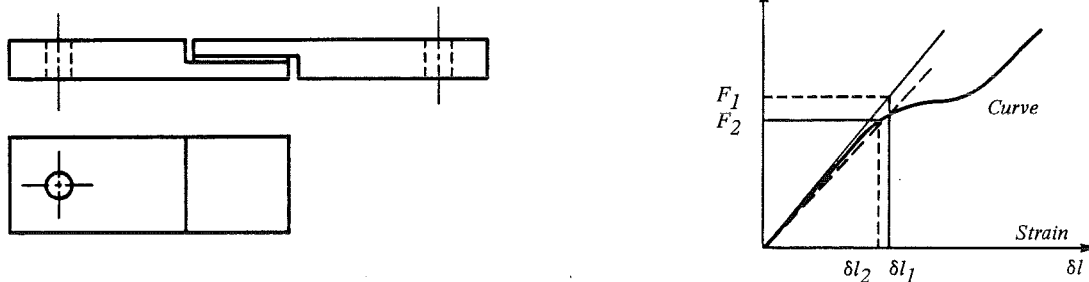


Fig. 9 - SHEAR TEST

A common test for elastomers is the peel test. This test does not give tensile or shear data but it does verify bonding to the propellant and the case.

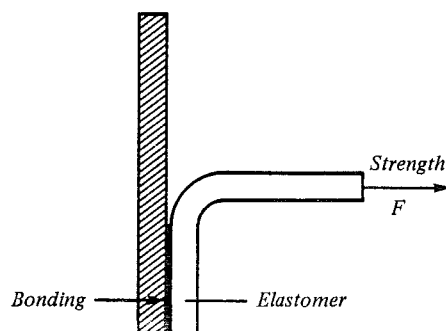


Fig. 10 - PEEL TEST

2.3. Thermal analysis

The criterion for thermal analysis is the maximum allowable temperature of the motor case. This temperature is defined by the structural capability of the case and the bonding integrity of internal insulation. Sometimes some equipment located near the motor case can be a limitation factor.

2.3.1. Ablation process by hot gases

At a specific time of combustion, three zones can be considered in the insulation thickness (see figure 11).

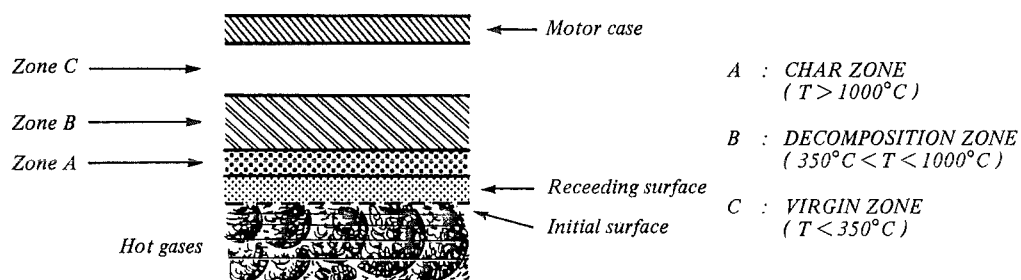


Fig. 11 - ABLATION PROCESS

In the virgin zone near the motor case (zone c) the temperature is low and the decomposition reactions are not initiated. The heat transfer is achieved by a conduction process. In the decomposition zone (zone B), a great part of the energy is absorbed by the chemical reactions which are in majority endothermic. In this zone the energy transfer is achieved by a both conduction and mass transfer process. In front of the combustion products, the rubber is fully decomposed and is at the state of carbon char.

On this chemical erosion effect is superposed a mechanical erosion due to the friction of boundary layer. This effect becomes preponderant for gas velocities exceeding 40 m/s.

2.3.2. Analysis method

The ablation process is a very complex phenomenon depending on the combustion products, the elastomer formulation and the boundary layer configuration. For these reasons, its accurate modelling for thermal analysis is very difficult. Simplified methods are used in usual practice. One of these methods is presented in figure 12. This method consists to assume on isothermal ablation of the rubber. The eroded thickness is supposed to be a result of a constant erosion rate. This erosion rate is estimated with results obtained in firing test. Some empirical correlations are made in order to take into account parameters such as exposure time, gas velocity or combustion pressure. In the remaining material, the heat transfer is achieved by a conduction process with equivalent thermal properties.

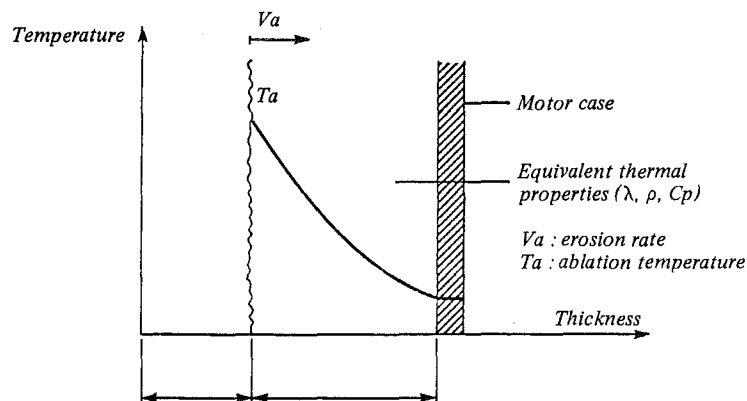


Fig. 12 - ANALYSIS METHOD

All the data needed for this calculation such as erosion rate, ablation temperature and equivalent thermal properties are obtained from firing test measurements.

2.4. Mechanical analysis

The mechanical analysis is the last step of internal insulation design. The loads can be thermal variations, flight loads or internal pressure at ignition.

Temperature variations can be induced by processing of propellant, handling or storage. These variations may induce stresses in the internal insulation by the difference of thermal expansion of the case and the propellant.

At motor ignition, the internal pressure creates different deformations of the case and propellant. The most severe conditions are obtained for ignition at low temperature. The effects of contraction of the grain due to temperature and expansion of the case due to internal pressure are directly cumulated.

Finite element analyses are used in order to verify the structural design of the case loaded with propellant. The results of a typical analysis are presented in figure 13 and 14, taking into account the cumulative effects of internal pressure at ignition and flight loads.

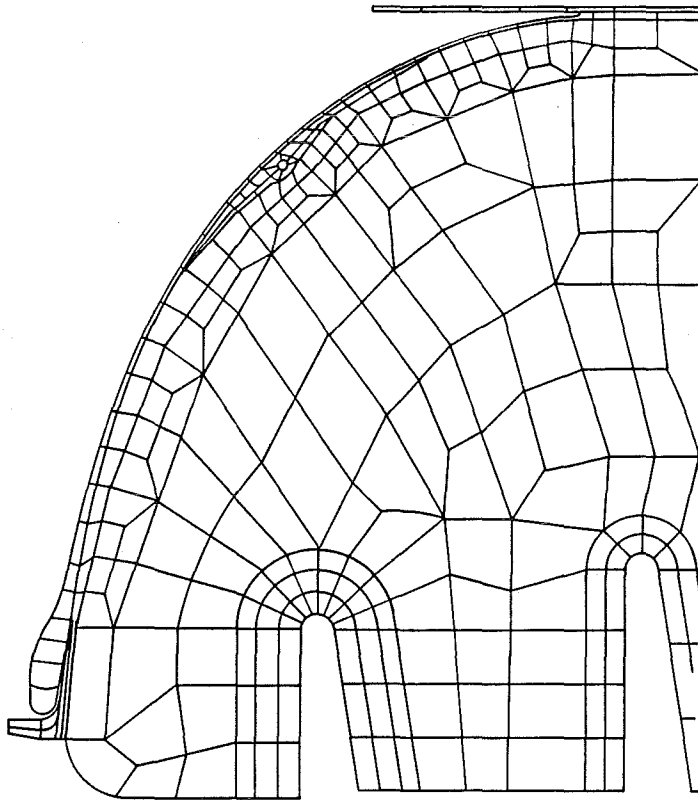


Fig. 13 - MODELING

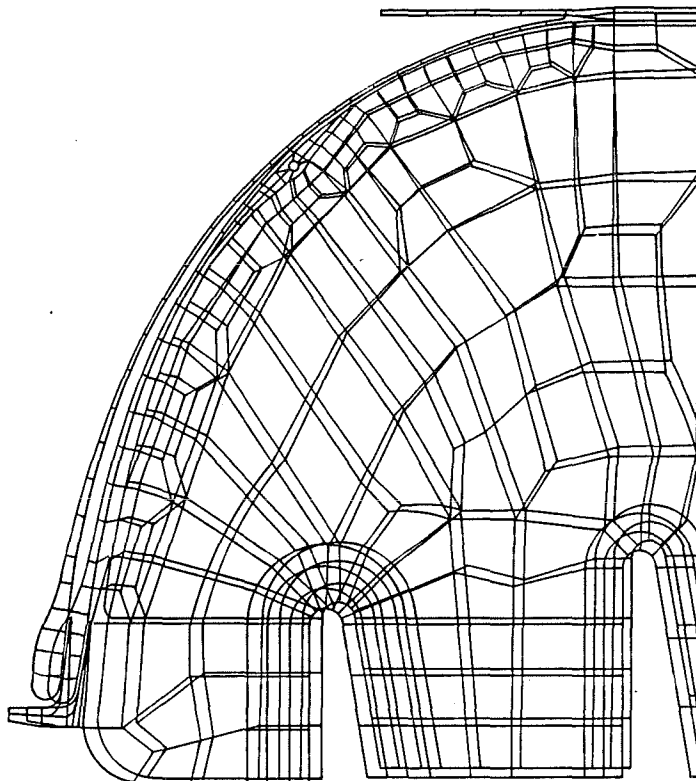


Fig. 14 - STRAIN CALCULATION

FINITE ELEMENT ANALYSIS

3. - INTERNAL INSULATION FABRICATION

The composition and fabrication of an elastomeric internal insulation are very similar to those of a classical reinforced plastic. The material consists of an elastomer such as EPDM or natural rubber, reinforcing fillers (carbon, silica or Kevlar) and different ingredients such as plasticizer, antioxidant and vulcanization agents. The fabrication of the part is made by the same processes as those used for reinforced plastics : molding, winding or lay-up.

3.1. Elastomer formulation

Some elastomers used for internal insulation are presented in table 1. Sometimes a formulation can use a mixing of these different ingredients.

NAME	ASTM ABBREVIATION	DENSITY
Natural	NR	0.93
Butyl	IIR	0.93
EPDM	EPDM	0.86
Neoprene or Polychloroprene	CR	1.23

Fillers have no chemical effect in the formulation of the rubber. They are used as reinforcement in order to improve thermal and mechanical properties of the product. The main fillers which have been used for internal insulation are carbon black, asbestos, silica or kevlar. The erosion resistance of the material is a function of the filler used.

Other ingredients are added to the formulation such as plasticizer, which are used to facilitate mixing of the ingredients, vulcanization agents, antioxidants, etc...

3.2. Fabrication of the part

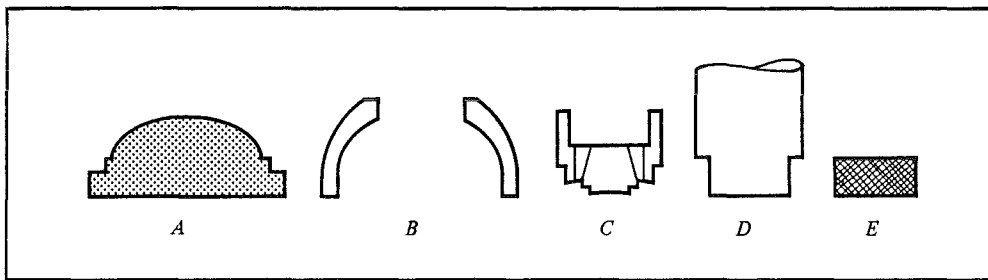
The fabrication of an elastomeric internal insulation involves 4 phases.

Initially a compounding process is used in order to blend the different ingredients. This operation uses internal mixers or rollmills. This step is an important phase of the process and the quality of the final product is greatly dependant on this operation.

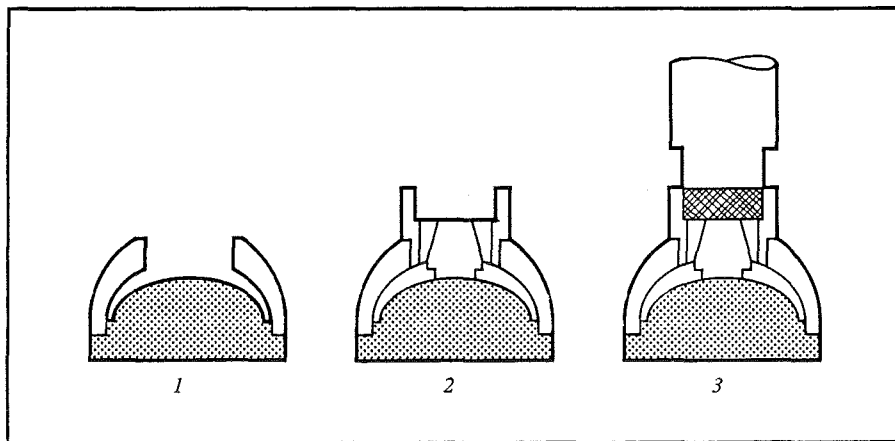
In a second step a calendaring process is used in order to give to the unvulcanized rubber the shape of sheets thus allowing the fabrication of the part.

The fabrication of the part is made by processes such as molding, lay-up or winding. A molding process (see exemple in figure 15) is well suited for small parts produced in large quantities. However the cost of tooling is very high and for reduced quantities, a lay-up process can be used (see figure 16). This type of process is difficult to automate. For this reason, winding process becomes more and more usual. This process presented in figure 17, leads to a more reproducible quality at a lower cost.

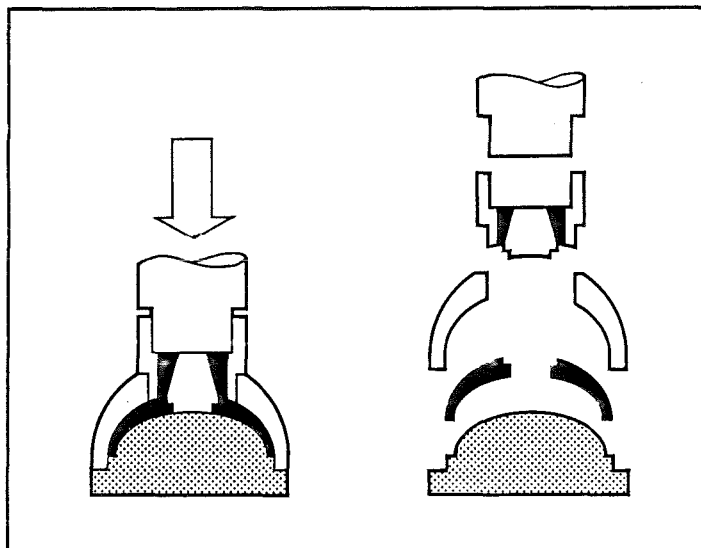
The vulcanization is an operation of curing under pressure, thus giving the final thermal and mechanical properties to the part. For molded parts, vulcanization can be performed by heating with electrical resistances incorporated into the mold.



A - B : TRANSFER MOLD
C : MATERIAL RESERVOIR
D : PISTON
E : MATERIAL



TOOL ASSEMBLED



VULCANIZATION

DEMOLDING

Fig. 15 - TRANSFER MOLDING PROCESS

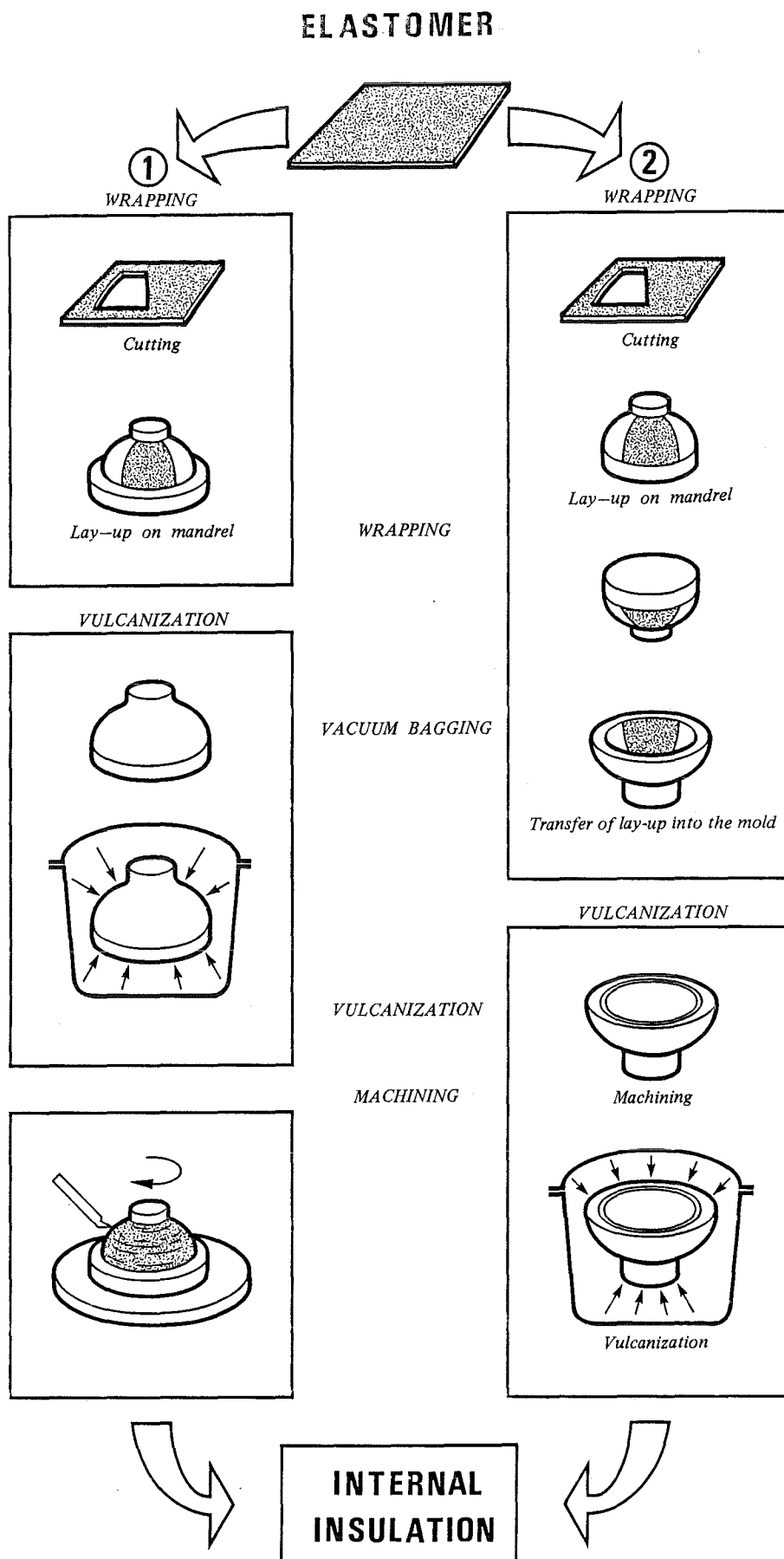
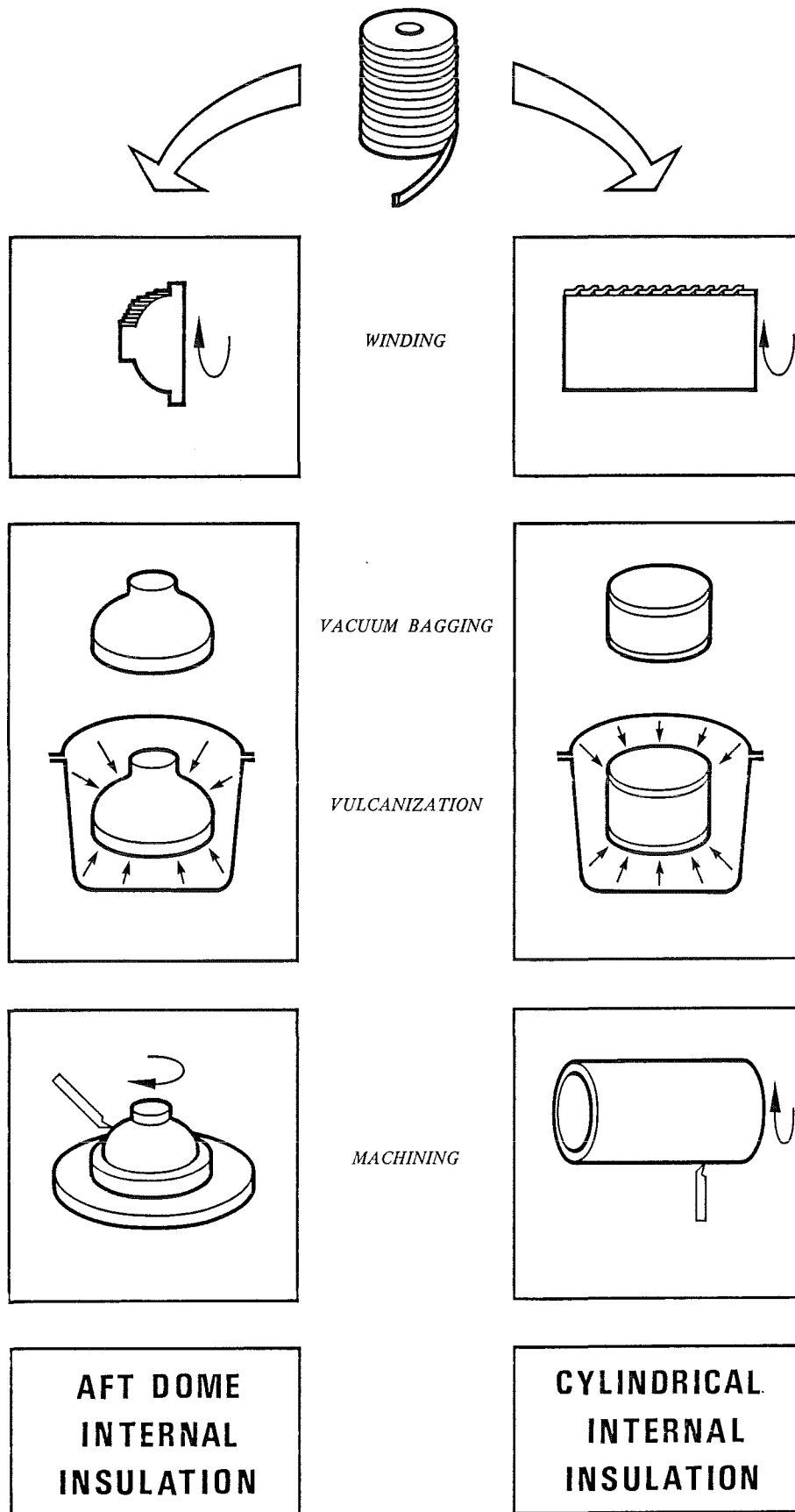


Fig. 16 - LAY - UP PROCESS

SPOOL OF CALENDERED RUBBER*Fig. 17 - WINDING PROCESS*

3.3. Integration into the motor case

The integration of internal insulation into the chamber depends on the technology used for the case construction. Thus for metallic chambers, the internal insulation is bonded into the case with a pressure applied by specific tooling. In the case of kevlar or graphite chambers, the filament winding process can be performed directly over a sand or metallic mandrel equipped with the internal insulation. Afterwards the mandrel is removed in order to cast the propellant into the chamber.

4. - CONCLUSION

The most important step of internal insulation design is the thermal analysis. This analysis is always performed using mainly experiments, correlations and simplified methods. However important improvements have been performed in the field of elastomer formulation, thus increasing the insulation performance and decreasing the density of the rubber.

OVERALL OPTIMIZATION OF SOLID ROCKET MOTOR

by

Mr A.Truchot
Agence Spatiale Européenne
Division STS-AR
8-10, rue Mario Nikis
75738 Paris Cedex 15
France

ABSTRACT

The overall optimization of a solid rocket motor consists of determining the most efficient configuration of the motor in terms of range or payload of the vehicle. After a presentation of the general requirements of a solid rocket motor, the different design parameters are detailed : operating conditions, geometric parameters and technologies used for each component. In order to achieve parametric studies, a computer program has been developed by SEP. The principle and main characteristics of this program are presented and two examples of application are given in order to illustrate the possibilities of the program.

1. - INTRODUCTION

Based upon the general requirements of a propulsion system, a great number of motor configurations are possible ; thus it is possible to change the operating conditions (pressure, duration), some geometric parameters (case length, nozzle submergence, etc...) and the technologies used for each component. All these parameters are closely linked and influence upon motor efficiency. The main objective of the optimization is to determine the most efficient configuration in terms of range or payload of the vehicle.

2. - REQUIREMENTS - OPTIMIZATION CRITERIA

The overall optimization of a solid rocket motor is an iterative process. The requirements of the propulsion system are a result of a trajectory calculation of the vehicle using the estimated performance of the motor. These requirements are associated with optimization criteria concerning either the range for a fixed payload, or the payload for a fixed range. These preliminary data enable the motor designer to determine the most efficient configuration of the motor. Then, a new trajectory calculation is performed, which gives new requirements and new optimization criteria. Several iterations are often required in order to obtain the most efficient configuration of the vehicle and its propulsion system.

2.1. Solid rocket motor requirements

The requirements of a solid rocket motor can be very different for ballistic, space or tactical applications ; however, they can be usually divided into the three following classes :

Performance requirements :

The performance requirements consist of a total impulse to be delivered by the motor, with certain limits to the burning time. The thrust-vs-time curve can be constant or as constant as possible. Sometimes a specific thrust-vs-time curve can be required ; this type of specification is usual for first stage of ballistic missile or space launcher, for which a high level of initial thrust enables a decrease of the gravity losses. Sometimes certain masses (total, inert or propellant) may be required.

Geometric requirements :

The envelope limit is usually a requirement of the vehicle designer. The geometric constraints are of great importance ; often the optimization consists to determine the most efficient configuration in a limited external volume of the motor ; moreover the motor configuration can result directly from these requirements ; it is the case of submerged nozzles for limited length motors or blast tube nozzles for tactical missile applications.

Other requirements :

Other requirements are of great importance ; thus, the objectives of cost, reliability and development time can restrict the use of certain efficient technologies, but not sufficiently demonstrated such as nozzle or case materials, TVC systems, etc...

2.3. Optimization criteria

The optimization is based upon criteria concerning either the range for a fixed payload or the payload for a fixed range. The optimization criteria are often given by partial derivatives indicating the influence of design parameters upon the range or payload of the vehicle.

An example of partial derivatives of range with respect to inert mass, propellant mass, specific impulse, and burning time is presented hereafter.

$$\begin{aligned}\frac{\partial P}{\partial m_i} &= 3 \text{ km/kg} && \text{(partial derivative with the inert mass)} \\ \frac{\partial P}{\partial m_p} &= 5 \text{ km/kg} && \text{(partial derivative with the propellant mass)} \\ \frac{\partial P}{\partial I_s} &= 50 \text{ km/s} && \text{(partial derivative with the specific impulse)} \\ \frac{\partial P}{\partial t_{cu}} &= -10 \text{ km/s} && \text{(partial derivative with the burning time)}\end{aligned}$$

The partial derivatives enable the comparison of a given motor configuration (with parameters m_i , m_p , I_s , t_{cu}) to the reference (with parameters $m_i(0)$, $m_p(0)$, $I_s(0)$, $t_{cu}(0)$) by calculating the range increment ΔP .

$$\Delta P = \frac{\partial P}{\partial m_i} (m_i - m_i^{(0)}) + \frac{\partial P}{\partial m_p} (m_p - m_p^{(0)}) + \frac{\partial P}{\partial I_s} (I_s - I_s^{(0)}) + \frac{\partial P}{\partial t_{cu}} (t_{cu} - t_{cu}^{(0)})$$

If the range increment ΔP is positive, the motor configuration is said to be more efficient than the reference.

Partial derivatives are in fact influence coefficients, which are only valid for small variations of motor parameters compared to the reference, which has been taken into account for the trajectory calculation.

3. - INFLUENCE OF DESIGN PARAMETERS

The design parameters of a solid rocket motor can be divided into three classes : the operating conditions (pressure, burning time), the geometric parameters (case length, nozzle submergence, exit cone half angle, etc...) and the technologies used for each component (propellant configuration, case and nozzle materials, TVC system, extendible exit cone, etc...). The variation of one of these parameters leads to a new configuration of the motor, requiring an accurate evaluation of its performance.

3.1. Operating conditions

It is often interesting to optimize the operating parameters of the motor ; thus, the chamber pressure has a direct influence upon the throat area, the nozzle dimensions and inert mass, the case inert mass, etc... Moreover these interactions are conflicting ; thus, an increase of pressure leads to a higher inert mass of the case (designed for internal pressure) and a lower one of the nozzle (decrease of the throat area).

The burning time can also be optimized ; this parameter influences throat area, nozzle dimensions and inert mass, thermal design of nozzle and internal insulation, etc...

In order to determine the optimum operating conditions, it is necessary to select several values of the maximum pressure and burning time. The performance of the motor will be evaluated for each couple of pressure and burning time. The results can be represented by the diagram illustrated in figure 1.

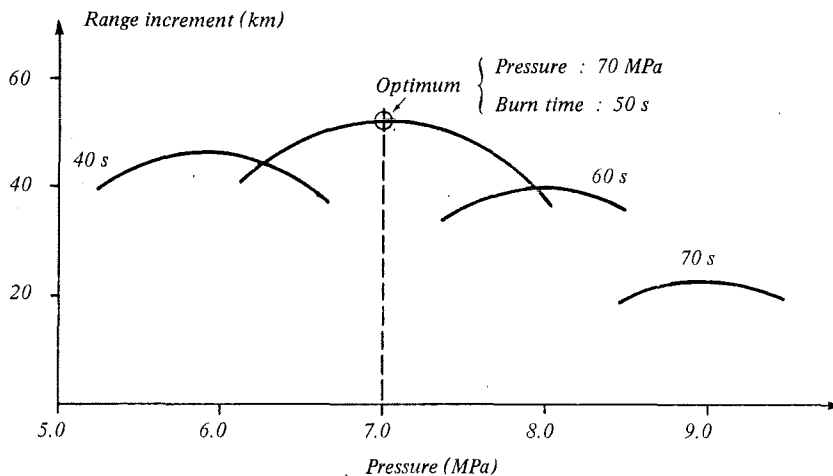


Fig. 1 - OPTIMIZATION OF PRESSURE AND DURATION

In this example, the optimum operating conditions are the following :

- . maximum pressure : 7.0 MPa
- . burn time : 50 s

3.2. Geometric parameters

The main geometric parameters of a solid rocket motor are presented in figure 2.

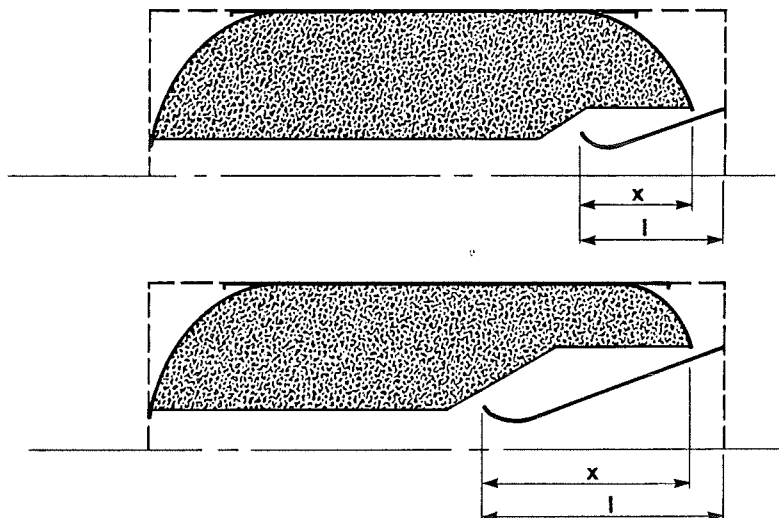


Fig. 2 - INFLUENCE OF NOZZLE SUBMERGENCE

The motor efficiency is a main function of these parameters. In order to illustrate the importance of the geometric parameters two configurations of a solid motor in a same external volume are represented in figure 3. The only difference between these two configurations is the nozzle submergence.

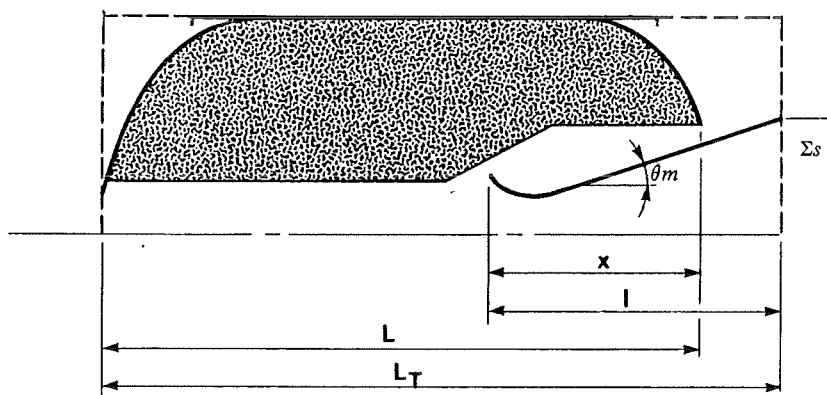


Fig. 3 - MOTOR GEOMETRIC PARAMETERS

As shown, this variation influences upon the nozzle inert mass, exit cone expansion ratio, propellant mass, case inert mass, etc... The optimal nozzle submergence will be greatly dependant on the partial derivatives with respect to inert mass, specific impulse and propellant mass. Other geometric parameters can be optimize : case length, exit cone expansion ratio and half angle, aft-opening diameter of the case, etc...

3.3. Technologies used for each component

Different technologies can be used for each component (propellant grain, case, nozzle, etc...). The use of a given technology can influence other design parameters. For instance, the optimum operating pressure is often greater with a solid rocket motor using a graphite filament wound motor case because of the better mechanical properties of graphite fibers compared to those of kevlar fibers or metal. For the different components, the technologies which can be used are the following :

a) Motor case :

The motor case can be metallic or composite. The first generations of composite motor case were made up of glass fibers. The use of kevlar fibers and more recently of graphite fibers has allowed on increase of performance. The use of a composite motor case leads to a lower inert mass of the motor.

b) Propellant grain design :

For a given propellant, the desired thrust-vs-time curve defines the burning area evolution. This evolution can be achieved by different grain shapes or burning rates, etc... The optimization of the propellant grain must be performed taking into account certain constraints : casting process, erosive burning, combustion instability, mechanical behavior, etc...

c) Internal insulation :

The design of internal insulation is a function of the combustion geometry ; the inert mass of internal insulation is a function of both the propellant grain design and the thermal properties of the selected rubber.

d) Nozzle and TVC system :

The motor performance depends on both nozzle specific impulse efficiency and inert mass. These two parameters are functions of the nozzle design : aerodynamic contour (expansion ratio, exit cone half angle deflection angle), nozzle configuration, selected liner and insulator materials (phenolic, carbon-carbon, etc...), TVC system, etc...

4. - COMPUTER AIDED PRELIMINARY DESIGN

In order to perform quickly and accurately parametric and sensitivity analyses, a computer program has been developed at SEP. Based upon data given by the user concerning performance or geometric requirements, the program builds the motor, component by component and estimates its performances (inert mass, propellant mass, specific impulse, etc...). This program enables the comparison of a great number of motor configurations and the investigation of the influence of design parameters. The principle and main characteristics of the program are presented in reference [1]. A brief summary is given hereafter and different examples of application are given in order to illustrate the possibilities of the program.

4.1. Principle

With the data given by the user, the program designs separately each component. This design phase uses simple models in order to obtain acceptable calculation time necessary to decrease the optimization time for parametric study. Afterwards, an iterative method is used to assemble the motor components. The outputs of the program consist of numerical data (geometric, performance) and graphical displays in order to verify the coherence of the solution. At the end of the program, a modification procedure is available in order to define a new configuration by changing only the desired parameters.

4.2. Characteristics of the program

The characteristics of the program which have been selected to facilitate the utilization are :

- . interactivity : the program user controls inputs and outputs data on a visual unit
- . visual graphics : graphics routines are incorporated, allowing a visualization of the calculated motor configuration
- . modular structure : this structure has been selected in order to facilitate extension to new technologies.

4.3. Data input

The data can be divided into two classes : data relative to requirements and data relative to each motor component.

a) Geometric and performance requirements :

Several options can be selected in the following list if they are not conflicting :

- . fixed diameter
- . fixed space envelope
- . fixed motor or propellant weight
- . fixed total impulse
- . fixed thrust-vs-time curve
- . fixed ideal velocity increment.

b) Data relative to motor components :

The program user must input the data relative to each component. For instance, for the motor case, the user must specify the technology used : metallic or composite, and select the design criterion : stress or strain limited, imposed stiffness.

4.4. Analysis principle

The central portion of the program consists of the automated design process. In a preliminary phase, a series of compatibility tests is performed ; the program verifies that data for each component are sufficient and not conflicting. Then each component is designed with a specific design routine. This step uses several data basis containing informations such as propellant characteristics, materials thermal and mechanical properties. The specific routine used to design each component is based on the technology used, the function to be achieved by the component and the design criteria. The models which have been developed are based on experience, state of the art, technology limits, simplified analyses and results from other computer programs. No use has been made from sophisticated analysis program such as aerodynamics or finite element codes. The reason for this, was the need of short computational time in order to decrease the duration of optimization time. At the end of the program, all the different components designed are assembled together, using an iterative process, taking into account the interactions between each component, the conformance to space envelope, etc...

4.5. Analysis results

After the assembly process, the final configuration of the motor is obtained. Two categories of results are available : firstly numerical results relative to performance or components parameters and secondly a drawing of the motor configuration with the possibility of zooms. Typical numerical results are presented in figure 4.

PROGRAM OUTPUT	
Motor diameter, m	1.600
Overall length, m	2.400
Motor weight, kg	6,155
Propellant weight, kg	5,670
Maximum pressure, MPa	6.7
Average pressure, MPa	6.1
Burn time, s	53.
Nozzle throat diameter, mm	180.
Expansion ratio, initial	16.8
average	15.8
Vacuum specific impulse, s	275.
Total impulse, MN.s	15.290
Volumetric loading	0.91
Web fraction	0.62
Port diameter, mm	350.
Port to throat ratio	3.78
Burn rate (7 MPa), mm/s	10.
Case length, mm	2.1
Aft boss opening diameter, mm	800.
Average exit cone angle, degrees	23.5
Maximum vector angle, degrees	5.

TABLE 1

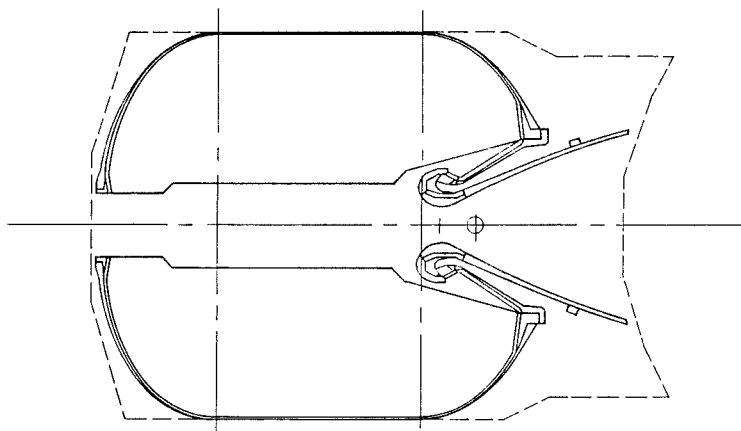


Fig. 4 - MOTOR CONFIGURATION

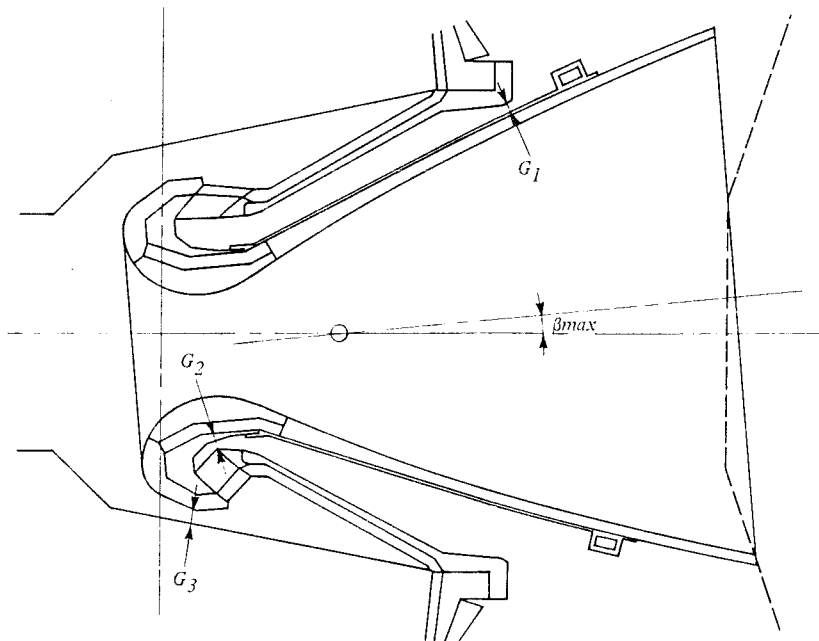


Fig. 5 - ZOOM OF THE NOZZLE

4.6. Accuracy

A comparison of results obtained by the program and by a more detailed design of the motor is presented in table 2. The accuracy obtained on inert mass and propellant mass is in the range of 2 to 3 %.

MASS	PROGRAM RESULTS (kg)	DETAILED DESIGN RESULTS (kg)
Case	357	363
Internal insulation	115	104
Nozzle	139	119
Igniter	7	8
Miscellaneous	5	10
Total inert mass	618	604
Propellant mass	11213	11188

TABLE 2

4.7. Applications

Two examples of applications will be presented hereafter. The first application is representative of a second or third stage of a ballistic missile. The second presents the developments of the program, which have been achieved in order to optimize the ARIANE V solid rocket boosters.

4.7.1. Optimization of a solid rocket motor in a fixed space envelope

The fictitious solid rocket motor studied is representative of a second or third stage of a ballistic missile. The design criterion is a fixed space envelope and the optimization criterion a maximum missile range. The motor to be optimized, incorporates the following technologies :

- . a kevlar filament wound case
- . an internal insulation made of EPDM rubber
- . an axisymmetric grain with a circular port
- . an high solid and aluminized propellant
- . a submerged contoured and movable nozzle using a carbon-carbon integral throat and entrance and carbon phenolic for the insulators and the exit cone
- . the thrust vector control device is a composite flexible bearing.

The general configuration of the motor is presented in figure 4. The optimization was conducted with the following parameters :

- . case length : L (m)
- . web fraction : e (mm)
- . maximum operating pressure : Pmax (en MPa)
- . burning time : tcu (en s)
- . nozzle submergence : x/L
- . exit cone half angle : Om (en °)

The nozzle expansion ratio has not be choosen as an independant parameter ; it is deduced from nozzle throat location and exit cone half angle. The iterative process, which has been used for the optimization is presented in figure 6.

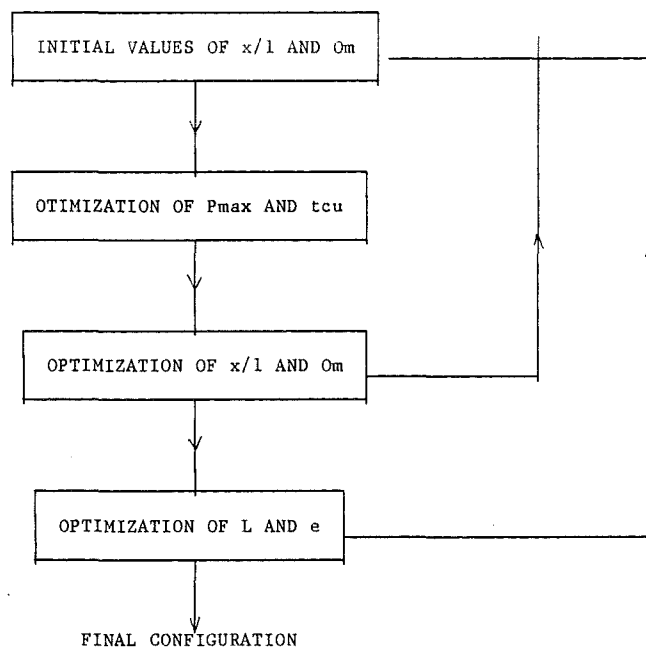


FIGURE 6

The optimization was based on partial derivatives with respect to burning time, inert mass, propellant mass and specific impulse. The total process has required the evaluation of two hundred motor configurations. The work has been done in two days. Typical results of step 1 and 2 are presented in figure 7 and 8.

The main characteristics of the optimum motor are presented in table 1. The visualisation of the motor is presented in figure 4. The optimum design parameters are the following :

. case length	: L = 2.1 m
. web fraction	: e = 379 mm
. maximum pressure	: P_{max} = 6.7 MPa
. burn time	: t_{cu} = 53 s
. nozzle submergence	: x/l = .61
. exit cone half angle	: O_m = 23.4°

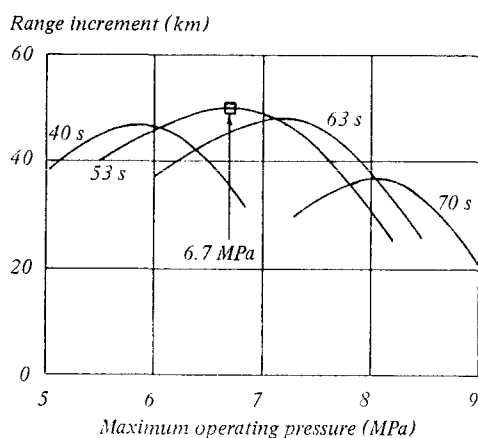


Fig. 7 — OPTIMIZATION OF PRESSURE AND DURATION

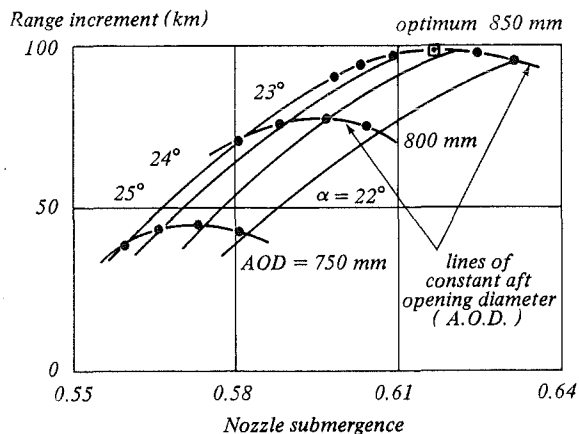


Fig. 8 - OPTIMIZATION OF NOZZLE SUBMERGENCE AND EXIT CONE HALF ANGLE

4.7.2. Optimization of ARIANE 5 solid rocket motor

The ARIANE 5 european launcher first stage consists of a central cryogenic stage and two strap-on solid rocket boosters. These boosters incorporate the following technologies :

- . segmented steel motor case
- . composite propellant : 86 % solid, 18 % aluminium
- . submerged movable nozzle hinged by a flexible bearing.

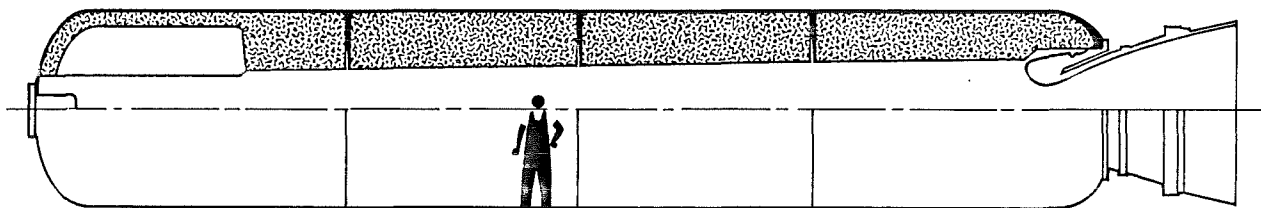


Fig. 9 - ARIANE 5 BOOSTER CONFIGURATION

The computer program has been adapted in order to achieve the optimization of these boosters. For this purpose, two modules have been developed to design the segmented case and grain.

Segmented case design module :

This module has the capability to design three to five segments of either identical or various cylindrical section lengths. The parameters taken into account are the following : mechanical properties of the selected material, geometric characteristics, forward and aft opening diameters, maximum expected operating pressure, safety factor and proof pressure ratio.

Segmented grain design module :

The required thrust-vs-time curve presented in figure 10 consists of a high thrust at lift-off followed by a regressive thrust phase to minimize aerodynamic loads during the transonic phase. At the end of the burn time, the only limitation is the maximum acceleration of the launcher. The grain configuration consists of center-perforated grain with a forward or aft finocyl star. Because of the dominant role of the thrust-vs-time requirement, it has been necessary to develop an efficient combustion module to calculate the burning area evolution. The grain module is based upon 1) internal ballistic aspects in order to produce the desired thrust-vs-time curve, 2) mechanical aspects, 3) internal flow field in order to avoid erosive burning.

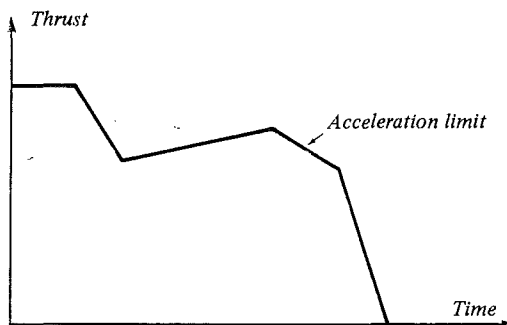


Fig. 10 - THRUST VS TIME SHAPE REQUIREMENT

In addition to these new modules, work has been done 1) on the internal insulation module to extend its capabilities to segmented grain, 2) on the nozzle module to adapt the model to large nozzles, 3) on the specific impulse prediction model.

This new version of the optimization program is extensively used in parametric studies, which are conducted by the designers in order to select the basic options, geometric and operating parameters. The main parameters which are studied are :

- . motor overall length and outside diameter
- . number of segments
- . length of cylindrical sections
- . location of the star section
- . thrust-vs-time curve parameters
- . maximum operating pressure
- . nozzle expansion ratio

Typical results obtained by the program are presented in figures 11 and 12.

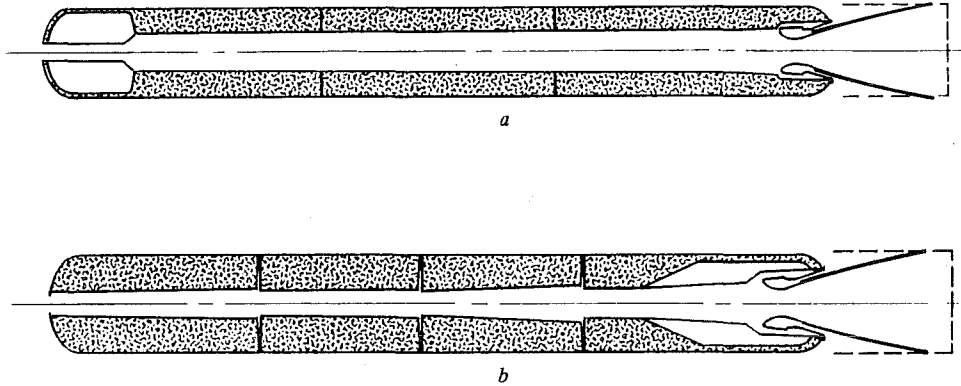


Fig. 11 - a - THREE SEGMENTS - STAR SECTION IN THE FORWARD SEGMENT
b - FOUR SEGMENTS - STAR SECTION IN THE AFT SEGMENT

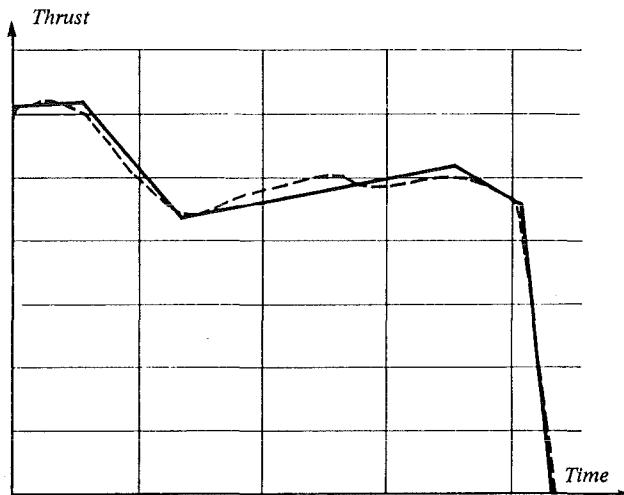


Fig. 12 - THRUST TIME COMPARISON

—— design requirement
---- actual from the code designed grain

5. - CONCLUSION

The development of automated design computer programs has allowed great simplifications of solid rocket motor preliminary design and optimization. The program, which has been presented in this paper, is an efficient tool for parametric studies and gives sufficient data to start the detailed design of each component. These programs must be continuously extended to new technologies or new applications.

ROUND TABLE DISCUSSION
Rijswijk, Netherlands, 7 April 1987

1. QUESTIONS CONCERNING NOZZLE PROBLEMS

1.1 Mr G.Kristofersen, NDRE, NO

With regard to nozzle inserts, there has been a trend from metallic (W, Mo) to graphite and to reinforced graphite. How does silicon carbide (SiC) fit into the picture?

Mr Truchot

The main drawback of silicon carbide is the lower melting point (about 2500 °C) than that of carbon-carbon (4000 °C). So silicon carbide can be used as a throat material only when the burning temperature of the propellant is low.

Mr Kristofersen

I thought that SiC could be used at 3000 °C.

Mr Truchot

No, I think it is too high! But an advantage of SiC is an excellent oxidation resistance, much better than that of carbon-carbon.

Mr Kristofersen

Is it possible, in order to enhance the oxidation resistance of a graphite, to impregnate it with SiC?

Mr Truchot

I think you talk about "overcoating" carbon with SiC? This technology has been used, but the main drawback is that the very thin layer of SiC is usually really very brittle, and when cracks go through this layer they propagate very quickly in the carbon material. I think the best solution is really to use a ceramic matrix.

Mr Kristofersen

Is it true even with a small burning time?

Mr Truchot

I think that the problem of the cracks in SiC could be critical.

Comment by Mr D.Reydellet

I think that if you manage to have a "good" layer of SiC and a "good" bonding between carbon and SiC, and if your burning time is short enough, you could have a good solution. But if the SiC is too brittle, or if the bonding is weak, or if the burning time is too long, you will run into difficulties. Anyway, it is better to put SiC *in* the carbon material and not only *on* the material.

1.2 Mr A.Mason, R.O.Summerfield, UK

Concerning materials for ITE, could the speaker quote any specific values for erosion rates of carbon-carbon throat inserts, giving details of propellant and motor performance to which they relate?

Mr Hildreth

I can't give you precise values for all kinds of propellants, including the whole range of aluminium percentage; I can say that the carbon-carbon erosion rate has an order of magnitude of 7 milliinches per second to 15 milliinches per second (about 0.2 mm/s to 0.5 mm/s). It is about one third or one fourth of that of a carbon phenolic material.

1.3 Mr Kristofersen, NDRE, NO

- a) More nozzles can be substituted for a large one. Is there an optimum for the number of nozzles?
- b) An annular nozzle can be looked upon as the limiting case for many small nozzles. Do annular nozzles have any future?

Mr Truchot

I think that the best solution for minimum weight is one single nozzle. But it may happen in some cases that several small nozzles are useful (for controlling the rolling movement, for instance).

Mr Kristofersen

I thought that one single nozzle was heavier than several small nozzles.

Mr Reydellet

I don't think so: when you look at the thermal insulation, for instance, you need much more weight for protecting the aft dome with several nozzles than with one single nozzle. In addition, the internal aerodynamics is very bad!

Mr Truchot

Furthermore, with several nozzles the case is generally much heavier, because of the weight of the bonding for the nozzles.

Mr Hildreth

I know that in USA some early booster type motors were using several nozzles, primarily for roll control purposes. Now, I know that almost all the motors which are designed now are using a single nozzle. I think that the first advantage is simplicity. My opinion is that the fewer nozzles you have for a large motor the better it is likely to be.

1.4 Mr R.J.Ballinger, British Aerospace, UK

Would anyone like to comment on the potential problem of aluminium deposition on the nozzle throat during the initial stages of burn? Is it taken into account in the initial design? Do nozzle materials influence the situation?

Mr Hildreth

For large nozzles, I think this phenomenon is negligible. In smaller designs, it could be more significant. It is generally ignored, because if there is some aluminium deposition at the very beginning of the firing it is generally removed very quickly. In RPL we have a test motor which is used for measuring the performances of the propellant formulations. We have thousands of firings with this motor; it has a bulk graphite throat of about one inch diameter. It seems that there is some evidence of aluminium deposit during the first second, or one second and a half. After that time, the graphite temperature seems to be sufficient for eliminating the deposition. The complete firing duration is about 5 to 6 seconds. But I don't think that this phenomenon was ever considered in the calculations.

Mr Ballinger

My concern was for tactical applications, for boost motors where we need the high practical specific impulse, with aluminium propellant, for high accelerations with very short burning time (1.5 to 2 seconds).

Mr Hildreth

I am not really familiar with air launched missiles; my best answer is that there could be a significant problem for you.

Mr Reydellet

It is basically a problem of wall temperature. The example given by Mr Hildreth shows that you have small throats, short burning time and a material with high diffusivity. You have a large amount of material to be put to a high temperature very quickly. So that wall temperature has not enough time to reach the alumina melting point. On the contrary, if you use a material having low diffusivity (carbon phenolic for instance), the thickness of the material to be heated will be much thinner. In this case, the equilibrium temperature will be reached for the wall very quickly. I don't guarantee the result, but it might help you if you have some difficulties.

2. QUESTIONS CONCERNING INTERNAL THERMAL INSULATION

2.1 Mr Raudsandmoen, Raufoss, NO

As both composite and strip laminate motor cases are very sensitive to leaks of hot gas through the insulation, could you please comment on how to reduce the risk of insulation leaks; e.g. material choice (type of rubber, fibre-filled, powder filled), method of application (spray or rotation insulation, insulation vulcanized into the case, bonded into the case, or winding on to the insulation).

Mr Truchot

This question was first put to Mr Denost, Mr Thorp and Dr Evans. But since composite cases cannot *alone* hold gas pressure without leaking, I must take this question. For composite cases it is essentially a problem of rubber insulation: only the rubber can prevent gas from getting out.

Mr Thorp

For strip laminate I must say that it is exactly the same as for monolithic cases: you have to protect it from the hot gases (3000 °K, typically). So there is no difference. What I must say is that we have to protect the case from water during the pressure proof test, because the resin we use is water sensitive. But, besides that exception, there is no difference with monolithic cases.

Mr Raudsandmoen

It seems to me that the consequences are very significant for composite cases.

Mr Denost

For composite cases, it is unreasonable to rely on the resistance of the case against hot gases if, for any reason, there is a thermal insulation failure or some leakage. The answer seems to be very rude, but it is only reality.

Mr Raudsandmoen

Does that mean that the best way to prevent the case from leaking is to wind on to the insulation?

Mr Denost

Not really. The designer must just make sure that the insulation will survive and protect the case. That is what is done generally.

Dr Evans

In addition, you will have to protect the case by an insulation during the hydroproof test. If you don't the case will likely be destroyed during the test.

3. QUESTIONS CONCERNING CASES

3.1 Mr Kristofersen, NDRE, NO

Filament winding is demonstrated for large motors. Is there a recommended lower limit with regard to motor diameter.

Dr Evans

The lower limit is established by the availability of small precise winding machines and somewhat by the size of fibre bundles commercially available. I have wound a lot of pressure vessels at 3 inches diameter with absolutely no difficulty on production size winding machines. Some demonstrations have been made for vessels of 1¼ inch diameter.

3.2 Mr Monvoisin, DGAIDEn, FR

Is there a rule or a method to define the succession of the hoop and helicoidal layers within the composite?

Dr Evans

In general it is preferred to alternate layers in a way that produces fibre direction symmetry about the mean radius or mid thickness of the laminate, to minimise warping of some plys under load. However, in practice, considerable liberty may be taken with this "rule" with little penalty if other behavioural characteristics are desired. For example, if the motor case structure is severely aeroheated during the post-burn flight period, one can somewhat thermally protect the helix layers, which provide bonding strength and stiffness, by placing most of them radially inboard and consequently concentrating the hoop layers to the outside where they serve as an insulator after they have performed their pressure vessel function.

Mr Denost

Generally, we alternate layers. The first reason is that we try to protect the layers that have to support higher loads (i.e. hoop layers). The second reason is that generally the mixing of layers helps to solve the problem of the bonding with the skirts, which are the cylindrical parts bonding the vessel to the rest of the missile. Since one must stop the hoop winding at the tangent line (because one cannot put hoop layers on the dome) we try to stop it as smoothly as possible, in order to avoid bending loads.

3.2 Mr Monvoisin, DGAIDEn, FR

The composite is damaged during the manufacturing process of the filament wound cases. That makes its mechanical properties decrease in comparison with unidirectional composite. What causes the damage? Is it possible to minimise this damage by slight changes in the manufacturing process?

Can the behaviour of glass, kevlar and graphite fibres be compared from this point of view?

Dr Evans

In my presentation I oversimplified by stating that the reduction in fibre strength achieved in a pressure vessel with respect to the inherent strength is due to "damage incurred in manufacture". There are other factors, including non-uniform fibre collimation and tensioning as a consequence of winding and cure (mandrel expansion before the resin becomes solid tends to more uniformly tension each fibre). Fibre/resin interaction can also cause reductions in delivered fibre strength. For example, high modulus resins result in high radial tensile loads being placed into each fibre and can cause severe strength loss in kevlar which is inherently quite weak in this direction.

Certainly, however, fibre damage during winding is a significant factor and is caused by fibre abrasion as the fibre is pulled under winding tension through and across the various contact points comprising the resin impregnation and fibre delivery systems. These kinds of damage are minimised in practice by ensuring that contact points are smooth and of large enough radius to avoid fibre damaging by bending. Even so, fibre damage does occur. Graphite or carbon is more sensitive to this phenomenon than kevlar or fibreglass.

3.3 Mr Monvoisin, DGAIDEn, FR

The graphite/resin composite is said to be more shock sensitive than the kevlar/resin composite. Do you take this factor into account when designing or manufacturing the cases?

Dr Evans

Graphite vessels do appear to be more "shock" or "impact" sensitive than those of glass and particularly kevlar. This tendency leads often to the use of kevlar or glass overwraps for added protection if the impact environment is severe.

3.4 Mr Sauvel, DGAIDEn/CAEPE, FR

During his presentation, Mr Denost spoke about the difficulty of making filament wound cases with openings of different sizes at the forward and the aft dome. Have you encountered this difficulty? If yes, how do you manage to solve it?

Dr Evans

Mr Denost correctly presented the typical solution for wound motor cases, where the aft polar opening which houses the nozzle is significantly larger than that of the forward opening. In practice, accommodation of such differences in polar opening is achieved by "deviating" both dome profiles and their winding angles and paths to "share the distress" by introducing shear stress field into both domes. For most vessels, a combined "deviation" for both domes of 10.15° can be accommodated. Resin properties of course influence how much deviation can be accommodated. Also, the path is not geodesic, so there is a tendency for the fibre to slip away from where it is placed.

Mr Denost

I agree with all these statements. All these methods are to be judged when coming to the winding machine and when one sees if it works or not.

3.5 Mr Thepenier and Mr Lucas, SNPE/USM, FR

For the optimisation calculations of the case, do you take into account the influence of the grain? If yes, how?

Dr Evans

In Hercules, we consider the interaction effects of propellant grain strain under pressure and the case stiffness (particularly hoop stiffness) during the preliminary motor design. It is a design trade. If propellant bore strains are predicted to be excessive as a result of lower case hoop stiffness than desired, then the hoop stiffness can be increased by the addition of more hoop wraps. The IM (intermediate modulus) graphite fibre like IM6 and IM7 with fibre modulus of 42×10^6 psi provides adequate case stiffness in most instances when the case is designed for pressure.

3.6 M. Vigier, Aérospatiale, FR

As a result of the studies concerning the graphite fibres, have you some results that can investigate the influence of ageing or of accidental shocks on their performance? Is the behaviour different from that which has been observed for other fibres (kevlar in particular)?

Dr Evans

It is a very difficult subject to be answered in a few words. With respect to the shock induced damage this is, as you know, a quite complex topic which cannot be easily addressed in abrupt response. But one can say that graphite pressure vessels subjected to impacts by sharp objects appear to undergo more strength loss than do those of either glass or kevlar. However in the context of generalized use of composite motor cases in a tactical missile environment, the larger question is how can one determine when an unacceptable damage level has been incurred after accidental impact, regardless of fibre choice. One other problem is how to get a criterion by using non-destructive techniques.

With respect to ageing, particularly under stress, I have seen no data to suggest that graphite fibre undergoes ageing losses. Kevlar and glass both exhibit creep rupture behaviour and consequently do not carry long term loads very well, but this characteristic is not important for motor cases. Matrix or resin dominated properties like compression and shear strength and stiffness are of course affected by resin ageing regardless of the fibre.

3.7 Mr Kristofersen, NDRE, NO

Cartridge loaded grain necessitates large ports, thereby requiring metal end rings. What is a typical propellant mass fraction for a small tactical rocket with cartridge loaded grain?

Mr Thorp

The mass fraction will depend very much on the requirements of the missile. Typically, if you have a very simple cylindrical body, and a long burning (end burning grain), with no requirement for a blast pipe, or attachments, you will probably have a mass fraction of about 0.8, with a light alloy or steel body. Graphite fibre can also be used, but it depends very much on the stiffness requirements.

At the other end of the scale, if you have a motor with wing-ring, long blast pipe, long attachments, the mass fraction can go down to 0.5 or 0.6.

I want to point out that strip laminate cases can be used with case bonded grain as well.

3.8 Mr Thepenier, SNPE/USM, FR

What is the factor of safety used for a "strip laminate" body? Is the strain under pressure for such cases similar to others?

Mr Thorp

The factor of safety used is exactly the same as for a monolithic steel case. If you choose a determined strip thickness, it may happen that you get a slightly higher margin of safety than desired, because of the nature of the laminate. But strip thickness can be modified to match exactly the factor of safety that you want.

The strain under pressure is the same as that for a monolithic case. The adhesive layer is capable of taking high shear loads, thus transmitting all loads to the strip.

3.9 Mr Holz, Thomson-Brandt, FR

Can a filament wound case for tactical missile be competitive (in terms of ratio propellant mass/missile mass) against a maraging steel case, if a first frequency made bigger than 70 Hz is required?

Dr Evans

A graphite motor case designed for pressure only will usually have an axial stiffness value about equal to that of aluminium of the same thickness (but the aluminium one has far less strength). If a greater stiffness is required to meet a given natural frequency, this may best be achieved by adding either a low angle helix layer or unidirectional layers. For this purpose the higher modulus fibres like HM ($E = 60 \times 10^6$ psi vs $E = 42 \times 10^6$ psi for IM) is advisable to minimise the quantity required. The graphite case approach may well not be competitive if the missile system requires a very high natural frequency or if there is a volume limited by available envelope.

4. QUESTIONS CONCERNING GRAIN PROBLEMS

4.1 Mr Calabro, Aérospatiale, FR

In the current propellant grains, the finocyl shape is mostly at the aft dome. In the older SRM, this shape (star) was at the forward dome; what are the criteria for choosing that location? In particular, if the shuttle's boosters were to be redesigned, would the same solution be chosen (in the forward dome)?

Mr Thrasher

I was not aware that there was a long term trend for moving the finocyl star from the forward end to the aft end of the motors; but I can find some reason for that. First, the tooling removal for the star shape is easier through the large port, which is usually located at the aft end. The second reason is that the star in the forward dome creates a big pressure drop from the forward to the aft dome, because of the big gas flow through the cylindrical bore of the grain. I know that there is some consideration about instabilities risk. The driving of longitudinal burning instabilities seems to be more effective if there is a star shape in the forward dome.

As far as the shuttle boosters are concerned, I am only aware of some problem about the star: there are some small cracks (that can be easily removed) due to thermal cool down. I see no reason to bring the star shape to the aft end. It is probably easier to manufacture the motor with the star in the forward dome.

4.2 Mr Gondovin, SNPE/CRB, FR

For the purpose of high energy (NEPE type) propellant grains structural analysis, which stress-free temperature do you assume — cure temperature or another temperature? (It is assumed that the grain is not pressure cured). In other words is there a significant cure shrinkage for that kind of propellant?

Mr Thrasher

I am not absolutely sure of the value, but it seems to me that I have seen some structural analysis assuming a cure shrinkage corresponding to a 10°F elevation of temperature.

Mr Gondovin

For that type of propellant, we don't have precise values. We only know that for classical propellants (CTPB for instance) there is no cure shrinkage. So we assume that the stress free temperature is the cure temperature.

Mr Thrasher

I guess that the common practice in USA for old propellants is to take a slight elevation of temperature.

4.3 Mr Thepenier, SNPE/USM, FR

In your model for calculating the margin of safety, how do you determine the value of FS (factor of safety)? Do you take into account for choosing this value the level of knowledge of the propellant characteristics? (Well-known or new propellant.) Do you need a reliability model?

Mr Thrasher

In USA, the FS is typically given by the SRM designer. It is a requirement. For boosters, we used a FS of 2 for bond-line critical points, and a FS of 1.5 for central bore critical point. We don't take into account the fact that, at the beginning, we don't have a lot of data relating to the propellant. The mechanical characteristics data box has to be developed during the programme. If the propellant doesn't satisfy the factor of safety, it has to be improved, or the design must be changed.

In addition, it is not a common practice in USA to assess a number for the structural reliability in rocket systems. There has been some attempt, I think, but the success was poor.

4.4 Mr Thepenier SNPE/USM FR

How do you use propellants which have "non classical" tensile curve (with two maxima for instance). What parameter of the curve do you take into account for designing the grain?

Mr Thrasher

It is a very difficult question. At first, if you use corrected stresses, you find the phenomenon much more often than if you use engineering stresses. My personal opinion is that something bad is happening to the propellant when you reach the first maximum. This could be a very wise criterion to be chosen. But sometimes, some people think that the second maximum could be used. Nobody knows who is right.

4.5 Mr Fleming, UK

In the paper of SNIA BPD no mention was made of the spin on erosive burning effect. Can these effects be important? (30% increase in burning rate.)

Mr Biagioni

We don't take into account this effect, but for the size of motor for which I have a personal experience, this effect is not so high. We consider it quite negligible, but the spin is not very high.

Mr Thepenier, SNPE/USM, FR

In the grain predesign, are criteria relating to mechanical strength pressure temperature taken in to account? What are the safety ratios that are used to achieve good operation during the lifetime under operational conditions?

Mr Biagioni

I am not a structural specialist. But I know that in my company, structural specialists do use mechanical criteria in the predesign, based on experimental correlations to take into account the effect of pressure and temperature — I have no value of factor safety in my mind now.

4.6 Mr Fleming, UK

"Base Bleed" is essentially a rocket propellant burning at low pressure (so acting as a gas generator) in a suitable motor at the rear of a shell (projectile) to extend range. Since such motors are now being produced in the hundreds of thousand per year (propellant by SNPE, Raufoss, ERT etc...), when does AGARD plan to study "BB"?

How would the members present here react to an independently organised meeting, perhaps towards the end of 1987, to consider quality control and testing?

Dr Zeller

At the last PEP meeting, there was a proposal from Mr Cruttenden (UK), about a meeting dealing with that kind of subject, including "base bleed". But, as far as I know, this subject has not been selected by AGARD for a next specialist meeting. I personally would be interested by a meeting on this subject.

D.Reydellet

In addition, I think you will find more interested people, if you ask people involved in gun propellant.

4.7 Professor De Luca, Politecnico di Milano, IT

Usually, a rocket motor is designed to be ignited, to give thrust during a certain duration, then extinguished. But what happens if you want to ignite, extinguish, then reignite, and so on..? And what if you want several levels of thrust? How much of your method can be used? How much must be changed?

Dr Zeller

It is really a very large question. There are several architectures that are possible: for instance for the short range attack missile, you have two grains that are separated, and that burn separately. There are some advanced studies using laser beams to interfere with burning. As a conclusion, one can say that it depends on the kind of architecture you choose: in certain cases you may have to develop new design methods.

Mr Reydellet

Concerning thrust modulation, I must say it is a very difficult problem. The main question is to find propellants that burn steadily in a large range of pressures. Even if you find them, you may encounter some difficulties for controlling the pressure level. As a conclusion, one can say that rocket propulsion has some limitations. Thrust modulation is one of them, and you must not try to compete in that field with other propulsion techniques that are more flexible.

ROUND TABLE DISCUSSION
Lancaster, California, USA, 23 April 1987

1. QUESTIONS PUT TO MR HILDRETH

1.1 Mr J.Gross, NWC, China Lake, US

How do you estimate nozzle erosion rates in the design process?

Mr Hildreth

99,99% is empirical based on past experience, subscale, fullscale; the range runs from about 7 to 15 milli-inches per second (0.2 to 0.5 millimetres per second) for carbon-carbon, depending upon whether you have aluminized or non-aluminized propellant.

Mr Gross

What is the relative cost of a carbon-carbon throat insert for a tactical motor compared to a graphite throat (i.e. ATJ)? — or compared to a pyrolytic graphite throat?

Mr Hildreth

I can't give you dollar values. I can give you only a general statement. If it is compared piece to piece, I think that the carbon-carbon piece will be more expensive. Depending on the kind of carbon-carbon you use, it can be moderately more expensive, or extremely. For instance, in one case, if you can make a log of 3D cylindrical weaved and cut a number of small throats in it, or if you use a 4D or multi D technology, you can make a huge billet and punch out a large number of pieces for tactical motors. It would be different for a space boost motor, where you have to weave every piece individually. In that case, I think there is no question: carbon-carbon is more expensive; however, you also have to consider that in general carbon-carbon nozzles are probably simpler; you don't need as much back-up materials, as much insulator materials. The whole nozzle design changes, which directly affects the cost. I don't know if, for tactical motors, a carbon-carbon based design is much more expensive than a phenolic or other technology design; I guess it is, probably, but it has also much higher performances. Concerning the pyrolytic graphite, I have no information on it: this technology appeared and disappeared in very few years.

1.2 Mr H.Platzek, NWC, China Lake, US

The extendible-exit-cone (EEC) does add a little more impulse to a motor, but it seems as if it's more than off-set by the increased complexity, increased inert weight. Have any type of quantitative studies been conducted to show how much is gained and what is the cost?

Mr Hildreth

Again, I don't have any precise number for you. I would only assume that, if there was not a pay-off, they wouldn't be used. But is it really for gaining performance or reducing the losses? For instance, where you have some geometrical constraint (vehicle length for submarine launched missiles) you can minimize the loss by using an EEC. Although EECs are complex and expensive, I know that they have been used in ballistic and space applications. So there must be a gain.

Comment by Mr Truchot

The complexity and the cost of EEC depends on the technology you use for carbon-carbon parts. If you use a 2D involute or 3D, large exit cones are very expensive. But if you have a less expensive technology, the cost can decrease. In addition, if the material allows simplification of the design, you can reduce the complexity and the cost. Anyway, if you compare the efforts you have to perform for gaining a few seconds of specific impulse by improving the propellant, I think that EECs are rather cheap (you can gain about 8 seconds in specific applications). Anyway, there is a trade-off to be made in every case.

Comment by Mr Reydellet

In addition, I can say that EECs are particularly interesting for submarine launched strategic missiles.

2. QUESTIONS PUT TO MR TRUCHOT

2.1 Mr B.Christensen, Hercules/Bacchus, US

What flow models are used for internal fluid flow calculations?

Are they viscous? Finite elements? Finite difference? Two-dimensional? Three-dimensional?

Mr Truchot

Currently in SEP, we have several computer codes. The first one is based on finite difference methods with only 2D capabilities. This code takes into account the viscous effect. The second code is a 3D code. It uses the methods of singularities. Finally, we have a third computer code which is still in development. It is a 2D, two-phase flow code.

Comment by Mr Zeller

In SNPE we have a 3D code; Ideal gas, one phase, inviscid, non turbulent. It uses a finite difference, unsteady method (Godounoff method).

Mr B.Christensen

How are erosion rates for internal insulators determined for new motors (no firing data for that motor available). What is the overall design strategy for internal insulators in a new motor?

Mr Truchot

We use empirical correlations and firing test results. For the first motor, we design some extra thickness. After the first test, we decrease the rubber thickness. If you know another method, you're invited to give more details. We would be very interested.

Mr Christensen

How do canted, submerged nozzles affect internal insulator char rates?

Mr Truchot

I have no personal experience of canted nozzles, but I guess that the canted nozzle is not a good design from the point of view of thermal insulation erosion in the aft dome.

Comment by Mr Reydellet

I think that the problem is more severe if the canted nozzle is *not* submerged.

Mr Christensen

What measurements (instrumentation) for internal insulators are taken during firings? Are the same made for flight and static motors?

Mr Truchot

In SEP, we measure the temperatures during the static firing test by putting thermocouples in the rubber.

Comment by Mr Reydellet

Usually we don't put thermocouples in rubber for flying tests, because we don't have a sufficient number of measurements. In addition, in France, we don't recover the stages after flight (even the first stage). Have you in the USA experienced some differences? If you have, have you some explanation?

Mr B.Christensen

Our experience is that we have seen over twice as much char as compared to static tests. These experiences were at first with silica-filled EPDM. We wonder if this applies to kevlar or asbestos filled materials. This phenomenon occurs in the forward dome. At this time, there is no satisfactory explanation; maybe a violent flow bringing hot gases to the forward dome, perhaps flight acceleration causes more charring in this area.

D.Reydellet

Under axial acceleration, the gap between the flap and the forward dome insulation is bigger than during static tests. So you may have more circulation in this gap leading to more heating of the flap surface and of the insulation.

Mr B.Christensen

It should be, but we also have this phenomenon with bonded forward dome.

2.2 Mr O.Casillas, UTC/CSD, US

What are the historical trends in the internal insulation technology (materials and processes) and what do you see in the future for insulating methods?

Mr Truchot

The first generation of rubber used asbestos fillers (10 years ago). The density of these rubbers was 1.5; the next generation was EPDM silica rubbers. We decreased the density to 1.1, with the same thermal properties and the same erosion resistance. Now, the modern compositions allow the density to decrease to 0.85. The trend for the future is to decrease the thermal diffusivity of the rubber, decrease the density and increase the erosion resistance.

2.3 Mr B.Lichtinger, UTC/CSD, US

What research is being performed to find new and lighter elastomers for insulators in place of EPDM?

Mr Truchot

I have no answer to that question. If you have some idea...

Mr B.Lichtinger

What additional losses are involved in the supersonic split line Thrust-Vector-Control (TVC) system over conventional systems?

Mr Truchot

At this time, we have only performed a demonstration test for that technology. The accuracy of the measurement during this test was not sufficient to detect the loss due to that effect. I guess there is some loss, but I can't give you any numbers.

3. QUESTIONS PUT TO DR EVANS**3.1 Mr B.Lichtinger, UTC/CSD, US**

Could you explain the significance and implication of fibre stress ratio in composite case design?

Dr Evans

Stress ratio is the ratio of the stress developed in the helix layer divided by the stress developed in the hoop layer. Another way to look at that: the lower the stress ratio, the more high stresses are in the hoop layers. Usually, the design drives to a failure in hoop layers, because that type of failure is more repeatable.

Mr B. Lichtinger

Could you explain Non Destructive Test (NDT) and inspection methods used to detect flaws in current composite motor cases?

Dr Evans

That is the subject of about a six months seminar! A lot of work has been done on this subject in this country by all propulsion companies for composites: ultrasonic, acoustic emission, cat-skin etc...; not only for cases, but for composite parts in general; as a matter of fact, for cases, only two kinds of NOC are routinely used: *X-RAY* for obvious unbounds and cracks, separations between the layers; and *proof-test*, which is the standard acceptance test criterion: if the case passes the proof-test, you have a good one. The other techniques are "non-state-of-the-art". The challenge is to develop a "finger-print" for each unique configuration, so that the comparison of the same configuration with various defects can be done.

Mr Lichtinger

What is your opinion concerning the future of composite cases in the new HLLV (Heavy Lift Launcher Vehicle) and future launch vehicles?

Dr Evans

My opinion is that the design of a new heavy launch vehicle is strictly an economic issue: the lowest price per pound in orbit. The composite cases used for thirty years in strategic system have certainly proved a sufficient reliability. The appear, in any judgement, to be cost-competitive, for satisfying the cost requirements.

3.2 Mr R. Leighton, USAF Astronautic Lab. Edwards, US

What role does the propellant grain structural integrity play in composite case design considerations? What situations might warrant consideration of the grain effects (stiffness contributions, inertia effects...)?

Dr Evans

The case and the grain have to be considered interactively, because the grain bore strain during motor pressurization is directly influenced by case (hoop layer) rigidity. With the strength of materials growing every day, and the case wall becoming thinner and thinner, one can have to put extra material for having a large web fraction. More generally, the stiffness is a concern for tactical applications, where natural frequencies of the motor are a design driver; during the operation time, the mass is decreasing, and the natural frequencies are changing dramatically; in addition, with aeroheating, the case stiffness is decreasing. This concern has to be taken into account seriously.

Mr Leighton

Likewise, how does the nozzle loading or the case enter into case design requirements? Also, how critical is the boss blow-out failure mode in case design requirement?

Dr Evans

The nozzle thrust force "unloads" the aft dome. This fact is routinely considered for the design of the polar reinforcement of the dome. In this area, the simplified netting analysis is not convenient. Furthermore, the problem is more critical when the opening becomes larger. We use the most powerful finite element code we have and, even so, we have encountered some surprises. If you need it (if the shear level is high) you can incorporate some helical reinforcement between layers.

4. QUESTIONS PUT TO MR DENOST**4.1 Mr D. Thrasher, USAF Astronautics Lab., Edwards, US**

Both speakers addressed netting analyses which define mandrel contours for geodesic and modified geodesic domes. Apparently, these analyses ignore the thickness build-up near the polar openings. How is the discrepancy addressed in practise?

Mr Denost

Knowledge of the precise thickness in every point of the dome is very important for the design. It has been necessary to develop a specific code for evaluating the thickness and validate it by experimental data. In particular, it is necessary to take into account the bandwidth of the filaments, and the winding angle (which varies very rapidly in this area). We have also to determine how to place the successive layers very precisely. Sometimes one can use local reinforcements, wafers for instance; but I think that since the quality of the theoretical predictions is not very good in this area, the wafers are often used as a security, but I don't think they are *always* necessary.

4.2 Mr Carrier, DREV, CA

Do you know of any public domain "Design handbook for composite cases for SRM"?

Mr Denost

I'm not aware of any publication, beside the two papers of this L.S., of course.

Mr Reydellet

There are a few specific courses in the French school, "Ecole Nationale Supérieure de l'Aéronautique et de l'Espace" (Toulouse, France), but they are in French.

5. QUESTIONS PUT TO MR THORP**5.1 Mr Platzeck, NWC, China Lake, US**

We heard of the strengths and advantages of strip laminate and filament cases that have been around some time, but still in limited use. What are some of the weaknesses or disadvantages of these types of cases?

Mr Thorp

I will speak only of strip laminate. At first, I must say that the "Rapier" system, which is one of the best missile systems in UK uses a solid rocket motor with a strip laminate case. The second generation of the Rapier will use also a strip laminate case. A number of other systems currently in production in UK use also strip laminate cases. I agree that all around the world it has a more limited use, but we will try to do something for that. This technology is applicable to high tensile steels, but not to light alloys. Particularly high length to diameter ratios are required, because if the ratio is smaller than 4, the size of the end rings becomes a problem, so that you are probably better off having an homogenous monolithic case. Another disadvantage is the aerodynamic heating that you may have with missiles fired from high speed aircraft, because at some temperature the resin starts to lose its strength. This phenomenon occurs from 100°C or 130°C. The strength decreases continuously, and at 200°C, you can run into trouble. The answer to this is to apply a thermal protection to the case. A lot of materials are available for that use. Another case where protection will be necessary is the underwater use; the protection will be necessary to protect the resin against humidity.

Dr Evans

I shall answer for the filament wound cases. Primarily, there is a problem of initial cost (due to materials and processes) that often excludes these technologies from tactical applications. The other problem is that composite cases are said to be more subject to damage under severe environments (aeroheating, impact...)

But requirements for tactical applications are becoming more and more ambitious every day. Composite cases could be a possible answer to the search for performance. But there could be some limitations with the complexity of design for some tactical motor cases. However, the data base for designing and manufacturing composite cases becomes greater and greater every day, so we can hope that we will be able in the future to solve technical and economical problems as well, specifically for mass production.

Mr Platzeck

I heard about bonding and rings to the strip laminate cases and bonding the strip laminate body, but no indication of the adhesive used, cleaning preparation, nor inspection procedure to ensure that the bond is acceptable.

Mr Thorp

Firstly, the adhesives we use are basically epoxide resins. We have two different adhesives, one for the strips and one for the end rings, because of the different requirements, but they are very similar; the strip adhesive is a high molecular weight resin; the end ring adhesive has a lower molecular weight. I have some very long chemical formulas down here. I don't intend to read them, but you are welcome to come and take a look at them.

Concerning cleaning and preparation, we take great care to degrease the strip when we receive it, then shot blast it; then we degrease it again before we put resin on it; when resin is applied, it is semi-cured and then it can be held for six to nine months before we use it.

Concerning inspection, for the strip and the resin, we use stringent methods (detailed chemical characterization for the resin, for instance). For the motor body, the ultimate inspection is the pressure proof test. Every case is proofed to a pressure well above the level of the maximum operation pressure. The body is measured very precisely before and after the test, to make sure that there was no movement of the end rings during that test. We have just tried to use some acoustic emission analysis during the pressure test, because the cases groan and moan a little bit. But it was just research. In addition, we have never used ultrasonic inspection methods for the case, but only for checking the propellant grain integrity.

5.2 J.Lu, USAF Aeronautics Lab, Edwards, US

I would like to know your opinion on the incorporation of fracture mechanics in motor structure design and service life prediction, and, also, the current status on fracture mechanics research in France and in UK.

Mr Thorp

Fracture Mechanics is not in my line; I think Mr Reydellet is more equipped to answer this question, for France and UK, and he has promised to do so.

Mr Reydellet

The fracture mechanics can be used for propellants, but I never heard that it can be used for composite cases. It is now very classical to use it for metallic alloys; but the advances on that subject don't come from rocket propulsion, but from aircraft applications. However, fracture mechanics can be used for metallic cases in SRM for different purposes.

The first is to assess the adequacy of non-destructive inspections for metallic cases: by measuring the K_{IC} of the materials, it is possible to calculate the size of the critical defect that will lead to failure under operating pressure, and compare this size to the smallest flaw that can be seen by non destructive tests. It is *not* advisable to have a very small critical size (1 mm is bad: 5mm is better!)

The second concern is the stress corrosion problem; if you have permanent stresses, you have to take into account the K_{ISCC} of your alloy (" K_I seuil de corrosion sous contrainte" in French), that is the value of K_I under which you cannot have stress corrosion.

The last concern could be a fatigue problem, if you have cyclic loads; in this case, you have to use another criterion, based on another threshold for K_I .

As a conclusion, all these methods are not quantitative design methods, but rather qualitative criteria (determined by experience), to be used in order to make sure that one will not be running into difficulties with a fracture mechanics problem.

Dr Zeller

I would like to point out that some work is being performed currently in France dealing with the kinetics of crack propagation in propellant grain. The AIAA paper of Mr Nottin which was given at the Joint Propulsion Conference last year can give you a good idea of what is done in France in that field. But it is at this time only research; it is not used as a routine acceptance criterion for current production.

6. QUESTIONS PUT TO DR ZELLER**6.1 Mr Lichtinger, UTC/CSD, US**

What work is France doing in the area of 1.1 class solid propellants?

Dr Zeller

The threshold between 1.1 and 1.3 propellants is not the same in USA and in France; in France, the 1.1 propellants begin at 240 cards of card-gap test, but the cards used have not the same thickness as in USA. In USA, 1.1 propellants have a NOL card gap test greater than 70 cards. This is equivalent to 90 French cards (according to an experimental program that we have performed). As a consequence, 240 French cards are equivalent to about 190 US cards. So, in France almost all cured propellants are 1.3, but some of them could be 1.1 in USA!

In the 1.1 US class category, we find extruded propellants (which are still very useful), cast double base or composite modified cast double base, and lastly the new high energy cross link double base or NEPE type propellants. All these propellants are 1.1 class in USA, and we routinely manufacture any kind of these propellants.

Mr Lichtinger

Can you provide me with a summary of your processing capabilities? How many mixers? What size? Pressure cure capabilities? Curing ovens? etc...

Dr Zeller

I shall not enter into details. For extruded and cast double base, we have manufactured so many grains every year, that it is an evidence that we have all necessary facilities. For NEPE and cross-link double base, we have all the facilities starting from the one pint mixer (for research centre) to the 420 gallons mixer (industrial production).

6.2 M.Carrier, DREV, CA

Can you tell us what is being done in Europe to experimentally validate the grain structural analysis codes that are used in all European projects?

Dr Zeller

In France, we use in-house developed 3D codes. We use these codes every time we develop a new case bonded grain. Since we have already successfully developed a lot of grains, I think that it is a kind of validation. In addition, during every engineering development, we usually perform "overtests", in order to assess the actual margin of safety of the grain (if necessary by obtaining mechanical failure). We can say that, roughly speaking, we have a good agreement with the calculations. We can also check the validity of the codes by using analog motors; a paper will be presented on the next AIAA propulsion meeting in San Diego on that subject. On the other hand I must say that *we don't use* transducers for measuring stresses in the propellant.

6.3 Mr Thrasher, USAF Astronautics Lab, Edwards, US

What sort of structural modelling capability is used within your grain design code? (Closed form, finite element or something else?)

Dr Zeller

At the very beginning of a project, we use closed form equations including the central port geometry and end effects. For special geometries, such as slotted tubes, we use the results of a parametric study using 3D finite element code calculations; we use them on a data base.

Mr Thrasher

Are structural deformations considered in your grain burnback analysis? If so, how?

Dr Zeller

No, we don't take into account the deformations of the grain for ballistic predictions.

7. QUESTIONS PUT TO MR THRASHER**7.1 Mr Platzeck, NWC, China Lake, US**

Some grain designs, especially radial slots, look impossible to inspect. How's it done?

Mr Thrasher

Most of the inspections are made visually; by using an endoscope, borescope or something similar.

Another technique is X-Ray, which can be useful to detect cracks (even radial cracks).

Computed tomography can be also effective, but it is for the future.

7.2 Mr Jones, Bristol Aerospace, CA

As a result of casting flow effects, the mechanical properties and burning rate of composite propellants vary with position and orientation in the motor. In the future, is it going to be necessary to allow for these effects in the design stage and how may they be predicted?

Mr Thrasher

This is definitely a real-world problem, because it really does happen; another problem is the effect of chemical migration and reaction which leads to mechanical properties gradient. Before looking if it will be "necessary", I would like to look if it will be "possible" to predict these phenomena: In fact, the flow of uncured propellant is a very complex rheological unstable phenomenon. I don't think it will be possible to obtain an advanced prediction tool. However, I think that the phenomenon is rather repeatable, when the distribution of aluminium and oxidisers are determined. It could be possible to dissect a motor and to look at the ballistical and mechanical gradients and anisotropy; these data could be taken into account in the analysis from a ballistical and structural point of view.

Dr Zeller

We have developed an internal ballistic code which can take into account gradients of burning rate with the location and orientation in the grain. The problem is that we have at this time no data to run this code!

8. QUESTIONS PUT TO ALL SPEAKERS**8.1 Mr B. Geisler, USAF Astronautics Lab, US**

In your experience, which factors do you believe have caused the majority of motor failures?

- a) poor design
- b) poor manufacture
- c) ageing and environmental factors
- d) other factors?

Mr Hildreth

I can speak of four examples: two involved spare boost motors and two others launch vehicle boosters. The failures of space boost motors were nozzle failure. In one case, it was obviously a bad design, not necessarily at the time of the design, but subsequently with the involute exit cone we had to improve the design and the technology, because we couldn't manufacture well enough.

The second one was a critical tolerances problem.

The first failure of launch vehicles was an excessive erosion problem in nozzle. This failure was the result of changes in material, over a period. It was neither a design problem, nor a manufacturing problem, but changes were made since the first design.

The second one is the really catastrophic accident that everybody knows. This failure occurred after many successful flights, so one cannot say that there was a catastrophic flaw in the design. Something particular must have happened to that particular segment, maybe in environmental conditions. So one has to put this failure in another category.

As a conclusion, I could say that the major problem we have is not only to have a good design, but also to manufacture it over a long period of time.

Mr Truchot

We only experienced failures during the development of the first generation of our strategic missiles. In one case, it was poor mechanical and thermal design of the nozzle (specifically with pyrolithic graphite throats).

Dr Evans

I would say at first that, relating to problems that appeared in the propulsion community in this country, I'm convinced that our customers have a certain responsibility. Rocket motors are basically very simple devices. They have a relative technological maturity; in the past ten years, we have seen a big pressure for decreasing the amount of money and work devoted to the effort of understanding what could be the necessary margins of safety. In addition, competition between manufacturers leads to propose fewer and fewer test articles in an engineering development. Furthermore, the search for performances has never been so great. This is, I think, what has pushed us in that direction.

Mr Denost

I have no personal experience of major failure in composite vessels. But I must say that the designer has to take into account a sufficient margin of safety to accept the variations that may occur during fabrication. He has to check that there is no potential danger: for instance critical areas where slight changes during the production phase may lead to a poor margin of safety. So, if in the future we meet some major failure, I think we shall have to look at first at the design.

Mr Thorp

The example I have now in my mind concerns a tactical missile with four SRM boosters, which must peel away at the same time. After some time in service, it appeared they were not peeling away at the same time. As a matter of fact, it was a problem of ageing of the propellant. Is it a design or an environmental problem? It is probably a combination of the two causes, plus the fact that insufficient testing was done in the development phase to prove the service life.

Dr Zeller

The most recent failure I have in mind occurred in an end-burning free-standing grain. The cause is probably a mixing between poor design and ageing. The failure was due to migration of nitroglycerine in the inhibitor; the result was an ignition in an area which was not predicted by ballistic codes, then overpressure and explosion of the case. During the engineering development of this motor not enough work was performed concerning the ageing, not only on the propellant by itself, but also ageing of the whole propellant grain in the real environment during its life. So I think the most important thing is to have a sufficient number of good ageing tests.

Mr Thrasher

At first, I would like to say that, in my opinion, a designer must apply all the knowledge that is available in a reasonable way (structural, ballistic...) In that context, I have only one example in my mind: that was really a design error. This concerns a free-standing grain, for a nozzle-less motor. The designer failed to consider that there was a gradient of pressure along the grain, and a very rapid peak of pressure grew up at the nozzle end of the grain; the grain collapsed, and there was a very effective explosion! Anyway, every other failure has been basically due to problems in designing, specifically because of the lack of realistic data for the analysis: the materials in the motors have often not the same properties as the properties used for the analysis. The lack of data in a sufficient spectrum of loading conditions causes major failures.

Additional Comment by Mr B. Geisler

Previously, we have put a lot of money into studying the ageing of the propellant. But, with the experience, we discovered that it was not the cause of failure: we'd better put more money in design and manufacture practices.

The other trend I see is that we are cutting the margin of safety continuously. We think we are smarter; we make the parts thinner and thinner, lighter weight, and when our understanding lacks a little bit, we have a failure.

The other frequent problem is to get out of the original design by slight modifications, after slight modifications... and so on... and what was once a good design no longer works.

BIBLIOGRAPHY

This Bibliography was compiled by CEDOCAR (CEntre de DOcumentation de l'ARmement) in consultation with the Director of the Lecture Series, Ingénieur en Chef de l'Armement D.Reydellet.

BIBLIOGRAPHY OF LECTURE SERIES N° 150
 "DESIGN METHODS FOR SOLID ROCKET MOTORS"

1. - Général Optimization

- 1.1 24063 C.CEDOCAR
 REFERENCE QUESTE : AE-024064
 titre ang. : User's manual for solid propulsion optimization code
 (spoc) volume 1 - technical description.
 Auteurs : ROYS G. P.
 Type de doc. : RAPPORT
 Langue : ENG
 No rapport : NTIS AD A 108224
 Source : NP. 240; 91 FIG. ; 24 REF. ; DP. 08/81; MICROFICHE
 résumé : Code de calculs pour optimiser les recherches
 concernant la propulsion de moteur fusée à propergol
 solide. Le spoc adaptable sur ibm 4341 et cdc 6600
 élabore un avant projet compte tenu des exigences des
 performances, des contraintes de conception et des
 limites d'opérations. Détermination des principaux
 composants moteur et de leurs possibilités en utilisant
 les dimensions et caractéristiques de base. Modèle de
 schéma d'optimisation non linéaire à partir de
 l'algorithme hooke et jeeves. Formulation du propergol,
 tuyère combustion, dimensionnements. Manuel 1 de
 l'utilisateur.
 Classification : 014
 Descripteurs : Moteur fusée ; Propergol solide; Modèle mathématique ;
 Non linéarité ; Calculateur numérique ; Optimisation ;
 Code ; Avant-projet ; Conception ; Analyse structurale ;
 Simulation analogique ; Combustion ; Rentabilité ;
 Fortran.
- 1.2 24062 C CEDOCAR
 REFERENCE QUESTE : AE-024063
 titre ang. : User's manual for solid propulsion optimization.code
 (spoc). Volume 2. User's code.
 Auteurs : ROYS G. P.
 Type de doc. : RAPPORT
 Langue : ENG.
 No rapport : NTIS AD A 108225
 Source : NP 217; 67 FIG. ; DP. 08/81 ; MICROFICHE
 résumé : Volume 2 du manuel d'utilisateur d'un code pour
 ordinateur qui exécute les avant-projets de détail
 de moteurs-fusée à combustion solide. Tous les
 composants principaux et les performances du moteur
 sont mathématiquement déterminés à partir des
 dimensions et des caractéristiques de base. Une
 méthode d'optimisation en recherche non linéaire
 basée sur l'algorithme de hooke et jeeves est
 utilisée pour établir les caractéristiques du moteur
 et optimiser l'un quelconque des paramètres. Les
 variables sont les propriétés du combustible, les
 dimensions du nez et des canaux.
 Classification : 014
 Descripteurs : Propulseur; Moteur fusée ; Produit combustion ;
 Propergol solide ; Conception ; Projet ; Projectile ;
 Ordinateur ; Logiciel ; Optimisation ; Algorithme ;
 Mise en oeuvre.

- 1.3 24064 C.CEDOCAR
REFERENCE QUESTE : AE-024065
titre ang. : User's manual for solid propulsion optimization code (spoc) volume 3. Programm description.
Auteurs : ROYS G. P.
Type de doc. : RAPPORT
Langue : ENG
No rapport : NTIS AD A 108226
Source : NP. 24; 8 FIG. ; DP. 08/81; MICROFICHE
résumé : Volume 3 du manuel d'utilisateur d'un code pour ordinateur qui détermine les avant-projets de détail de moteurs-fusée à combustible solide. Tous les composants principaux et les performances du moteur sont calculés à partir des dimensions et caractéristiques de base. Une méthode d'optimisation en recherche non linéaire basée sur l'algorithme de hooke et jeeves est utilisée pour établir les caractéristiques du moteur et optimiser l'un quelconque des paramètres. Les variables sont les propriétés du combustible, les dimensions du nez et des canaux.
- Classification : 014
Descripteurs : Propulseur; Moteur fusée; Produit combustion; Propergol solide; Conception; Projet; Projectile; Ordinateur; Logiciel; Optimisation; Algorithme; Mise en oeuvre; Programmation.
- 1.4 155533 C.CEDOCAR
NUMERO : C-84-003334
titre fr. : (Conception assistée par ordinateur des moteurs fusées à propergols solides).
titre ang. : Computer aided preliminary design of solid rocket motors
Auteurs : JACQUES L. ; ROUX J.
Affiliation : (1) Société Européenne de Propulsion, Saint Médard en Jalles (France)
type de doc. : Publication en Série
Langue : ENG
Titre publi. : AIAA Paper (US)
Source : NO 83-1254 (06/83); 8 P; 13 fig. ; 1 tabl.
AIAA/SAE/ASME 19th Joint Propulsion Conference, Seattle, WA. ; 27-29/06/83
CODEN : AAPRAQ
localisation : 05; Me 300-1
Classif. : 2108
résumé : Description du programme de calcul de la configuration d'un moteur en fonction des critères appliqués à chacun de ses composants. Exemple d'application à un étage de missile balistique de portée maximum.
- source analyse : INFO/SJ
Code Cosati : 21 08
Descripteurs : - Moteur fusée propergol solide * ; Conception assistée par calcul * ; Etude conception moteur fusée * ;
- Missile balistique ; Performance système propulsion ; Configuration système propulsion ; Structure moteur ; Programme calculateur .
- 1.5 1216 C.CEDOCAR
REFERENCE QUESTE : AE-001217
titre ang. : Advanced air launched missile rotor design methods.
Auteurs : ROYS G. P.
Type de doc. : RAPPORT
Langue : ENG
No rapport : NTIS AD A 108634
Source : NP. 42 ; 10 FIG. ; 13 REF. ; DP. 09/81 ; MICROFICHE
résumé : Rapport sur un projet en 3 phases pour la mise au point d'un programme d'ordinateur pour calculer l'avant-projet de moteurs-fusée à propergol solide. Tous les composants principaux et les caractéristiques sont déterminés numériquement. Une optimisation basée sur l'algorithme de hooke et de jeeves sert à déterminer le compromis idéal pour des paramètres. Les contraintes choisies sont les paramètres précités, les formes. Les variables sont la formulation du propergol, le rendement de combustion, les dimensions de la tuyère, etc.
- Classification : 014; 023
Descripteurs : Propulseur; Moteur fusée; Méthode; Calcul numérique; Logiciel; Propulsion chimique; Propergol solide; Optimisation; Combustion; Caractéristique aérodynamique; Missile.

1.6 98253 C.CEDOCAR

NUMERO : C-82-002087
 titre fr. : (Les moteurs - fusées à combustible solide).
 autre titre : Raketnye divigateli tvierdogo topliva
 Auteurs : FAKHROUTDINOV I. K.
 type de doc. : Ouvrage
 Langue : RUS
 éditeur : Mashinostroenie (Moscou)
 Source : (1981), 223 P. ; 87 ref. ; 101 fig. ; 10 tabl. ;
 3 phot.
 localisation : 05 ; 440-132
 Classif. : 2108
 résumé : Théorie et pratique de la fabrication des moteurs -
 fusées à combustible solide. Calcul des paramètres ;
 questions d'organisation et questions économiques
 concernant la fabrication et la conception de ces
 moteurs.
 source analyse : CAEN/D1.EX/MP
 Code Cosati : 21 08
 Descripteurs : - Moteur fusée propergol solide * ; Etude conception * ;
 - Paramètre ; Protection thermique ; Charge propulsive ;
 fiabilité ; Technologie ; Etude théorique ; Etude technique ;
 Monographie ; Ouvrage ;
 Identificateurs : Combustible solide * ; Publication soviétique.

1.7 124194 C.CEDOCAR

NUMERO : C-82-018365
 titre fr. : (Bases théoriques sur la conception des moteurs-fusées
 à combustible solide).
 autre titre : Teoreticheskie osnovy proekirovaniia RDTT
 Auteurs : EROKHIN B. T.
 type de doc. : Ouvrage
 Langue : RUS
 éditeur : Mashinostroenie, Moscou
 Source : (1982), 206 P. ; 81 ref. ; 38 fig. ; 8 tabl.
 localisation : 05 ; Numéro CEDOCAR/440-482
 classif. : 2108
 résumé : Modèles physique et mathématique pour la conception
 des moteurs-fusées à combustible solide. Méthode
 mathématique d'optimisation des caractéristiques géométriques
 des moteurs-fusées à combustible solide.
 source analyse : CAEN/MP
 Code Cosati : 21 08
 Descripteurs : - Etude conception moteur fusée * ; Moteur fusée propergol
 solide * ; Etude conception * ;
 - Modèle mathématique ; Tuyère moteur fusée ; Chambre
 combustion ; Etude théorique ; Ouvrage ;
 Identificateurs : Publication soviétique ; Optimisation.

1.8 8631 C.CEDOCAR

NUMERO : C-79-001619
 titre fr. : (Etude thermique, analyse et performances d'un système
 rotatif à propergol solide).
 titre ang. : Thermal design, analysis, and performance of a solid
 propellant spin system
 Auteurs : HWANGBO H. ; EBY R. D. ; SUMMER P. R.
 Auteur coll. : Agence Spatiale Européenne
 type de doc. : Publication en Série
 Langue : ENG
 Titre publi. : ESA Symposium "SP"
 Source : NO 139 (11/78) ; PP. 365-373 ; 9 ref. ; 17 fig. Munich
 (10-12/10/78)
 CODEN : ESFPA4
 localisation : 05 ; M.3091-4
 classif. : 2108
 résumé : Modèle de calcul des caractéristiques balistiques,
 thermiques et d'écoulement de fluide. Prédiction des
 performances en vol.
 source analyse : CAEN/DA
 Code Cosati : 21 08
 Descripteurs : - Moteur fusée propergol solide * ; Etude conception
 moteur-fusée * ; Commande attitude satellite * ;
 - stabilité attitude ; Analyse thermique ; Balistique ;
 Ecoulement fluide ; Modèle mathématique ; Corps rotation ;
 Générateur gaz.

2. - Case Design

2.1 51378 C.CEDOCAR

NUMERO : C-80-FO4021
 titre fr. : Enroulement filamenteux de fibres non métalliques.
 Conception et réalisation de structures de propulseurs
 à poudre.
 Auteurs : LAMALLE J. ; CABANEL D.
 Affiliation : (1,2) SNIAS, St Médard en Jalles
 type de doc. : Publication en Série
 Langue : FRE
 Titre publi. : Institut National des Sciences et Techniques Nucléaires ;
 Saclay (FR)
 Source : NO 22 (1980), PP 355-382; 25 fig. (22e Colloque de
 Métallurgie de Saclay, 19-20 et 21/6/79)
 CODEN : PCMLA2
 Isbn : 2-225-66132-4
 localisation : 05; M.5570
 Classif. : 1104
 résumé : Conception et dimensionnement de structures de propulseurs à
 poudre réalisées par enroulement filamenteux de fibres non-
 métalliques. Les différents matériaux utilisables ; les
 procédés de fabrication et de contrôle; les moyens mis en
 oeuvre; des réalisations de la SNIAS.
 source analyse : Auteur-ATRE/PZ
 Code Cosati : 11 04
 Descripteurs : - Composite matrice epoxy *; Construction filament enroulé *;
 Réservoir propergol *;
 - Plastique renforcé fibre verre ; Propulseur; Fusée ;
 Résistance structure ; Calcul structure : Bobinage ;
 Mémoire congrès ;
 Identificateurs : Kevlar matériau *; Matériau préimprégné : Saclay congrès ;
 1979 année ;

3. - Propellant Grain Design

3.1 1480 C.CEDOCAR

NUMERO : C-79-000221
 titre fr. : (Optimisation des performances des propergols solides à additifs métalliques)
 titre ang. : Performance optimization of metallized solid propellants
 Auteurs : SWAMINATHAN V. ; RAJAGOPALAN S.
 type de doc. : Publication en Série
 Langue : ENG
 Titre publi. : Propellants and Explosives ; (DE)
 Source : VOL.3, NO 5 (10/78), PP. 150-155 ; 15 ref. ; 3 tabl.
 CODEN : PREX2S
 Issn : 0340-7462
 localisation : 05
 Classif. : 1901
 résumé : On cherche à déterminer la composition optimale d'un type de propergol solide contenant un additif métallique en vue d'obtenir l'impulsion spécifique maximale. On a utilisé la méthode de projection des gradients, proposée par Rosen. On présente et discute les résultats.
 source analyse : ATRE/PO
 Code Cosati : 19 01
 Descripteurs : - Propergol solide * ; Impulsion spécifique *
 - Liant propergol solide ; Chaleur formation ; Poids moléculaire ; Modèle mathématique ;
 Identificateurs : Propergol métallisé *

3.2 147252 C.CEDOCAR

NUMERO : C-83-015378
 titre fr. : (Analyse dynamique de structures viscoelastique utilisant la méthode des éléments finis incrémentale).
 titre ang. : Dynamic analysis of viscoelastic structures using incremental finite element method
 Auteurs : CHEN W. H. ; LIN T. C.
 Affiliation : (1) National Tsing-Hua University, Hsinchu, Taiwan.
 type de doc. : Publication en Série
 Langue : ENG
 Titre publi. : Univelt, Advances in Astronautical Sciences (US)
 Source : VOL 50 (1983), PP. 710-722 ; 23 ref. ; 6 fig. NCKU/AAS. International Symposium Tainan-Taiwan, 29-31/12/81 (Part II)
 CODEN : ADASA9
 Issn : 0065-3438
 Isbn : 0-87703-166-51
 localisation : 05; Me 920
 classif. : 2011
 résumé : Présentation d'une méthode simple et efficace, qui ne comprend pas de transformations intégrales basée sur le principe variationnel d'Hamilton, pour étudier des structures viscoelastiques de géométrie complexe, soumises à des charges dynamiques. Modélisation du comportement constitutif, technique de résolution. Deux exemples illustratifs montrent la précision de la méthode. Etude des effets transitoires des structures viscoelastiques soumises à des charges instationnaires.
 source analyse : INFO/SN
 Code Cosati : 20 11
 Descripteurs : - Viscoélasticité * ; Analyse dynamique structure *
 - Propergol fusée solide ; Aube turbine gaz ; Méthode élément fini ; Dépendance du temps ;
 Identificateurs : Charge variable

3.3 174955 C.CEDOCAR

NUMERO : C-84-015323

titre fr. : Influence directe des contraintes sur la vitesse de combustion des propergols solides composites.

titre ang. : The direct effects of strain on burning rates of composite solid propellants.

Titre conf. : 20th Joint Propulsion conference

LIEU DE CONF. : Cincinnati (US)

DATE CONF. : 1984/06/11-1984/06/13

Auteurs : LANGHENRY M.T.

Affiliation : Auburn Univ. AL (US)

Auteur coll. : American Inst. of Aeronaut. and Astronaut. ; SAE ASME

type de doc. : Mémoire Congrès

Langue : ENG

Titre publi. : AIAA Papers (US)

Source : NO 84-1436; 8 p.; 12 ref. ; 9 fig. ; 1 Tabl. ; DP. 1984

CODEN : AAPRAQ

Issn : 0146-3705

localisation : 05; ME.300-1

résumé : Présentation d'un modèle mathématique permettant de prévoir l'augmentation de la vitesse de combustion due aux contraintes mécaniques dans un propergol composite solide. Ce modèle attribue cette augmentation à la capacité des flammes à pénétrer dans les petites fissures et les vides qui se forment lorsque le propergol se déforme. Le nombre et la dimension des fissures sont obtenus en appliquant une analyse de propagation de défaut à partir d'une distribution initiale aléatoire due à la décohésion sous contraintes des particules de liant et d'oxydant.

source analyse : INFO/CR

Code Cosati : 19 01 ; 20 11

Descripteurs : - Propergol composite *; Combustion propergol *;
Relation déformation contrainte * ;
- Performance système propulsion ; Vitesse combustion :
Moteur fusée propergol solide ; Propagation fissure ;
Modèle mathématique ; Thermodynamique statistique ;
Propagation flamme

Identificateurs : Facteur intensité contrainte

4. - Nozzle Design

4.1 53667 C.CEDOCAR

NUMERO : C-80-F04680
 titre fr. : Prédiction du comportement des matériaux phénoliques ablatifs.
 Auteurs : BONNET C.
 Auteur coll. : Advisory Group for Aerospace Research and Development
 type de doc. : Publication en Série
 Langue : FRE
 Titre publi. : AGARD Conference Proceeding (FR)
 Source : VOL. CP-259, NO 30 (7/79), PP. 30 1-30. 16 ; 7 ref. ; 25 fig.
 CODEN : AGCPAV
 Isbn : 92-835-0243-4
 localisation : O5 ; Me 372-15
 classif. : 2108
 résumé : Exposé destiné à montrer les efforts accomplis pour améliorer les méthodes de fabrication des matériaux composites ablatifs et des pièces, mettre au point de nouvelles méthodes d'analyse et des programmes de calcul permettant de prédire le comportement mécanique et thermique des pièces de tuyère en tir, caractériser ces matériaux aux températures d'utilisation.
 source analyse : CAEN/MS
 Code Cosati : 21 08
 Descripteurs : - Moteur fusée propergol solide * ; Matériau composite * ,
 tuyère moteur fusée * ; matériau ablation *
 - résine phénolique ; résistance mécanique ; Résistance thermique ; Procédé fabrication ;
 Identificateurs : Comportement matériau .

4.2 180094 C.CEDOCAR

NUMERO : C-85-F00952
 titre fr. : Etudes aérodynamiques liées au développement des divergents déployables.
 Titre conf. : 21e colloque d'aérodynamique appliquée.
 LIEU DE CONF. : Ecully (FR)
 DATE CONF. : 1984/11/07-1984/11/09
 Auteurs : VENABLES A. : LARUELLE G.
 Affiliation : ONERA (FR) ; ONERA (FR)
 type de doc. : Mémoire Congrès
 Langue : FRE
 Titre publi. : AAAF Notes Techniques (FR)
 Source : NO 18 ; 71 p. ; 16 Ref. ; 38 Fig. ; ONERA TP 1984-149 ; DP. 1984/4T
 CODEN : AAAN2Y
 Issn : 0243-0177
 Isbn : 2-717-00794-6
 localisation : O5 ; M 1180
 résumé : Dans le but d'augmenter la portée d'un missile balistique à encombrement donné, on étudie l'adaptation de divergents déployables pour les étages supérieurs. Description des diverses configurations de ces divergents, exposé des méthodes de calcul utilisées pour l'estimation des efforts, essais effectués pour vérifier les résultats.
 source analyse : INFO/MS
 Code Cosati : 21 08 ; 12 01
 Descripteurs : - Tuyère moteur fusée * ; Calcul mathématique * ; Tuyère divergente * ;
 - Etude conception tuyère ; Missile balistique ; Mesure pression ; Essai soufflerie ; Moteur fusée propergol solide
 Identificateurs : Moteur missile * ; Méthode calcul ; Mesure écoulement.

4.3 202235 C.CEDOCAR

NUMERO : C-86-002072
 titre fr. : Conception et optimisation de systèmes de propulsion
 utilisant des tuyères chanfreinées.
 titre ang. : The design and optimization of propulsion systems
 employing scarfed nozzles.
 Titre conf. : 21st AIAA/SAE/ASME/ASEE Joint Propulsion Conference
 LIEU DE CONF. : Monterey US
 DATE CONF. : 1985/07/08-1985/07/10
 Auteurs : LILLEY J.S.
 Affiliation : US Army Missile Command, Redstone Arsenal, US
 Auteur coll. : AIAA/SAE/ASME/ASEE
 type de doc. : Mémoire Congrès
 Langue : ENG
 Titre publi. : AIAA Paper (US)
 Source : NO AIAA851308 ; 24 p. ; 5 ref. : 20 fig. ; 6 tabl. ;
 DP 1985
 CODEN : AAPRAQ
 Issn : 0146-3705
 localisation : 05 ; ME 300-1
 résumé : Description d'une étude comportant deux phases :
 utilisation d'un modèle mathématique de performances
 d'un système de propulsion pour évaluer l'influence de
 la géométrie des tuyères sur leurs performances.
 Utilisation des résultats de cette première phase pour
 la conception et l'optimisation de tuyères, dévoyées et
 chanfreinées, en fonction de la mission du missile qu'elles
 équipent.
 source analyse : INFO/CR
 Code Cosati : 21 08
 Descripteurs : - Moteur fusée propergol solide * ;
 - Performance système propulsion ; Etude conception moteur
 fusée ; Ecoulement symétrie axiale ; Tuyère dévoyée ;
 Etude conception tuyère
 Identificateurs : Missile tactique.

REPORT DOCUMENTATION PAGE			
1. Recipient's Reference	2. Originator's Reference AGARD-LS-150 (Revised)	3. Further Reference ISBN 92-835-0454-2	4. Security Classification of Document UNCLASSIFIED
5. Originator	Advisory Group for Aerospace Research and Development North Atlantic Treaty Organization 7 rue Ancelle, 92200 Neuilly sur Seine, France		
6. Title	DESIGN METHODS IN SOLID ROCKET MOTORS		
7. Presented at			
8. Author(s)/Editor(s) Various	9. Date April 1988		
10. Author's/Editor's Address Various	11. Pages 248		
12. Distribution Statement	This document is distributed in accordance with AGARD policies and regulations, which are outlined on the Outside Back Covers of all AGARD publications.		
13. Keywords/Descriptors			
<div style="display: flex; justify-content: space-between;"> <div> Solid propellant rocket engines Solid rocket propellants </div> <div> Rocket engine components Design </div> </div>			
14. Abstract			
<p>This Lecture Series will try to summarize the current state-of-the-art in designing solid rocket motors and their components. The aim is to collect the experience of several countries in using new technologies and new methods which have been developed over the past ten years.</p> <p>Specific sessions will deal with propellant grain, cases, nozzle, internal thermal insulations; the question of the general optimization of a solid rocket motor will be emphasized.</p> <p>The material in this revised publication was assembled to support a Lecture Series under the sponsorship of the Propulsion and Energetics Panel and the Consultant and Exchange Programme of AGARD presented on 18—19 April 1988 in London, United Kingdom, 21—22 April 1988 in Saint-Aubin de Medoc, France, 25—26 April 1988 in Neubiberg, Germany and on 28—29 April 1988 in Rome, Italy.</p>			

<p>AGARD Lecture Series No.150 (Revised) Advisory Group for Aerospace Research and Development, NATO DESIGN METHODS IN SOLID ROCKET MOTORS Published April 1988 248 pages</p> <p>This Lecture Series will try to summarize the current state-of-the-art in designing solid rocket motors and their components. The aim is to collect the experience of several countries in using new technologies and new methods which have been developed over the past ten years.</p> <p>Specific sessions will deal with propellant grain, cases, nozzle, internal thermal insulations; the question of the general optimization of a solid rocket motor will be</p> <p>P.T.O</p>	<p>AGARD-LS-150 (Revised)</p> <p>Solid propellant rocket engines Solid rocket propellants Rocket engine components Design</p>	<p>AGARD Lecture Series No.150 (Revised) Advisory Group for Aerospace Research and Development, NATO DESIGN METHODS IN SOLID ROCKET MOTORS Published April 1988 248 pages</p> <p>This Lecture Series will try to summarize the current state-of-the-art in designing solid rocket motors and their components. The aim is to collect the experience of several countries in using new technologies and new methods which have been developed over the past ten years.</p> <p>Specific sessions will deal with propellant grain, cases, nozzle, internal thermal insulations; the question of the general optimization of a solid rocket motor will be</p> <p>P.T.O</p>	<p>AGARD-LS-150 (Revised)</p> <p>Solid propellant rocket engines Solid rocket propellants Rocket engine components Design</p>
<p>AGARD Lecture Series No.150 (Revised) Advisory Group for Aerospace Research and Development, NATO DESIGN METHODS IN SOLID ROCKET MOTORS Published April 1988 248 pages</p> <p>This Lecture Series will try to summarize the current state-of-the-art in designing solid rocket motors and their components. The aim is to collect the experience of several countries in using new technologies and new methods which have been developed over the past ten years.</p> <p>Specific sessions will deal with propellant grain, cases, nozzle, internal thermal insulations; the question of the general optimization of a solid rocket motor will be</p> <p>P.T.O</p>	<p>AGARD-LS-150 (Revised)</p> <p>Solid propellant rocket engines Solid rocket propellants Rocket engine components Design</p>	<p>AGARD Lecture Series No.150 (Revised) Advisory Group for Aerospace Research and Development, NATO DESIGN METHODS IN SOLID ROCKET MOTORS Published April 1988 248 pages</p> <p>This Lecture Series will try to summarize the current state-of-the-art in designing solid rocket motors and their components. The aim is to collect the experience of several countries in using new technologies and new methods which have been developed over the past ten years.</p> <p>Specific sessions will deal with propellant grain, cases, nozzle, internal thermal insulations; the question of the general optimization of a solid rocket motor will be</p> <p>P.T.O</p>	<p>AGARD-LS-150 (Revised)</p> <p>Solid propellant rocket engines Solid rocket propellants Rocket engine components Design</p>

<p>emphasized.</p> <p>The material in this revised publication was assembled to support a Lecture Series under the sponsorship of the Propulsion and Energetics Panel and the Consultant and Exchange Programme of AGARD presented on 18—19 April 1988 in London, United Kingdom, 21—22 April 1988 in Saint-Aubin de Medoc, France, 25—26 April 1988 in Neubiberg, Germany and on 28—29 April 1988 in Rome, Italy.</p> <p>ISBN 92-835-0454-2</p>	<p>emphasized.</p> <p>The material in this revised publication was assembled to support a Lecture Series under the sponsorship of the Propulsion and Energetics Panel and the Consultant and Exchange Programme of AGARD presented on 18—19 April 1988 in London, United Kingdom, 21—22 April 1988 in Saint-Aubin de Medoc, France, 25—26 April 1988 in Neubiberg, Germany and on 28—29 April 1988 in Rome, Italy.</p> <p>ISBN 92-835-0454-2</p>
<p>emphasized.</p> <p>The material in this revised publication was assembled to support a Lecture Series under the sponsorship of the Propulsion and Energetics Panel and the Consultant and Exchange Programme of AGARD presented on 18—19 April 1988 in London, United Kingdom, 21—22 April 1988 in Saint-Aubin de Medoc, France, 25—26 April 1988 in Neubiberg, Germany and on 28—29 April 1988 in Rome, Italy.</p> <p>ISBN 92-835-0454-2</p>	<p>emphasized.</p> <p>The material in this revised publication was assembled to support a Lecture Series under the sponsorship of the Propulsion and Energetics Panel and the Consultant and Exchange Programme of AGARD presented on 18—19 April 1988 in London, United Kingdom, 21—22 April 1988 in Saint-Aubin de Medoc, France, 25—26 April 1988 in Neubiberg, Germany and on 28—29 April 1988 in Rome, Italy.</p> <p>ISBN 92-835-0454-2</p>

AGARD

NATO  OTAN

7 rue Ancelle • 92200 NEUILLY-SUR-SEINE
FRANCE

Telephone (1)47.38.57.00 • Telex 610 176

**DISTRIBUTION OF UNCLASSIFIED
AGARD PUBLICATIONS**

AGARD does NOT hold stocks of AGARD publications at the above address for general distribution. Initial distribution of AGARD publications is made to AGARD Member Nations through the following National Distribution Centres. Further copies are sometimes available from these Centres, but if not may be purchased in Microfiche or Photocopy form from the Purchase Agencies listed below.

NATIONAL DISTRIBUTION CENTRES

BELGIUM

Coordonnateur AGARD — VSL
Etat-Major de la Force Aérienne
Quartier Reine Elisabeth
Rue d'Evere, 1140 Bruxelles

ITALY

Aeronautica Militare
Ufficio del Delegato Nazionale all'AGARD
3 Piazzale Adenauer
00144 Roma/EUR

CANADA

Director Scientific Information Services
Dept of National Defence
Ottawa

LUXEMBOURG

See Belgium

DENMARK

Danish
Ved Id
2100 C



National Aeronautics and
Space Administration

Postage and Fees Paid
National Aeronautics and
Space Administration
NASA-451

Official Business
Penalty for Private Use \$300



R

FRANCE

O.N.E.
29 Ave
92320

Washington, D.C.
20546

**SPECIAL FOURTH CLASS MAIL
BOOK**

L2 001 LS-150 88051B3000161D
DEPT OF THE AIR FORCE
ARNOLD ENG DEVELOPMENT CENTER (AFSC)
LIBRARY/DOCUMENTS
ARNOLD AF STA TN 37389

ishment

AGARD

GERMANY

Fachinf
Physik
Karlsruhe
D-7514

GREECE

Hellenic
Aircraft
Departn
Holargos

ICELAND

Director of Aviation
c/o Flugrad
Reykjavik

UNITED KINGDOM

Defence Research Information Centre
Kentigern House
65 Brown Street
Glasgow G2 8EX

UNITED STATES

National Aeronautics and Space Administration (NASA)
Langley Research Center
M/S 180
Hampton, Virginia 23665

THE UNITED STATES NATIONAL DISTRIBUTION CENTRE (NASA) DOES NOT HOLD
STOCKS OF AGARD PUBLICATIONS, AND APPLICATIONS FOR COPIES SHOULD BE MADE
DIRECT TO THE NATIONAL TECHNICAL INFORMATION SERVICE (NTIS) AT THE ADDRESS BELOW.

PURCHASE AGENCIES

National Technical
Information Service (NTIS)
5285 Port Royal Road
Springfield
Virginia 22161, USA

ESA/Information Retrieval Service
European Space Agency
10, rue Mario Nikis
75015 Paris, France

The British Library
Document Supply Division
Boston Spa, Wetherby
West Yorkshire LS23 7BQ
England

Requests for microfiche or photocopies of AGARD documents should include the AGARD serial number, title, author or editor, and publication date. Requests to NTIS should include the NASA accession report number. Full bibliographical references and abstracts of AGARD publications are given in the following journals:

Scientific and Technical Aerospace Reports (STAR)
published by NASA Scientific and Technical
Information Branch
NASA Headquarters (NIT-40)
Washington D.C. 20546, USA

Government Reports Announcements (GRA)
published by the National Technical
Information Services, Springfield
Virginia 22161, USA



Printed by Specialised Printing Services Limited
40 Chigwell Lane, Loughton, Essex IG10 3TZ

ISBN 92-835-0454-2